The cytosolic fate of ricin A chain in target cells

Philip John Hart

BSc. (Hons.) Biochemistry (First Class)

University of Warwick

A Thesis Submitted for the Degree of

Doctor of Philosophy

Department of Biological Sciences

University of Warwick

July 2010

Contents

List of Figures

List of Tables

List of Abbreviations

The following is a complete list of uncommon abbreviations used in this thesis. It excludes those covered by the *Système international d'unités*

2YT	2× yeast extract, tryptone medium
4-PB	4-phenyl butyrate
AAA	ATPase associated with various cellular activities
a.a.	amino acid
AP	alkaline phosphatase
ADP	adenosine diphosphate
Aha	Activator of Hsp90 ATPase
ALLN	N-Acetyl-Leucinyl-Leucinyl-Norleucinyl-CHO
AMPK	Adenosine monophosphate activated protein kinase
ApoB	apolipoprotein B
AT	antitrypsin
ATP	adenosine triphosphate
ATX	ataxin
a.u.	arbitrary units
BAG	Bcl-2 associated athanogene
BCIP	5-bromo-4-chloro-3-indolyl phosphate
BiP	binding protein
β-me	β-mercaptoethanol
BSA	bovine serum albumin
°C	degrees Celsius
C01	CCT018159
cAMP	cyclic adenosine monophosphate
cGMP	cyclic guanosine monophosphate
CCT	chaperone containing TCP-1
Cdc	cell division cycle
cf.	confer
CFTR	cystic fibrosis transmembrane conductance regulator
CHIP	C-terminus of Hsc70 interacting protein
Ci	Curies
Cnx	calnexin
CoA	co-enzyme A
COP	coat protein
CPI	Complete protease inhibitors
CPY	carboxipeptidase Y
Crt	calreticulin
CTA1	Cholera toxin A chain
CTD	c-terminal domain
Cue	coupling of ubiquitination to ER degradation
Da	Daltons
Derlin	degradation in the ER associated protein
DHFR	dihydrofolate reductase
DMSO	dimethyl sulfoxide
Doa	dead on arrival
DOI	duration of infection
DSG	deoxyspergualin
Dsk	dark skin
DTT	dithiothreitol
DUB	de-ubiquitinating factors
EE	early endosomes
EDEM	ER-resident degradation enhancing mannosidase
ER	endoplasmic reticulum
ERAD	endoplasmic reticulum associated degradation
ERAD-L	~ (lumenal faults)
ERAD-M	~ (membrane faults)
ERAD-C	~ (cytosolic faults)
FBX	F-box
FGF	fibroblast growth factor
g	gravity
GA	geldanamycin
gp	glycoportein
GFP	green fluorescence protein
GTP	guanosine triphosphate
Grp	glucose regulated protein
h	hours
Hdj	human DnaJ homologue
HERP	homocysteine-induced ER stress regulated protein
HIP	Hsc70 interacting protein
Hmg-	3-hydroxy-3-methyl-glutaryl-
HOP	Hsp70/90 organising protein
Hrd	Hmg-CoA reductase degradation
HRP	horseradish peroxidise
Hsc	heat shock cognate
HSF	heat shock factor
Hsp	heat shock protein
HSPBP	hsp binding protein
Htm	homologous to mannosidase
IC_{50}	concentration required to effect 50% inhibition
IL-2	interleukin-2

IPTG	isopropyl β-D-1-thiogalactopyranoside
Kar	karyogamy
kDa	kilodaltons
Lipofect.	lipofectamine
Log	logarithm
Lys	lysine
mRNA	messenger ribonucleic acid
Min	minutes
Mns	mannosidase
MOPS	3-(N-morpholino)propanesulfonic acid
n	number
NAC	nascent chain associated complex
N.B.	nota bene (note well)
NBT	nitroblue tetrazolium
NECA	N-ethyl-5'-carboxamido adenosine
NEF	nucleotide exchange factor
NLS	nuclear localisation signal
Npl	nuclear protein localisation
OS	Oligosaccharide sensing
P	pellet (note capital)
p	particle (note lower case)
p	probability value (note italics)
Ψ	water potential
PAGE	polyacrylamide gel electrophoresis
PAP	pokeweed antiviral protein
PDI	protein disulfide isomerise
pH	potenz hydrogen
pI	isoelectric point
POPC	1-palmitoyl-2-oleoyl-*sn*-glycero-3-phosphocysteine
POPS	1-palmitoyl-2-oleoyl-*sn*-glycero-3-phosphoserine
PPI	peptide prolyl isomerise
Pre	pre-incubation
Rab	Ras-like proteins from rat brain
RA	radicicol
Rad	radiation sensitivity abnormal
RE	recycling endosomes
Rel.	relative
RFP	RING-finger protein
RING	really interesting new gene
RIP	ribosome inactivating protein
RMA	RING-finger motif with membrane anchor
RNA	ribonucleic acid
RNAi	interfering ribonucleic acid
rRNA	ribosomal RNA
Rpt	regulatory particle
RTA	ricin toxin A chain
RTB	ricin toxin B chain
S	Svedberg units (always prefixed by a number)
S	soluble (never prefixed by a number)
SD	standard deviation
SDS	sodium dodecyl sulfate
Sec	secretory
SEL	suppressor of lin-12-like
SEM	standard error of the mean
SERCA	sarcoplasmic / ER Ca^{2+} ATPase
SF9	*Spodoptera frugiperda* cell line 9
Skp	S-phase kinase-associated protein
SOB	super optimal broth
Ssa	stress seventy sub-family A
Ste	sterile
SV40	Simian vacuolating virus 40
t	time
TAg	Large T antigen
Tat	twin arginine transport
TCA	trichloroacetic acid
TEB	thioesterase B gene
TEMED	tetramethylethylenediamine
TGN	*trans*-Golgi network
TPR	tetratricopeptide repeat
TPST	tyrosyl protein sulfotransferasse
TRC	tumour repressor in renal carcinoma
Tris	Tris-(hydroxymethyl)-aminomethane
Ub	ubiquitin
Ubc	ubiquitin conjugating
Ubx	ubiquitin regulatory 'x'
UCSF	University of California, San Francisco
UDP	uridine disphosphate
UGGT	UDP-glucose:glycoprotein transferase
Ufd	ubiquitin fusion degradation
UPS	ubiquitin-proteasome system
v/v	volume/volume
v/w	volume/weight
WT	wild-type
Ydj	yeast DnaJ homologue
Yos	yeast oligosaccharide sensing

Acknowledgements

Thanking everyone who has helped me form this thesis is an impossible task, so I have to thank the most important people. Professors Mike Lord and Lynne Roberts and Doctor Robert Spooner have all been monumentally kind to me during my four years of study. This kindness has been manifested in many forms: freely discussing speculation, evaluating results, the occasional beer and the accommodation of my work- and writing-styles. I'm told the latter can be unnecessarily abstruse, so thank you for your patience!

I must also thank Professor Jörg Höhfeld of the University of Bonn and his protégés, Doctors Christian Rogon, Michael Dreiseidler and Verena Arndt. They were especially helpful in providing constructs and stocks of purified protein. At Warwick, I would like to thank Kat Moore for inducting me into the lab and tutoring me for my first year, as well as Dr. J. Cook, Dr. Alice Rothnie and Dr. Paola Pietroni for technical assistance and advice. Professor John Ellis also deserves thanks for helping us to critique the initial stages of the project and for rigorously defending a lot of the core precepts that lie at the heart of chaperone biology (especially whenever a slip-of-the-tongue was made).

Outside of academia, I would like to thank my family for being eternally supportive. Mum, for all the tea and for letting me convert the dining room into a study; Dad, for all the encouragement and incentive. Finally, I would like to dedicate the effort I have put into the writing of this document to my two late Grandmas, for many happy memories.

Declaration

All the results presented in this thesis were obtained by the author at the University of Warwick, whilst under the supervision of Professors J.M. Lord and L.M. Roberts. This is the case unless it is explicitly stated otherwise. All sources of information have been specifically acknowledged by means of reference.

Results in this thesis which have been published before are highlighted by the publication attached at the rear. These published results fundamentally include: co-chaperone over-expression experiments; Hsc70 assays where the inhibitor, deoxyspergualin, has been used *in vivo*; and Hsp90 inhibitor work using acute geldanamycin and radicicol treatments *in vivo* (with wild-type toxin).

None of this work has been used in any previous application for a degree at any other institution. This work was funded by a BBSRC studentship.

Summary

Ricin is a heterodimeric, toxic plant protein. It is able to deliver its catalytic A chain (RTA) into the cytosol of target cells. RTA crosses the endoplasmic reticulum (ER) membrane into the cytosol, masquerading as a substrate of ER-associated degradation (ERAD) to do so. Therein, RTA inactivates ribosomes. This thesis shows that RTA is prone to lose solubility *in vitro* near the physiological temperature and pH of target cells. This instability is hypothesised to cause RTA to misfold in the ER lumen, promoting chaperone and membrane interactions therein. Fittingly, this thesis shows that Grp94, a lumenal chaperone, promotes the toxicity of RTA, and that liposomes constructed of negatively-charged phospholipid interact with RTA *in vitro*. This instability resembles that of other toxic A chains that exploit ERAD. Cholera toxin A chain and pertussis toxin A chain, for instance, are also relatively unstable (Pande *et al*., 2007 & 2008).

The Hrd1 complex now seems the strongest candidate for retrotranslocating RTA from the ER lumen (Li *et al*., 2010). In the cytosol, the proteasomal cap has been shown to be involved in downstream processing of RTA – enabling toxicity (Li *et al*., 2010). This thesis reports that, in mammals, the balance of cytosolic chaperones and their co-factors helps to dictate the success of retrotranslocated RTA, putatively by determining its escape from terminal degradation in the proteasomal core. The effect of these chaperones occurs at a stage beyond access of the toxin subunit to the ER, and can result in both activation and inactivation of cytosolic RTA.

It has been shown that, on one hand, Hsc70 is responsible for activating RTA. Hsc70 may aid RTA in attaining an active conformation in the cytosol after retrotranslocation. Alternatively, it might supplant the effectors of its degradation. On the other hand, Hsc70 also enters RTA into a sequential triage with Hsp90. Unlike Hsc70, Hsp90 deactivates RTA. This effect is dependent upon the lysines of this toxin subunit, suggesting Hsp90 may participate in the lysine-ubiquitination of RTA. Supporting this conclusion, Hsc70 and Hsp90 can both ubiquitinate RTA *in vitro*. This ubiquitination can be promoted if RTA is first incubated with liposomes. This implies that RTA may be particularly vulnerable to ubiquitination during retrotranslocation, where it might also be partially solvated by phospholipid. Contrasting to RTA, Hsp90 actually aids the toxicity and dislocation of ER-retrotranslocating cholera toxin A chain (Taylor *et al*., 2010). It seems that RTA may have fortuitously evolved to exploit Hsc70 rather than Hsp90 to promote its cytosolic activation. Provocatively, the hydrophobic C-terminal tail of RTA demarcates it from a homologous toxin, saporin, which does not exploit ERAD to achieve toxicity. Indeed, this region may be an adaptation RTA has acquired to promote interaction of the toxin subunit with Hsc70, which even seems to occur in RTA's native, folded state. This interaction may be another reason why the region is apparently significant to the cytotoxicity of the protein (Simpson *et al*., 1995)

Finally, because the reactivation of RTA after retrotranslocation involves proteins with broad specificity (Hsc70, Hsp90), this thesis hypothesises that this pathway may operate for other ERAD substrates. Prior investigators have shown isolated examples of this phenomenon. For example the degradation-independent retrotranslocation of extracellularly-applied luciferase (Giodini & Cresswell, 2008) and of endogenous calreticulin (Afshar *et al*., 2006). This thesis hypothesises that the success of a protein in being reactivated post-dislocation will be determined by stringency of the cell's chaperone network, the propensity of the substrate to be degraded, and its propensity to refold. As a protein which is toxic to the cell when refolded in the cytosol, RTA will be a useful tool to investigate this putative, broadly relevant, post-dislocation activation pathway.

CHAPTER 1:
Introduction

1.0 Ricin: occurrence, mode of action and the original applications of its study

Ricin is a potently toxic protein of the castor oil plant, *Ricinus communis.* The mature protein is found throughout the tissues of its native host at low levels. However, it is especially concentrated in the endosperm of the plant's seeds, from which commercially valuable castor oil can also be extracted (Alexander *et al*., 2008). Consumption of as few as four of these poisonous seeds can be a mortal dose for an adult (Wedin *et al*., 1986). This extreme toxicity first provoked Stillmark (1888) to discover the agent responsible: the protein, ricin.

The protein itself is a heterodimer, comprising a galactose-binding lectin moiety of 34kDa disulfide-bonded to an rRNA N-glycosidase of 32kDa (Olsnes & Pihl, 1973). These are denoted ricin toxin B chain (RTB) and ricin toxin A chain (RTA) respectively. Its bipartite structure and function makes ricin analogous to a broad class of two-component complexes with similar operational arrangement – known collectively as AB-toxins. The B chain of these complexes generally has a cell-binding role, helping to localise the holotoxin to the site where the A chain thereafter exerts a cytotoxic activity. This arrangement is also true of ricin (Lord & Robert, 1998). Ricin is also member to a large family of ribosome inactivating proteins (RIPs), which are subdivided into two main types (I & II) by the presence or absence of a B chain. Type I RIPs do not possess a lectin B chain, whereas type II RIPs, like ricin, do (Lord *et al*, 1994). It is thought that these proteins serve an integral function in their native hosts as they are found in well over 50 different species spread among 13 taxonomic families (Hartley *et al*., 1996).

RTB binds specifically to β1-4 linked galactosides. Therefore, it is able to bind glycoproteins and perhaps even glycolipids that are abundant on the cell surface (Baenziger & Fitte, 1979). This ensures the holotoxin can adsorb to the exterior of target cells, promoting the indiscriminate endocytosis of the protein. A small portion of the internalised holotoxin can then find its way into a compartment from where RTA, the ribosome-inactivating N-glycosidase, can be translocated across the membrane into the cytosol (Hazes & Read, 1997; Wesche *et al*., 1999). Therein, it may encounter its substrate: the ribosome. The catalytic activity of RTA specifically targets a single, highly-conserved adenine of 28S rRNA, cleaving it from the phosphodiester backbone of a short stem-loop structure (Endo *et al*.,

1987). After this depurination, the ribosome irreversibly stalls during translation as it can no longer bind mechanistically-essential elongation factors (Stirpe & Battelli, 2006).

As the production of ribosomal RNA accounts for 70% of all transcription even under unstressed conditions (Granneman & Tollervey, 2007), the cell has only a limited capacity to compete against the catalytic activity of RTA. To emphasise the overwhelming extent of this burden, a single RTA is able to inactivate 2000 ribosomes per minute *in vitro* (Sandvig & Van Deurs, 2002). The target cell, unable to maintain its protein complement, nor to adapt its protein expression in response to dynamic environmental and internal cues, ultimately dies. Indeed, after intoxication of an animal host by any major route, both apoptosis and necrosis are observed in affected tissues (Sha *et al*., 2010). Rao *et al*. (2005) show that, in a simplified culture of HeLa cells, viability is lost through a primarily apoptotic route.

Surprisingly, despite their wide distribution among plants and the attention of significant research, the physiological role of RIPs in their native hosts remains a subject of debate (Hartley *et al*., 1996). Foremost, ricin has been suggested to have a role in warding off herbivores (Olsnes & Pihl, 1982). However, it seems inconsistent that as many as 36 hours may pass after ingestion of a lethal dose before the first signs of toxicity become manifest (Wedin *et al*., 1986). By this time a greedy herbivore may have already consumed a significant quantity of the plant, although it is possible that toxicity could have influenced forager behaviour over a greater timescale. Nevertheless, why synthesise a large, metabolically-costly protein to fulfil this job? Why not synthesise a more prudent secondary plant substance (examples of which are reviewed in Hruska, 1988), which could achieve a similar and more immediate reduction in edibility?

Responding to these quandaries, multiple other reasons have been posed to explain the abundance of ricin and other similar toxins (Table 1.1). For example: they may have roles as storage proteins, fuelling the growth of seedlings as they make the transition from heterotrophic reliance upon seed reserves to autotrophy (Hartley *et al*., 1996). Alternatively, it has been suggested that RIPs have antiviral roles, causing localised deactivation of host cells at sites of viral infection (Chen *et al*., 1991). This might be especially important near to the germ-line, where ricin is particularly concentrated. RIPs may even be important as antifungal agents (Jach *et al*., 1995). However, these arguments are based upon the effects of exogenous RIPs upon non-native hosts (such as dilute pokeweed antiviral protein sprayed upon tobacco leaves). Indeed, often they do not appear to bestow any additional resistance to

viruses and fungi in their native contexts (as reviewed in Hartley *et al*., 1996). Ultimately, it may be that a combination of these activities explains the pervasiveness of RIPs and the heavy accumulation of ricin in castor seeds, which can be as much as 5% of total protein content (Lord *et al*., 1994).

Table 1.1 – Examples of ribosome inactivating proteins

Species	Common name	RIP name	Type	Reference
Adenia digitata	Wild granadilla	Modeccin	II	Gasperi-Campani *et al*., 1978
Adenia precatorius	Rosary pea	Abrin	II	Wei *et al*., 1974
Cucurbita pepo	Marrow	Pepocin	I	Yoshinari *et al*., 1996
Diathus caryophyllus	Carnation	Dianthin 30/32	I	Stirpe *et al*., 1981
Phytolacca ameriacana	Pokeweed	Pokeweed antiviral protein	I	Irvin, 1975
Ricinus communis	Castor oil plant	Ricin	II	Lord *et al*., 1994
Sambucus nigra	Elderberry	Nigrin b/f	II	Citores *et al*., 1996

Regardless of the physiological role of ricin in *Ricinus communis*, its potent toxicity has been exploited by humans in a number of therapeutic, investigative and criminal applications (reviewed in both Hartley *et al*., 1996; and Lord *et al*., 1994). Some examples of its use include, as:

(1) An active moiety in antibody-conjugated immunotoxins that are used to destroy cancerous cells, or else allogeneic T lymphocytes from donated bone marrow.
(2) A tool in developmental biology used to ablate cell lineages under the control of stage- or tissue-specific promoters.
(3) A transgenically-expressed antiviral and antifungal agent in plants.
(4) A tool to investigate the secretory pathway.

(5) An abortifacient.

(6) A way to kill other humans.

For these reasons, and because of the potential future uses of the toxin in related contexts, the mechanism of ricin is the subject of ongoing scientific interest.

1.1 Biosynthesis of ricin in its native *Ricinus communis*

The overall route by which ricin invades a target cell has been introduced, but the molecular mechanisms governing this feat have not been elaborated upon. To appreciate the fortuitously ingenious trafficking route the holotoxin undertakes, the biogenesis of the protein should be made clear. Unlike its heterodimeric, mature form, ricin is initially translated as one contiguous chain with a signal peptide – holistically known as 'preproricin' (Hartley *et al*., 1996). During its synthesis, the emergence of an N-terminal signal peptide from the exit tunnel of the ribosome ensures the translational complex is targeted to the endoplasmic reticulum membrane (Martoglio & Dobberstein, 1998). There, the nascent polypeptide is co-translationally channelled into the lumen of the endoplasmic reticulum (ER) through the Sec61 translocon. As the translating polypeptide is incrementally driven through this membrane pore by the machinations of the ribosome, several modifications occur.

First, the signal peptide is cleaved by the lumen-facing activity of signal peptidase. Then, as four primary-sequence embedded N-glycosylation sites emerge from the translocon, they become core-glycosylated (Lord, 1985)[1] by a complex adjacent to the translocon, the oligosaccharyl transferase, OST, complex. Finally, the signal peptide-cleaved, glycosylated polypeptide folds into its native secondary and tertiary structural elements, which are stabilised by the formation of five intra-chain disulfide bonds (Rutenber & Robertus, 1991).

This folded, signal-peptide cleaved protein, referred to as 'proricin', exits the ER by vesicular flow and is targeted to vacuolar protein bodies by a twelve-residue region linking RTA and RTB (Frigerio *et al*., 2001). Upon entry to this vacuolar compartment, the targeting sequence is proteolytically excised, liberating the familiar, heterodimeric form of the toxin that we refer to as ricin (Butterworth & Lord, 1983). The five disulfide bonds that originally formed in the ER lumen persist in the final structure: four stabilise RTB, whilst the fifth maintains

[1] These asparagine-linked oligosaccharides have no impact upon the final toxicity of ricin, as their absence has little effect upon the toxin's efficacy (Rapak *et al*., 1997)

the only remaining covalent bridge between RTB to RTA. The differences between these three forms are summarised graphically in Figure 1.1.

This series of post-translational processing events minimises the possibility that the toxic activity of RTA is ever accidentally exposed to the cytosol of the host cell. Not only is the protein compartmentally sealed off from host ribosomes at the moment of its synthesis, but even if it were inadvertently translated into the cytosol, uncleaved preproricin is unable to depurinate the ribosomes which are the substrate of the mature toxin (Richardson *et al.*, 1989). This, along with the fact that many plant ribosomes are RIP-resistant (Frigerio *et al.*, 1998; Hartley *et al.*, 1996), prevents the *accidental* death of the host organism.

Figure 1.1 - The various forms of ricin during biogenesis of the mature holotoxin

Showing preproricin, proricin and ricin. Core N-glycosylation is indicated by the chain of attached circles and squares. Disulfide bonds are indicated by "x". One of these bridges RTA & RTB. The 22 amino acid signal peptide and the 12 amino acid linker are shown by the white rectangles, which are progressively excised in the subsequent maturation. RTA is shown in purple. RTB is shown in green. The graphics for the image below were produced using Paintshop Pro X2, Corel.

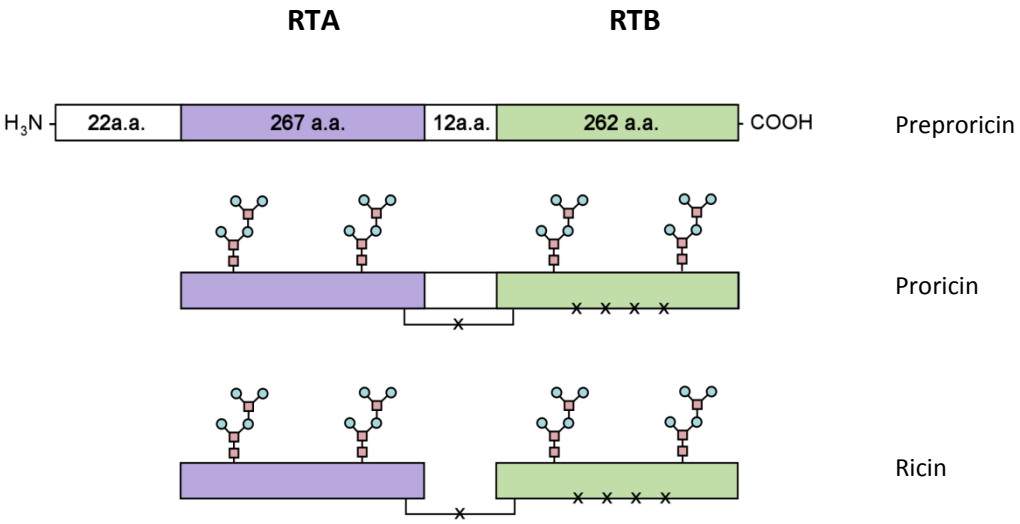

1.2 The three-dimensional structure of ricin holotoxin

The fully-folded structure of mature ricin was determined to a resolution of 2.5Å by Rutenber & Robertus (1991). A rendering of this structure is printed in Figure 1.2. The detail in the following section provides a summary of this structural information, with interpretation derived from it paraphrased from Lord *et al*. (1994).

Ricin toxin A chain (RTA) **–** The enzymatically active, N-glycosidase moiety of the holotoxin possesses eight α-helices and a single β-sheet. These elements account for roughly half of the 267 amino acid subunit. The N-terminal 40% of the polypeptide folds into a discrete conformational unit comprising two of these α-helices and the β-sheet. Adjunct to this domain, the polypeptide is arranged into a bundle of five α-helices, which nestles behind the N-terminal β-sheet. The central helix of this α-helical cluster bears the active site residues of the N-glycosidase activity (Glu177 and Arg180), to which the appropriate stem-loop structure of rRNA must be accessible. The C-terminal portion of the polypeptide folds into another, independent conformational unit centred upon the eighth α-helix. This discrete region, apposed to the active site helical bundle, helps produce the binding cleft of the enzyme. Importantly for future reference, the opposite side of this cleft-forming domain (the C-terminus) is hydrophobic and interacts with RTB. This region also houses the disulfide bridge which covalently links the two subunits.

Ricin toxin B chain (RTB) **–** The lectin moiety of the ricin holotoxin is 262 amino acids long, and is divided into two lobes that are both competent for galactoside binding. These lobes are homologous, having arisen from gene duplication, and each comprises three repeated sub-regions derived from an archaic galactose-binding motif. Only two of these sub-regions – one in each of the two lobes – retain galactose-binding properties. However, even these sites bind galactose in an attenuated fashion relative to other sugar-binding proteins. This weak-binding (combined with the wide variety of receptors competent to be bound on the typical target cell) has meant that it has been difficult to identify significant cell surface receptors for the holotoxin. Indeed, if any are specifically important in the intoxication process, they have not yet been found.

Figure 1.2 - The three-dimensional structure of the ricin holotoxin

Showing the three-dimensional structure of ricin, as published by Rutenber & Robertus (1991). The polypeptide chain is coloured so that the C-terminus region of each chain is blue – progressing through the spectrum to red at the N-terminal of both RTA and RTB. This image was produced using the UCSF Chimera package from the *Resource for Biocomputing, Visualization, and Informatics* at the University of California, San Francisco. Depth is implied by the fading in colour saturation.

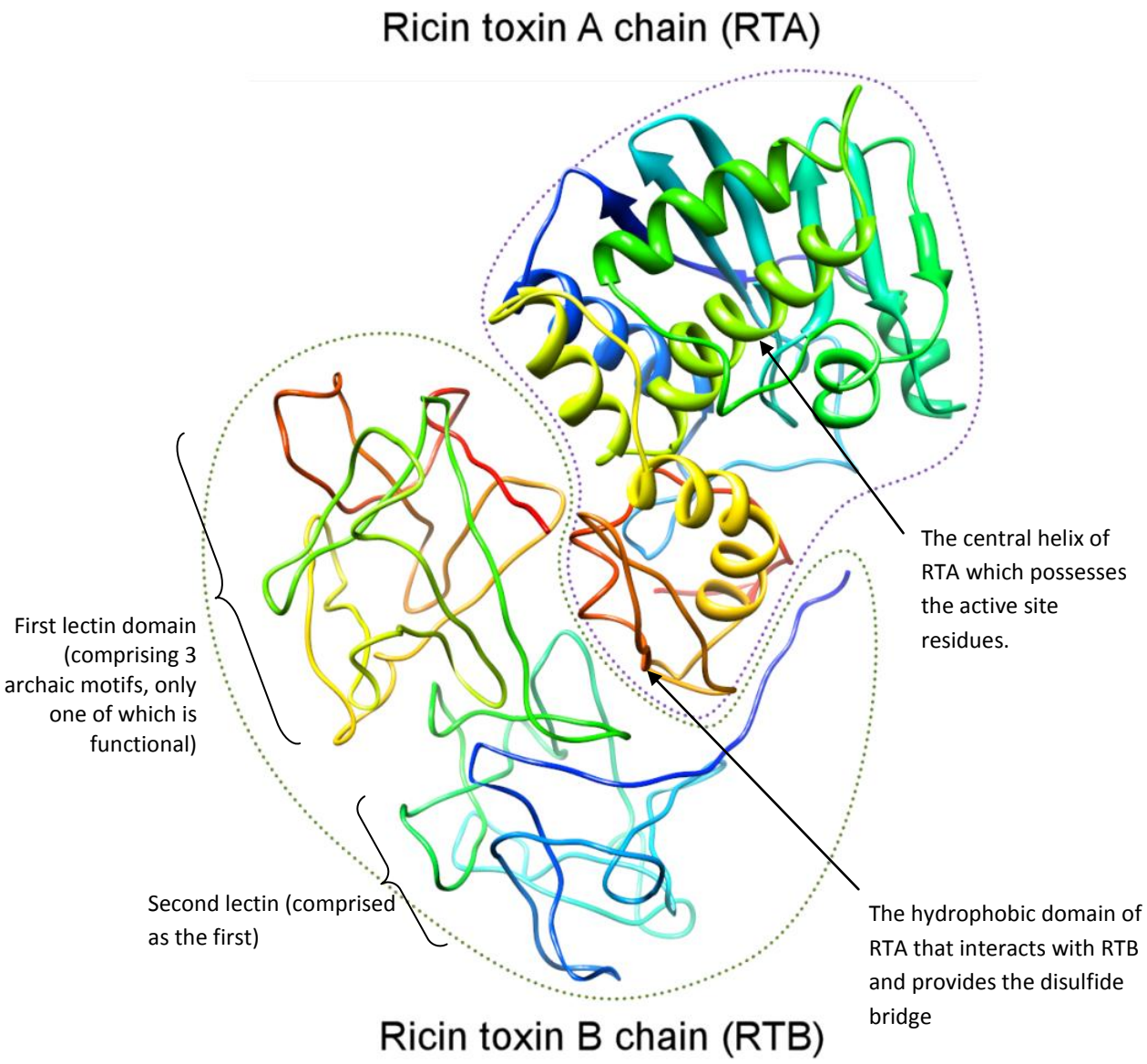

1.3 Intoxication of a target cell

When mature ricin is exposed to target cells, intoxication proceeds via a series of events that can be divided into distinct stages. These stages are:

(1) Binding at the target cell's surface, followed by indiscriminate endocytosis.
(2) Retrograde trafficking to an endomembrane compartment where the phospholipid bilayer can be crossed.
(3) Translocation of active RTA across the membrane into the cytosol.
(4) Inactivation of target ribosomes.

The novel content of this thesis focuses upon putative molecular interactions the toxin might make on either side of the translocated membrane and the ramifications this may have upon downstream processing of the protein by the target cell. To provide appropriate context to these unique findings, the earlier stages of toxin trafficking are summarised below.

1.3.1 Transit of ricin from the cell surface to the translocation-competent compartment

Estimates suggest that the average HeLa cell possesses as many as $\sim 3 \times 10^7$ independent cell-surface galactosides that may be bound by RTB (Spooner *et al*., 2004). This abundance causes the holotoxin to be broadly adsorbed to the cell surface, resulting in its internalisation by a variety of endocytic routes – both clathrin-dependent and clathrin-independent (Simpson *et al*., 1998). Some of these routes deliver ricin to the lysosome, wherein it is degraded. Others deliver the holotoxin to early and recycling endosomes (EEs & REs, respectively) that stain positively for the trafficking molecule, Rab5 (Moisenovich *et al*., 2004).

Much of the toxin which accesses these Rab5-positive compartments is still subject to recycling to the plasma membrane, or else to being diverted to the lysosome (Van Deurs *et al*., 1986). However, a small portion is transported from these endosomes to the *trans*-Golgi network (TGN), which is the onward route for toxicity (Van Deurs *et al*., 1988). Trafficking to the TGN is Rab9-independent (which regulates transport from late endosomes to the TGN), implying a direct transport of ricin from specifically *early* endosomes to the TGN (Lauvrak *et al*., 2002). Consistently, Ütskarpen *et al*. (2006) showed that ricin intoxication was sensitive to siRNA knockdown of Rab6A and Rab6, which collectively regulate early endosome-to-TGN transport.

Ricin is subsequently transported from the TGN to the ER, wherein fluorescence can be observed if cells are intoxicated with a GFP-ricin construct (Liu *et al*., 2006). Only a minuscule quantity of toxin eventually achieves a cytosolic destination relative to that which is internalised at the cell surface. Data from Rapak *et al*. (1997) also corroborated the trafficking route described above in a series of elegant experiments. They produced a holotoxin where the constituent RTA was tagged with vacant glycosylation and sulfation sites. After intoxication of mammalian cells with this holotoxin, they observed that glycosylated, sulfated RTA could be retrieved from the cytosol. These modifications are performed by oligosaccharyl transferase of the ER (Yan *et al*., 1999) and tyrosyl-protein sulfotransferate (TPST) of the Golgi (Spooner *et al*., 2008a), respectively. Thus, it showed that toxin which had gained access to the cytosol had, at one stage during intoxication, co-localised with both of these activities. Supporting this hypothesis, increasing the transport of ricin to the Golgi and the ER under experimentally-controlled conditions increases the cytotoxicity of ricin. Indeed, Morre *et al*. (1987) observed that mammalian cells were sensitised to ricin when pre-treated with monensin (which increases the flow of protein traffic into the Golgi cisternae). Consistent with these findings, addition of a C-terminal Golgi retention motif to ricin, YQRL, had a predictably sensitising effect (Zhan *et al*., 1998), as did addition of the ER retrieval motif, KDEL (Wales *et al*., 1993). As native ricin lacks these sequences, it is unknown how it achieves an ER localisation. Contrastingly, cholera toxin, another example of an AB-toxin where the A chain dislocates from the ER into the cytosol, actually possesses a C-terminal KDEL (Majoul *et al*., 1998). Curiously, however, cholera toxin can also navigate to the ER if its KDEL sequence is removed (Lencer *et al*., 1995). In such a case it might be transported to the ER in a more serendipitous fashion, like ricin. For instance, these toxins might hitch-hike upon other proteins that, themselves, have appropriate retrieval sequences.

Day *et al*. (2001) hypothesised that ricin might disengage from its original, cell-surface binding partner after endocytosis. This would enable it to re-engage with escapee residents of the ER or Golgi which possess KDEL motifs. Indeed, Day *et al*. (2001) demonstrated that ricin could bind to an iconic ER chaperone, calreticulin, *in vitro*.[2] Curiously, however, cells

[2] N.B. This binding occurred only between holotoxin and calreticulin and not between RTA and calreticulin. Furthermore, it could be disrupted by the inclusion of lactose in the incubation, but was not dependent on the glycosylation of the ricin holotoxin. This implied it was the lectin activity of RTB that was responsible for the interaction (Day *et al*., 2001).

remain sensitive to ricin when wider KDEL retrieval is prevented by inhibition of the COPI apparatus, preventing Golgi to ER transport (Chen *et al.*, 2003). This suggests that there is a significant alternative route to the ER that remains to be investigated.

1.3.2 Rationalising the ER as the ultimate endomembrane destination

Whilst the exact nuances of ricin's retrograde trafficking remain obscure, the final destination of the holotoxin in the secretory pathway seems very likely to be the ER lumen (Rapak *et al*, 1997; Liu *et al.*, 2006; Sandvig *et al*., 1991). This finding is consistent with a multitude of other AB-toxins that are also transported to the ER (e.g. cholera toxin – Majoul *et al*., 1998; Pseudomonas exotoxin A and Shiga toxins – as reviewed in Watson & Spooner 2006). Fittingly, there are abundant machineries in the ER which facilitate the translocation of polypeptides across the membrane, which is what RTA must do to reach cytosolic ribosomes. Foremost among these machineries is the Sec61 translocon and its accessory factors, which are responsible for importing proteins into the ER. Complementing this apparatus are the components of endoplasmic reticulum associated degradation (ERAD), which collectively promote the export of undesirable polypeptides to the cytosol. There, they are hydrolysed by the 26S proteasome (Meusser *et al*., 2005; Werner *et al*., 1996).

From the perspective of the toxin, the directionality of polypeptide movement during ERAD seems the most appropriate to exploit. However, how could it evade the proteasomal destruction which is usually the tacit outcome of the process? Hazes & Read (1997) were first to report that RTA and the active moieties of many other ER-trafficking toxins (e.g. cholera toxin; shiga toxin; pseudomonas exotoxin, pertussis toxin) have low lysine complements compared to polypeptides of similar length. This implied the physiological role of these toxins exposed them to a situation where the replacement of these residues would be of benefit to the protein's function. As proteasomal degradation is greatly promoted by lysine-linked polyubiquitination (Thrower *et al*., 2001), it seemed the toxins had evolved to escape this modification. Perhaps they had done so to evade polyubiquitination during a particularly vulnerable, ERAD-like translocation into the cytosol? Summarily, investigative interest grew out of this hypothesis into two areas of research:

(1) what features of ricin could make it appear like an ERAD substrate; and, moreover,
(2) what factors of the canonical ERAD machinery might ricin exploit?

Before experimental observations that probe these quandaries are introduced, this chapter continues by providing a background to the physiological role, nature and dynamics of this essential quality control pathway.

1.4 Endoplasmic reticulum associated degradation (ERAD)

The endoplasmic reticulum is the first endomembrane compartment which proteins of the secretory pathway encounter. Whether these proteins are co- or post-translationally translocated into the ER from their site of synthesis, they are all transiently accommodated by the narrow aperture of the Sec61 translocon *en route* to this organelle (Van den Berg *et al*., 2004; Tian & Andricioaei, 2006). This means that all polypeptides that are secreted into the lumen emerge into it in a substantially unfolded, translocation-competent state. In this state they transiently expose hydrophobic regions to the lumenal environment. These regions have a tendency to self-aggregate, forestalling the acquisition of native structures, so promoting the accumulation of dysfunctional ones. To mitigate these detrimental side-reactions, there are abundant chaperones in the ER lumen that temporarily bind these regions. This shield of chaperones persists until enough contiguous polypeptide has emerged from the translocon to enclose hydrophobic stretches within appropriately hydrophilic encasements. Indeed, the lumenal equivalent of the Hsc70 molecular chaperone, BiP (Kar2 in yeast), binds imported polypeptides as they emerge, ensuring just that (Hammon & Helenius, 1994).

Nevertheless, the folding process often goes awry if the capacity of the cell to successfully nurture the folding of nascent protein is exceeded. This occurs under conditions of, for instance, heat or oxidative stress, nutrient starvation; or after translational errors and mutation (Schröder & Kaufman, 2004; McClellan *et al*., 2005). Moreover, under *unstressed* conditions, the subunits of multimeric complexes can be synthesised in incorrect ratios, yielding orphan polypeptides that lack the partners that usually complement their native state (Vanhove *et al*., 2001). Even after having assumed a native state, proteins remain subject to varying degrees of regressive unfolding – whether these are stochastic or stress-induced. This results in the ongoing potential for terminally-misfolded conformers to be generated.

To prevent the accumulation of misfolded species in the secretory pathway and to ensure that detrimental gain-of-function misfolds are not communicated to neighbouring cells, they are degraded. Some proteins of the secretory pathway are transported to the lysosome, wherein they are hydrolysed by proteases (McCracken & Brodsky, 2006). As a drastic measure at times of stress, the entirety of overloaded compartments can be degraded by autophagy

(Kincaid & Cooper, 2007). Often, however, misfolded proteins are isolated in the early stages of the secretory pathway, preventing their transmission to downstream organelles and neighbouring cells. These proteins are degraded by cytosolic 26S proteasomes, the process which is designated 'ERAD' (Werner *et al*., 1996).

However, removal of unwanted polypeptides from the ER lumen to the cytosol is no trivial task. Indeed, each ERAD client investigated to date is managed by a – sometimes vastly, sometimes subtly – distinct retinue of facilitators (as reviewed by Nakatsukasa & Brodsky, 2008). Still, there are common procedures that unite all ERAD pathways. In brief:

(1) Misfolded substrates have to be recognised, which is usually achieved by a combination of membrane factors, lingering associations with chaperones and lumenal lectins.
(2) The recognition factors bridge an interaction of the substrate with the retrotranslocation machinery. This machinery is contributed to by a miscellany of membrane-associated and membrane-integral complexes that may accommodate exit of the polypeptide from its ER locale (i.e. form a pore).
(3) Finally, upon the cytosolic side of the ER membrane, there are co- and post-translocational processing events which effectively drive extraction of the misfolded polypeptide from the membrane compartment and prepare it for degradation by the 26S proteasome.

The variety of ways in which these steps are achieved is outlined in the following sections.

1.4.1 How the cell identifies ERAD candidates

Quality control pathways in the ER must resolve terminally-misfolded polypeptides from those which are only transiently unfolded and those which are actually appropriately folded. However, the nature of a conformational faults can vary greatly, a corollary to the variety of stresses, mutations and chance events a cell may endure. Moreover, a fault can be localised to distinct phases of the ER environment: the lumen, the core of the lipid bilayer itself, or even to the cytosolic side of the ER membrane. Because of this diversity of 'symptoms', the array of factors implicated in the diagnosis of ERAD substrates is complex, providing a variety of contingencies (reviewed in Määttänen *et al*., 2010). Contrastingly, downstream of substrate recognition, the similarity between initially separate pathways increases, converging upon the final, rude, step of degradation in the proteasomal core (Carvalho *et al*., 2006).

All the same, detection of ERAD clients relies upon two related, general attributes: chronic residence in the ER lumen and chronic exposure of hydrophobic regions (Määttänen *et al*., 2010). Retention in the ER can occur if a conformer fails to display appropriate export motifs on its surface (Ellgaard & Helenius, 2003). Retention would also occur if a client had a lingering interaction with ER chaperones, as would be the case when a misfolded protein recurrently displays hydrophobic regions to the solvent (Vanhove *et al*., 2001).

One of the best-elaborated mechanisms measuring prolonged ER-residency is the so-called 'mannose timer' shown in Figure 1.3. The information that follows is discussed more broadly in reviews by Wang & Ng (2008); Eriksson *et al*. (2004); and Määttänen *et al*. (2010). First, nascently secreted proteins with appropriate N-X-(S/T) glycosylation sites become core-glycosylated in the ER ($[N$-acetyl-glucosamine$]_2$[mannose$]_9$[glucose$]_3$). This core glycan is then subjected to the sequential activities of relatively fast-acting ER-resident glucosidases. These trim the two terminal glucose residues of the glycan, which promotes interaction of the glycoprotein with the ER lectins: calreticulin (Crt) and calnexin (Cnx). These lectin chaperones specifically recognise the monoglucosylated form of the glycan, an interaction which a final glucosidase can liberate the client from by removal of the last glucosyl moiety. Freed glycoproteins remain competent to rejoin interactions with calreticulin and calnexin if an ER-localised UDP-glucose:glycoprotein transferase (UGGT1) restores the terminal glucose residue. Such is the case if the protein fails to be exported. However, if the glycoprotein is misfolded it will stay in the ER for an especially long time. This is caused by prolonged chaperone interactions and failure to qualify for export to downstream compartments. In this case, a slow-acting mannosidase (e.g. EDEM1/2/3 in mammals, or Htm1/Mns1 in yeast) removes a mannose residue from the glycan. This modification prevents UGGT1 from binding the glycoprotein, and irreversibly removes it from the calreticulin/calnexin cycle. The glycan generated by EDEM is thereafter competent for interaction with another ER lectin, OS-9 (in mammals; Yos-9 in yeast), which bridges it to downstream ERAD components (Qian *et al*., 2008).

Figure 1.3 – Schematic of the mannose timer.

The pathway is described in text above. The large blue circle denoted 'P' represents the client protein in the ER. The smaller blue squares attached represent *N*-acetyl glucosamine residues; blue circles mannose residues; blue triangles represent glucose residues. "Onward transport" can be facilitated by vesicle sorting receptors that recognise protein cargoes and interact with the cytosolic COPII machinery. Note EDEM is a mammalian protein; in yeast it is called mannosidase I.

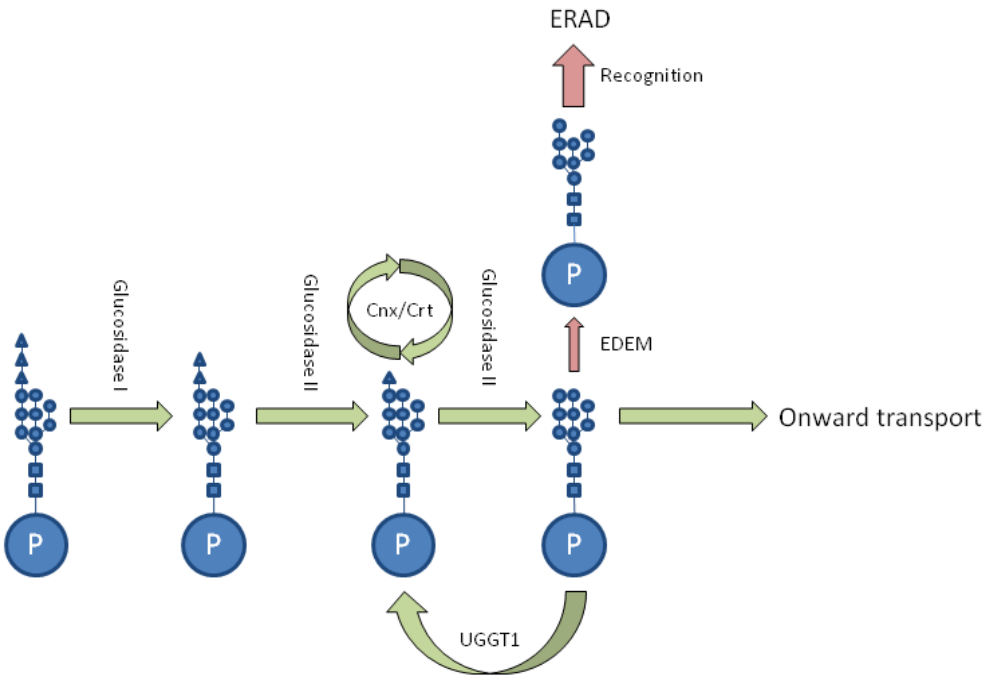

Other routes by which clients may be co-opted onto ERAD pathways are less clear. However, they must exist to cater for proteins which are not glycosylated. What is more, not every glycoprotein is subjected to the mannose timer mechanism. Indeed, some glycoproteins are able to persist in the ER for long periods of time, in complexes with chaperones. For instance immunoglobulin heavy chains, which are retained in complex with BiP until their light chain binding partners are secreted into the lumen (Vanhove *et al*., 2001). Alternative mechanisms determining ERAD candidacy may be stochastically driven like the mannose timer. However, they might rely more simply upon prolonged chaperone interaction rather than a deterministic glycan switch. Indeed, OS-9 – which interacts with membrane integral ERAD machinery – can be found in complexes with two lumenal chaperones: Grp94 and BiP. The joint properties of these proteins may form an integral client-sensing gating complex to downstream ERAD effectors (Eletto *et al*., 2010; Kabani *et al*., 2003).

Unfortunately, it remains difficult to differentiate potential gating functions of lumenal chaperones from purely chaperoning activities, given that aggregation prevents ERAD (McCracken & Brodsky, 2006). It is also unclear whether Grp94 has a role in 'herding' the client to the chaperone machinery, or whether it is itself responsible for maintaining the complexes involved in handling the client (an argument made in a review by Nakatsukasa & Brodsky, 2008). The line therefore blurs between chaperone, gating arbiter and complex maintainer.

1.4.2 Membrane complexes involved in ERAD – multi-functional pores?

After recognition, substrates are passed to membrane-integral complexes. These membrane-associated assemblies are one of the most interesting aspects of ERAD, given the various tasks they must fulfil. All recognise substrates, accommodate their exit from the ER membrane, and recruit cytosolic factors involved in downstream degradation. In *Saccharomyces cerevisiae*, there are two major complexes centred on two distinctive E3 protein:ubiquitin ligases: Doa10 and Hrd1 (these complexes and their associates are given a pictorial review by Kawaguchi & Ng, 2007). E3 protein:ubiquitin ligases are responsible for the ubiquitination of their substrates, a modification which fosters their interaction with the proteasome (Thrower *et al*., 2001). Remarkably, the Doa10 and Hrd1 complexes handle starkly different substrates.

1.4.2.1 ERAD-L & ERAD-M: The Hrd1 complex of *Saccharomyces cereivisiae*

Substrates with conformational faults localised to the lumen are directed to the Hrd1 pathway (Figure 1.4). They are initially recognised by a presumptive 'gating complex' that may comprise Yos9, Kar2, and Grp94 (Eletto *et al*., 2010; Kabani *et al*., 2003). This triumvirate of factors associates with the lumenal domain of an integral membrane protein, Hrd3, to which they are thought to pass clients like a mutant of the soluble protein α1-antitrypsin, i.e. α1-antitrypsin null Hong Kong (α1-AT NHK; Christianson *et al*., 2008), and glycoproteins (Eletto *et al*., 2010). Hrd3 can also independently recognise and retain misfolded ER proteins, e.g. soluble, mutant carboxipeptidase Y (CPY*) without the direct aid of the gating complex (Gauss *et al*., 2006; and references in Hirsch *et al*., 2009). However, it seems reasonable to think that it works synergistically with the soluble chaperone complex to audit the contents of the ER. Hrd3, in turn, is bound stoichiometrically to the transmembrane E3 ligase, Hrd1 (Gardner *et al*., 2000). The E3 ligase activity of Hrd1 is required for the degradation of CPY* in the cytosol (Li *et al*., 2010; Bordallo & Wolf, 1999). This shows that degradation by other ERAD machinery cannot compensate in this context. Gardner *et al*. (2000) show that Hrd1 over-expression without the correlate up-regulation of Hrd3 leads to the promiscuous degradation of folded lumenal proteins. This demonstrates that the task of selecting misfolded clients is delegated to the other, upstream, factors.

The Hrd1 complex is also involved in the degradation of proteins with transmembrane aberrations, such as the Parkin-associated endothelin-like receptor, Pael-R (Omura e*t al*., 2008). Problematic transmembrane domains might precipitate irregular structural phenotypes in connected lumenal domains. These would be recognised by soluble machinery. However, it has also been shown that a transmembrane helix of Hrd1 can detect tell-tale hydrophilic residues embedded in the otherwise hydrophobic core of the membrane, facilitating their transfer of the offending protein to a degradation pathway (Omura *et al*., 2008).

How Hrd1 substrates are channelled through the membrane after their recognition – a process known as 'dislocation' or 'retrotranslocation' – is unknown. It has been hypothesised that Hrd1 forms part of a conduit through the membrane by merit of its six transmembrane helices (Omura *et al*., 2008). It could even assemble the true pore components. Indeed, Hrd1 also associates with Usa1, a transmembrane protein which recruits Derlin-1 to the complex (Hirsch *et al*., 2009). Derlin-1, which also bears six transmembrane helices, is another potential pore constituent. It is required for the degradation of a set of clients with mostly

lumenal (rather than intra-membrane) faults, such as the transmembrane human V2 vasopressin receptor (Schwieger *et al*., 2008). It could be that Derlin-1 specifically tailors the dimensions of the membrane pore for such clients (Yihong *et al*., 2004).

After partially emerging onto the cytoplasmic face of the ER membrane, dislocated proteins are thought to be subjected to lysine-ubiquitination by the cytoplasm-facing RING finger ubiquitin ligase of Hrd1 (Hirsch *et al.*, 2009). The ubiquitination cascade that leads to the priming of transferred ubiquitin residues is also enabled by membrane-associated proteins. An E2 enzyme, Ubc7, is tethered to the membrane by interaction with the transmembrane protein called Cue1, which interacts with Hrd1 (Bazirgan & Hampton, 2008). E2 ubiquitin-activating enzymes are involved in the sequence of reactions which prime ubiquitin for the ligation reaction that is catalysed by an E3 ubiquitin ligase's activity. After ubiquitination, the substrates of the pathway converge with those of the Doa10 route, which is outlined next.

1.4.2.2 ERAD-C: The Doa10 complex of *Saccharomyces cerevisiae*

ERAD clients that are embedded in the ER membrane and which have cytosolic faults are degraded by a complex including Doa10 (Figure 1.4). As Doa10 contains fourteen transmembrane domains, it has been suggested that it may form a pore (Kreft *et al*., 2006). Membrane integral substrates of this complex include the mutant α-factor transporter, designated Ste6*, and the plasma membrane H^+-ATPase, abbreviated to PMA1 (Ravid *et al*., 2006). Much like Hrd1, Doa10 is accompanied by membrane-integral proteins which activate its E3 ligase activity. These include: Ubc7, Ubc6 & Cue1 (Huyer *et al*., 2004). Interestingly, Doa10 also contributes to the degradation of soluble cytoplasmic proteins, like the Mat alpha2 receptor (Swanson *et al*., 2001). However, such substrates do not appear to require downstream extraction machinery to facilitate this process (Ravid *et al*., 2006). Metzger *et al*. (2008) studied an example of this pathway, using a soluble, cytosolic orotidine 5-phosphate decarboxylase with a degradation-promoting C-terminal tag (Ura3-CL).

Precisely how valid substrates are distinguished by the Doa10 complex is unknown; the identification of a simple 'switch' is lacking. Still, it has been shown that cytoplasmic chaperones, e.g. Hdj1 and Ydj1 (Hsp40s) and Ssa1 (Hsc70), are required for the execution of the route (Metzger *et al*., 2008; and references in Nakatsukasa & Brodksy, 2008). These chaperones might be required at any number of stages during the process (e.g. in complex assembly, or an anti-aggregation role), but it has been proposed that they might gate the complex, analogous to the way Yos9/Kar2/Grp94 might gate the Hrd1 pathway in the lumen.

Figure 1.4 – The ERAD-C, ERAD-L and ERAD-M complexes

The following figure is heavily influenced by the Cell Snapshot produced by Kawaguchi & Davis (2007). Unlike their figure, machinery downstream of the E3 ligase is omitted for clarity (as these are discussed in the next section of this introduction). ERAD substrates are the fleshy-pink wiggles and transmembrane domain proteins marked with asterisks (the asterisk denotes the topology of the conformational fault the substrates bears). 1) Substrates are recognised for ERAD-L by a combination of the mannose timer and the gating complex formed by chaperones Kar2, Grp94 & Yos9 (Christianson *et al*., 2008). 2) Substrates are recognised for ERAD-M by a transmembrane domain of Hrd1 (Omura *et al*., 2008), as well as by the mannose time mechanism and Yos9. 3) Substrates are recognised for ERAD-C by a combination of Doa10 and putatively a gating complex consisting of Hsp40s (Ydj1 & Hdj1) and Hsc70 (Ssa1) – see Nakatsukasa & Brodksy (2008).

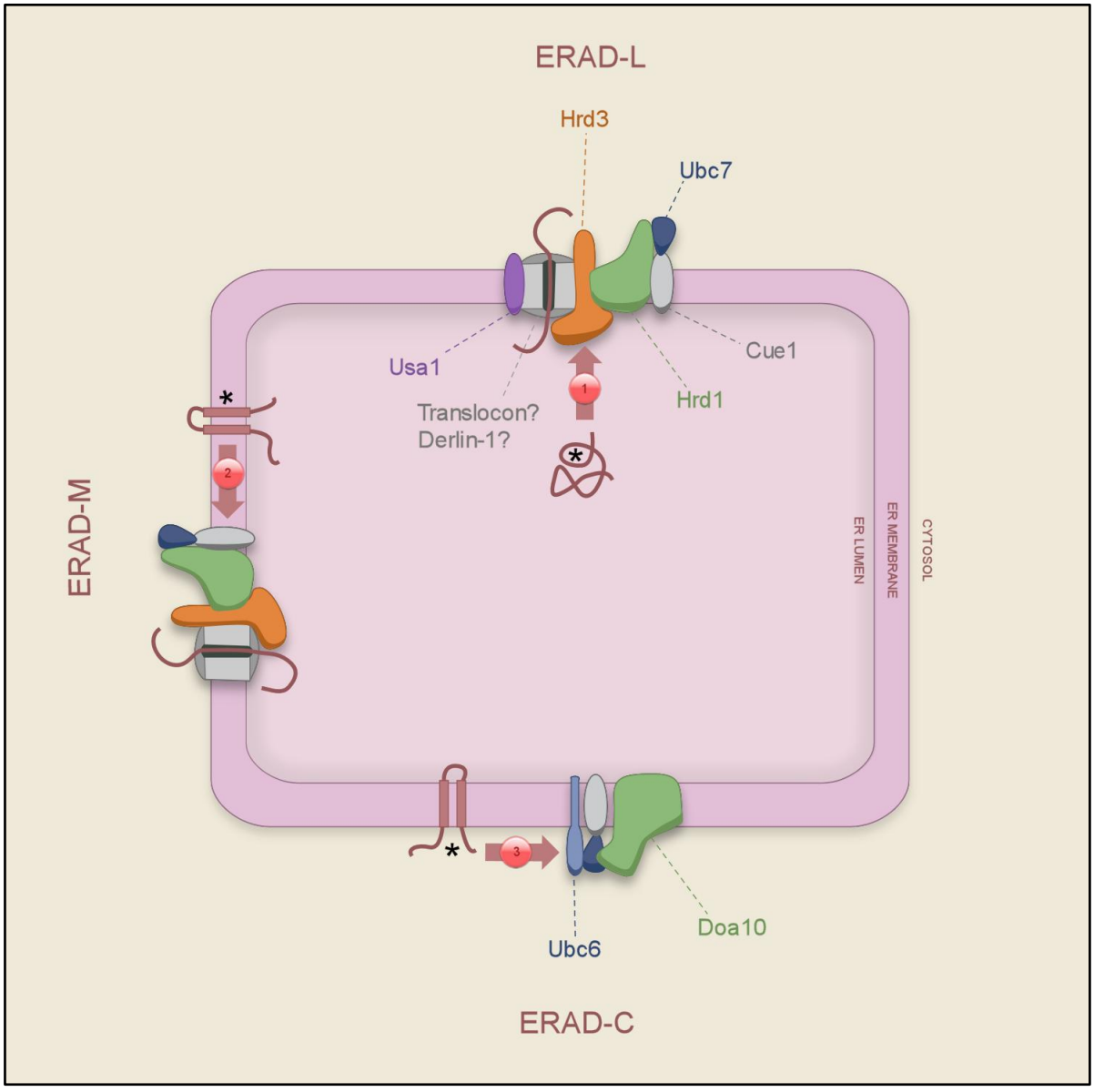

1.4.2.3 A role for the Sec61 translocon in polypeptide export?

Early in the ERAD field it was proposed that the Sec61 translocon might simply be co-opted for the retro-translocation process. With the aid of supplementary, ERAD-specific factors it could become a 'dislocon'. However, as Sec61 is important for the initial translocation of these polypeptides into the ER, it has been difficult to differentiate import failure from export success. Nakatsukasa & Brodsky (2008) make a comprehensive review of arguments for and against its involvement. Pilon *et al.* (1997) note that *conditional* Sec61 mutants are deficient in the retrotranslocation of ERAD clients like CPY* when shifted to Sec61-inactive conditions. Additionally, if the ERAD of a glycoprotein is reconstituted *in vitro* using microsomes, retrotranslocation can be prevented if translating ribosomes are first bound to Sec61 (Gillece *et al*., 2000).

Hebert *et al.* (2010) argue against Sec61 involvement because the minimal diameter of a glycoprotein is 20Å. They compare this to the aperture of the related, Archaeal SecY, which is too narrow, at 3Å (Van den Berg *et al*., 2004). Prior investigators, however, have shown that the mammalian translocon may be more flexible, its inner enclosure stretching to a diameter of 40-60Å during polypeptide import (Hamman *et al*., 1997). Nevertheless, Nakatsukasa & Brodsky (2008) review how experimenters have consistently failed to isolate Hrd1/Doa10 complexes containing Sec61. Moreover, they cite numerous studies where integral membrane substrates are efficiently degraded even when the translocon has been disrupted (using conditional mutants). One thought they express is that formation of Sec61-inclusive complexes may be transient, explaining why they may not have been observed to date.

Need there be a physical pore at all for some substrates? Ploegh (2007) speculates that misfolded proteins might exit the ER environment attached to lipid droplets. His model suggests that insertion of neutral lipid into the bilayer can form discrete, lens-like domains. These could be ejected into the cytosol as lipid droplets. Microdomains of these droplets could possess bilayer-like properties, or 'wrinkles'. Such domains would permit the accommodation of integral membrane proteins, including chaperones like calnexin.[3] This would expose their lumenal domains to the cytosol, where they could be recognised by quality control. Ploegh (2007) argues that it is plausible that soluble lumenal protein could be transported as well, piggy-backing upon integral-membrane proteins with chaperoning

[3] Which are consistently found associated with lipid droplets, along with BiP (Ploegh, 2007).

properties. Correct or not, this creative speculation highlights how a definitive pore has not yet been identified by the field. This particular issue, therefore, is in need of both clarification and – perhaps – novel thinking like Ploegh's.

1.4.3 Driving extraction from the ER membrane in *Saccharomyces cerevisiae*

The components mentioned so far recognise ERAD clients and accommodate them through the membrane. They also ubiquitinate them as they emerge into the cytosol. However, how client proteins are *driven* through the membrane remains to be explained. Other modes of protein translocation require the expenditure of energy to determine their unidirectionality. Indeed, transport is often coupled to the hydrolysis of ATP or GTP by the facilitating translocase and client-bound chaperones, or by the coupling of the process to the dissipation of an electrochemical gradient (Table 1.2).

The provision of energy during ERAD falls to different factors according to the substrate in question. Two complexes containing ATPases associated with assorted cellular activities (AAA proteins) are generally involved. These are Cdc48, or else subunits of the 19S proteasomal cap (Nakatsukasa & Brodsky, 2008). It is thought that these might act as motors, dragging substrates from the membrane (Figure 1.5). In some cases, the progressive polyubiquitination of client lysines might help ratchet the client into the cytosol. The same modification also improves the ability of Cdc48 and the proteasomal cap subunits to bind the substrate (Meusser *et al*., 2005).

Cdc48 is a soluble, hexameric protein that is both an 'unfoldase' and a protein complex 'segregase' (Schuberth & Buchberger, 2005; Ye *et al*., 2004). Given these generic properties, its role extends beyond ERAD. It is involved in, for instance: membrane fusion, transcriptional activation, cell cycle control, apoptosis and is also functionally implicated as a molecular chaperone (Wang *et al*., 2004). Tailored to these various roles, Cdc48 has multiple co-factors which 'plug-in' to its fundamental activity. During ERAD, Cdc48 is tethered closely to the Doa10/Hrd1 core membrane complexes by the transmembrane protein, Ubx2 (Schuberth & Buchberger, 2005). Beyond Ubx2, there are broadly three classes of Cdc48 ERAD co-factors:

(1) Ubiquitin-binding proteins such as Ufd1/Npl4 which help Cdc48 bind clients with greater avidity (Schuberth & Buchberger, 2005).

(2) A substrate-processing enzyme, PNGase (peptide-N_4-(acetyl-β-glucosaminyl)-asparagine amidase), removes N-linked glycans from glycoproteins. This is a prerequisite for their proteasomal degradation (Fagioli *et al*., 2001; Kim *et al*., 2006). PNGase and Ufd1/Npl4 can bind to Cdc48 at the same time (Raasi & Wolf, 2007), suggesting the tight coupling of binding and deglycosylation.

(3) The co-factors Rad23/Dsk2 bridge Cdc48 to the proteasome, with built-in ubiquitin-like domains (Raasi & Wolf, 2007).

Holistically, the Cdc48 complex therefore links three processes that facilitate proteasomal degradation: substrate binding, substrate processing and, ultimately, substrate transfer to the proteolytic complex. Substrates that use Cdc48 can be any of the three classes of ERAD substrate: soluble and lumenal e.g. CPY*; transmembrane with lumenal faults, e.g. Hmg-CoA reductase; or transmembrane with cytosolic faults, e.g. $CFTR^{\Delta F508}$ (Rabinovich *et al*., 2002; Gnann *et al*., 2004).

A certain subset of clients can be extracted from the ER by the proteasome alone, e.g. pro-alpha-factor (Lee *et al*., 2004; reviewed in Meusser *et al*., 2005). Indeed, proteasomes associate very closely to Sec61 *in vivo* (Ng *et al*., 2007). Lee *et al*. (2004) pinpointed that the 19S cap of the proteasome alone is sufficient to facilitate the extraction of pro-alpha-factor from ER-derived microsomes. Subsequent addition of the 20S core complex caused the degradation of the retrotranslocated substrate, reconstituting the ERAD pathway entirely. This same finding showed that degradation was not intrinsically coupled to extraction. The cap complex comprises 19 individual proteins. Nine of these segregate into a polyubiquitin-binding lid (the first example of a ubiquitin binding protein was mammalian s5a / yeast Rpn10 of this lid complex – Van Nocker *et al*., 1996). A decameric base unit contacts the core particle; 6 of these are AAA proteins, like Cdc48. This ring helps to unfold substrates, an activity which may be useful for prising a protein from the ER membrane (Lee *et al*., 2004).

Recently, Lipson *et al*. (2008) identified that certain subunits of the 19S cap are ERAD-specific, e.g. Rpt4. Other subunits may have a more general role in regulating access to the core particle (e.g. Rpt2). Lipson *et al*. (2008) also showed that degradation of some substrates, like CPY*, depends on both Cdc48 and the proteasomal cap. They hypothesised that they could work redundantly – in parallel – or sequentially during extraction. Li *et al*. (2010) noted that different versions of the same ERAD substrate (RTA, in fact) depended on

one or the other for extraction. This would support a partially redundant mechanism, where Cdc48 and Rpt4 can recognise distinct client features, rather than a sequential one (Figure 1.5).

One question that arises is: if the proteasome can extract substrates as Cdc48 does, then why duplicate the extraction machinery? It is thought that the intercession of this protein between retrotranslocation and degradation provides useful regulatory properties; properties which the cap does not have, such as glycan removal. Despite this, Kim *et al.* (2006) review how a number of glycoproteins do not actually require PNGase to facilitate their degradation, such as CPY*, T cell receptor α chain (TCR-α), and class I major histocompatability complex (MHC) proteins. Ironically, a processing buffer like Cdc48 – physically separating client extraction and client degradation – might be significant to the toxicity of ricin in the mammalian context.

Figure 1.5 - Cdc48 and the proteasomal cap drive extraction of ERAD substrates.

The following figure is heavily influenced by the Cell Snapshot produced by Kawaguchi & Davis (2007). It shows the Cdc48 and proteasomal mechanisms of extraction from the ER (Meusser *et al.*, 2005). Cdc48 is recruited to the Doa10 and Hrd1 complexes by Ubx2 (left-most model). Ubiquitin chains are indicated by the contiguous chain of little blue circles. Some substrates can use proteasomal caps to facilitate extraction (centre model). The proteasome complex binds to Sec61 (Ng *et al.*, 2007). Some substrates use both Cdc48 and the proteasomal caps. Lipson *et al.* (2008), formulated parallel (leftmost and centre models) and sequential (right-most model) modes of extraction. Purple arrow indicates sequential transfer of substrate.

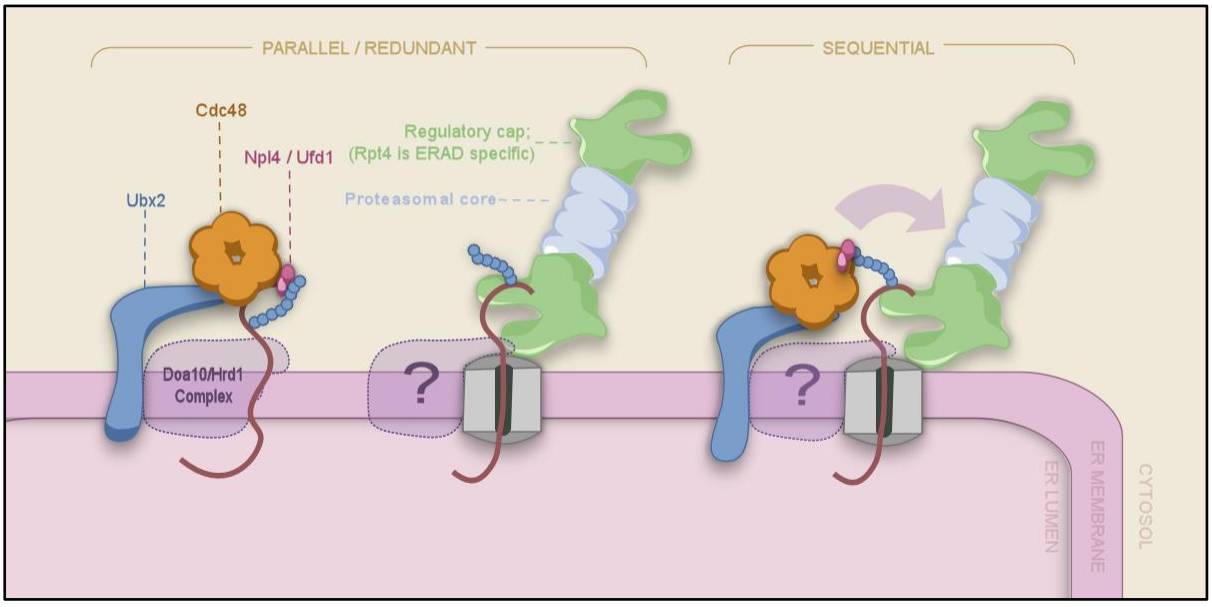

Table 1.2 - Protein Import Pathways and their Driving Forces

Collated from the sources in the right-hand column. 'TAP' refers to the transporter associated with antigen processing, whereby exogenous proteins are translocated into the ER lumen and associated with MHC class I molecules. 'AAA' stands for ATPase associated with assorted cellular activities. This table is intended to be representative and not comprehensive. ΔpH indicates a proton gradient separated by a selectively-permeable membrane. ΔΨ indicates an electrochemical gradient across a membrane.

Pathway Moniker		Dominant 'driving' forces	Further Reading
ER import	Co-translational	Ribosome-driven chain extension	Corsi & Schekman, 1996
	Post-translational	Brownian motion coupled to a BiP-dependent ratchet.	Corsi & Schekman, 1996
	TAP transporter	ATP hydrolysis by translocases.	Ehses *et al.*, 2005.
Mitochondrial Import (Post-translational)	To the inner-membrane space	ΔΨ between inner & outer membranes.	Wiedemann *et al.*, 2004.
	To the matrix	ΔΨ and Brownian motion coupled to a matrix-localised Hsp70 ratchet.	
Chloroplast Import (Post-translational)	To the stroma	ATP & GTP hydrolysis by translocases.	Soll & Schleiff, 2004.
	To the thylakoid lumen	ΔpH, which controls pore dynamics.	Robinson & Bolhuis, 2004.
Bacterial secretion		ATP hydrolysis by SecA upon the *cis*-side of the membrane.	Driessen & Nouwen, 2008.
ER export		AAA proteins of Cdc48 and the proteasomal cap. An ubiquitin ratchet may also provide synergy.	Meusser *et al.*, 2005.

1.4.4 Unique characteristics of mammalian ERAD

The machineries of mammalian ERAD are more elaborate than those of yeast (Table 1.3). This reflects the broader array of clients and more complex layers of regulation that both multi-cellularity and developmental pathways demand. Indeed, the key apparatuses that *Saccharomyces cerevisiae* possesses are all represented and some are expanded. However, in contrast to *Saccharomyces cerevisiae*, the mammalian cohort of ERAD-implicated E3 ligases is supplemented by a soluble, cytosolic set (reviewed in Nakatsukasa & Brodsky, 2008; Ballinger *et al.*, 1999). The degradation of both the cystic fibrosis transmembrane conductance regulator (CFTR) and apolipoprotein B (ApoB) epitomises the participation of

these soluble E3 ligases in ERAD. CFTR is a large, polytopic plasma membrane protein that is avidly degraded by ERAD (Alberti *et al*., 2004). This degradation occurs to a disease-causing extent in people who are homozygous for the mutant $CFTR^{\Delta F508}$. In this version of the protein, the conformation of a cytosolic ATP-binding cassette is disrupted (Alberti *et al.*, 2004; Hirsch *et al*., 2009). Hsc70 detects the prolonged ER-residency this fault causes (Albert *et al.* 2004), much as its yeast ortholog, Ssa1, may recognise clients at the outset of the Doa10 pathway (Metzger *et al.*, 2008). Prolonged association of Hsc70 with $CFTR^{\Delta F508}$ leads to an increased chance of polyubiquitination. This polyubiquitination is promoted by the soluble, Hsc70-dependent, Hsc70-binding E3 ligase called CHIP (Alberti *et al*., 2004). CHIP ubiquitinates both client and chaperone, leading to client degradation by localisation of the client-bound complex to the proteasome (Minami *et al*. 1996; Alberti *et al*., 2003). This pathway is quite distinctive, in that it delegates the entirety of the recognition and polyubiquitination processes to soluble, cytosolic factors.

This functional contribution of CHIP to the ERAD of $CFTR^{\Delta F508}$ highlights the potential significance of another two soluble E3 ligases that have been implicated in ERAD, yet have no yeast correlates. One is FBX2, which recognises and ubiquitinates glycoproteins (Yoshida *et al*., 2002). The other is Parkin, which is analogous to CHIP in that it selects its substrates in an Hsc70-dependent manner (Pratt *et al*., 2010). Their exact preference for substrates and prevalence of their involvement in ERAD, however, is not well understood.

Interestingly, a core E3 ligase of yeast, Hrd1, has two homologues in mammals. One is very similar to Hrd1, whilst the other (gp78) has acquired an ubiquitin-binding domain much like yeast's Cue1. Morito *et al*. (2008) showed that this motif gates access of substrates to gp78's RING-finger domain, which cannot start ubiquitin chains *de novo*. They speculate that other E3 ligases work upstream of gp78. Indeed, they show that gp78 co-operates in this manner with another mammal-specific transmembrane E3 ligase, RMA1, in the degradation of $CFTR^{\Delta F508}$ (Morito *et al*., 2008).

The participation of these three complexes – gp78, RMA1 and Hsc70/CHIP – in the degradation of $CFTR^{\Delta F508}$ highlights a good example of redundancy between E3 ligases (Morito *et al*., 2008). Adding to this picture, if $CFTR^{\Delta F508}$ is exogenously expressed in yeast, the Doa10 complex facilitates its degradation (Younger *et al.*, 2004). The homolog of Doa10 in mammals, TEB4, has only recently been identified (Kreft *et al.*, 2006; Nakatsukasa and

Brodsky, 2008). It therefore remains unclear whether it also handles $CFTR^{\Delta F508}$ in the mammalian context.

Table 1.3 - Select factors implicated in both Yeast and Mammalian ERAD

This table is much as printed in Nakatsukasa & Brodsky (2008). Derlin-1 can be immunoprecipitated with those proteins which are underlined (with additions made as noted by Hebert *et al*. 2010). Additional homologs have also been added, as per Raasi & Wolf (2007).

Mammals		Yeast *(Saccharomyces cerevisiae)*
Cytosol- and membrane-associated		
P97-UFD1-NPL4		Cdc48-Ufd1-Npl4
CHIP	Soluble E3 ligases	(No obvious correlate)
FBX2		(No obvious correlate)
Parkin		(No obvious correlate)
ATX3		Ufd2
Rad23		Rad23
N-glycanase		Png1
Membrane-associated		
HRD1-SEL1L		Hrd1-Hrd3
gp78		(Hrd1-like & Cue1-like domain)
RMA1, TRC8 & RFP2 (Transmembrane E3 ligases).		(No obvious correlates)
TEB4		Doa10
Ubc6e		Ubc6
Ubc		Ubc7
HERP		Usa1
VCP-interacting membrane protein (VIMP) & ERASIN		Ubx2
Derlin-1, -2 and -3		Der1
Sec61		Sec61
(Incorporated into gp78)		Cue1
ER lumen- and membrane-associated		
OS-9 and XTP3-B		Yos9
EDEM-1, -2 and -3		Htm1 (now Mns1).
BiP		Kar2
PDI		PDI

Apolipoprotein B (ApoB) is the other cited example of a substrate whose ERAD is contributed to by CHIP. However, its ERAD is notable for different reasons as well. ApoB is a core constituent of low-density and very-low density lipoproteins, which are involved in cholesterol transport (Shepherd, 1994). During import into the ER, ApoB is loaded with lipid and cholesterol. However, if either is absent, then the N-terminal domain no longer associates with ApoB-specific lumenal factors that facilitate its co-translational translocation (Gusarova *et al*., 2001; Brodsky *et al*., 2007). After dissociation of these factors, translation in the cytosol continues, but the remaining peptide is not passed through the pore, instead distending a misfolded loop into the cytosol. This loop is subsequently recognised by both Hsc70 and Hsp90, which target it for degradation by cooperation with CHIP (Gusarova *et al*., 2001). The protein is therefore degraded in a co-translational, co-translocational manner in response to regulatory cues from the lumen.

Interestingly, this "aborted" translocation pathway functions more broadly at times of stress (Oyadomari *et al*., 2006). That is, when the ER is overcome with unfolded protein. This curtails the escalation of the ER's quality control burden (Kawaguchi & Ng, 2007). Negative feedback from the lipid content of the lumen also regulates the ERAD of proteins like HMG-CoA reductase (Song *et al*., 2005). Such feedback appears to be a recurring theme, as there exists an ERAD-implicated E3 ligase that directly senses sterols and down-regulates the proteins responsible for their synthesis, designated TRC8 (Lee *et al*., 2010; Nakatsukasa & Brodsky, 2008; Brauweiler *et al*., 2007). Given Ploegh's (2007) speculation about the involvement of lipid droplets in the egress of ERAD substrates from the ER, this poorly-characterised category of lipid-sensing factors may hold greater significance for the field of ERAD. For instance, the wider integration of lipid and protein homeostasis. This remains to be determined.

1.5 Ricin and the ERAD pathway it might exploit

Over the years, building experimental evidence has suggested that ricin exploits ERAD to dislocate RTA into the cytosol. Inhibition of the proteasome results in the sensitisation of mammalian cells to ricin (Wesche *et al*., 1999), implying RTA (originally applied at the cell surface as part of a holotoxin) is a candidate for degradation by the complex. However, this observation could be descriptive of an ultimately cytosolic location rather than of an ERAD-style retrotranslocation. Similarly, Deeks *et al*. (2002) showed that introducing additional lysines into RTA decreased its toxicity, suggesting the subunit was exposed to the

ubiquitination machinery of the cell during intoxication. Whether this was the ubiquitination machinery of an ERAD-specific process, or simply of cytosolic quality control remained a question. Clarifying this issue, Li *et al.* (2010) showed that RTA synthesised in the cytosol of yeast, without a signal peptide, is rather stable. This indicates some process predisposes RTA to degradation specifically during intoxication. Indeed, Argent *et al*. (2000) report that folded RTA is strikingly resistant to protease digestion *in vitro*. The obvious process that might render RTA vulnerable to protease digestion *in vivo* is an unfolding step associated with ERAD (Fagioli *et al*., 2001; Beaumelle *et al*., 1997; Argent *et al*., 1994).

In the mammalian context, the sensitivity of cells to cholera toxin (which also has a lack of lysines and is targeted to the ER) is affected in cells where the ERAD machinery has been mutated. Teter *et al*. (2003) identified a mutant cell-line which was resistant to cholera toxin and which degraded a soluble, lumenal ERAD substrate, α1-AT NHK, more efficiently. Teter & Holmes (2002) identified a ricin-resistant cell line which simultaneously exhibited the reduced degradation of α1-AT, owing to decreased dislocation rather than a fault in cytosolic degradation machinery. The properties of both cell lines linked the function of ERAD to the fate of an ER-dislocating toxin. Using a different approach, Slominska-Wojewodzka *et al*. (2006) showed that targeted interference with a component of mammalian ERAD (i.e. EDEM) affected the toxicity of ricin.[4]

In yeast, convincing evidence has suggested RTA exploits ERAD. Most comprehensively, an entire set of factors was identified by Li *et al*. (2010). They showed that both toxicity and degradation of lumenally-expressed RTA is strongly inhibited by the following deletion strains: Δ*hrd1*, Δ*der1* and Δ*hrd3*. Promisingly, these findings corroborate well with the finding that (in HeLa cells) the ER-targeted, lysine-deficient cholera toxin uses Derlin-1 and Hrd1 (and its orthologue, gp78) to access the cytosol (Bernardi *et al*., 2008 & 2010). Toxicity and degradation of lumenally-expressed RTA in yeast was inhibited in other genetic backgrounds as well, albeit less strongly. These backgrounds included: Δ*usa1*, Δ*ubx2*, Δ*ubc7* & Δ*cue1*, which, consistently, are knockouts of proteins associated with the Hrd1 complex. The involvement of these factors was notably independent of lysine-ubiquitination and of the E3 ubiquitin ligase activity of Hrd1 (Li *et al*., 2010). Speculatively, this indicates that many

[4] In a complex series of observations, Slominska-Wojewodzka *et al.* (2006) observed that up-regulated EDEM protected cells against ricin intoxication. However, when the EDEM·client interaction was subsequently interrupted with kifunensine or puromycin, they observed a relative promotion of toxic activity in these cells relative to the wild-type. They hypothesised that ricin exploits EDEM to gain access to the dislocon.

factors ascribed ‘ubiquitination’ functions have other roles too, e.g. as scaffolding proteins, or even pore components. Overall, these findings suggest that RTA undertakes a route into the cytosol which closely identifies with ERAD-L – that of a soluble lumenal substrate in yeast.

Downstream of the retrotranslocation complex, candidates for the motor driving extraction have also been studied. Marshall *et al.* (2008) showed that the efficient extraction of RTA from the ER of tobacco protoplasts is dependent upon Cdc48. Cells expressing dominant-negative versions of this protein retain much of their protein-synthetic capability when they express ER-targeted RTA (whereas wild-type protoplasts do not). Marking a point of difference between tobacco, Li *et al*. (2010) show that Cdc48 and its cofactor, Npl4, are not required for the extraction of RTA^{WT} in *Saccharomyces cerevisiae*. This difference highlights how alternate ERAD arrangements may be perpetuated in the mammalian context, a context which is especially relevant to this thesis.

Interestingly, the ERAD of a severely misfolded mutant of RTA, RTAΔ, was dependent upon Cdc48 and its co-factors Png1, Rad23, and Dsk2 in yeast (Li *et al*., 2010; Kim *et al*., 2006; Hosomi *et al*., 2010). Kim *et al.* (2006) report that Png1 (PNGase) can form a dimeric complex with Rad23, helping target glycosylated RTAΔ to the proteasome. It may be that the ERAD machinery can distinguish the two forms of RTA. Alternatively, an intrinsic property of RTA^{WT} may ensure that it exits the ER by a tailored, Cdc48-independent route. Li *et al*. (2010) hypothesise that the extraction motor driving RTA may, instead, be a subunit of the proteasomal cap.

There is yet comparably little clarification of the ERAD machinery which ricin might exploit in mammals. However, investigators have carefully explored how ricin might *qualify* for such a process. Most ERAD candidates travel across the membrane as monomers, free of disulfide bonds (Fagioli *et al*., 2001). Thus, it was anticipated that RTA might conform to this ideal. Therefore, RTA would have to lose its connection to RTB somehow during intoxication. Indeed, it is quite clear that RTB is not an absolute requirement for the retrotranslocation of RTA, as lumenally-targeted RTA is potently toxic to both yeast and plants (Marshall *et al*., 2008; Li *et al*., 2010). Moreover, over-expressing RTB in the ER lumen of plant and mammalian cells actually inhibits toxicity by potentially sequestering RTA therein (Frigerio *et al*., 1998; Spooner *et al*., 2004). Providing a possible answer for how RTA might be released from RTB *in vivo*, Spooner *et al*. (2004) showed that it was possible to generate monomeric RTA by incubating the holotoxin with protein disulfide

isomerase (PDI). Given PDI is an enzyme of the ER, it is – or its homologues are – ideally situated to fulfil this role *in vivo*.

After liberation from RTB, RTA more closely resembles an ERAD substrate. It is technically no longer a 'native' protein, having lost the partner to which it is in complex with for most of its lifetime. This might be recognised by the cell, manifested in the exposed C-terminal patch of RTA. Correspondingly, mutations in this region negatively impact upon cytotoxicity (Simpson *et al*., 1995). Speculatively, it might be that this hydrophobic stretch in the wild-type interacts with ERAD-promoting chaperones of the ER. Alternatively, it has been suggested that this region provokes interaction with the ER membrane instead, so inducing misfolding, which could *thereafter* promote ERAD (Day *et al*., 2002; Mayerhofer *et al*., 2009). Indeed, Mayerhofer *et al*. (2009) show that incubation of RTA with liposomes containing negatively-charged phosphatidyl-serine (POPS) leads to disruption of the toxin subunit's secondary structure *in vitro*. Feasibly, this might contribute to the acquisition of a translocation-permissive conformation. Mayerhofer *et al*. (2009) show that the C-terminus of RTA embeds into microsomal membranes, demonstrating that a functional role for this domain might exist *in vivo*.

Demonstrating that unfolding of RTA is important to the productive, toxic route, Beaumelle *et al.* (2002) conducted a series of experiments using an RTA-dihydrofolate reductase complex (RTA-DHFR). They observed that holotoxin containing RTA-DHFR was still cytotoxic (albeit far less effective than wild-type toxin). If they co-treated cells intoxicated with this adulterated holotoxin with methotrexate (a DHFR-inhibitor), toxicity was reduced compared to without. They hypothesised that this was because of the tight-folding of the DHFR whilst bound to methotrexate. Similarly, when Argent *et al*. (1994) introduced a disulfide bond into RTA, they also observed a reduction in toxicity – and proposed a similar explanation. The acquisition of at least a partially-unfolded state therefore seems integral to retrotranslocation.

Overall, there are tenable ideas that suggest how RTA may ensure its recognition as an ERAD substrate (Mayerhofer *et al*., 2009; Simpson *et al*., 1995). Given what is known of yeast, there are also good protein candidates to target for investigation (Li *et al*., 2010). Moreover, Bernardi *et al*. (2010) recently identified that CTA1 retrotranslocation is promoted by Hrd1 and gp78 in the mammalian context. RTA's dearth of lysines helps it to escape the lysine ubiquitination that would usually be performed by the ERAD complex it uses (Deeks

et al., 2002). This putatively attenuates the sequence of interactions that would otherwise deliver the toxin subunit to the proteasome. However, it remains unclear how RTA might attain an active conformation after retrotranslocation, thus resolving itself from the majority of proteins which await degradation on the cytosolic face of the membrane. Indeed, RTA is unfolds for the process (Beaumelle *et al*., 2002; Argent *et al*., 1994) and is unable to attain an active conformation spontaneously (Argent *et al*., 2000). A mechanism to fold to a catalytic conformation therefore becomes crucial. Perhaps not without its own significance, this refolding must also occur in a cellular compartment which is not native for this fragment of a secreted plant protein.

Experiments have shown that RTA becomes a molten globule at a threshold of around 45°C, and that the toxin subunit cannot spontaneously refold from this state (Argent *et al*., 2000). Because of this, it has been speculated that a third-party might be required to ensure that a correct folding pathway is assumed *in vivo* after retrotranslocation (Argent *et al*., 2000). Interestingly, Argent *et al*. (2000) showed that active RTA could be generated *in vitro* if the molten globule state of the protein was incubated with substrate ribosomes. It was thus proposed that the ribosome could perform this process *in vivo*. Nevertheless, it is unclear what aspect of the ribosome is responsible for this effect. It could be that co-purified proteins, such as small quantities of cytosolic chaperones bound to ribosomal protein (as reported for Hsp90 by Kim *et al*., 2006), are responsible for the phenomenon. Indeed, *in vivo* where such chaperones are abundant, they might be expected to intercede before an interaction with the ribosome is possible. These protagonists of cytosolic quality control may be responsible for the salvage of RTA during intoxication.

1.6 Cytosolic quality control & chaperones

Much like in the ER lumen, the cytosol has to nurture the folding of nascent polypeptides. Arguably, the 'folding problem' in this compartment may be graver because of high local concentrations of identical, unfolded nascent polypeptides as they are translated from polysomal mRNA (Ellis & Hartl, 1999). Unique stresses demand unique machinery. In mammalian cells, growing protein chains interact with the ribosomally-localised nascent chain associated complex, NAC, which may have chaperoning properties (Young *et al*., 2004). Like the ER, added to the burden of nascent chains is the regressive misfolding of mature protein at times of stress (McClellan *et al*., 2005). Fittingly, there are abundant chaperones that cater to the prophylaxis, amelioration and elimination of the various

conformational complaints that can arise (Young *et al*., 2004). Interestingly, there is also the need to keep proteins destined for other compartments in a translocation-competent – unfolded or partially-unfolded – state. Chaperones are involved in this process too (Young *et al*., 2003).

Like lumenal chaperones, these protein buffers help polypeptides to avoid non-native states without themselves becoming a permanent, covalently-attached component of the final structure (Ellis & Hartl, 1999). Via numerous mechanisms, their transient interaction reduces the frequency of off-pathway folding events that lead to permanent loss of function and aggregation (Markossian & Kurganov, 2004). However, there are also times when the folding capacity of the cell is exceeded. Under such conditions, distinct quality control compartments consisting of concentrated misfolded protein arise: inclusion bodies. These dynamic structures sequester aberrant proteins, waylaying degradation and refolding. At the same time they mitigate the toxic effect of aberrant conformers which would otherwise be soluble (Kaganovich *et al*., 2008). They store a 'folding debt', if you will. Two qualitatively distinct 'misfolding compartments' exist in both yeast and mammals, suggesting careful regulation of their formation in eukaryotes. First, there is a juxta-nuclear, endoplasmic reticulum inclusion for ubiquitinated proteins involved in ERAD. This compartment is studded with proteasomes and chaperones (Kaganovich *et al*., 2008). Second, there is a perivacuolar compartment that enlarges when the prior is saturated. It consists of *terminally* misfolded, insoluble protein. Some proteins, for example amyloidogenic species, are immediately sent to the latter compartment rather than being kept in the first (Bagola & Sommer, 2008). This kind of audit is indicative of the careful decisions the quality control machinery is capable of.

It is important to note that chaperones, by definition, do not impose specificity – that is they do not fold proteins like origami. Rather, they increase the efficiency of folding, the exact secondary and tertiary qualities of which are encoded by the primary sequence of the client (Ellis & Hartl, 1999). Some exceptional 'steric chaperones' do impart specific conformational cues before being segregated from the final structure, but they usually have a dedicated substrate, or are themselves initially part of the protein they chaperone, such as the cleavable presequences of zymogens (Ellis & Hartl, 1999). In all likelihood, these would be too specific in function to contribute to the successful refolding of retrotranslocated RTA. The more generalised chaperones of the cytosol, however, may be of functional significance to RTA.

In the cytosol, Hsp90s and Hsc70s and a variety of other 'holding-type' chaperones (of up to ~200kDa) bind to misfolded conformers (Ellis & Hartl, 1999; Young *et al*., 2004; Markossian & Kirganov, 2004). Unique to the cytosol, larger, complex chaperones of greater than 800kDa actually fully encapsulate folding proteins (or individual protein domains; Young J.C., *et al*., 2004). This sequesters them from the cytosolic milieu, with which they might adversely associate whilst filtering through non-native conformations that converge upon the native state (Ellis & Hartl, 1999). The following sections describe these chaperones in more detail.

1.6.1 Hsc70

One of the most abundant cytosolic chaperones, Hsc70, binds to short regions of unfolded, extended, hydrophobic polypeptide (Flynn *et al*., 1991). On average, binding-competent motifs arise every thirty-six residues in the mammalian proteome (Bukau & Horwich, 1998). This makes the potential clients of Hsc70 very broad indeed. The chaperone itself is divided into two highly-conserved, independently-folded regions: an ATPase domain at the N-terminus and a peptide-binding domain at the C-terminus (Shaner & Morano, 2007). Turnover of the N-terminal ATPase is coupled to a conformational rearrangement that alters the affinity of the chaperone for clients. The ATP-bound state binds clients loosely, whereas subsequent ATP hydrolysis leads to a state which binds clients with high affinity (Sondermann *et al*., 2001). Crucial to the diversity of clients and roles that Hsc70 has, cycling between nucleotide-governed conformations is controlled by both the intrinsic properties of the chaperone itself and a myriad of regulatory co-factors (Young *et al*., 2003). By such manipulation, co-factors can contribute to the context in which a client is initially bound by Hsc70, the timing of client residency, and the interaction of the client with downstream cellular machineries.

Despite functional dependence on co-chaperones *in vivo*, ATPase turnover by Hsc70 can occur in their absence. Indeed, substrate binding alone stimulates ATP hydrolysis. However, this step in the cycle is rate-limiting unless a J-domain-containing co-chaperone is present (Sondermann *et al*., 2001). J-domain containing proteins are abundant in the cell and stimulate the ATPase activity of Hsc70 (Walsh *et al*., 2004; Bukau & Horwich, 1998). These proteins have a variety of localisations and their various J domains stimulate Hsc70 with different potencies. Some J-domain proteins also bind prospective Hsc70 clients, like Hsp40 does, regulating their access to the chaperone's peptide binding site (Cintron & Toft, 2006;

King *et al*., 2001). Thus, in the locality of a J-domain protein the concentration of Hsc70 chaperoning activity is much increased (Young *et al*., 2003).

The client/ADP-bound complex can be stabilised by another co-chaperone, HIP (Sondermann *et al.*, 2001; King *et al.*, 2001). A further class of co-chaperone, those with nucleotide exchange factor (NEFs) activities, antagonises HIP by promoting the open conformation of Hsc70. This permits the release of bound clients – especially if they are able to swiftly conceal the hydrophobic region that led to the initial chaperone interaction. If the client is not able to do so, then repeated rounds of interaction with the chaperone can occur. Examples of NEFs include the BAG-domain proteins (Alberti *et al*., 2003), HspBP1 (Alberti *et al*., 2004) and the independent chaperone Hsp110, which curiously contains an Hsc70-like N-terminus of ambiguous functionality (Hrizo *et al*., 2007; Shaner & Morano, 2007). Exemplifying a final effect upon the N-terminal ATPase, the co-chaperone, CHIP, can stabilise the 'open', ATP-bound conformation (Kampinga *et al.*, 2003). Thus, at every stage of its ATPase cycle, Hsc70 is subjected to regulation, making it a complex machine at the heart of protein interactions in the cell.

Aside from influencing the nucleotide-bound state, co-chaperones can also link Hsc70 to parallel quality control machineries operating in the cytosol. One mammalian J-domain protein, Hsj1, bears an ubiquitin-interacting motif and so – for instance – can reiteratively load ubiquitinated chaperone clients onto Hsc70 (Westhoff *et al*., 2005). The BAG-domain proteins in particular have diverse functions: BAG-1 has an ubiquitin-like domain for associating with the proteasome (Alberti *et al.*, 2001; Alberti *et al.*, 2003). BAG-2, on the other hand, directly opposes BAG-1 by not having the attached ubiquitin-like domain. This means it blocks un-ubiquitinated Hsc70 clients from interacting with the proteasome, so promoting the client to freely diffuse into the cytosol instead (Arndt *et al*., 2005; Dai *et al*., 2005). Last, the co-chaperone, CHIP, as introduced earlier for its role in ERAD, possesses an E3 ligase activity that can be focussed upon chaperone-bound substrates (Ballinger *et al*., 1999; Connell *et al*., 1999; McDonough & Patterson, 2003; Murata *et al*., 2001). As such, Hsc70 is not just an aid to protein folding. Pivotally, it is also able to facilitate the degradation of substrates if they linger in its binding site (Esser *et al*., 2004).

1.6.2 Hsp90

Hsp90 operates as a dimer. Each component monomer comprises four conserved regions: an N-terminal region; a flexible, highly-charged linker region; a middle domain; and a C-

terminal domain. The C-terminal domain is responsible for the persistent dimerisation of the chaperone and also a regulatory role (Retzlaff *et al*, 2009), whilst the N-terminal region houses an ATPase (Buchner, 1999). The turnover of the dimer's two ATPase domains is mutually inter-dependent and coupled to an interaction between N-termini (Buchner, 1999; Vaughan *et al*., 2008; Hessling *et al*., 2009). This results in the oscillation of Hsp90 between two over-arching conformations (Figure 1.6a). First a polarised, deformed ring structure (ATP-bound) and second, a V-shaped dimer (while ADP-bound, or vacant of nucleotide). Curiously, Mickler *et al*. (2009) found that the coupling of ATP turnover to conformational rearrangement is actually quite weak and that the domain rearrangements of the chaperone are governed more strongly by stochastic fluctuations.

Despite being the most abundant chaperone of the mammalian cytosol and the subject of intense study, the qualities which distinguish Hsp90's clients have not been precisely determined (Prodromou & Pearl, 2006). Moreover, the mechanistic significance of the domain rearrangements described above – with regards to the chaperoning properties of the protein – is unknown (Richter *et al*., 2007). Nevertheless, suggestions have been made. For instance a hydrophobic patch formed at the interface of the N-termini may be important for substrate binding, as well as sites in the middle domains, Figure 1.6a (Richter *et al*., 2007). However, the field still seems vague on the matter. Placing the question of mechanism aside for now, it is thought that Hsp90 recognises proteins that are relatively close to their native state (compared to Hsc70, at least). Indeed, Hsp90 participates in the latter stages of steroid hormone receptor maturation (King *et al*., 2001) and in the quaternary assembly of multi-component complexes (Imai J. *et al*., 2003; Kim *et al*., 2006), as opposed to sensing more elemental aspects of protein structure (such as an extended polypeptide chain). Fittingly, rather than 'enclosing' substrates in any fashion, it is thought that clients are bound on Hsp90's surface (Buchner 1999).

Like those of Hsc70, the co-factors contributing to Hsp90's function are diverse. They range in purpose from participating directly in protein folding and regulating the chaperone's ATPase cycle to scaffolding Hsp90 to other factors (Buchner 1999; Vaughan *et al*., 2008). Many are protein prolyl isomerases (Buchner, 1999). Some are substrate-specific and involved in client-recognition. For example there is Cdc37, which is a co-factor specifically implicated in the recognition of client kinases. Cdc37 also inhibits ATP turnover by Hsp90 and helps load bound kinases onto the chaperone (Siligardi *et al*., 2002). Aha1, on the other hand, promotes ATP hydrolysis and the interaction of the dimer's N-termini (Hessling *et al*.,

2009; Vaughan *et al.*, 2008). Hsp90 also liaises with CHIP and other E3 ligases like Skp1 (via the Sgt1 adaptor – Zhang *et al.*, 2008). This diversity of co-chaperones means cytosolic Hsp90 can be organised into versatile, discrete, functionally-differentiated complexes – tailored to the needs of disparate clients.

Figure 1.6 – The conformational cycle of Hsp90.

a) Hsp90 assumes predominantly an elongated V-structure when ADP-bound, and a circular, distorted ring when ATP-bound. Putative substrate binding domains are highlighted in pink. One is putatively formed between N-terminal domains when they dimerise, as indicated. The other sites are thought to be located upon the middle domains of the protein. The C-terminal domains (blue) are responsible for dimerisation in both the ATP and ADP-bound state. See text for references. b) The steroid hormone receptor pathway, as described in text in section 1.6.3 (from King *et al.*, 2001). The client is denoted by the red squiggle.

a. The conformational cycle of Hsp90

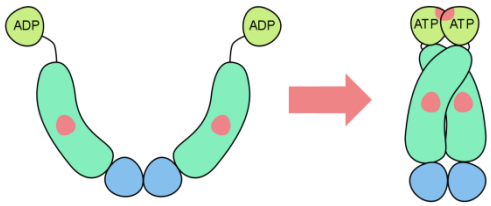

b. Steroid hormone receptor maturation pathway

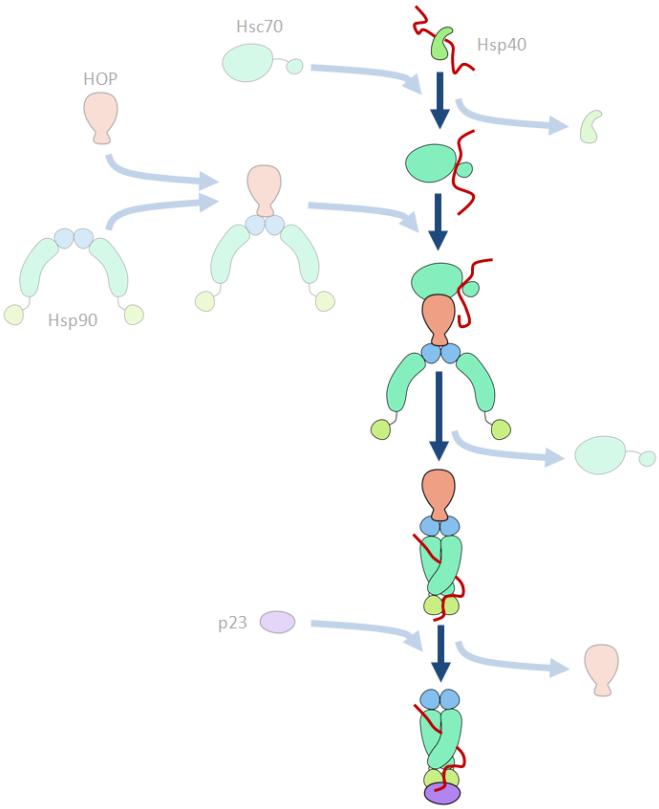

1.6.3 Hsc70 and Hsp90 working together using HOP

Distinctively, there is one co-chaperone called HOP (Heat shock protein 70/90 organising protein) which can physically scaffold Hsp90 to Hsc70 (Odunuga *et al*., 2004). This laterally integrates two neighbouring chaperoning machineries in the cytosol, permitting a co-ordinated response to misfolded protein. The interaction of HOP with Hsc70 and Hsp90 is mediated by dedicated tetratricopeptide (TPR) motifs, which are not inter-changeable (Song & Masison, 2005).

Much work has been produced that showing that HOP promotes the processive transfer of substrates from Hsc70 to Hsp90 (Figure 1.6b). King *et al*. (2001) reports a 'folding pathway' involving both Hsc70 and Hsp90 that leads to optimal activation of steroid hormone receptors *in vitro* and *in vivo*. In this pathway, clients are initially recognised by Hsp40 and Hsc70, a complex which is then stabilised by the co-chaperone, HIP (Hsc70 interacting protein). Stabilisation by HIP increases the probability of the complex encountering free HOP·Hsp90, which specifically recognises the client-, ADP-bound state of Hsc70. HIP is displaced, resulting in a tripartite chaperone complex of Hsp90·HOP·Hsc70 (with bound client). HOP binding promotes Hsc70's nucleotide exchange, leading to the transfer of bound steroid hormone receptor to the dimeric Hsp90. After transfer to Hsp90, HOP and Hsc70 dissociate from the complex. Hsp90 undergoes nucleotide exchange and finally associates with p23, another co-factor, which prolongs the lifetime of the complex (Morishima *et al*., 2003) by preventing ATP hydrolysis (Vaughan *et al*., 2008). This prolonged residency maintains the long-term activity of the client receptor. Dissociation, however, permits the receptor to revert to a signalling-incompetent form which can go through successive rounds of 'pseudo-maturation' (King *et al*., 2001). The chronic requirement for Hsp90 by steroid hormone receptors has muddied the chaperone field somewhat; such clients have a protracted association with chaperones rather than a transient association, as defined by Ellis & Hartl (1999).

This HOP-mediated pathway, at the time of writing, was given the most recent overview by Pratt *et al*. (2010). With regards to the mechanism of Hsp90, the authors speculated that the chaperone associates with the 'cleft' elements of multi-domain, multi-protein complexes. However, what consistently recognisable themes could unite molecularly-different clefts in disparate proteins is unknown. An observation that was made early in the field is that Hsp90 homologues are inessential to the survival of prokaryotes, whereas they are essential to the

survival of eukaryotes (Caplan *et al*., 1999). One big difference between these kingdoms of life is how widespread multi-domain proteins are; eukaryotes have accreted many more multi-domain proteins in their genomes than prokaryotes (Koonin *et al*., 2000). Given the implication of Hsp90 in ordering clefts (Pratt *et al*., 2010), and its involvement in the assembly and maintenance of macromolecular complexes (Imai *et al*., 2003; Kim *et al*., 2006), this prevalence might be why Hsp90 is so essential to eukaryotes: i.e. the relative arrangement of functionally-associated domains.

1.6.4 CCT (Hsp60)

The best studied mammalian chaperone is CCT, which is a large hetero-hexadecameric, double-ringed complex. The two back-to-back rings house central cavities that transiently accommodate clients during a strictly-regulated binding cycle co-ordinated to rounds of ATP hydrolysis (Kosmaoglou, 2008). In mammals, the rings each comprise eight different subunits (Gómez-Puertas *et al*., 2004). Each is also capable of housing a separate client, although their cycles of binding are linked in an out of phase manner, meaning the complex only ever binds one client at a time (Bukau & Horwich, 1998). CCT assists in the folding of an estimated 10% of newly synthesised mammalian proteins and may have a particular preference for proteins with β-strands (Kitamura *et al*., 2006). Its mechanism makes it very distinct from Hsc70 and Hsp90, in that it can encapsulate entire single-domain proteins, or individual domains of much larger structures (Young *et al*., 2004).

Most work regarding this chaperonin's activity has stemmed from the study of orthologues: the Archaeal thermosome and the prokaryotic GroEL/GroES (Gómez-Puertas *et al*., 2004). These differ slightly in mechanism and conformational arrangement to CCT, and so the mechanism described here is specific to CCT. CCT begins its client-binding cycle in an open conformation competent to bind clients, which occurs via the apical domains of each ring (Gómez-Puertas *et al*., 2004). Specific subunits are involved in this interaction, which may vary between substrates. Unlike prokaryotic GroEL, this interaction occurs mainly between charged and polar residues rather than hydrophobic ones, and interaction with the substrate occurs whilst it is in a partially-ordered state rather than an unstructured one (Kosmaoglou, 2008; Gómez-Puertas *et al*., 2004). The binding of substrate is likely to be multivalent and to become progressively more so after the initial interaction (Gómez-Puertas *et al*., 2004). Each subunit of the ring in which the client is held binds ATP. ATP hydrolysis leads to the iris-like convergence of α-helical, lid segments of each subunit, enclosing the client (Zhang *et al*.,

2010). The sequential nature in which ATP-binding and hydrolysis occurs is thought to affect the conformation of the domains to which the client is bound, meaning it is mechanically re-orientated (Gómez-Puertas *et al*., 2004). Nucleotide exchange may then occur, which (if CCT is similar to GroEL) results in conformational changes that result in re-opening of the cavity and disassociation from the client (Zhang *et al*., 2010). This mechanism of segregation enables the client to pursue the native state encoded by its primary sequence without interference from the primary sequences of improperly-folded, neighbour proteins.

1.6.5 p97

Introduced in the earlier context of ERAD, mammalian p97 (or plant/yeast Cdc48), is a homohexameric protein with ATPase activity. As well as its role in ERAD, it also has a chaperoning role (Kobayashi *et al*., 2007; Markossian & Kirganov, 2004). It forms an offset, concentric ring structure, with monomers fanning out from a central pore. Misfolded or ubiquitinated substrates are thought to bind initially to the periphery of the protein, between adjacent subunits (Jentsch & Rumpf, 2006; Halawani & Latterich, 2006).

Kobayashi *et al.* (2007) show that p97 is able to both re-solubilise and re-activate heat-denatured luciferase from insoluble, inactive aggregates. However, it is unclear exactly how the ATPase cycle of the protein and the domain rearrangements it promotes is coordinated to this activity. Multiple competing models are discussed by Pye *et al*. (2006). Jentsch & Rumpf (2006) speculate that, much like Hsc70, the ATPase cycle of p97 may be regulated by coordination with multiple co-factors. Pye *et al*. (2006) also speculate that some co-factors could even transduce the conformational rearrangements p97 makes into distinct mechanical operations. Indeed, quite unlike the other chaperones discussed, it is thought that p97 works actively as an 'unfoldase' (Halawani & Latterich, 2006). DeLaBarre *et al*. (2006) note a high local concentration of arginine residues lines the central pore of the protein. The side chains of these residues resemble guanidine, a notable protein denaturant. They compare the local frequency of arginyl residues to "8M guanidine", a concentration capable of denaturing most proteins. Therefore, p97 could break apart aggregates in a fashion regulated by its ATPase cycle, giving misfolded proteins a second chance at acquiring a native state.

1.6.5 Small heat shock proteins (sHsps)

The proteins that make up this divergent class of chaperone range in size from 15-42kDa (Kosmaoglou *et al*., 2008). They come together to form higher order, oligomeric complexes of between 9 and 50 subunits (Cashikar *et al.*, 2005). Unlike the other chaperones mentioned, it is deemed that they are regulated primarily by phosphorylation and temperature rather than by cycles of ATP binding and hydrolysis (Kosmaoglou *et al*., 2008). Some sHsps form into defined oligomeric structures with rotational symmetry, whereas others seem more dynamic, stackable and modular. There are ten such proteins in humans, each sharing a 90-reside α-crystallin domain (Haslbeck *et al.*, 2005).

Outlining their fundamental mechanism, Kosmaoglou *et al.* (2008) state that sHsps specifically recognise unfolded stretches of polypeptide. Cashikar *et al*. (2005) review that some become insoluble after heat shock, co-aggregating in large complexes with misfolded proteins. Indeed, unlike other chaperones, oligomeric sHsps can bind more than one client at the same time (Haslbeck *et al*., 2005). This incorporation into bodies of misfolded protein apparently ensures that aggregation is not irreversible, and facilitates the smoother, lateral co-operation of such aggregates with other chaperones of the cytosolic matrix (Haslbeck *et al*., 2005). Effectively, sHsps hold denatured proteins in a folding-competent state, collecting a 'reservoir' of unfolded species. Subsequent 'reactivation' is the preserve of other proteins, such as p97 and the Hsc70/Hsp90 chaperone system (Cashikar *et al*., 2005).

1.6.6 Which chaperones are of novel investigational interest in the context of ricin?

Where a study should begin to discern which chaperones might aid RTA is a good question. Which chaperones could resolve RTA from other substrates destined for degradation? To refine this starting point, further questions can be asked, for instance:

(1) Do these chaperones function in analogous pathways?
(2) Is their activity localised to the ER membrane?
(3) Are they likely to recognise RTA?

And, perhaps more tenuously:

(4) Could they feasibly integrate with the mammalian equivalents of the Hrd1 complex, which is the best candidate for the extraction of RTA in yeast (Li *et al*., 2010)?

Hsc70 seems a plausible candidate for being able to interact with RTA, given the frequency of its binding sites across the proteome. Its activity is also known to be localised to the ER membrane in a regulated manner, given that it is involved in the ERAD of apolipoprotein B (Gusarova V. *et al.*, 2005) and $CFTR^{\Delta F508}$ (Jiang *et* al., 2001). In addition, Hsc70 acts as a gating complex for yeast Doa10, the homolog of which in mammals is TEB4 (Nakatsukasa & Brodksy, 2008). Hsc70 is also known to promote the insertion of tail-anchored proteins directly into the ER (Rabu *et al*., 2008). If that role could be reversed under the right conditions, in part, it would be interesting to speculate whether RTA might benefit from it. Hsc70 has other protein transport roles too, for instance in maintaining proteins destined for post-translational import in a translocation competent state. Mechanistically, Hsc70 can also perform "entropic pulling" of translocating proteins, dragging them through the membrane, Table 2 (Corsi & Schekman, 1996; Wiedemann *et al*., 2004). What we know of Hsc70's chaperoning abilities and its precedent involvement in protein transport pathways therefore make it a very interesting target for study.

As Hsp90 can work in tandem with Hsc70 by merit of HOP, it also seems like a good candidate to investigate. Its activity is likewise localised to the ER membrane in some instances. The ERAD of ApoB and $CFTR^{\Delta F508}$ are, again, notable examples of this (Gusarova *et al*., 2005; Loo *et al*., 1998). Provocatively, Giodini & Cresswell (2008) also identified that Hsp90 was responsible for the cytosolic refolding of an exogenously applied protein. These investigators showed that luciferase is endocytosed and transported to the ER of cultured dendritic cells. Therein it is exported to the cytosol by an ERAD-like mechanism.[5] Whilst this may be a rather specific case study in an immune-specialised cell, it vouches for the plausible interruption of Hsp90 in the later stages of ERAD. This 'interruption' apparently leads to the liberation of folded, functional polypeptide (luciferase) rather than degradation. Thus, Hsp90 is evidently involved in a pathway which uncouples retrotranslocation from degradation. Instead, degradation is apparently supplanted with Hsp90-mediated refolding. This makes it an interesting study as well.

CCT is an arguably poorer candidate for investigation, given it is implicated in the folding of only 10% of newly-synthesised proteins (Kosmaoglou *et al*., 2008). Moreover, it is thought to recognise mainly β-sheet structures (Kitamura *et al*., 2006). RTA, on the other hand, is

[5] In that it was blocked by Pseudomonas exotoxin A (which binds to Sec61) and could be reconstituted using ER-derived microsomes and cytosolic Cdc48 (Giodini A. & Cresswell P., 2008).

largely α-helical. Its role also seems to be specific to folding rather than interlinked with a pathway leading to degradation (McClellan *et al*., 2005). Thus, it would perhaps make sense for the cell to segregate it away from localities of the cell where proteins are destined for degradation. Small heat shock proteins, on the other hand, may be interesting targets to study, but their role seems to be passive – dependent on downstream factors like Hsc70, Hsp90 and p97 to deliver folded structures from the misfolded proteins they buffer (Haslbeck *et al*., 2005). Therefore, study of the downstream 'reactivators' seem more likely to yield a positive, interesting result.

Finally, the p97 complex also seems like an interesting candidate for interacting with and perhaps reactivating retrotranslocated RTA. Of course, this protein is integral to a variety of ERAD routes, and evidence has already suggested that the plant homologue, Cdc48, contributes to extraction of active RTA from the ER of tobacco protoplasts (Marshall *et al*., 2008). In yeast, however, Cdc48 does not seem to be required for the extraction of RTA (Li *et al*., 2010). As these works have already pursued the involvement of Cdc48/p97 in extraction of RTA from the ER membrane, the study of Hsc70 and Hsp90 in particular seems to provide the most novel investigational target.

1.7 Thesis aims

In light of the information above, this thesis aims to determine whether cytosolic chaperones – Hsc70 and Hsp90 – participate in a functional interaction with RTA during intoxication of target cells. It will explore whether these intracellular aids to protein-folding have an impact on the cytotoxicity of ricin in a representative mammalian cell line, HeLa cells, which have been widely used to characterise the mechanism of ricin before now (Watson & Spooner, 2006). The first arm of this investigation will use inhibitors to examine the putative role of these chaperones during intoxication *in vivo*. As Hsc70 and Hsp90 are integral to the function of a cell in a multiplicity of ways (and many inhibitors are pleiotropic to different degrees), this will be tested with a number of reagents.

With the involvement of these chaperones tested, this thesis continues to explore the mechanisms by which their impact upon cytotoxicity might be executed *in vitro*. This is examined first by looking at reconstitutions of the processes that these chaperones are known to facilitate *in vivo* and *in vitro* for *bona fide* substrates, and seeing whether RTA is also candidate to the same phenomena. The outcome of these experiments will further clarify the possibility that a chaperone·RTA complex can form and will also be informative of the

potentially wider array of fates that might be imposed by such interactions in the cellular context, where the chaperones interlink with – for instance – the ubiquitin proteasome system (UPS). Factors which might influence the candidacy of RTA as a client of these chaperones are also given consideration, e.g. factors which might potentially demarcate the recognition of RTA as a misfolded protein in the ER and those which might promote its stability in the cytosol and renaissance as a stable protein.

Finally, the course of this thesis returns to a genetic approach, by looking at whether the normal outcome of the interaction can be changed, predictably, by altering the levels of mechanistically-elaborated co-chaperones.

CHAPTER 2:

Materials & Methods

2.0 Suppliers of reagents

The reagents used throughout this thesis were acquired from the following suppliers. Suppliers are listed in alphabetical order (with reagents purchased from them in alphabetical order underneath the title of each supplier). Proteins are also included if they were not purified during the course of study.

Autogen Bioclear
geldanamycin

Avanti Polar Lipids
POPC (phospholipid)
POPS (phospholipid)

Bio-Rad
Bradford reagent

Cook J., Warwick University
saporin (*S. officinalis*)

Fisher Scientific
acetic acid
acrylamide
calcium chloride
chloroform
citric acid
coumaric acid
disodium hydrogen phosphate
EDTA
ethanol
formaldehyde
formamide
glucose
glycerol
glycine
hydrogen chloride
luminol
magnesium sulfate
methanol
NN'-methylene *bis*-acrylamide
penicillin

Fisher Scientific - continued
phenol
potassium acetate
potassium chloride
potassium dihydrogen phosphate
sodium acetate
sodium chloride
sodium dodecyl sulphate
sodium hydroxide
streptomycin
TCA
TEMED
Tris

Formedium Ltd.
galactose

GE Healthcare
bromophenol blue
BSA

Helena Biotech
agarose

Höhfeld J., University of Bonn
E1 (from wheat)
E2 (UbcH5b; *H. sapiens*)
BAG-5, (*H.sapiens*)
CHIP, (*H.sapiens*)
Tau protein (micro-tubule assoc.)

Invitrogen
Lipofectamine
pluronic acid

Invitrogen – continued
SeeBlue Plus2 Markers

Marvel
milk albumin (fat-free)

Merck Biochemicals
tryptone
yeast extract
magnesium chloride

Nippon Kayaku Co.
deoxyspergualin

Perkin-Elmer
[^{35}S]-methionine
scintillant (Optiphase S-mix)

Promega
BCIP
NBT

Roche
Complete protease inhibitors

Sigma-Aldrich
aniline
ammonium persulphate
ATP
β-mercaptoethanol
dithiothreitol
ethidium bromide
fetal calf serum
glutamine

Sigma-Aldrich - continued
lactose
lithium chloride
MOPS
phenylmethylsulfonyl fluoride
RNase A
Ponceau S reagent (solid)
phenol red
polyethylene glycol-8000
rubidium chloride
sodium azide
TNM-FH (medium)
triton X-100
Trypan blue
$Tween_{20}$
ubiquitin (bovine source)

Tocris Life Sciences
CCT018159
4-phenyl butyrate
radicicol

Vector Laboratories
ricin toxin B chain

VWR International
ammonium
manganese chloride
SF9 cells

2.1 Antibodies

The primary antibodies detailed in Table 2.1 were used for immunostaining throughout the results sections of this thesis. Secondary antibodies are detailed in Table 2.2.

Table 2.1 – List of primary antibodies used in this thesis

'M' indicates monoclonal. 'P' indicates polyclonal. The 'dilution' column notes the dilution factor at which each antibody was used during staining.

Antibody	Source	M	P	Supplier (Catalogue number)	Dilution
α-BAG-5	mouse	x		Höhfeld J., University of Bonn	10^{-3}
α-γ-tubulin	mouse	x		Sigma-Aldrich (T6557)	10^{-4}
α-Grp94	rat	x		Stressgen (SPA-850)	10^{-4}
α-Hsc70	rabbit		x	Stressgen (SPA-816)	10^{-4}
α-Hsc70/Hsp70	mouse	x		Stressgen (SPA-820)	10^{-4}
α-Hsp90	rabbit		x	Stressgen (SPA-846)	10^{-4}
α-HOP	mouse	x		Stressgen (SRA-1500)	10^{-4}
α-Luciferase	mouse	x		Höhfeld J., University of Bonn	10^{-4}
α-RTA	rabbit		x	Spooner R.A., University of Warwick	10^{-4}
α-TAg	mouse	x		Leppard K.N., University of Warwick	10^{-3}
α-Tau protein	mouse	x		Höhfeld J., University of Bonn	10^{-4}

Table 2.2 – List of secondary antibodies used in this thesis

'M' indicates monoclonal. 'P' indicates polyclonal. The 'dilution' column notes the dilution factor at which each antibody was used during staining.

Antibody	Conjugate	Source	M	P	Supplier (Catalogue Number)	Dilution
α-mouse / rat	AP	goat		x	Promega (S372B)	10^{-4}
α-rabbit	AP	mouse	x		Sigma-Aldrich (A1949)	10^{-4}
α-mouse	HRP	donkey		x	Fisher Scientific (SA1-100)	10^{-4}
α-rabbit	HRP	goat		x	Sigma-Aldrich (A0545)	10^{-4}
α-rabbit	Alexa-Fluor 680nm	goat		x	Invitrogen (A21076)	10^{-3}

2.2 DNA vectors

The following DNA vectors were used throughout this thesis. Note that this table mixes viral and plasmid vectors.

Table 2.3 DNA vectors used in this thesis

The experimental application of each is denoted by the columns labelled 'P' (indicates those vectors used for purification) and 'O' (those vectors used for over-expression studies in HeLa). The 'host' column denotes the organism from which the protein's DNA sequence was originally sourced. References are given to provide an example of the plasmids' prior uses. *Indicates work with this plasmid has not yet been published.

Protein	Host	Vector	P	O	Reference
BAG-1S	*H. sapiens*	pcDNA		x	Alberti *et al*., 2002
BAG-2	*H. sapiens*	pcDNA		x	Arndt *et al*., 2005
BAG-5	*H. sapiens*	pcDNA		x	Höhfeld J. (University of Bonn)*
CHIP	*H. sapiens*	pcDNA		x	Arndt *et al*., 2005
HIP	*R. rattus*	pcDNA		x	Demand *et al*., 1998
HOP	*R. rattus*	pcDNA		x	Demand *et al*., 1998
Hsc70	*R. rattus*	Baculovirus with pVL1393-*hsc70*	x		Höhfeld & Jentsch, 1997
Hsp40	*H. sapiens*	pET	x		Höhfeld & Jentsch, 1997
LacZ	*E. coli*	pcDNA		x	Ladds G. (University of Warwick)
RTA	*R. communis*	pUTA	x		Deeks *et al*., 2002
RTA^{0K}					
RTA^{6K}					
TAg	SV40 virus	SV40 virus		x	Stubdal *et al*., 1996

2.4 Solution composition

The following list details the composition of solutions referenced multiple times throughout the methods sections.

Bradford reagent (5× stock)	0.05% Coomassie Blue (w/v) 24% ethanol (v/v) 43% phosphoric acid (w/v)
Coomassie Blue solution	0.2% Coomassie Blue (w/v) 7.5% acetic acid (v/v) 50% ethanol (v/v)
de-stain	40% methanol (v/v) 10% acetic acid (v/v)
DMEM	See Dulbecco *et al.* (1959)
DMEM (supplemented)	As DMEM, plus: 10% FCS 0.4mM glutamine 25 units.mL^{-1} of penicillin 189 units.mL^{-1} of streptomycin.
lysis buffer	15mM Tris 150mM NaCl 1% triton X-100 (w/v) 0.1% SDS (w/v) 2mM NaN_3 15% glycerol (w/v) made to pH7.5 with HCl
PBS	8g.L^{-1} NaCl 0.2g.L^{-1} KCl 1.44g.L^{-1} $Na_2HPO_4.12H_2O$ 0.24g.L^{-1} KH_2PO_4 made to pH7.4 with HCl.
PBS-T	As PBS, plus: 0.1% $Tween_{20}$
trypsin solution	8g.L^{-1} NaCl 0.38g.L^{-1} KCl 0.1g.L^{-1} Na_2HPO_4 1g.L^{-1} glucose 3g.L^{-1} Tris 0.0015% phenol red (w/v) 2.5g.L^{-1} trypsin made to pH7.7 with HCl
TBS	10mM Tris 150mM NaCl; made to pH8 with HCl
TBS-T	As TBS, plus: 0.05% $Tween_{20}$ (w/v)
transfer buffer	14.42g.L^{-1} glycine 3.03g.L^{-1} Tris 0.1g.L^{-1} SDS 20% methanol (v/v)
Terrific broth	12g.L^{-1} tryptone 24 g.L^{-1} yeast extract 0.4% glycerol (v/v) 0.017M KH_2PO_4 0.072M K_2HPO_4
2YT	16g.L^{-1} tryptone 10g.L^{-1} yeast extract 5g.L^{-1} NaCl

2.5 Methods

The structure of this section is laid out in the order that the reader will encounter these methods in the results chapters.

2.5.1 Culture of HeLa cells

HeLa cells were grown as a monolayer in supplemented DMEM. Monolayers were cultured in 75mL Falcon flasks, or else flat-bottomed dishes. Monolayers were incubated at 37 °C with an ambient 5% $CO_{2(g)}$.

Cells were passaged after monolayers reached confluency. To do this, cells were first washed by flushing them with 5mL of trypsin solution. They were then incubated with a further 5mL of trypsin solution for 15 minutes at 37 °C with 5% $CO_{2(g)}$. An appropriate volume of the resultant cell suspension was then discarded, and the remainder diluted as desired with supplemented DMEM. Diluted suspensions were transferred to fresh 75mL Falcon flasks.

2.5.2 Assaying the IC_{50} of ricin to HeLa cells with respect to protein synthesis

2.5×10^4 cells in 100μL of DMEM were seeded into each well of a 96-well plate (an haemocytometer from Neubauer was used to calculate appropriate dilution factors). These plates were then left overnight at 37 °C with ambient 5% $CO_{2(g)}$.

Each 96-well plate was typically demarcated in halves, with one half (4 rows × 12 columns) constituting a coeval set of negative controls and the second half acting as the positive control. The cells upon one half of the plate will have typically been subjected to some form of pre-treatment, as described in the appropriate results section. After this period of pre-treatment, medium is removed and cells are treated with one of 11 graded doses of ricin in 100μL of supplemented DMEM. The ricin dilutions typically halve from a maximum concentration of 100ng mL^{-1} (variations as specified in text). One column of 1 × 8 wells is not treated with ricin, as a control. Note that, in experiments where the effects of pharmacological agents were tested, these agents were included during the ricin treatment as well.

After 4 hours of incubation with the graded doses of ricin (37 °C in 5% $CO_{2(g)}$), wells were washed with 100μL of PBS. Then, 1μCi of [^{35}S]-methionine in 50μL of PBS was added to each well. This labelled amino acid was incorporated into protein by the residual protein synthetic capability of the toxin and toxin-untreated cells. To enable this labelled, cells were

incubated for 30 minutes (37°C, 5% $CO_{2(g)}$). After labelling, wells were washed 5 times with 5% TCA (w/v in H_2O) to precipitate protein. Finally, 50µL of scintillant (Optiphase Supermix from Perkin Elmer) was added to each well and the fluorescence intensity across the plate measured by a scintillation counter (Microbeta Trilux 1450).

During data analysis, the fluorescence intensity from wells not treated with ricin was used as a standard for 100% protein synthesis. Note that positive and negative controls (i.e. inhibitor treated and inhibitor untreated cells, in most cases) possessed independent standards for this value (Figure 2.1). This accounted for the relative toxicity of different pre-treatments. The fluorescence intensity from wells containing each graded dose of ricin was then related to the 100% value for protein synthesis. This enabled the construction of a sigmoidal dose-response curve. A program developed by R.A. Spooner was then used to produce a line of best fit through the acquired data. The IC_{50} was calculated from the regression of this line. The IC_{50} of the positive control dataset was then compared to the IC_{50} of untreated cells to yield a fold-change in ricin sensitivity. This protocol is derived from that published in Spooner *et al*. (2006). Note that the overall toxicity of the pre-treatment itself could be determined by comparing the fluorescence intensity of ricin-untreated. The intensity from positive-controls was compared to negative-controls to get a percentage effect (Spooner *et al*., 2008).

Figure 2.1 Setup of the Cytotoxicity Assay

Diagram of the organisation of a 96-well plate.

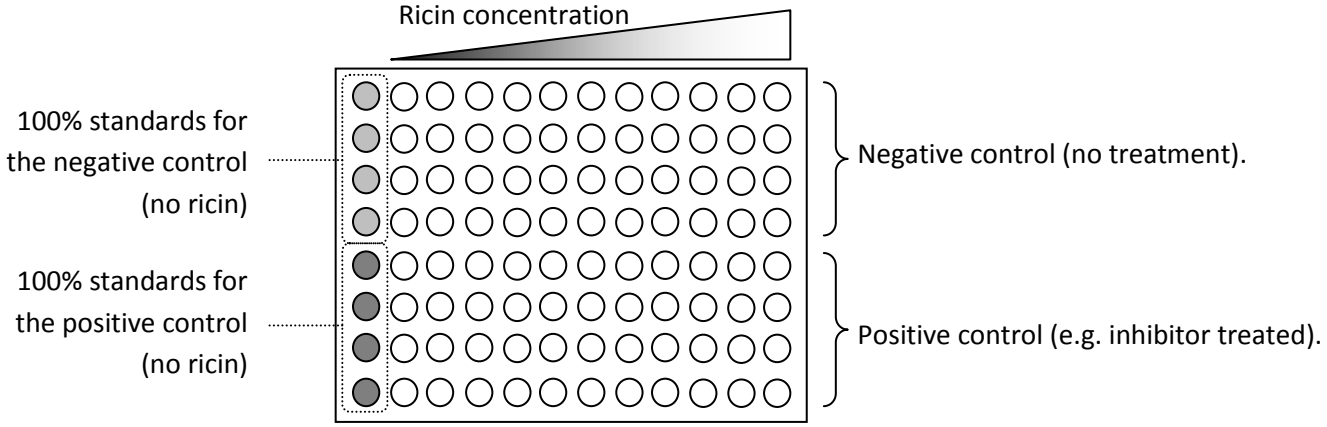

2.5.3 Assaying toxin trafficking time

Cells were seeded into a Falcon 96-well plate as before. Plates were divided in half, one half comprising the negative control and the other the positive (each half pre-treated as described in text). At strictly timed intervals, columns of wells were treated with a standard, killing dose of ricin (100ng mL^{-1}). As before, one 1 × 8 column of wells was no treated with ricin, to provide a standard for 100% protein synthesis. After incubation (37°C, 5% $CO_{2(g)}$), cells were then labelled with [^{35}S]-methionine (as before in section 2.5.2, for 30 minutes). The incorporation of this into acid-precipitable material was then quantified, also as in section 2.5.2.

The resultant data were assembled into a time-response curve (as per Hudson T.H. & Neville D.J., 1987). This plots the logarithm of protein synthesis vs. the length of ricin incubation. The linear phase of this plot is then regressed back to 100% protein synthesis. The time at which protein synthesis is equal to 100% is defined as the holotoxin's trafficking time. Positive controls were compared to appropriate negative controls (as described) to get a percentage change in trafficking time under various treatments.

2.5.4 Collection of detergent soluble lysates

Detergent-soluble lysates were collected from confluent monolayers cultured in 6 well plates. First, the plates containing monolayers were removed from the 37 °C incubator and cooled on ice for 5 minutes. The supplemented DMEM in which the monolayers had been cultured was then removed. Each of the wells was then washed twice with 1mL of PBS.

Lysis buffer containing Triton X-100 (and Complete protease inhibitors; one tablet per 50 mL) was added to each well (to a volume of 0.5mL). This was left for a period of 5 minutes, shaking on ice (or until cell membranes had dissolved, leaving punctuate nuclei – as observed by microscopy). After this period, the lysis buffer in each well was washed repeatedly over the residue of the monolayer until the remaining layer of organic material could be seen to detach. The resulting lysate was then collected in an Eppendorf tube and the 10000 ×*g* supernatant (10 minutes at 4 °C) collected. This final centrifugation step was to remove cell debris.

2.5.5 Bradford assay

The Bradford assay was used to determine the protein concentration of cell lysates. 1, 5 and 10 μL of the lysed sample was added to 1mL of 20% Bradford reagent (v/v) in water and the absorbance at 595nm recorded. A calibration curve was generated by producing an array of solutions at known concentrations of BSA (in an equivalent buffer to the samples tested). Absorbance was plotted against known protein concentration in Microsoft Excel, and the linear phase of the curve was regressed. The concentration of samples was then determined using the formula for the regressed equation and the absorbance of each sample (and appropriate dilution factor, where appropriate).

2.5.6 SDS-PAGE

Samples destined for SDS-PAGE were first mixed with loading buffer to make a final concentration (with sample) of 0.1% SDS (w/v); 0.0625M pH6.8 Tris/HCl; 1.25% β-mercaptoethanol (v/v) and 2.5% glycerol (w/v); and bromophenol blue (qs). These samples were boiled at 95°C for 5 minutes. They were then spun in a micro-centrifuge for 5 seconds and loaded onto a polyacrylamide gel.

The resolving portion of this gel constituted polyacrylamide to the concentration indicated in the appropriate results section (w/v; 38:1 with NN' methylene *bis*-acrylamide). The remaining constituents of the gel were as follows: 0.78M Tris/HCl pH9.2; 0.01% SDS (w/v); 0.01% ammonium persulphate (w/v) and 0.05% TEMED (v/v). The stacking portion of the gel constituted: 3.7% acrylamide (w/v; 38:1 with NN' methylene *bis*-acrylamide); 0.17M Tris/HCl pH6.8; 0.06% ammonium persulphate (w/v); 0.01% SDS and 0.3% TEMED (v/v).

After sample loading, gels were subjected to a current of 30mA through the stacking portion of the gel, and 45mA through the resolving portion. Empty lanes were loaded with an equivalent volume of loading buffer to prevent wavefront distortion.

2.5.7 Blotting of polyacrylamide gels onto nitrocellulose

After separation by SDS-PAGE, samples were blotted onto nitrocellulose (Hybond-ECL, Amersham, GE Healthcare). Sheets of nitrocellulose were sandwiched with the gel between two flat electrodes and filter paper (3mm, Whatman). The gel and filter paper were doused in transfer buffer. A current of 200mA was passed between the electrodes for 2 hours.

2.5.8 Immunostaining of nitrocellulose blots

Blotted nitrocellulose was first blocked from non-specific binding of antibodies by incubation in 5% non-fat Marvel (w/v) in TBS-T for 1 hour, while shaking. The nitrocellulose was then exposed to the primary antibody (at an appropriate dilution) in 1% non-fat marvel (w/v) in TBS-T for 1 hour and 30 minutes, while shaking. The antibody-stained nitrocellulose was then washed three times in 1% non-fat marvel TBS-T (w/v), for 15 minutes each time. The secondary antibody was then incubated in the same manner as the first, but in 1% non-fat marvel TBS-T for 1 hour and 30 minutes while shaking. The blot was then washed in 1% non-fat marvel TBS (without tween), thre times (for 15 minutes each time). Blots were developed using either ECL or AP protocols depending on the nature of the secondary antibody's conjugate.

2.5.8.1 Alkaline phosphatase development of nitrocellulose blots

Blots stained with secondary antibodies which were conjugated to alkaline phosphatase were developed according to the Promega protocol. The nitrocellulose was bathed in 5mL of 100mM Tris-HCl pH9.0; 150mM NaCl; 1mM $MgCl_2$; 0.33% (v/v) NBT; 0.165% (v/v) BCIP. BCIP and NBT were added last. Pink colour was allowed to appear on the blot until a desired intensity had been reached. At this point, the colour-producing reaction was stopped by the addition of 5mL of 0.2mM EDTA.

2.5.8.2 ECL development of nitrocellulose blots

Blots with secondary antibodies conjugated to horseradish peroxidise were developed in accord with the GE Healthcare protocol. Equal volumes of solution 1 (0.1M Tris / HCl pH8.5; 2.5mM luminol; 0.4mM coumaric acid) were added to solution 2 (0.1M Tris / HCl pH8.5; 0.018% H_2O_2). This was incubated for 1 minute at room temperature, shaking. The blots were then exposed to Kodak Biomax Scientific Imaging film for an empirically determined length of time. Exposed films were then processed in an AGFA Curix 60 X-ray film developer, as per the operator's instructions.

2.5.8.3 Odyssey imaging of nictrocellulose blots

The stages leading to visualisation of bands by this method were exactly as for AP and ECL protocols. However, PBS-T and PBS were used rather than TBS-T and TBS respectively. Additionally, incubation and washes with the secondary antibody were performed in the dark

to prevent bleaching of the fluorophore conjugate. The blot was dried in the dark between sheets of filter paper and scanned using a LICOR scanner.

2.5.9 Other staining techniques

2.5.9.1 Ponceau S staining of nitrocellulose blots

Nitrocellulose blots were washed in 5mL Ponceau S solution (0.1% Ponceau [w/v]; 5% acetic acid [v/v]) for 10 minutes. Background staining was then removed by washing the blot in distilled water until a good signal:noise ratio was achieved (as determined by eye). If this blot was to thereafter be used in an immuno-stain, residual Ponceau reagent was washed off using TBS before probing with antibody.

2.5.9.2 Coomassie staining after SDS-PAGE

After electrophoresis, acrylamide gels were evenly soaked in 10mL of Coomassie Blue solution. At a point where the gel had acquired a deep blue colour, the Coomassie solution was poured off and the gel was soaked evenly in de-stain solution (on a shaker). To achieve the appropriate ratio of signal:background staining intensity, the de-stain solution may have been replaced multiple times, as determined by eye.

2.5.9.3 Silver staining after SDS-PAGE

After electrophoresis, gels were washed in 50% methanol (v/v). The methanol solution was replaced every 30 minutes for a total incubation of 2 hours. The gel was then exposed to the silver stain (0.8% silver nitrate [w/v]; 1.4% ammonium [v/v]; 1.71% NaOH [w/v]; in water) for 5 minutes, whilst rocking gently on a shaker. The silver-loaded gel was then washed 4 times in distilled water, and left for 10 minutes, still shaking. Bands were produced by flooding the gel with silver stain developer (0.0125% citric acid [w/v]; 0.15% formaldehyde [v/v]). This developed the brown colour of stained bands. At an empirically determined endpoint, the development was halted by submerging the gel in de-stain.

2.5.10 Transformation of bacterial cultures with plasmid DNA

An aliquot of competent cells was thawed on ice (DH5α for plasmid amplification; JM101, or BL21 for protein expression, as stated). 2μL of plasmid DNA was then added to this aliquot and incubated on ice for a further 30 minutes. This mixture was then heat shocked at 42°C for 2 minutes and returned to ice for a further 5 minutes. If the plasmid contained a

kanamycin resistance gene, transformed cultures were then allowed to recover at 37°C for an hour before the next step. After recovery, or if the plasmid did not encode a kanamycin resistance gene, the transformed cells were spread on plates with nutrient agar containing the appropriate antibiotic (for selection of transformed colonies). Plates were then incubated overnight at 37°C.

2.5.11 Production of rubidium chloride competent cells

An aliquot of *E.coli* cells of the desired strain was thawed on ice and then inoculated into 10mL of SOB medium (20g.L^{-1} peptone; 5g.L^{-1} yeast extract; 10mM NaCl; 2.5mM KCl). This inoculated culture was then grown overnight at 37°C in a shaking incubator. After incubation, 500µL of the culture was used to inoculate 50mL of SOB medium (supplemented with 250µL of 1M $MgSO_{4(aq)}$ and 125µL of 2M $MgCl_{2(aq)}$). This culture was then incubated at 37°C until an optical density of 0.48 was reached (compared to medium alone, at a wavelength of 600nm). The culture was then placed onto ice for 15 minutes and the cell aggregate collected by centrifugation.

The cell aggregate was resuspended in 16.6mL of buffer (constituents: 100mM rubidium chloride; 50mM manganese chloride; 30mM potassium acetate; 10mM calcium chloride; 15% glycerol [w/v]) and put on ice for 15 minutes. The cell aggregate was, again, collected by centrifugation. This cell pellet was resuspended very carefully in 4mL of a different buffer (constituents: 10mM MOPS; 10mM rubidium chloride; 75mM calcium chloride; 15% glycerol [w/v]). The resuspension was then incubated on ice for 15 minutes before aliquoting (into 100µL volumes). Each aliquot was snap-frozen upon dry ice and then transferred to a -80°C freezer for long-term storage.

2.5.12 Purification of RTA

RTA was purified by a method that is described by Deeks *et al*. (2002). Appropriate plasmids were transformed into *E.coli* JM101 and grown in 50mL of Terrific Broth (overnight at 37°C). This starter culture was then inoculated into 500mL of 2YT media and grown for 2 hours at 30°C. Expression of ricin A chain was induced by adding IPTG to this culture to a final concentration of 1mM. Cells were then incubated for an additional 4 hours.

The RTA-expressing cells were finally harvested by centrifugation at 10000 ×*g*, resuspended in sodium phosphate buffer (pH6.4) and lysed by sonication. Cell debris was removed by another 10000 ×*g* centrifugation. The supernatant was loaded onto a 50mL carboxymethyl-

Sepharose CL-6B (Pharmacia) column equilibrated with the sodium phosphate (pH6.4) buffer. After washing with a further 1L of buffer to remove unbound material, 100mL of sodium phosphate buffer containing 100mM sodium chloride was passed through the column. A gradient of up to 300mM sodium chloride was then used to elute the column. Fractions containing RTA were identified by SDS-PAGE and pooled.

2.5.13 Reassociation of RTA and RTB

RTA was associated with RTB by a protocol also described by Deeks *et al*. (2002). 50µg of purified RTA was added to 100µg RTB (Vector Labs) in a total volume of 1mL PBS. Also contained in the PBS buffer was 0.1M lactose and 2% β-mercaptoethanol. This reducing mixture was dialysed overnight against the same buffer without any β-mercaptoethanol. This dialysed sample was then dialysed again, into simple PBS (no lactose; over the course of three nights).

Reassociated RTA and RTB was then purified from RTA by passing the dialysed solution down a 1mL agarose-immobilised lactose column (Sigma-Aldrich). This column was washed with PBS to remove unbound RTA. PBS containing 100mM galactose to elute reassociated holotoxin and monomeric RTB. The concentration of reassociated holotoxin was determined by silver-staining of the RTA band (after reducing SDS-PAGE in parallel to standards of known concentration).

2.5.14 The solubility assay

500ng of RTA was added to a volume of 20µL reaction buffer in an Eppendorf tube. The reaction buffer was 10mM MOPS-HCl; 50mM KCl; pH7.2. Other components may have been added as described in text, e.g. inhibitors, liposomes, cytosolic extracts, chaperones and ATP. This mixture was then centrifuged for 5 seconds in a microfuge to mix the components. Following mixing, samples were incubated at the indicated temperature (typically 37 ºC or 45 ºC) for 15 minutes. Samples were then spun at 16000 ×*g* for 10 minutes at 4 ºC. The supernatant and pellet were both retained. Each fraction was mixed with an appropriate quantity of loading buffer and boiled for 5 minutes. Boiled samples were then vortexed and spun in a microfuge for 5 seconds (vortexing and mixing was performed twice). Samples were separated in parallel by SDS-PAGE, then silver-stained. The intensity of neighbouring pellet/soluble RTA bands was quantified relative to one another using TotalLab.

Assays containing liposomes only - Where indicated in assays with liposomes, a detergent treatment may have been used after the incubation at the specified temperature. This treatment consisted of putting all samples on ice for 5 minutes after the 15 minute incubation. Triton X-100 was then added to the samples at a concentration of 1% (w/v) and left for ten minutes at room temperature (or an equivalent volume of buffer, in negative controls). The rest of the protocol was then elicited as normal.

Assays containing cytosol only - Some assays had a complex mix of proteins in the incubation, which posed difficulties in downstream SDS-PAGE analysis. In such cases, it was first determined whether any underlying band ran on the gel in a similar fashion to RTA (so determining whether quantification would be possible). In the case of incubations with cytosol, an equivalent concentration of pellet and soluble fractions from "cytosol alone" was loaded onto gels alongside pellet and soluble fractions from "cytosol with RTA". These "cytosol alone" lanes were used approximate the background signal emanating from the inclusion of cytosol during quantification by TotalLab.

2.5.15 The aniline assay (for quantifying the catalytic activity of RTA)

The aniline assays in this thesis were conducted with the same method as described by Chaddock *et al*. (1993). Yeast ribosomes were kindly provided by Dr. J. Cook, having been prepared also as described in Chaddock *et al*. (1993). Ribosomes were first incubated in buffer (25mM Tris-HCl; 25mM KCl; 5mM $MgCl_2$; at pH7.5) for 5 minutes at 30°C. The indicated concentration of RTA was then added. RTA and ribosomes were incubated together for 2 hours at 30°C to allow depurination. The reaction was then stopped by the addition of 0.5% SDS (w/v) in 50mM Tris-HCl (pH7.6). Ricin-treated rRNA was then phenol/chloroform extracted and treated with acetic aniline, pH4.5 (as described in Chaddock *et al*., 1993). This cleaves the phosphodiester backbone at the site of specific depurination by RTA. The resultant fragment band can then be visualised by separating the rRNA by denaturing agarose:formamide gel electrophoresis (see Chaddock *et al*., 1993), staining with ethidium bromid and quantification relative to untreated controls.

2.5.16 Production of liposomes

All lipids used in this thesis were obtained from Avanti Polar Lipids (Alabaster, Alabama). Liposomes containing 100% 1-palmitoyl-2-oleoyl-sn-glycero-3-phosphocholine (POPC) or 100% 1-palmitoyl-2-oleoyl-sn-glycero-3-[phosphor-L-serine] (POPS) were prepared using an Avestin Inc. (Ottawa, Canada) Liposofast extruder. The lipid was first dried of solvent (chloroform) by flushing with gaseous nitrogen overnight (at least 12 hours) under vacuum. Buffer (10mM MOPS; 50mM KCl) was added to make a final lipid concentration of 1mM. This suspension was freeze-thawed (dry ice / 37 ºC) 5× to reduce multilamellar vesicles. Vesicles were then flushed, at room temperature (21ºC) through the extruder (fitted with a 100nm pore size polycarbonate filter) using gaseous nitrogen 10×. Resulting liposomes were stored at 4ºC and used within a day.

2.5.17 Purification of Hsp40

Hsp40 was purified as per the method outlined in Minami *et al*. (1996). The pET/Hsp40 plasmid was transformed into *E.coli* BL21(DE3) cells and grown at 37°C overnight in 500mL of 2YT. 0.4mM IPTG was then added, and the incubation extended for another 2 hours. These Hsp40-expressing cells were lysed by sonication in a buffer (20mM MOPS-HCl; 20mM KCl; 1mM EDTA; pH7.2; 1mM phenylmethylsulfonyl fluoride). The 10000 ×*g* supernatant of the sonicate was loaded onto a DEAE-Sepharose column (GE Healthcare) and eluted with the MOPS-HCl buffer with an ionic gradient of 20mM to 100mM KCl. Fractions containing Hsp40 were determined by SDS-PAGE and Coomassie staining. Pooled fractions containing Hsp40 were then loaded onto a Source 30S column (GE Healthcare) and eluted with a graduated buffer containing 100-300mM KCl. Fractions were analysed by SDS-PAGE and Coomassie staining, again, to determine the Hsp40 fractions which were to be pooled.

2.5.18 Purification of Hsc70

Three 1L flasks of SF9 cells (at a density of 1.2 million cells per millilitre) were infected with baculovirus containing pVL1393-*hsc70* at a multiplicity of infection of 10:1. This was left shaking at 30°C for 3 days. Cells were induced to express Hsc70 with the addition of 1mM IPTG for 4 hours. The cell aggregate was then collected by centrifugation. Hsc70 was purified from these cells in a 3-stage process. Cells were first lysed in Buffer A containing 1% triton X-100 (this buffer's other constituents were as follows: 20mM MOPS-HCl; 20mM

KCl; 1mM EDTA; pH7.2; 1mM phenylmethylsulfonyl fluoride). The homogenate was centrifuged for 30 minutes at 14000 rpm in a Beckman JA-14 rotor. The supernatant from this centrifugation was then centrifuged again for a further 60 minutes, this time at 45000 rpm in a 45 Ti rotor. Three sequential columns were used to remove protein impurities. After each column, eluted fractions were analysed by SDS-PAGE and Coomassie staining for Hsc70 content and pooled for loading onto the next column. The columns were, in order: DEAE-Sepharose (GE Healthcare), which was eluted with Buffer A, with a gradient of up to 1M KCl. The second column was an ATP-agarose column (Sigma-Aldrich), which was eluted with Buffer A containing up to 2mM ATP. The third column used was a Source 30Q column (GE Healthcare), which was eluted with Buffer A (containing from 0 to 1M KCl).

2.5.19 Production of a cytosolic extract

3×75mL flasks of HeLa cells were incubated until they were occupied by confluent monolayers. The HeLa cells were then made into a suspension using trypsin solution. The cells were collected from this suspension by centrifugation (10000 ×*g*, 10 minutes). This was resuspended in 5mL of 10mM MOPS-HCl (pH7.2) / 50mM KCl and the cells lysed by being passed repeatedly through a narrow, ice-cold metal casing containing metal ball bearings. The resultant solution was clarified by an hour centrifugation at 120000 ×*g*. The supernatant was dialysed into 5L of 10mM MOPS-HCl (pH7.2) / 20mM KCl overnight to remove small molecules. The final cytosol preparation was aliquoted into 20µL volumes and snap-frozen on dry ice before storage at -80°C

2.5.20 Ubiquitination assay (mediated by Hsc70/CHIP)

The ubiquitination protocol is described in Arndt *et al.* (2005). Hsc70, CHIP (E3), Hsp40, E1 and E2 (UbcH5b) were mixed together in the concentrations indicated in the appropriate results sections, with the substrate. The total reaction volume was made up to 20µL. The constituents of the buffer into which these proteins were diluted was as follows: 20mM MOPS-HCl, pH7.2; 100mM KCl; 1mM ATP; 1mM DTT; 1mM $MgCl_2$; 0.001% phenylmethylsulfonyl fluoride). Ubiquitin was supplied at a concentration of 2mg.mL^{-1}. Reactions were incubated under the indicated conditions (usually 2 hours, 37°C). The reaction was stopped by addition of the reducing running buffer for SDS-PAGE.

Often, a pre-treatment is given before the addition of E1, E2, ubiquitin and CHIP. Where this is so, it is described in the appropriate results section.

2.5.21 Lipofectamine transfection

As described by the Invitrogen protocol, with the modifications mentioned in text.

2.5.22 Viral infection of HeLa cells

HeLa cells were seeded into flat-bottomed dishes at a density of 2.5×10^5 cells per millilitre and grown overnight in supplemented DMEM. In the morning, DMEM was washed off with PBS and left bare. At a multiplicity of infection of 10:1, virus-containing DMEM was added to the bare HeLa cell monolayers. The medium in which the virus was diluted contained no fetal calf serum. Infections in six-well plates used a total volume of virus of 200μL per well. In 96-well plates, 25μL was used per well. This virus solution was rocked over the monolayers once every 10 minutes for an hour. Supplemented DMEM was then added and the cells incubated for the desired length of time.

2.5.23 Measuring the turbidity of an RTA-containing incubation

Two approaches were used. In both methods, RTA was added to buffer (10mM MOPS; 50mM KCl; HCl to pH7.2) at a concentration as indicated. Depending on the method, this solution was then incubated in an Eppendorf floating in a 45°C water bath (20μL aliquots were taken at time points and their absorbance at 320nm recorded relative to buffer alone). Or else, alternatively, a cuvette with the solution in was placed in a spectrophotometer (hooked up to a water bath set to 45°C) and the absorbance at 320nm recorded at each timepoint was recorded over time (so negating the need for aliquots being taken).

2.5.24 Amplification of plasmid DNA

An aliquot of *E.coli* DH5α were transformed with the appropriate plasmid (as per 2.5.10) and then grown in 50mL of terrific broth overnight. The cell aggregate from this (the 10000 ×*g* pellet) was collected and resuspended in 5mL of buffer (50mM glucose; 10mM EDTA; 25mM Tris-HCl pH8.0). To this, 10mL of a solution containing 1% SDS (w/v) and 0.2M NaOH was added. This was mixed vigorously. After mixing, 5mL of a solution containing $250 g.L^{-1}$ potassium acetate and 15% acetic acid (v/v) was added. This was mixed and then centrifuged at 10000 ×*g*.

The supernatant was mixed with 20mL of isopropanol and incubated at -20°C for 10 minutes. Subsequent to this, the 10000 ×*g* (4 minutes) pellet was collected and dissolved in 1.5mL of TE (10mM Tris-HCl, 1mM EDTA, pH8.0). 2mL of 5M LiCl was added to the resuspension,

precipitating the RNA. RNA was removed by centrifugation at 10000 ×g for 4 minutes. The supernatant was resuspended in ethanol, mixed vigorously, and stored at -20°C for 4 hours. The 10000 ×g pellet (4 minutes), containing the plasmid DNA, was then collected and washed with 95% ethanol.

Contaminant RNA was degraded by resuspending the DNA pellet in 0.5mL TE with 40μg.mL^{-1} RNase A for 30 minutes at 37°C. Purified DNA was then precipitated with a buffer containing 20% PEG-8000 (w/v) and 2.5M NaCl. This DNA was collected by a 5minute spin at 13500 rpm in an Eppendorf micro-centrifuge; the pellet was dissolved in 0.5mL TE and subjected to phenol/chloroform extraction – twice – to remove contaminant protein. Finally, the DNA was precipitated from the chloroform by addition of 1mL ethanol and 50μL of 3M sodium acetate. The precipitate was collected by a final spin in a micro-centrifuge (5 minutes; 13500rpm). The pellet was washed with ethanol, air-dried and then dissolved in 0.5mL of TE. The optical density of this solution at 260nm was then measured (relative to TE alone) to determine the DNA concentration of the preparation.

CHAPTER 3:

Pharmacological inhibition of chaperones influences the cytotoxicity of ricin.

3.0 An introduction to why cytosolic chaperones might interact with RTA

RTA is thought to exploit an ERAD-like pathway in order to gain access to the cytosol. The pathway which facilitates this process in mammals is largely unknown. However, a route involving Hrd1, like in yeast (Li *et al*., 2010), is expected to be utilised. This is particularly so because cholera toxin A-chain (CTA1) has been shown to be retrotranslocated by its mammalian orthologues gp78/Hrd1 (Bernardi *et al*., 2010). More broadly, however, the facilitators of RTA's retrotranslocation will putatively fall under four classes:

(1) Recognition proteins.
(2) Membrane-bound proteins that form a pore.
(3) Cytoplasmic proteins which drive the extraction of RTA.
(4) Cytoplasmic proteins responsible for resolving RTA from a proteolytic fate.

Very little is known about the cytosolic interactions RTA makes in mammalian cells, except that the 26S proteasome is responsible for degrading two-thirds of the population which gains access to this compartment (Wesche *et al*., 1998). As evidence has already been acquired which suggests RTA interacts with certain chaperones of the mammalian ER lumen, it may be that RTA will also be recognised by chaperones in the cytosol. Slominska-Wojewodzcka *et al.* (2006) suggests that the ER lectin-like chaperone, EDEM, recognises ricin holotoxin, promoting delivery of RTA to the retrotranslocation apparatus. Their data, however, do not imply that EDEM is absolutely necessary for the intoxication process. It has also been shown that ricin holotoxin can be reduced to monomeric RTA and RTB by the ER-resident chaperone PDI (Spooner *et al*., 2004). However, PDI does not seem to be responsible for subsequently unfolding RTA (R.A. Spooner, personal communication). This differentiates it from CTA1, which uses the interaction to induce a translocation-competent, substantially-unfolded state (Moore *et al*., 2010).

More specific reasons exist for why RTA may be stabilised or else recognised by chaperones in the cytosol. RTA is effectively an orphaned subunit when isolated from RTB (Marshall *et al*., 2008) and may no longer constitute a 'native' protein from the perspective of the cytosol's quality control machinery. Monomeric RTA also bears a solvent-exposed hydrophobic C-terminus. This domain is crucial for cytotoxicity (Simpson *et al*., 1995). It is

thought that this domain could begin the membrane or chaperone interactions in the ER that lead to retrotranslocation (Day *et al.*, 2002; Mayerhofer *et al.*, 2009). These 'non-native' qualities would be transposed to the cytosol after retrotranslocation and could feasibly prompt recognition by quality control pathways therein. Moreover, to traverse the potentially narrow aperture of a membrane pore such as that of the Sec61 translocon (Van den Berg *et al.*, 2004; Tian & Andricioaei, 2006), RTA is likely to have to be partially-unfolded. For this reason it is thought that impediments to the unfolding of RTA hinder cytotoxicity (Beaumelle *et al.*, 2002; Argent *et al.*, 1994). As purified RTA cannot fold to an active conformation from a heat-induced molten globule *in vitro* (Argent *et al.*, 2000), a third party is invoked. This factor would assist RTA in regaining a catalytic conformation after retrotranslocation. It need not be a protein binding partner, but could be another quality of the cytosolic environment, such as the redox environment, pH, crowding or other.

Prior to this study, the only established third party for a putative, cytosolic reactivation process was the ribosome itself. Argent *et al.* (2000) observed that incubation of partially-unfolded, molten globule-like RTA with salt-washed ribosomes yielded active A chain. Inspired by this observation, it was proposed that the ribosomes studding the cytosolic surface of the ER provided a practically-situated scaffold upon which nascently retrotranslocated RTA could refold. However, given that chaperones like Hsc70 and Hsp90 are abundant and often involved in ERAD, this thesis investigates whether these evolutionarily-obligated facilitators of protein folding might supersede an interaction with the ribosome *in vivo*.

Both Hsc70 and Hsp90 have been ascribed roles in ERAD-like pathways before now (Alberti *et al.*, 2004; Gusarova *et al.*, 2001). Co-operating with them in this function is a cohort of co-factors which regulate their ability to help clients refold productively. They also interlink them with the ubiquitin-proteasome pathway (Ballinger *et al.*, 1999). This enables Hsc70/Hsp90 to allot conformationally aberrant clients for degradation if they bind recurrently (Ballinger *et al.*, 1999). Two substrates that are subjected to Hsc70- and Hsp90-dependent degradation and which are localised to the ER membrane are the non-native (albeit functional) transmembrane protein, $CFTR^{\Delta F508}$ (Alberti *et al.*, 2004) and the co-translationally, co-translocationally stalled ApoB (Gusarova *et al.*, 2001), which were introduced earlier in this thesis. As RTA crosses the ER membrane to get into the cytosol, it is possible that the topology of the toxin subunit appears analogous to that of $CFTR^{\Delta F508}$ or ApoB at an intermediate stage in the process. If this is the case, then RTA might interact

with Hsc70 and Hsp90 during its membrane transit in a way that is similar to how $CFTR^{\Delta F508}$ or ApoB do during their ERAD.

Like ApoB and $CFTR^{\Delta F508}$, it is plausible that the net outcome of this chaperone interaction with RTA may, likewise, be degradation. Indeed, a chaperone interaction could even mediate the post-retrotranslocational, lysine-dependent degradation of RTA that Deeks *et al*. (2002) observed. However, in contrast to ApoB and $CFTR^{\Delta F508}$, the significant phenotypic contribution of this interaction with RTA could be the *smaller* population that survives it and benefits from chaperone binding. After all, only a single cytosolic molecule of RTA is thought to be required to deactivate a cell (Lord & Roberts, 1998). With these ideas in mind, this thesis contemplates two possibilities; that Hsc70/Hsp90 might:

(1) Aid RTA attain an active conformation in the cytosol.
(2) Assign RTA to a proteolytic fate.

It may also be that recognition of RTA by Hsc70 and Hsp90 withstands the retrotranslocation process itself. These chaperones could influence the survival of RTA in a significant, chronic fashion as the toxin subunit diffuses between substrate ribosomes. This prospect is roundly considered.

3.1 Experimental approach

One of the core techniques used throughout this thesis is the cytotoxicity assay. This procedure is used to determine the IC_{50} of ricin, which is defined herein as the concentration of toxin that inhibits 50% of cellular protein synthesis under standardised culture conditions. To calculate this value, a dose-response curve is produced. This curve is constructed by treating parallel cultures of cells with serial dilutions of ricin. After a subsequent incubation to permit intoxication, the rate of residual protein synthesis is measured. This is achieved by labelling the intoxicated cells with [^{35}S]-methionine and quantifying the eventual incorporation of this radioactive amino acid into acid-precipitable protein (unincorporated [^{35}S]-methionine is washed away before quantification).

This technique provides a very sensitive method by which the effects of cytosolic RTA can be detected. Indeed, as RTA inhibits protein synthesis in a catalytic fashion, a single instance of cytosolic RTA may be sufficient to significantly compromise the functional ribosomal complement of an entire cell (Sandvig & Van Deurs, 2002). Thus, very small changes in the concentration of cytosolic RTA can have a significant effect upon the protein synthetic

capability of a cell. If the cytotoxicity of ricin is helped or hindered by a particular pre-treatment, or condition, then a shift in the dose-response curve relative to a series of untreated, parallel controls will be observed. On a linear plot of increasing relative protein synthesis (*y*-axis) vs. increasing ricin concentration (*x*-axis), a protective treatment will shift the curve to the right. Protein synthesis at each concentration of toxin will be bolstered. On the other hand, a sensitising treatment will shift the curve to the left, reducing the protein synthesis observed at each dose. By comparing such relative shifts, it is possible to screen for treatments which affect the intoxication process.

This technique is crucial for research into the mechanisms by which ricin invades the cytosol because only a small concentration of enzymatically active RTA ultimately reaches this destination relative to that which binds at the cell surface. To render a sense of proportion, it is estimated that a mere 5% of the ricin which is internalised from the cell surface reaches the TGN upon endocytosis (Van Deurs *et al.*, 1988). Thereafter, a much smaller portion of TGN-localised holotoxin will gain access to the ER because of vesicular recycling from the various intermediary compartments back to the cell surface (Van Deurs *et al.*, 1986). Moreover, when in the ER itself, because reduction by PDI and the acquisition of a translocation-competent state may be inefficient (Spooner *et al.*, 2004; Hudson & Neville, 1987), even less is expected to subsequently retrotranslocate. Finally, even after crossing the membrane into the cytosol, Deeks *et al.* (2002) showed that roughly two-thirds of RTA that does so is rapidly degraded by proteasomes.

This series of filtering steps means that a relatively tiny proportion of RTA eventually reaches the cytosol in a soluble, active conformation. This small yet significant quantity makes use of techniques like co-immunoprecipitation problematic. It is technically difficult to differentiate the significant sub-population of cytosolic RTA from the relatively vast majority of that which floods the secretory pathway and cell surface. If the binding with a hypothesised interacting protein is transient and the target protein is in huge excess, then the problem of identifying its interaction with RTA is multiplied. Instead, determining the IC_{50} of the toxin in a variety of controlled treatments provides a more practical experimental approach.

As inhibitors of Hsc70 and Hsp90 were commercially available and easily supplemented into this experimental system, it was immediately possible to test whether these chaperones were

important in the cytotoxicity of ricin. Table 3.1 introduces the panel of inhibitors which have been utilised throughout this thesis to this end.

Table 3.1 – Chaperone inhibitors and their targets.

*As primarily assigned to these inhibitors. Off-target effects do occur, and are evaluated throughout the discussion of results.

Inhibitor	Full designation	Target*	Reference
DSG	15-deoxyspergualin	Hsp70/Hsc70	Nadeau *et al.*, 1994.
GA	geldanamycin	Hsp90	Whitesell *et al.,* 1994.
RA	radicicol	Hsp90	Sharma *et al.,* 1998.
C01	C01018195	Hsp90	Sharp *et al.,* 2007.
NECA	N-ethyl-5'-carboxamido adenosine	Grp94	Immormino *et al*., 2004.

At this juncture, it seems pertinent to stress that the IC_{50} assay measures the average difference in toxicity between negative and positive control cells. That is, the effect is averaged over the entire population of intoxicated cells. This does not allow for the differentiation of discrete sub-populations of cells, which might be functioning in an operationally distinct manner. As a complementary or alternative technique, fluorescence-activated cell sorting (FACS) would allow for the resolution of any such distinct populations of cells, rather than an average measure like IC_{50}. Synthesis of a fluorescent reporter protein could be activated during intoxication, and the cells could then be counted after incubation by this technique.

3.2 Deoxyspergualin, an inhibitor of Hsc70, protects HeLa cells from ricin intoxication

Hsc70-type chaperones are inhibited by the peptidomimetic, deoxyspergualin (DSG), which structurally mimics a short peptide (Figure 3.1). Despite this similarity, DSG is not thought to bind to the peptide-binding domain of Hsc70, as a client protein would (Nadler *et al*., 1998). Rather, DSG binds to a C-terminal motif of the chaperone – the tetrapeptide 'EEVD'. This interaction stimulates the ATPase activity of Hsc70 *in vitro*, perturbing the dynamics of its normal interaction with clients (Nadler *et al*., 1998).

Figure 3.1 - The molecular structure of the Hsc70 inhibitor, DSG

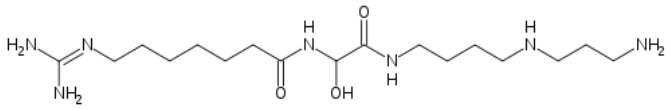

In vivo, it was observed by Jiang *et al*. (1998) that the disease-causing ERAD of mutant $CFTR^{\Delta F508}$ is rectified by treating host cells with DSG. This treatment disrupts an $Hsc70{\cdot}CFTR^{\Delta F508}$ complex, permitting the maturation and subsequent delivery of the functional protein to the plasma membrane, when it would otherwise be degraded (Jiang *et al.*, 1998). Subsequently, it has been shown that interplay of Hsc70 with specific, pro-degradation co-factors (i.e. BAG-1 and CHIP) is responsible for this degradation (Alberti *et al.*, 2004). DSG evidently prevents the overly-stringent degradation of $CFTR^{\Delta F508}$ by disrupting these complexes, alleviating the diseased phenotype (Jiang *et al.*, 1998). For this reason, DSG is currently being tested in clinical trials for cystic fibrosis.

The effect of DSG on the IC_{50} of ricin intoxication – As published by our laboratory in Spooner *et al.* (2008), when HeLa cells were treated with $50\mu g.mL^{-1}$ DSG[6] during intoxication with ricin, they were protected ~2-fold relative to untreated cells (Figure 3.2a & c). This implies that, at the IC_{50}, there is 50% less catalytic activity from cytosolic RTA in DSG-treated cells than there is in control cells. This 2-fold effect appears to be the maximum the dose can yield, given that pre-treatment for an hour does not yield any additional change in protection (as shown by the overlapping error bars in Figure 3.2c). Similarly, a protracted incubation for 16-hours results in little change in protection (Spooner *et al.*, 2008). This implies the effect of DSG results from an acute disruption of Hsc70 rather than an indirect, chronically-induced one. This would suggest that Hsc70 normally promotes the activity of RTA in target cells.

As an aside, it should be noted that DSG-treatments unavoidably included lactose, which is the excipient with which the inhibitor is stored after synthesis. However, any effects of this sugar (such as interfering with the binding of the lectin-bearing holotoxin to target receptors) have been accounted for by the treatment of control cells with an equivalent concentration of lactose.

[6] The concentration used in the rescue of $CFTR^{\Delta F508}$ *in vivo* (Jiang *et al.*, 1998)

The effect of DSG on ricin trafficking times – It was possible that treatment of cells with DSG could interfere with trafficking of ricin from the plasma membrane to the ER. This could be the case if significant trafficking proteins were Hsc70-dependent. Thus, a series of experiments were conducted which examined the length of toxin-incubation required before the first signs of ricin cytotoxicity could be observed (a technique described by Hudson & Neville, 1987). HeLa cells were challenged with a killing dose of ricin for varying lengths of time, after which their ability to incorporate [^{35}S]-methionine into nascent, acid-precipitable protein was examined. The length of time before the first signs of toxicity could be observed was then calculated and compared to parallel controls, giving an estimate of toxin trafficking time. Figure 3.2e shows the time-response curves generated from this assay, and Figure 3.2f shows the relative trafficking times that were quantified from them. These results were published in Spooner *et al*. (2008). DSG-treated cells have a trafficking time which is 103% that of controls (standard deviation, SD ±1%; n=3). This demonstrates that inhibition does not severely delay delivery of RTA to the cytosol.

The effect of DSG alone upon protein synthesis – Figure 3.2d shows that DSG has little effect upon protein synthesis by itself. Importantly, even if there were such an effect (as is the case for other treatments used later in this chapter), this would not contribute to the shift in the dose-response curve observed. This is accounted for: each dose-response curve is normalised to internal standards for 100% protein synthesis. For DSG-treated datasets, the 100% value for protein synthesis was provided by cells which were treated with DSG/lactose, and not with ricin. Similarly, for lactose-treated cells, the 100% standard was provided by cells which were treated with just lactose, but not with ricin.

Potential off-target effects of DSG - Although DSG affects Hsc70-type chaperones of the cytosol, it is important to stress that the lumenal paralogue of these chaperones, BiP, is unaffected by DSG. This is because it does not possess the C-terminus 'EEVD' motif (Brodsky, 1999). Therefore, if the protection owes to an effect upon the chaperone complement of the cell, BiP is probably not that which is affected. DSG does, however, have a putative effect upon the activity of cytosolic Hsp90, as this protein does bear the C-terminus 'EEVD' motif to which DSG binds (Nadeau *et al.*, 1994).[7] It was important to clarify whether the effects of DSG owed to an interaction with Hsc70 or with Hsp90.

[7] Note that the lumenal paralogue of cytosolic Hsp90, Grp94, is unaffected by DSG as it (like BiP) lacks the C-terminal 'EEVD' motif.

Figure 3.2 – The Hsc70/Hsp70 inhibitor, deoxyspergualin (DSG), protects cells from ricin.

HeLa cells were seeded into a 96-well plate at a density of 2.5 x 10^5 cells per well. They were then grown overnight at 37°C. Half were subsequently treated (for the time indicated) with:

- ● 100µg.mL^{-1} lactose and 50µg.mL^{-1} DSG, and the other half with:
- ○ 100µg.mL^{-1} lactose alone.

Serial dilutions of ricin were then added and the cells were incubated for 4 hours at 37°C. Subsequently, cells were washed with PBS and incubated with 1µCi of [^{35}S]-methionine per well for 30 minutes. Incorporation of this into acid-precipitable material was then quantified using a scintillation counter. a) Dose-response curves showing the protective effect of treating cells with DSG coeval to application of toxin (representative from a set of three). b) Shows the protective effect of a 1-hour pre-treatment with DSG before application of ricin (representative from a set of three). c) The average protective effect of acute and 1-hour pre-treatments with DSG, by comparison of IC_{50}. Cells treated with DSG coeval to application of toxin were protected 1.90-fold (standard deviation, SD: ±0.55; n=3) compared to control cells. Those cells pre-treated (denoted 'pre') for one hour with DSG were protected 2.02-fold (SD: ±0.38; n=3) relative to control cells. d) Shows the effect of DSG upon protein synthesis in the absence of ricin. In all cases, error bars show the standard error of the mean (SEM) between 3 independent sets of experiments.

e) Time-response curves showing the trafficking time of ricin. HeLa cells were seeded into each well of a 96-well plate and grown overnight at 37°C. At time nought, every well was supplemented with fresh medium containing 100µg.mL^{-1} lactose and 50µg.mL^{-1} DSG (●), or else with medium containing 100µg.mL^{-1} lactose alone (○). Each row of cells was then treated for a different length of time (as indicated) with a lethal dose of ricin (100ng.mL^{-1}). Residual protein synthesis in each well was then determined. Protein synthesis at each timepoint was normalised to controls not treated with ricin. Lines of best fit were then drawn through the exponential phase of the datasets and this portion of the data was regressed using Microsoft Excel. The time at which this equation satisfied 100% synthesis for each series was then used to compare control and inhibitor-treated cells. f) The trafficking time for DSG-treated cells was 103% of lactose-treated controls (SD ±1%; n=3; error bars show SEM).

(Figure 3.2 – continued.)

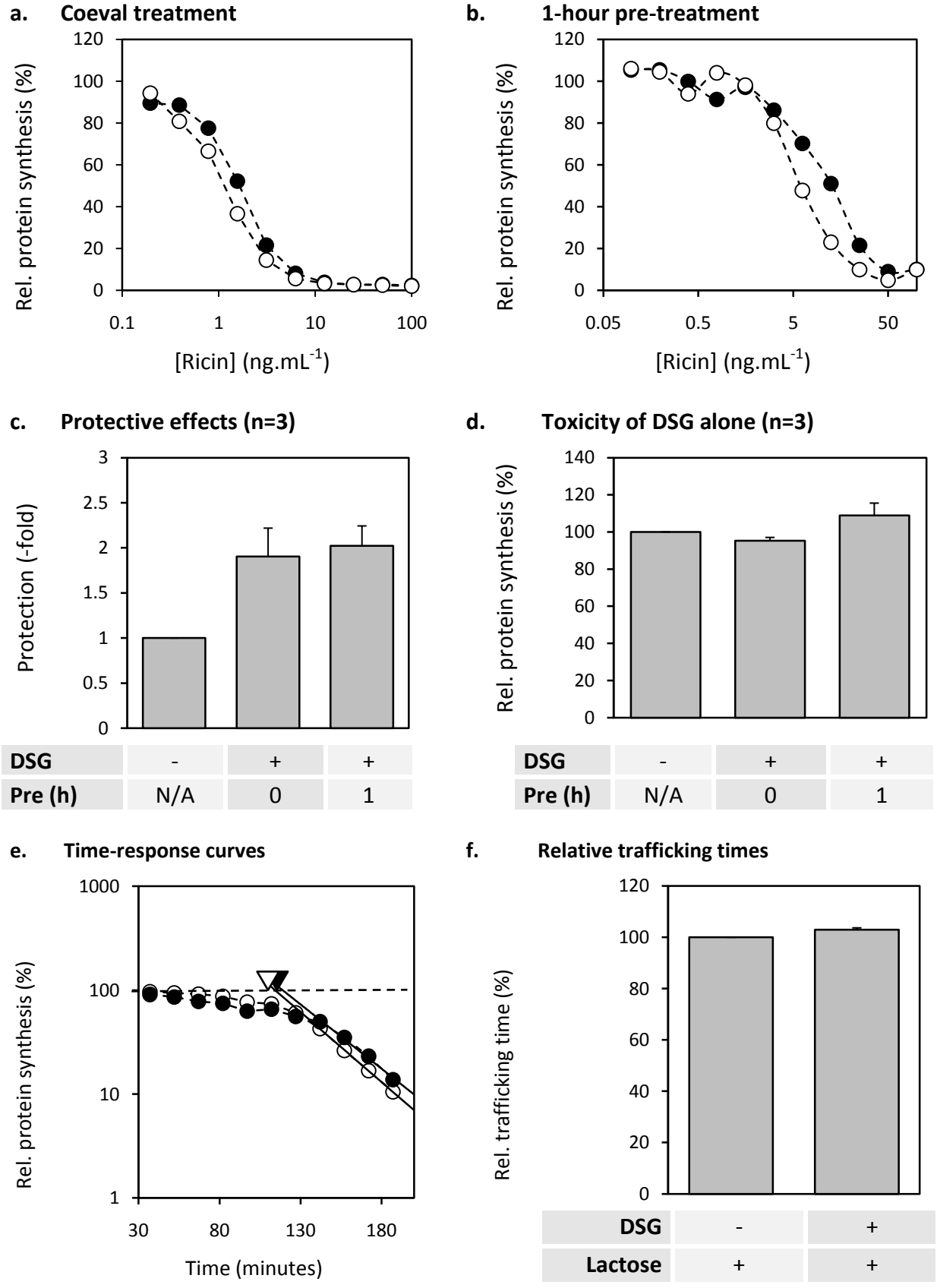

3.3 Inhibitors of Hsp90 sensitise HeLa cells to ricin intoxication

To distinguish the *potential* effect of DSG upon Hsp90 from its *well-established* effects upon Hsc70 (Jiang *et al.*, 2001), inhibitors of Hsp90-type chaperones were used in a similar set of assays. Three Hsp90-inhibitors were used, Figure 3.3. These were: geldanamycin (GA), radicicol (RA) and CCT018159 (C01). Advantageously, RA and GA are both known to have no effect upon the ATPase cycle of Hsc70 (Schulte *et al.*, 1998).

Figure 3.3 - Molecular structures of the three Hsp90 inhibitors: radicicol, CCT018159 and geldanamycin.

These chemical structures were rendered using two softwares: ISISDraw and PaintShopPro PHOTO X2.

a. radicicol (RA)

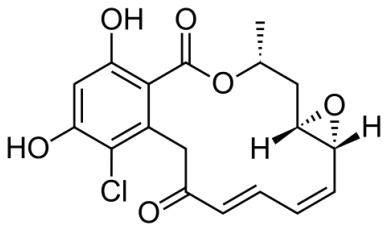

b. CCT018159 (C01)

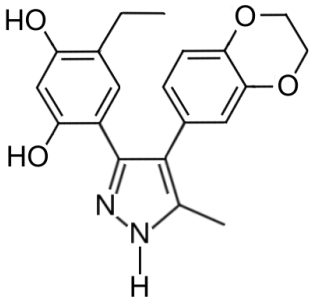

c. geldanamycin (GA)

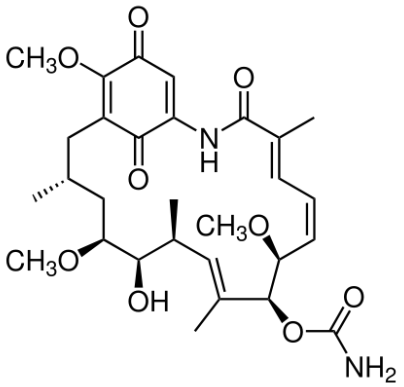

Each of these molecules has an affinity for the ATP-binding pocket in the N-terminal domains of the Hsp90 dimer (Schulte *et al.*, 1998). Their binding is therefore completely different to DSG. Despite no obvious, structural similarity each mimics the contacts that are made by ADP in the site where they bind (Roe *et al.*, 1999; Sharp *et al.*, 2007). Thus, they compete with nucleotide for occupancy of the site and render Hsp90 in a protractedly 'open' conformation (Roe *et al.*, 1999; Sharp *et al.*, 2007). Stebbins *et al.* (1997) proposed another mechanism. Stebbins *et al.* (1997) remarked upon the similarity of the N-terminal inhibitor-

binding pockets to substrate (peptide) binding sites. The authors postulate that clients may actually be bound in these sites during their interaction with Hsp90. If so, the binding of inhibitor might also compete with the client. Thus, the inhibitory effect of these compounds upon Hsp90 may be elicited by multiple mechanisms. The concerted effect would still be dissociation of Hsp90·client complexes.

Model clients which are dissociated from Hsp90 by GA/RA include: luciferase (Schneider *et al.*, 1996); the tyrosine kinase, src (Whitesell *et al.*, 1994); glucocorticoid receptors (Whitesell & Cook, 1996); and the oncogenic Raf (Sharma *et al.*, 1998). Importantly, this has variable, substrate-dependent outcomes. In the case of luciferase, dissociation leads to increased degradation if the luciferase has been heat-treated. In this case, the lack of interaction with Hsp90 evidently leaves the client in a state vulnerable to proteases (Schneider *et al.*, 1996). In the case of the glucocorticoid receptor, inhibition of Hsp90 results in the loss of its functional signalling from target cells. However, it is thought that the receptor persists in an immature, non-signalling state rather than being degraded (Whitesell & Cook, 1996).

Similarly, Loo *et al.* (1998) showed that 0.18μM (0.1μg.mL^{-1}) geldanamycin prevents the maturation of the ERAD candidate CFTR^{WT} when applied to cells stably-expressing the protein. The authors infer that an interaction of Hsp90 with CFTR^{WT} is important for its maturation from the ER. This contrasts to the maturation-prohibiting effect that Hsc70 has upon CFTR$^{\Delta F508}$ (Jiang *et al.*, 1998).

3.3.1 The effect of geldanamycin on ricin intoxication

HeLa cells were treated with 1μM GA whilst challenged with ricin. Compared to control cells, which were simply treated with DMSO (the solvent in which GA was dissolved), GA-treated cells were unexpectedly sensitised ~2-fold to ricin (Figure 3.4). GA, itself, appears toxic to HeLa cells (Figure 3.4c), but as the dose-response curves for each treatment were normalised to internal controls, this effect is compensated for in the determination of the IC_{50}. These results were published by our laboratory in Spooner *et al*. (2008).

This sensitisation obviously opposes the effect of DSG (a ~2-fold protection), and implies that approximately twice as much toxin reaches the cytosol in an active conformation when Hsp90 is inhibited in this manner. First, this evidence helps to clarify that the protection

caused by DSG does not result from an inhibitory effect upon Hsp90. Second, it would seem that Hsc70 and Hsp90 antagonise each other's role in the intoxication process:

(1) On one hand, Hsc70 promotes the activity of RTA in the cytosol.
(2) On the other hand, the action of Hsp90 inhibits the activity of RTA in the cytosol.

The effect of GA on ricin trafficking times - Like for DSG, it was important to determine whether GA had an effect upon the retrograde transport of ricin through the secretory pathway. This was especially important as Hsp90 inhibition reportedly interferes in the function of Rab proteins (Barzilay *et al.*, 2004; Liu *et al*., 2009) and ricin trafficking has been shown to be dependent upon Rab proteins, e.g. Rab6A and Rab6A' (Utskarpen *et al.*, 2006). There was effectively no difference between GA-treated and control cells (GA-treated cells had a trafficking time 101% that of controls; SD ±11%; n=3; as published in Spooner *et al*., 2008). The sensitising effect of GA resulted from a post-trafficking event.

Potential off-target effects of GA - As well as three cytosolic isoforms of Hsp90, mammalian cells also possess a lumenal paralogue, Grp94 (Chen *et al.*, 2005). It is possible that GA inhibits this lumenal counterpart, which has been implicated in delivering ERAD substrates to the retrotranslocation apparatus. The ERAD client α1-AT NHK is thought to be one such Grp94 client (Eletto *et al*., 2010). Because of this potential conflation, it was important to investigate whether the effect of geldanamycin resulted from an effect upon cytosolic or lumenal Hsp90 paralogues.

Figure 3.4 – The Hsp90 inhibitor, geldanamycin (GA), sensitises cells to ricin.

HeLa cells were treated with 1μM GA coeval to ricin-treatment, but otherwise treated as before. a) A typical set of dose-response curves from a total of three independent experiments, comparing cells treated with medium containing DMSO (○) to medium laden with GA (●). b) This yielded a 2.14-fold sensitisation (SD ±0.80; n=3). c) Shows the effect of GA incubation alone upon protein synthesis, relative to DMSO-treated cells. d) Trafficking times were calculated as before. Trafficking time of GA-treated cells was 101% (SD ±11%; n=3) that of DMSO-treated controls. In all cases, error bars show the SEM between four independent sets of experiments.

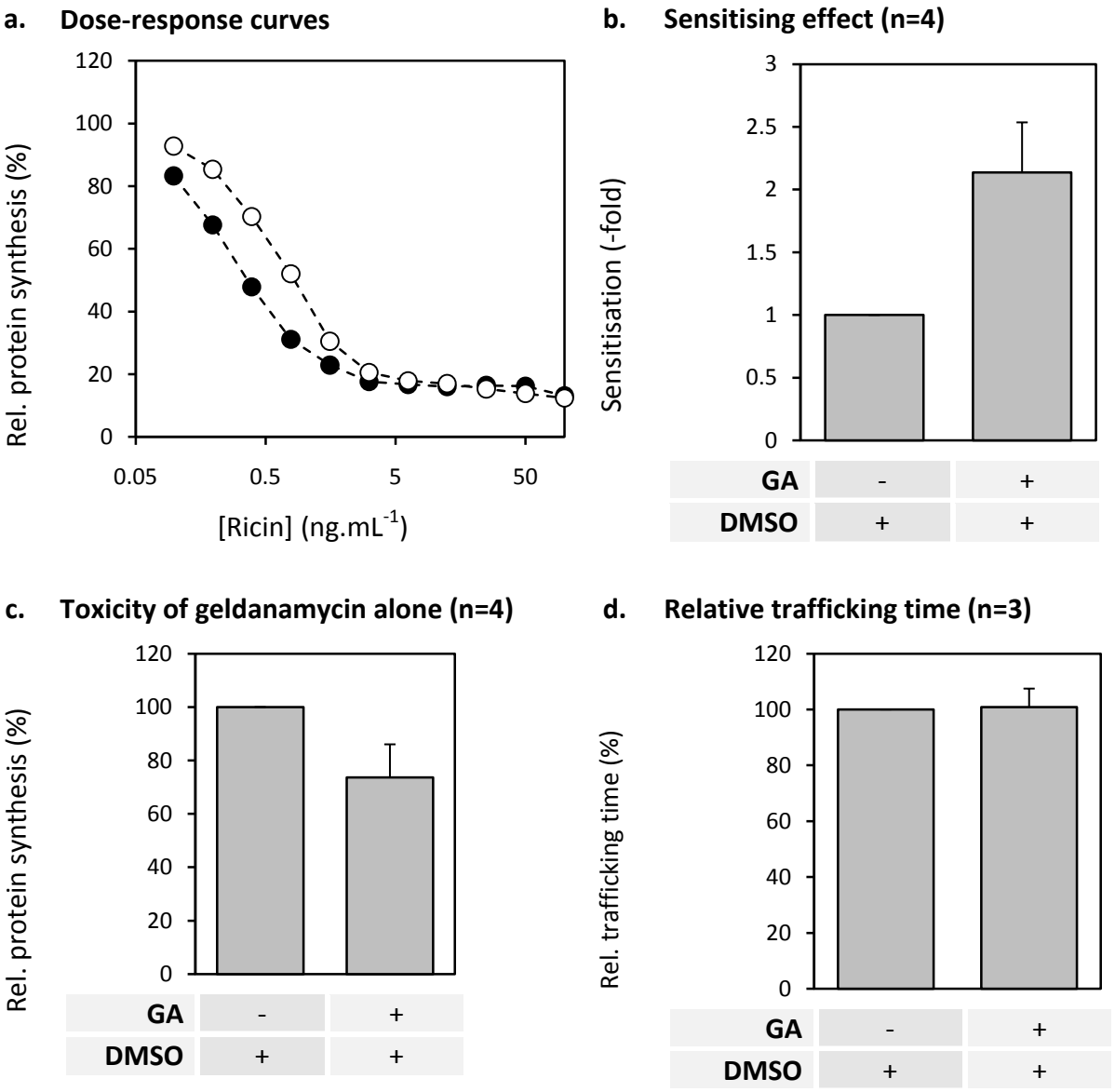

3.3.2 The effect of radicicol on ricin intoxication

The Hsp90 inhibitor, radicicol (RA), has a five-fold reduced affinity for Grp94 than GA (Barzilay *et al.*, 2004; Taylor *et al*., 2010). Therefore, its relative effect upon Grp94 will be diminished. Nonetheless, RA is still regarded as an inhibitor of Grp94 (Eletto *et al.*, 2010). When HeLa cells were treated with 1μM RA, they were sensitised 1.71-fold (SD ±0.46; n=3) to ricin (Figure 3.5a & b). These results were published in Spooner *et al*. (2008). This value is approximately equivalent to that of geldanamycin (2.14-fold sensitisation; SD ±0.80; n=3). Like GA, it appears that this effect also resulted from a post-trafficking interaction, as the trafficking time was similar to control cells, Figure 3.5d (published in Spooner *et al*., 2008).

3.3.3 The effect of CCT018159 on ricin intoxication

Finally, the Hsp90 inhibitor, CCT018159 (C01), was examined for its effects on ricin intoxication. C01 was used at a concentration of 3.2μM (its IC_{50} with respect to the ATPase activity of mammalian Hsp90-β *in vitro* – Sharp *et al.*, 2007). This treatment sensitised cells to ricin (Figure 3.6), but to a greater extent than either GA or RA: 2.36-fold (S.D. ±0.24; n=3). C01 also had demonstrably little effect upon trafficking time (Figure 3.6d).

Unfortunately, little data exists to show whether C01 possesses off-target effects on lumenal Grp94. However, it has – like GA and RA – no effect upon the ATPase activity of Hsc70 (Sharp *et al.*, 2007). The greater sensitisation this chemical causes could obviously result from a variety of possibilities: unknown off-target effects; a greater inhibitory effect upon Hsp90; or even a reduced rate of removal from the cell by P-glycoprotein (Sharp *et al.*, 2007).

Remaining problems with interpreting the results of Hsp90 inhibition - Despite the reliably sensitising effects of each Hsp90 inhibitor, problems interrupt the straightforward interpretation of these results. For instance it is possible each inhibitor affects Grp94. Moreover, inhibition of Hsp90 leads to the induction of Hsp70 expression in the cytosol (Shen *et al.*, 2005; Shu *et al.*, 2005). The following sections attempt to clarify whether each of these effects contribute to the sensitisation observed here.

Figure 3.5 – The Hsp90 inhibitor, radicicol (RA), sensitises cells to ricin.

HeLa cells were treated with 1μM RA coeval to ricin-treatment, but were otherwise treated as before. a) A typical set of dose-response curves from a total of three independent experiments, comparing cells treated with medium containing DMSO (○) to medium laden with RA dissolved in DMSO (●). b) This produced a 1.71-fold sensitisation (SD ±0.46; n=3). c) Shows the effect of RA incubation alone upon protein synthesis, relative to DMSO-treated cells. d) Trafficking times were calculated as before. Trafficking time of RA-treated cells (●) was 93% (SD ±8%; n=3) that of DMSO-treated controls (○). In all cases, error bars show the SEM between three independent sets of experiments.

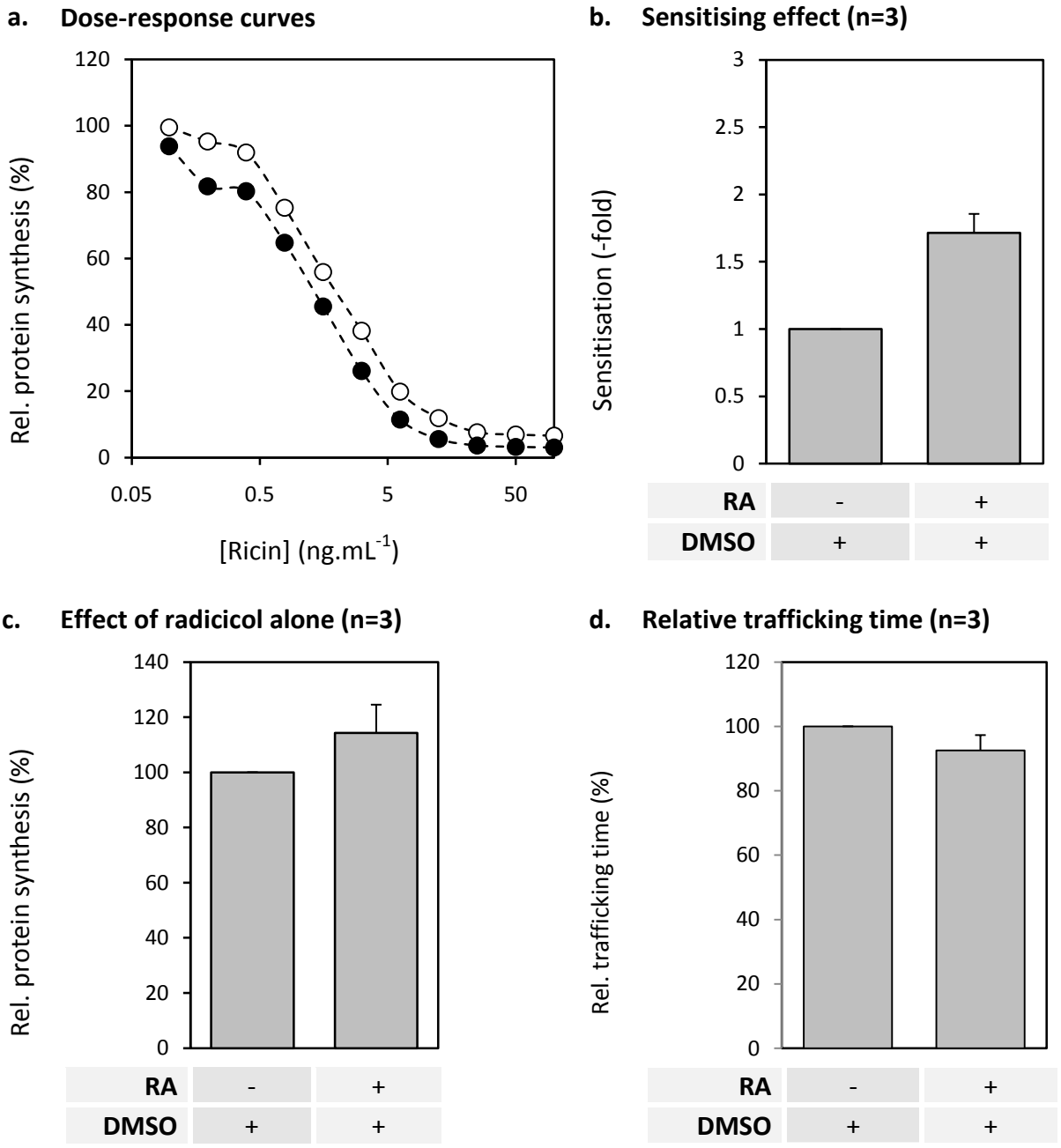

Figure 3.6 – The Hsp90 inhibitor, C01018159 (C01), sensitises cells to ricin.

HeLa cells were treated with 3.2µM C01 coeval to ricin-treatment, and otherwise treated as before. Controls were treated with DMSO as this was the solvent in which C01 was dissolved. a) A typical set of dose-response curves from a total of three independent experiments, showing C01-treated cells (●) and cells treated with an equivalent volume of DMSO (○). b) This produced a 2.36-fold sensitisation (SD: ±0.24; n=3). c) Shows the effect of C01 incubation alone upon protein synthesis, relative to DMSO-treated cells. d) Trafficking times were calculated as before. Trafficking time of C01-treated cells (●) was 97% that of DMSO-treated controls (○). (SD ±6%; n=3.) In all cases, error bars show the SEM between three independent sets of experiments.

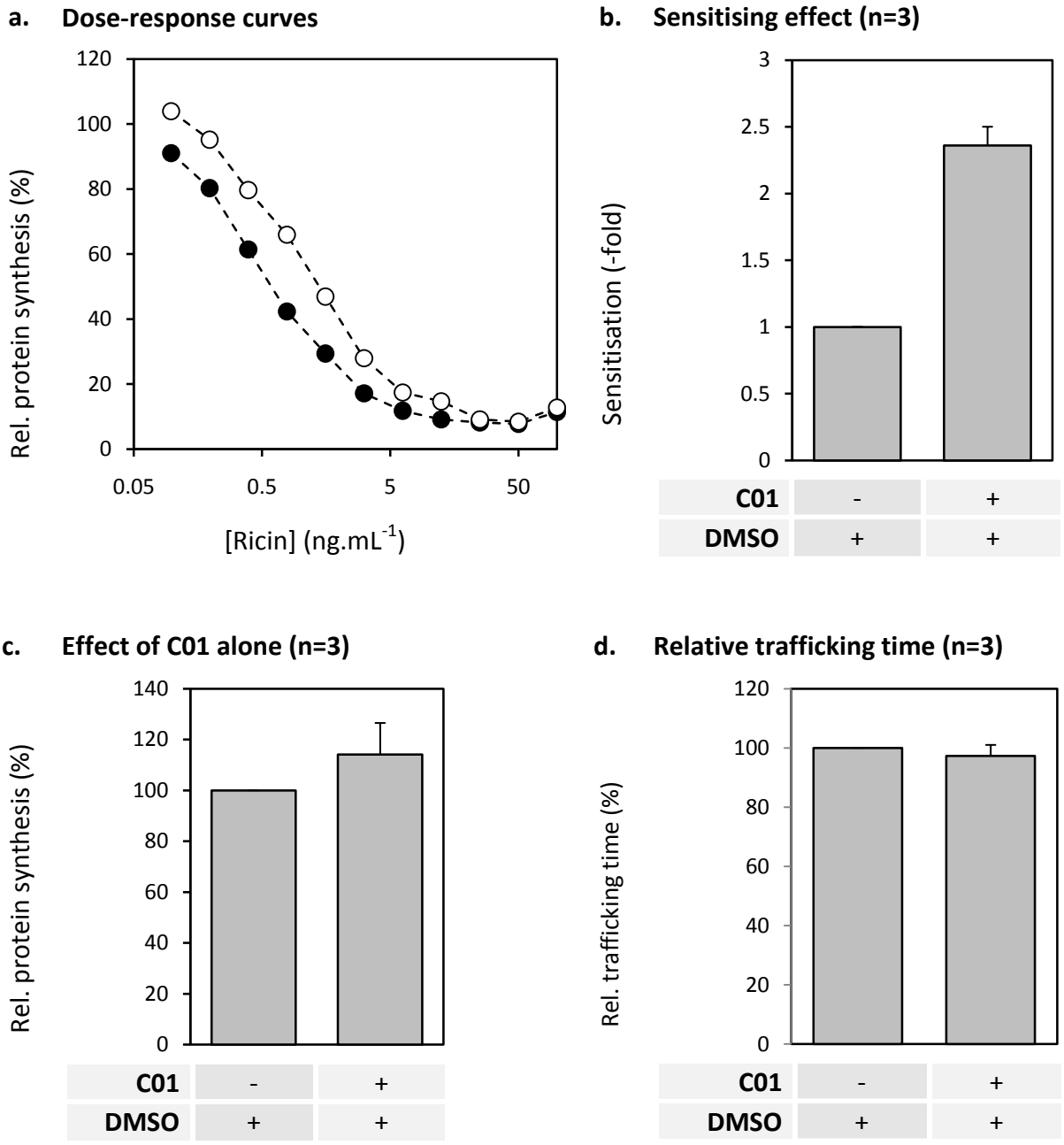

3.4 The effect of N-ethyl-5'-carboxamido-adenosine (NECA) on ricin intoxication

NECA is a Grp94-specific inhibitor which does not bind to cytosolic Hsp90 (Rosser & Nicchitta, 2000; Eletto *et al*., 2010). Thus, it may be used as a tool to differentiate the activities of cytosolic Hsp90 from Grp94. As published in Spooner *et al.* (2008), when HeLa cells were treated with 1μM NECA, they were *protected* 1.48-fold (SD ±0.24; n=5) relative to DMSO-treated controls (Figure 3.7a & b). Much like with the other inhibitors, the trafficking time of the ricin holotoxin appeared unaffected (Figure 3.7d). Feasibly, Grp94 could aid with the presentation of the RTA to the retrotranslocation apparatus (as it does for α1-AT NHK - Eletto *et al*., 2010). The low degree of protection could reflect how the pathway is redundant with other routes, or that NECA is not a very effective Grp94 inhibitor.

It may seem odd that paralogues Grp94 and Hsp90 direct opposite outcomes for RTA. However, these chaperones are divided by a membrane which demarcates separate 'ambitions' for the toxin subunit. Lumenal RTA requires recognition as an ERAD substrate to attain a cytosolic localisation. Being recognised as misfolded in the ER is thus a boon for the activity of the toxin. Contrastingly, having attained a cytosolic localisation, being recognised as misfolded will retard its activity by increasing the chances it is degraded. Therefore, this model suggests Grp94 and Hsp90 have a united tendency to recognise RTA as misfolded.

Unfortunately, it is important to note that NECA possesses off-target effects. For example, it is an agonist of adenosine receptors and inhibits both cAMP and cGMP phosphodiesterases (Brambilla *et al.*, 2000). Intracellular signalling caused by these effects might alter the quality of the cytosolic environment into which RTA enters. The coeval application of the inhibitor with the application of toxin would have partially limited such chronic, induced effects. Nevertheless, it stands to reason that the protective effect of NECA could be pleiotropic.

Figure 3.7 - *N*-ethylcarboxamidoadenosine (NECA) protects cells from ricin.

HeLa cells were treated with 1µM NECA coeval to ricin-treatment, and otherwise treated as before. Controls were treated with DMSO as this was the solvent in which NECA was dissolved. a) A typical set of dose-response curves from a total of three independent experiments, showing NECA-treated cells (●) and cells treated with an equivalent volume of DMSO (○). b) This produced a 1.48-fold protection (SD ±0.34; n=5). c) Shows the effect of NECA incubation alone upon protein synthesis, relative to DMSO-treated cells. d) Trafficking times were calculated as before. Trafficking time of NECA-treated cells (●) was 96% (SD ±3%; n=3) that of DMSO-treated controls (○). In all cases, error bars show the SEM between three independent sets of experiments.

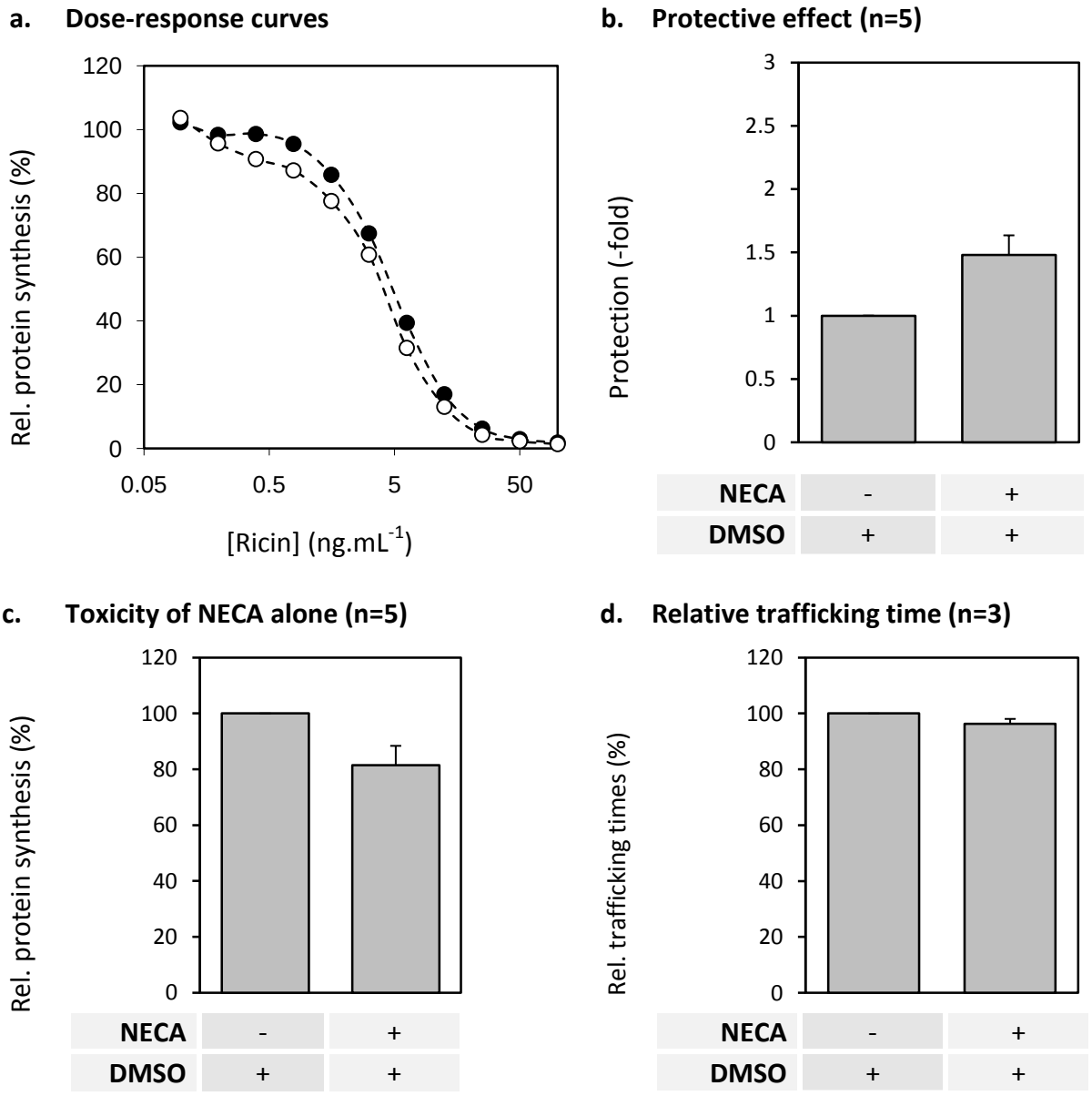

3.5 Hsp90 inhibitors induce the expression of Hsp70.

It is consistently observed that inhibition of Hsp90 induces the expression of cytosolic Hsp70, even at concentrations of as little as 1μM (Shen *et al.*, 2005), such as is used throughout this thesis. This effect is dependent upon the transcription factor, Heat shock factor 1 (HSF1; see Shen *et al.*, 2005). Normally, Hsp90 interacts with HSF1 and masks nuclear localisation sequences on this cytosolically located transcription factor. However, when Hsp90 is inhibited (or binding to a sudden surfeit of unfolded clients), HSF1 sheds its contingent of chaperones and is transported to the nucleus. Therein it *trans*-activates genes with heat shock elements to their promoters, including Hsp70 (Shen *et al.*, 2005).

As the protective effect of DSG upon ricin intoxication indicated a role for Hsc70-type chaperones in the cytotoxicity of ricin, it was important to determine whether the phenomenon of Hsp70 up-regulation caused the sensitising effects of GA/RA/C01 treatments. Figure 3.8 shows two immunoblots where HeLa cells have been incubated with either RA or GA, confirming that induction of Hsp70 occurs under our laboratory conditions (published in Spooner *et al*., 2008). Inducible Hsp70 is noticeably up-regulated at 4-hours post-incubation.[8] Examination of the same lysates for cytosolic Hsp90 shows no obvious change in levels. Grp94, on the other hand, is visibly up-regulated at least 8-16 hours after treatment (as shown by very weakly-stained bands marked out be black arrowheads in Figure 3.8). Lawson *et al*. (1998) report that both ER-resident Grp94 and BiP are induced under similar conditions.

In the preceding sections, the sensitising effects of GA, RA and C01 were determined after a coeval treatment of ricin and inhibitor. Because of this it was expected that the change in IC_{50} observed would be a result of acute effects rather than chronic, induced ones such as changes in protein expression. However, residual protein synthesis in prior assays was measured after a total period of 4 hours' incubation. It might be, therefore, that the level of Hsp70 (or of BiP/Grp94) increases swiftly enough in response to GA/RA to have a significant effect upon the intoxication process. On the other hand, delivery of the significant portion of active toxin to the cytosol takes closer to ~1 hour after binding to the cell surface

[8] Reassuringly, these observable changes in expression provide evidence that RA and GA are both functional under the conditions used in this thesis.

than 4 hours (Hudson & Neville, 1987; Spooner *et al*., 2008). Thus, the matter needed testing.

Figure 3.8 – Cells incubated with either RA or GA display increased levels of Hsp72 and Grp94, but constant expression of Hsp90

Cells were incubated with 1μM of the indicated inhibitor for the indicated length of time, or with DMSO for 16 hours (-). Detergent soluble lysates were then collected, analysed by SDS-PAGE, blotted onto nitrocellulose and immunostained for the indicated proteins and γ-tubulin (as a loading control). Bands were visualised by an alkaline phosphatase development. As Grp94 bands are faintly stained, they have been highlighted using black arrowheads.

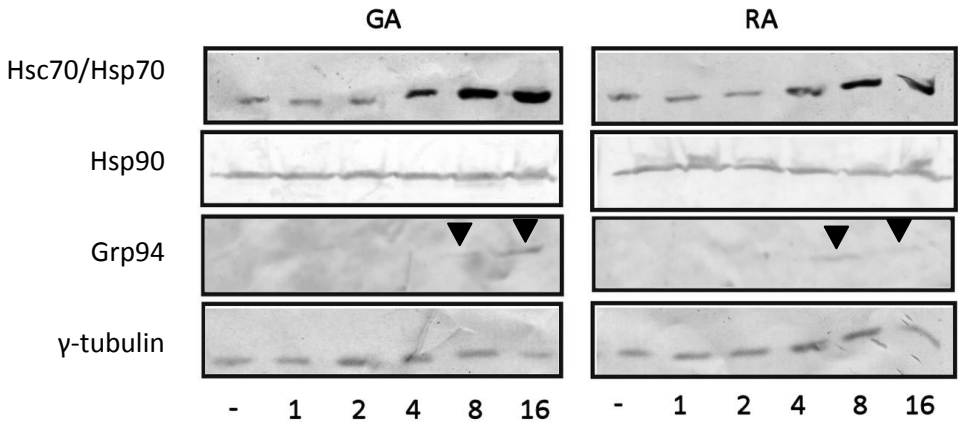

3.5.1 The effect of chronic incubation with Hsp90 inhibitors upon ricin intoxication

Cells were incubated from 0 to 16 hours with either GA or RA, and then assayed for their sensitivity to ricin relative to DMSO-treated controls. Upon lengthened incubation, the sensitising effects observed with RA and GA treatments were found to diminish (Figure 3.9). After 16-hours of pre-incubation, cells were even *protected* from ricin (N.B., 'protection' is any value of less than 1-fold sensitisation). This transition to protection implies a separate effect is induced by the treatment rather than the inhibitor simply becoming ineffective over time. The reciprocal of the sensitisation index gives the protective effect, which is 1.43-fold in the case of a 16-hour pre-treatment with RA (SD ±0.21; n=3) and 2.13-fold in the case of GA (SD ±0.18, n=4).

As a rise in Hsp70 levels correlate to this shift from sensitisation to protection, they may account for it. Alternatively, a rise in the expression of ER chaperones Grp94/BiP might be the cause. On the other hand, acute inhibition of Grp94 and Hsc70-type chaperones both resulted in protection. Therefore, another question arises: why would promoting their activity by increasing their expression also lead to protection? Rational suggestions can be made to explain such a disparity, if induction of Grp94/Hsp70 is responsible for the chronic effect of GA/RA:

(1) Inducible Hsp70, which is weakly expressed in unstressed conditions (Callahan *et al.*, 2002), may treat RTA differently from Hsc70. Indeed, its effects are not strictly being examined under DSG-treatments. Thus, although it is similar to Hsc70, Hsp70 might hinder RTA. Such differentiation has precedents:

   a. Hsp70 has increased affinity for clients than does Hsc70 (Callahan *et al.*, 2002), changing the dynamics of an interaction with RTA.

   b. Hsc70 and Hsp70 have opposite effects upon the maturation and degradation of epithelial sodium channels (Goldfarb *et al.*, 2006).

(1) Increased Hsp70 may dilute a relatively static background of deterministic co-factors. Thus, antagonism may exist between co-factor independent activities of Hsc70/Hsp70 and the impositions made upon them by the quality of the co-chaperone environment.

(3) Up-regulation of Grp94 (or BiP) might alter the dynamics of the chaperone matrix, altering the balance between client sequestration in the ER and client ERAD.

The effect of chronic Hsp90 inhibition may not necessarily be associated directly with chaperones either. Imai *et al*. (2003) showed that prolonged inhibition of Hsp90 leads to the reduction of 26S proteasome complexes, and a general reduction in the abundance of the 19S cap. It could be that this modification interferes with retrotranslocation, as the proteasome has previously been hypothesised as a motor driving extraction of misfolded polypeptides from the ER (Kalies *et al*., 2005; Lipson *et al*., 2008), and has been shown to be involved in the retrotranslocation of RTA in yeast (Li *et al*., 2010).

Figure 3.9 – Chronic pre-treatment with both GA and RA protect cells from ricin.

HeLa cells were pre-incubated (pre) with 1μM GA for a) 0-, b) 4-, c) 8- and d) 16-hours before ricin-treatment. Dose-response curves from each assay are shown, comparing cells treated with medium containing DMSO (○) to medium laden with GA and DMSO (●). e) and f) Show, respectively, the tabulated and graphical changes in the IC_{50} of ricin under these conditions relative to DMSO-treated controls. g) - l) Show figures equivalent to a) through f), but where 1μM radicicol was used rather than geldanamycin. Error bars show SEM in all cases.

Figures a) through f) are on the next page.

g) through to l) are on the subsequent page.

a. 0-hour (coeval) GA incubation

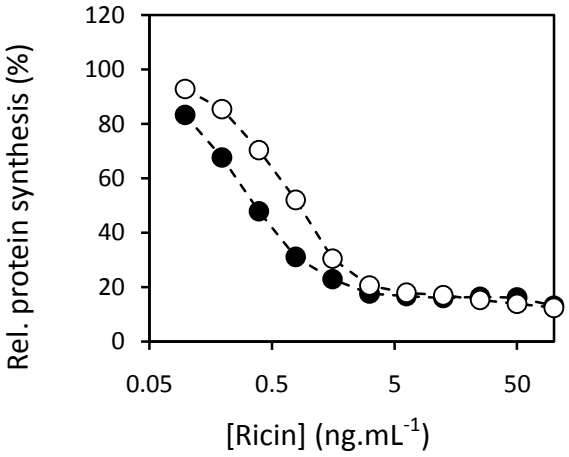

b. 4-hour GA pre-incubation

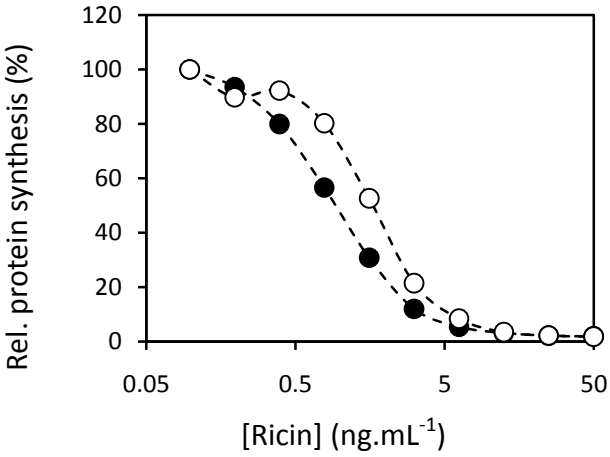

c. 8-hour GA pre-incubation

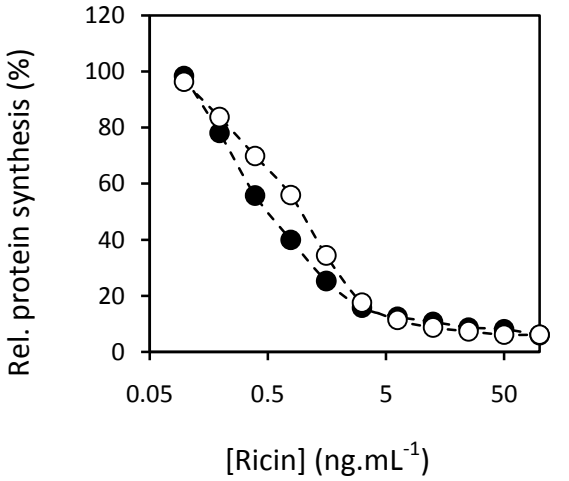

d. 16-hour GA pre-incubation

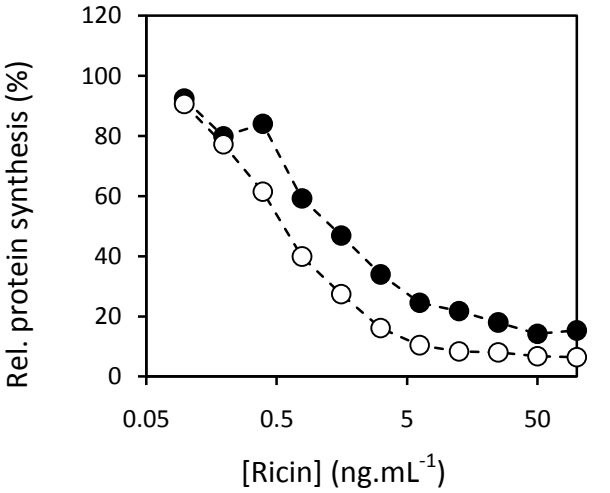

e. Tabulated GA protective values (n=4)

Incubation (hours)	**Sensitisation** (-fold; n=4)	**Standard deviation** (-fold)
0	2.14	0.80
4	1.70	0.83
8	1.13	0.52
16	0.47	0.18

f. Change in IC_{50} relative to control (n=4)

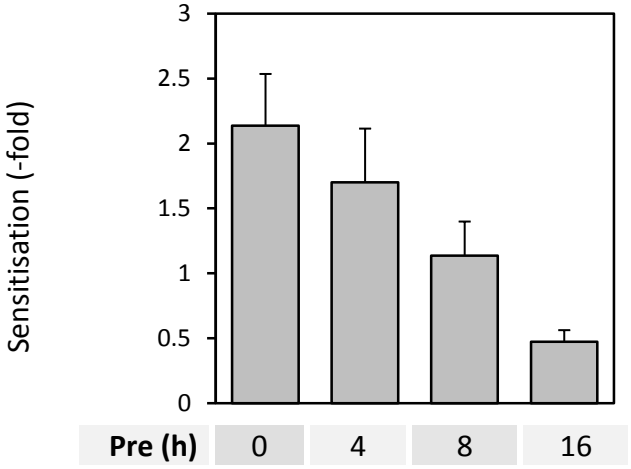

(Figure 3.9 – continued.)

g. 0-hour (coeval) RA incubation

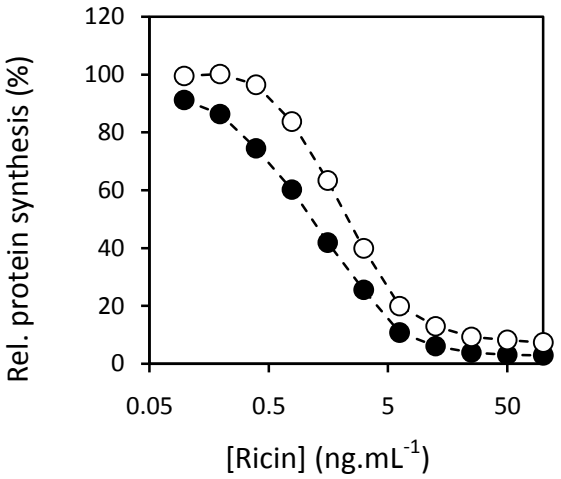

h. 4-hour RA pre-incubation

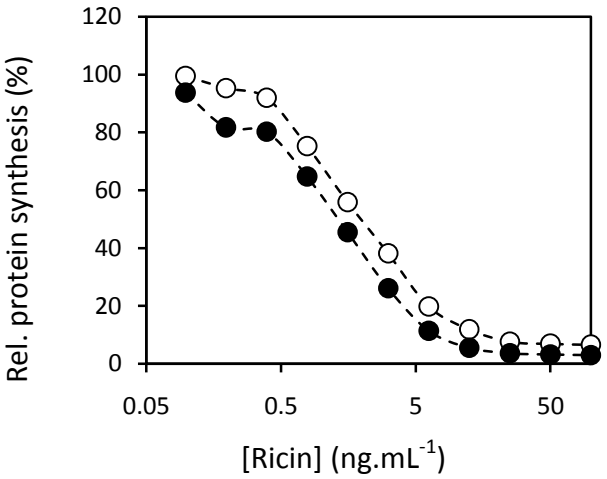

i. 8-hour RA pre-incubation

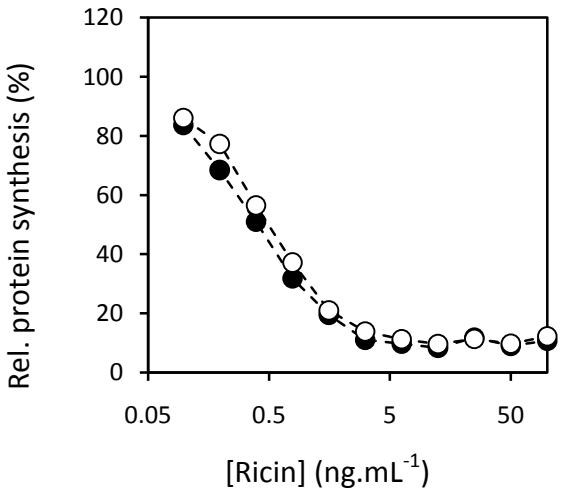

j. 16-hour RA pre-incubation

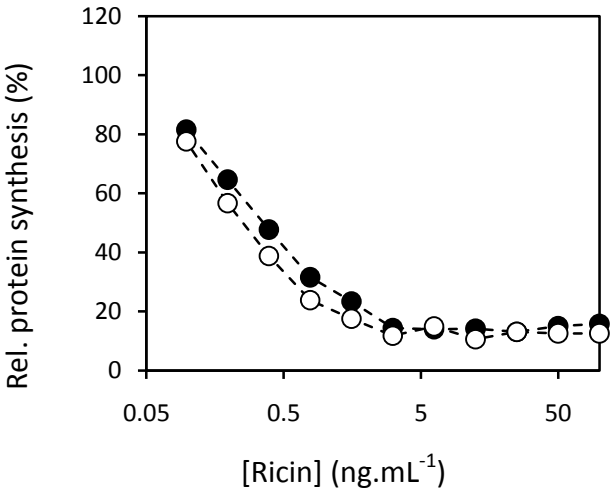

k. Tabulated RA protective values (n=3)

Incubation (hours)	**Sensitisation** (-fold; n=4)	**Standard deviation** (-fold)
0	1.71	0.46
4	1.65	0.46
8	1.31	0.24
16	0.70	0.21

l. Change in IC_{50} relative to control (n=3)

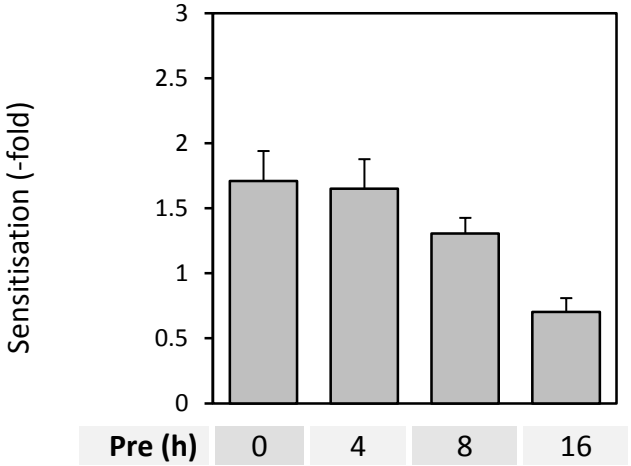

3.5.2 The effect of chronic incubation with 2mM 4-phenylbutyrate

It has been reported that chronic (72-hour) treatment of HeLa cells with 2mM 4-phenylbutyrate (4-PB) in the growth medium leads to down-regulation of Hsc70 mRNA by promoting its degradation (Rubenstein & Lyons, 2001). This results in a subsequent reduction in Hsc70 levels (Rubenstein & Lyons, 2001). When cells were treated in this fashion in our laboratory, a small reduction of Hsc70 was observed by the immunostain of cell lysates (Figure 3.10a & b). When cells were treated similarly for 72 hours with 2mM 4-PB and then challenged with ricin, they were protected relative to cells which were treated with the chemical coeval to the time of toxin application (1.55-fold; SD ±0.22; n=3; see Figure 3.10c & d). This small protection implies that when there is less Hsc70, less toxin activity is observed in the cytosol. This is in accord with the hypothesised role of Hsc70 as a promoter of ricin toxicity.

Unfortunately, 4-PB also has off-target effects, including: activation of cell differentiation, *trans*-activation of genes and cell cycle arrest (Wang *et al*., 2008). Furthermore, the slight reduction in Hsc70 observed may not be significant in a system where it is potentially already saturating. Problematically, a genetic approach to the down-regulation of Hsc70 would be just as fraught with off-target effects, resulting from the vital housekeeping role of this chaperone. Indeed, knocking out Hsc70 and its cytosolic paralogues entirely is reported to be a nonviable approach (reviewed in Whitesell & Lindquist, 2005). Therefore, alternative methods of investigation have been sought to investigate the role of Hsc70 *in vitro* (see subsequent chapters).

Figure 3.10 – Chronic incubation with 4-PB leads to the reduced intensity of Hsc70 immunostaining & protects cells from intoxication.

HeLa cells were plated at a density of 2.5 x 10^5 cells per well in a 6-well plate and then incubated in medium with or without 2mM 4-PB for 72 hours. Detergent-soluble lysates were then collected, electrophoresed, blotted onto nitrocellulose and immunostained via an alkaline phosphatase development. a) Shows the average intensity of Hsc70 bands in 4-PB treated cells relative to controls (normalised to 1), as quantified by TotalLab. Independent lanes were corrected for loading inaccuracies via the co-staining of γ-tubulin, the levels of which were assumed to be unaffected by the treatment. b) Shows the series of three independent experiments from which the quantification in "a" was derived. 10µg of protein is loaded per lane. Staining from α-Hsc70 reactivity is marked with the grey arrowhead; reactivity with α-γ-tubulin is marked with a white arrowhead. c) 72-hour incubation with medium containing 2mM 4-PB down-regulates Hsc70 mRNA production in Hela cells (Rubenstein & Lyons, 2001) and garners a 1.55-fold protection (SD: ±0.22, n=3) relative to acutely-treated controls. d) Shows example dose-response curves from one assay of three independent repeats. e) Shows the effect of the 4-PB alone upon protein synthesis, relative to untreated cells. Error bars show SEM in all cases.

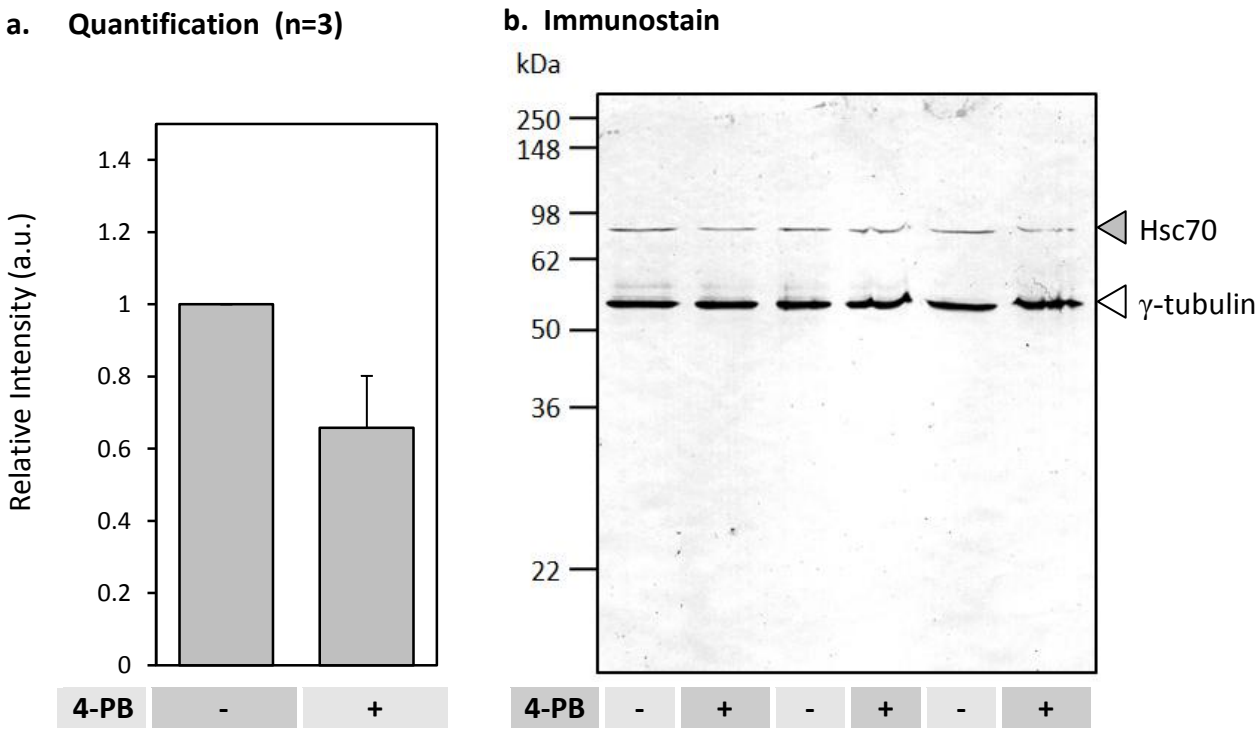

(Figure 3.10 – continued.)

● 72-hour 2mM 4-phenylbutyrate pre-treatment

○ Coeval 2mM 4-phenylbutyrate treatment

c. Protective Effect (n=3)

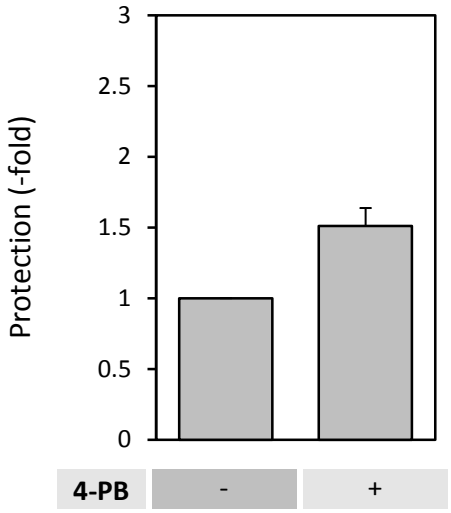

d. Dose-response curves

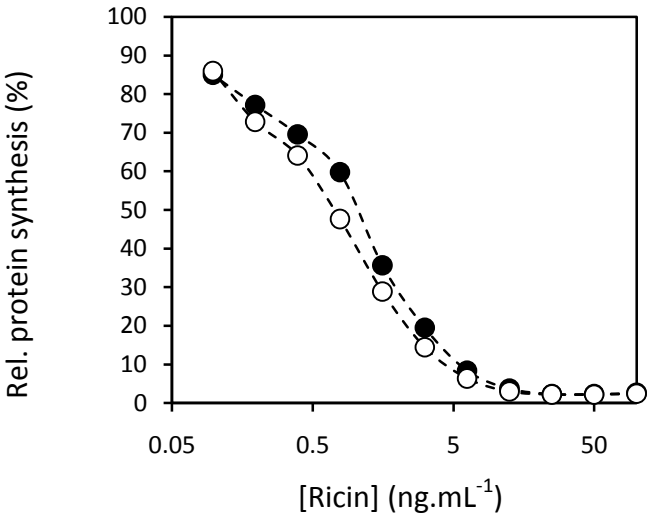

e. Effect of 4-PB alone (n=3)

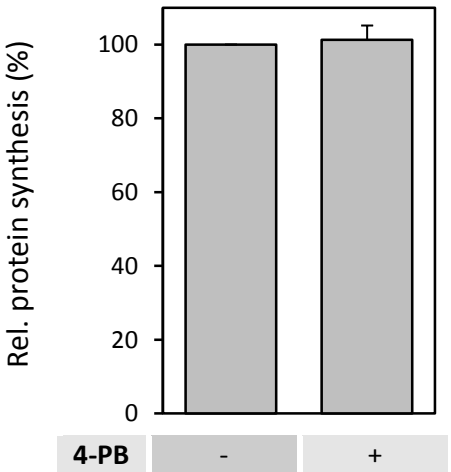

3.5.3 The effect of a heat shock upon the susceptibility of cells to ricin

If the chronic effects of GA/RA resulted from the up-regulation of Hsp70, then a heat shock inducing the same response might also protect cells from ricin intoxication. Parallel plates of cells were either heat-shocked for 10 minutes at 45°C, or incubated at 37°C. After a subsequent period of 2 hours at 37°C, IC_{50} was determined by the usual protocol. The lag was imposed to ensure that the heat shock response would be induced by the time the toxin reaches the cytosol (as reported by Burdon *et al.*, 1982).[9]

The result of three independent assays (Figure 3.11a & b) showed an average sensitisation of 1.04-fold (SD ±0.23; n=3), which is essentially the same as controls. This was unexpected, given that manipulation of heat-shock proteins in earlier assays had obvious and consistent protective or sensitising effects. It could be that a number of antagonising responses are induced by heat-shock, fortuitously neutralising one other. Among these responses would be various other chaperone levels (e.g. functionally-implicated Hsp90); the configuration of the proteasome (Beedholm *et al.*, 2004); and potentially competition from a backlog of ERAD candidates.

Obviously, this study could be broadened by examining a panel of different temperature heat-shocks, transecting different times post-stress, and by clarifying the expression of Hsp70 and Hsp90 in the cytosol in each case. However, it was deemed more valuable to pursue assays which began to refine the broadening array of interpretations the data to this point provoked. At this juncture, the following hypotheses seem the strongest:

(1) Grp94 putatively helps direct lumenal RTA to the retrotranslocation apparatus;
(2) Hsc70 activates cytosolic RTA;
(3) Hsp90 inactivates cytosolic RTA;
(4) Long-term Hsp90 inhibition induces an effect which protects cells from ricin.

[9] Note that – unlike previous assays – control and heat-shocked cultures had to be on different plates so that their temperatures during the treatment could be independently regulated.

Figure 3.11 – A 10 min heat shock at 45°C does not alter the susceptibility of cells to ricin

Cells were plated into two plates at a density of 2.5×10^5 cells per well and grown overnight at 37°C. Heat-treated plates were then incubated at 45°C for 10 minutes and returned to 37°C, whereas control plates were left in the incubator for this period. After 2 hours passed, the IC_{50} of each set of cells was determined by the usual method. a) Shows dose-response curves, heat-shocked (●) and control (○). b) Shows the average effect of this treatment (n=3). Error bars show SEM.

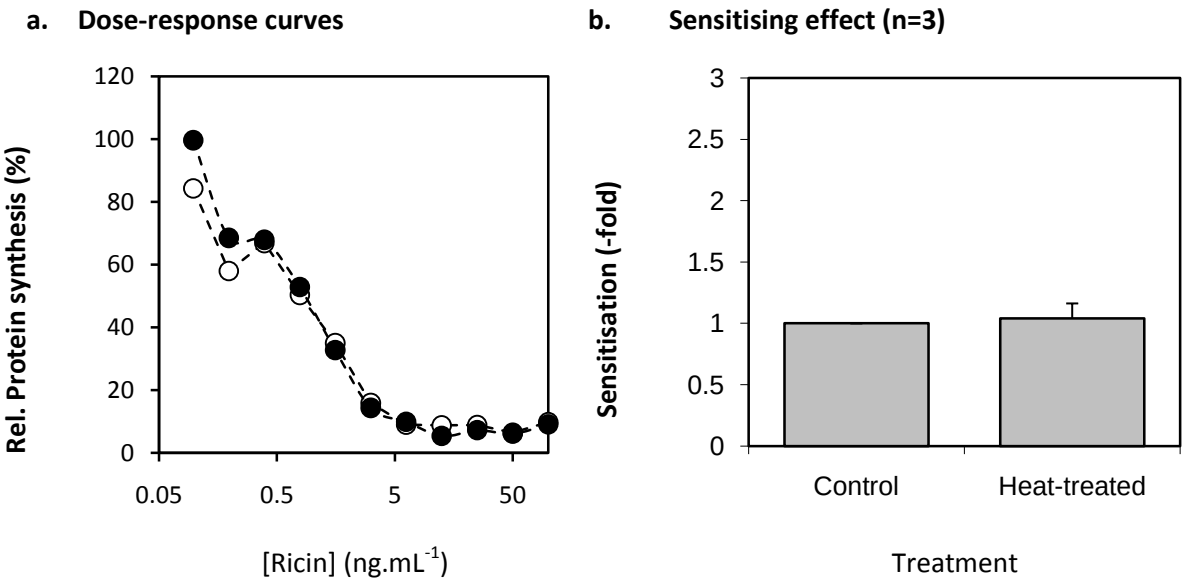

3.5.4 The effect of deoxyspergualin dominates that of radicicol

During the conformational maturation of substrates like luciferase, certain kinases and steroid hormone receptors, Hsc70 and Hsp90 are known to work together in a sequential triage (Pratt *et al*., 2010). This pathway delivers native, functional proteins from non-native, inactive conformers (Murphy *et al*., 2003; Johnson *et al*., 1996). In these pathways, the co-chaperone HOP dynamically links Hsp90 to Hsc70. Its binding preferences and effects upon the ATPase cycle of each chaperone promotes the passage of substrates from Hsc70 to Hsp90 (Johnson *et al*., 1998; Hernandez *et al*., 2002; Gross & Hessefort 1996).

To test whether this kind of sequential pathway was commensurate with the observations made in this thesis, or whether Hsc70 and Hsp90 competed for binding to RTA, a dual-treatment approach was used (Figure 3.12). Cells were treated with both DSG and radicicol at the time of toxin addition. The net effect of this treatment was a protection of 1.85-fold (SD ±0.48; n=3), which compares well to the effect of DSG alone (1.90-fold protection; SD ±0.55, *cf.* section 3.2). If Hsc70 and Hsp90 were competing with one another for binding RTA, dual inhibition would mitigate the opposite effects of these chaperones. However, this does not seem to be the case. Rather, it appears that the sensitising effect of radicicol is dependent upon the activity of Hsc70. These findings have been published in Spooner *et al*., 2008).

Figure 3.12 - The effect of DSG dominates the effect of radicicol

The protective effect of treating HeLa cells coevally with 50µg.mL^{-1} DSG, 1µM RA (●) was determined via cytotoxicity assay, as before. The controls used were treated with an equivalent concentration of DMSO and lactose (○) to account for their inclusion in the DSG and RA preparations. a) Shows typical dose-response curves. b) Shows the average protective effect at the IC_{50} relative to the controls (n=4). Error bars show SEM.

a. Dose-response curves

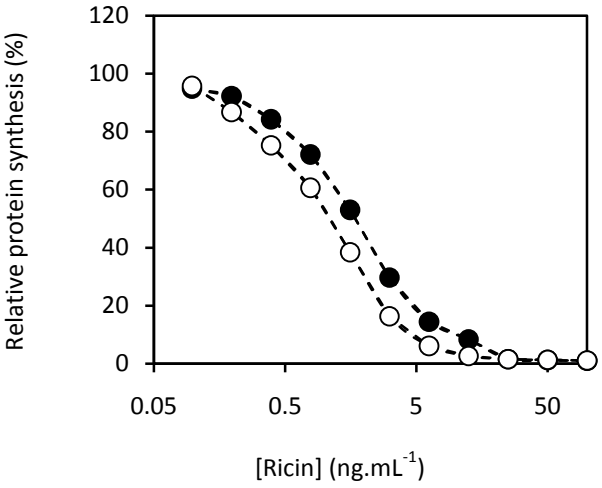

b. Protective effect (n=4)

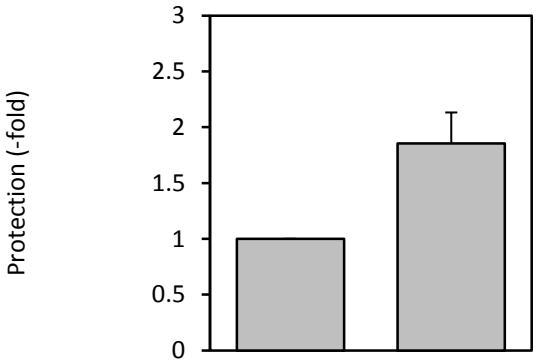

Lactose	+	+
DMSO	+	+
DSG	-	+
RA	-	+

3.5.5 Ricin itself does not provoke alterations in Hsc70/Hsp70 nor Hsp90 expression

As an aside to the main direction of this chapter, intoxication of a cell by ricin could itself promote changes in protein expression or activity. It has been hypothesised that ricin may have evolved a way of promoting a cytosolic environment that is permissive of its intoxication (Spooner & Watson, 2006).

Spooner & Watson (2006) proposed that, as ricin B-chain is a lectin with two binding sites, the holotoxin may be able to dimerise adjacent cell surface receptors. This could lead to the induction of internal signalling cascades, which could alter protein activity (Spooner & Watson, 2006). As binding to the cell surface and access of RTA to the cytosol are separated by ~1-hour (Hudson & Neville, 1987), this may be enough time for protein expression (or indeed activity) in the cytosol to become significantly affected as well. Of interest to this study is whether Hsc70, Hsp70 and Hsp90 chaperones are affected.

HeLa cells were incubated with minute doses of ricin for different lengths of time. Detergent soluble lysates were then collected and tested for changes in Hsp90 and Hsp70/Hsc70 expression (Figure 3.13a). By the method used, no apparent change in any of these proteins was detected.[10] Figure 13.3b shows corroborating data generated by R.A. Spooner (University of Warwick), which was interpreted by L. Zeef (University of Manchester). As part of a transcriptomic approach, HeLa cells were treated with 50 $ng.mL^{-1}$ ricin for up to 4 hours. Afterward, global transcriptional changes were measured using a technology from Affymetrix. Figure 3.13b shows the relative levels of Hsp90AA1 mRNA after such treatment over time (Hsp90AA1 is one of three cytosolic Hsp90 paralogues - Chen *et al.*, 2005). It would appear that, if ricin does affect relative protein expression ahead of entry to the cytosol, Hsp90 and Hsc70/Hsp70 are not among those which are affected.

[10] Although it may be that a saturating level of Hsc70/Hsp70 staining hides a relatively slight induction of Hsc70/Hsp70.

Figure 3.13 – The effect of ricin incubation on Hsp90 / Hsp70 expression in HeLa cells.

a) HeLa cells were seeded into and grown overnight in a 6-well plate at a density of 2.5 × 10^6 cells per well. They were then incubated with the stated concentration of ricin in culture medium for the indicated length of time. Detergent soluble lysates were finally collected and 10µg of protein loaded into each lane for SDS-PAGE. The gel was then blotted onto nitrocellulose and immunostained for Hsp90, Hsp70/Hsc70 and γ-tubulin, before development by an alkaline phosphatase protocol. Shown below is a representative assay from a set of three independent repeats. b) The data in the following figure is published here courtesy of R.A. Spooner (University of Warwick), who treated HeLa cells with 50 ng.mL^{-1} ricin for up to 4 hours and observed changes in mRNA levels by a transcriptomic approach using Affymetrix technology. Data from these assays were interpreted by L. Zeef (University of Manchester).

a. Immunostain

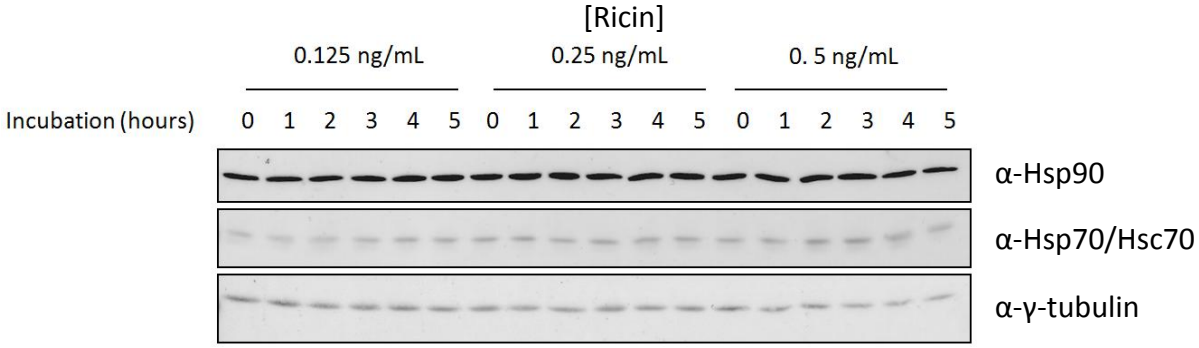

b. Quantification of Hsp90AA1 mRNA intensity

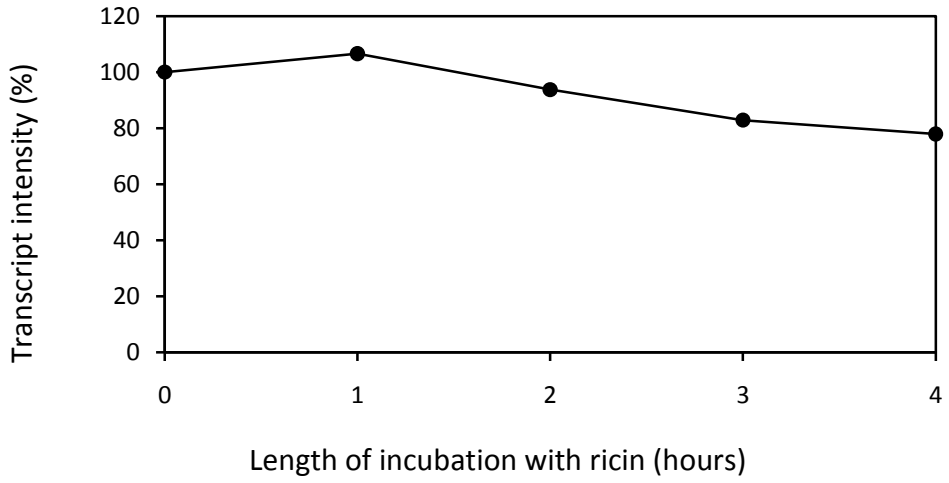

3.6 The effect of altering RTA's lysine complement upon the sensitising properties of radicicol

The experimental approach undertaken to this point has been constrained by the potentially pleiotropic effects of the inhibitors used (and, moreover, the pleiotropic effects of inhibiting the chaperones themselves). To try and better ratify whether the effects of these inhibitors resulted from a direct mode of action upon RTA, a new approach was devised.

I take this opportunity to re-state two of the primary rationales for studying the involvement of cytosolic chaperones in ricin cytotoxicity:

(1) Nascently retrotranslocated, unfolded RTA may benefit from an interaction with cytosolic chaperones which promote the acquisition of an active conformation.
(2) While still unfolded, RTA may be recognised by the same chaperones and targeted for proteasomal degradation.

As Hsc70 and Hsp90 work in concert with the ubiquitin-proteasome pathway, they may be able to send RTA to the proteasome directly. If so, this transfer might be mediated by lysine ubiquitination. As discussed earlier, RTA possesses remarkably few lysines, which help it to avoid terminal degradation (Hazes & Read, 1997). Indeed, Deeks *et al*. (2002) showed that increasing the lysine complement of RTA reduces the potency of the holotoxin. Therefore, if the sensitising effect of Hsp90-inhibition was augmented or diminished for holotoxins whose constituent RTA subunit had an altered lysine complement, conclusions could be drawn about the physical outcome of its interaction with RTA.

3.6.1 Purification of RTA^{0K}, RTA^{WT} and RTA^{6K}

To produce the holotoxin variants used in the proposed assay, recombinant, monomeric RTA and purified RTB had to be acquired. RTB was purchased commercially (Vector labs); the RTA variants, however, had to be purified from transformed cultures of *E.coli*. More explicit details on the protocol used can be found in the Chapter 2. However, a précis on the purification procedure is given here for ease of reference.

Genes for expressing RTA variants: RTA^{0K} (no lysines), RTA^{WT} (bearing two endogenous lysines) and RTA^{6K} (six lysines) were each separately transformed into *E.coli* JM101. Cultures of each were grown and RTA expression was induced. Cultures were then centrifuged, lysed by sonication and further clarified by centrifugation. Clarified sonicates were then fractionated by ion-exchange chromatography upon a 50mL CM-Sepharose CL-6B

column. Aliquots from the fractions obtained were analysed by Coomassie staining after SDS-PAGE for RTA content (Figure 3.14a-c). Those fractions containing RTA (and no impurities) were pooled.

Figure 3.14 – Purification of RTA variants.

Purification of clarified sonicates containing RTA^{WT}, RTA^{6K}, or RTA^{0K} from an *E. coli* culture. Continuous fractions (enumerated consecutively) were analysed by SDS-PAGE and Coomassie blue staining. Fractions containing RTA with no impurities were pooled. a) Shows purification of RTA^{WT}, b) RTA^{0K} & c) RTA^{6K}. In a), lane A comprises 10µL of crude sonicate; B is 10µL of the supernatant after centrifugation of the sonicate, whilst C is 10µL of the flow-through from the column as it washed with 100mM NaCl in pH 6.4 sodium phosphate. In all cases, the black triangle indicates bands corresponding to the molecular weight of RTA.

a. Purification of RTA^{WT}

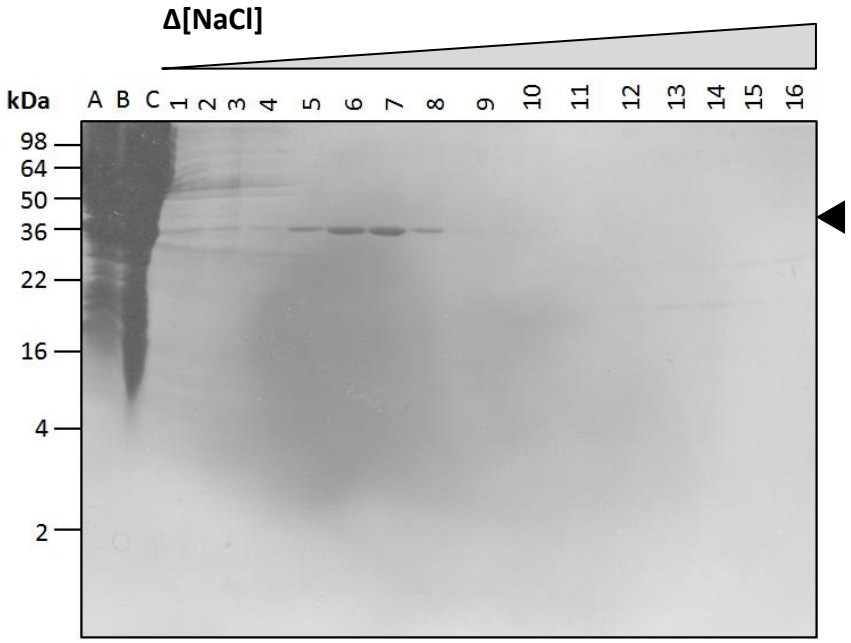

(Figure 3.14 - continued.)

b. Purification of RTA^{0K}

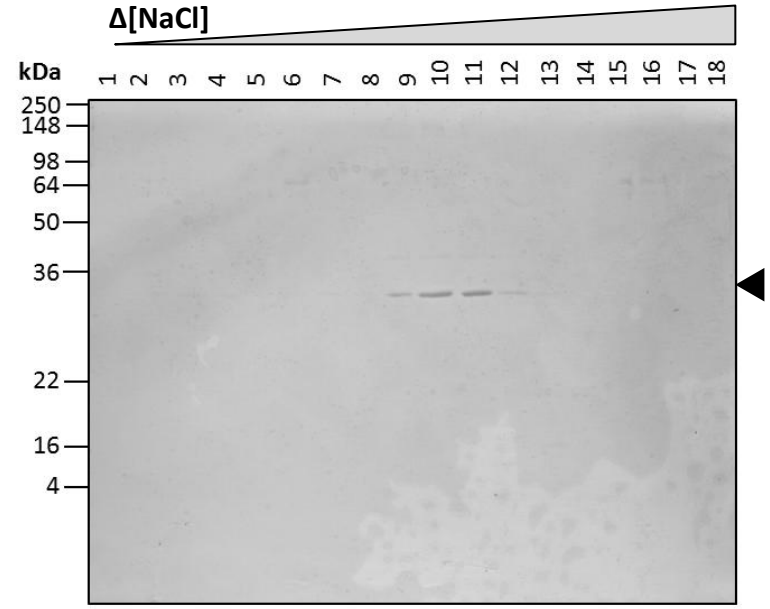

c. Purification of RTA^{6K}

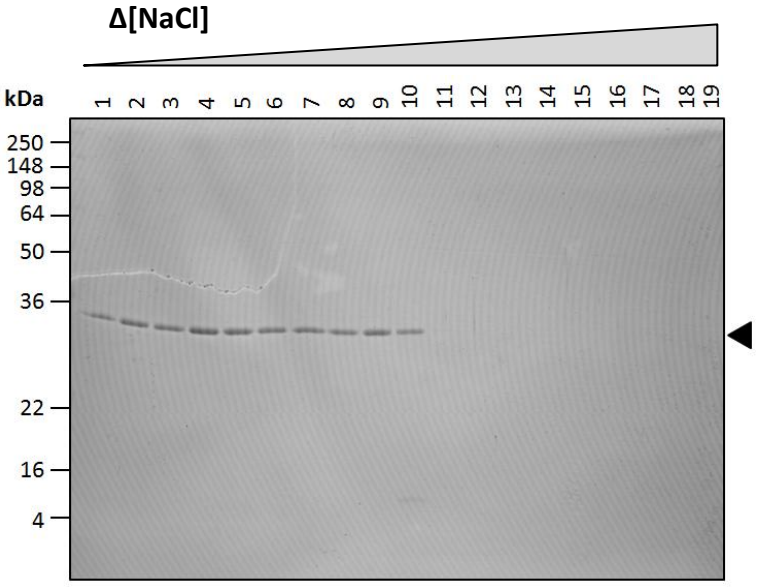

After pooling RTA-containing fractions, each relatively dilute RTA preparation was concentrated by centrifugation in Centricons (protocol as described by Millipore). The purity of each preparation was then analysed by Coomassie staining after SDS-PAGE. This can be observed below (Figure 3.15Figure).

Figure 3.15 – Purity of RTA^{WT}, RTA^{0K} and RTA^{6K} preparations after centrifugal concentration.

20µg of RTA (as estimated by the absorbance of the concentrated solutions at 280nm and the molar extinction coefficient, which is 0.77 for a 1mg.mL^{-1} solution in sodium phosphate – Chaudry G.J. *et al*., 1993) was loaded per lane. For comparison, 20µg of purified RTB (Vector labs) was run in parallel in the final lane. The gel was stained with Coomassie blue.

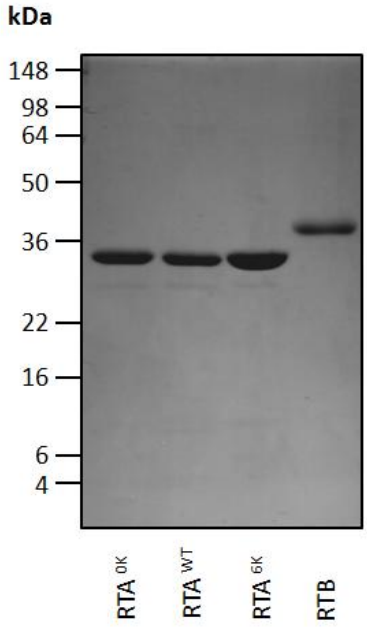

3.6.2 Association of recombinant RTA with RTB

To generate holotoxin from monomeric RTA and RTB, RTA had to be joined to RTB via a disulfide bond. For a full account of the association protocol, please refer to Chapter 2. However, a précis is given here. RTA was added to RTB, with RTA in 2:1 excess (w/w) with 2% (v/v) β-mercaptoethanol and 100mM lactose. The β-mercaptoethanol and lactose were then removed by consecutive rounds of dialysis. The resultant solution was passed down an immobilised α-lactose column (Sigma-Aldrich) to remove monomeric RTA. Monomeric RTB and holotoxin were eluted with a dilute galactose solution (to which RTB

binds in preference to lactose). Galactose was removed from this solution by dialysis, yielding a solution of purified RTB and reassociated holotoxin.

Reassociated holotoxin solutions were finally concentrated by centrifugation using YM-10 Microcons (Amicon). They were quantified by silver-staining (Figure 3.16). As some free, monomeric RTB existed in the final preparations, the concentration of holotoxin was calculated by comparison of RTA band intensity to standards of known concentration (40, 80, 120 & 160ng). Notice that RTA of the reassociated holotoxin migrates faster as it is not subjected to glycosylation when expressed in *E. coli*.

Figure 3.16 – Quantification of reassociated holotoxin

Three recombinant RTAs with varying complements of endogenous lysine residues were reassociated with RTB. The concentrations of the final aliquots of reassociated holotoxin were compared to standards of known concentration using a silver stain. The indicated volume of each reassociation (0K, WT & 6K RTA) was loaded in triplicate.

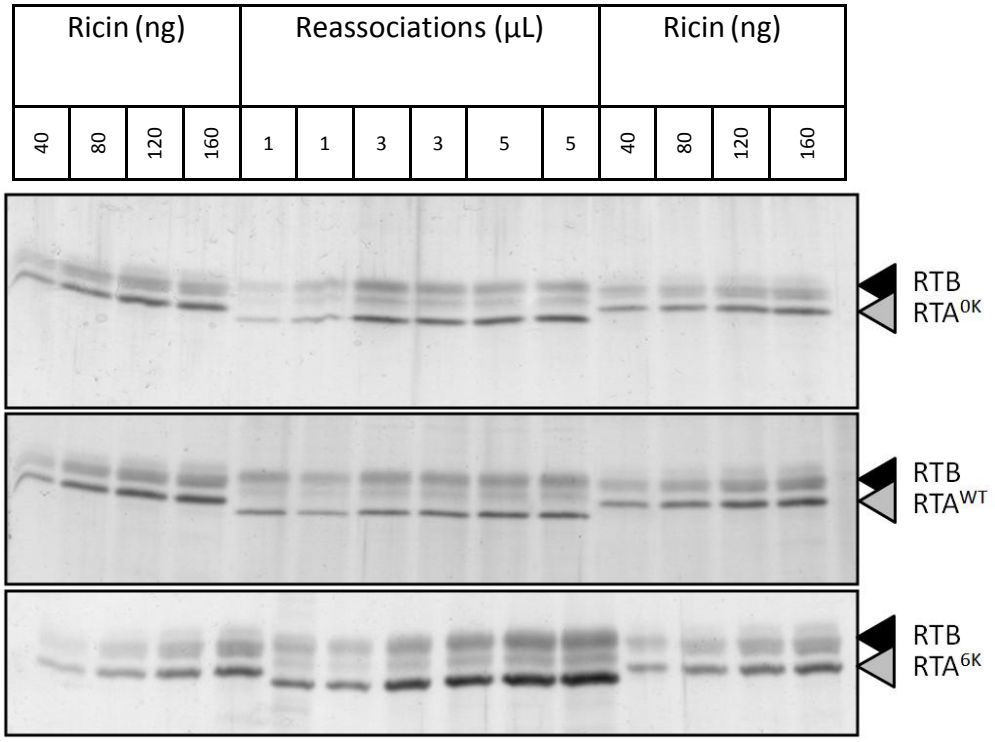

3.6.3 The inhibitory range of the reassociated holotoxins

With the concentrations of the reassociated holotoxins approximated, it was possible to explore whether the reassociated, recombinant proteins shared the same lysine-dependent trend in cytotoxicity as reported by Deeks *et al.* (2002). The efficacy of each in reducing protein synthesis was tested (Figure 3.17). As would be predicted, the IC_{50} of holotoxin containing RTA^{6K} was greatly increased relative to RTA^{0K} and RTA^{WT}. Again, this is presumably due to a greater propensity to become polyubiquitinated upon the cytosolic side of the ER membrane (Deeks *et al*., 2002), reducing the concentration of active RTA in the cytosol.

Quite unlike Deeks *et al*. (2002) RTA^{0K} is significantly more toxic than RTA^{WT}. This suggests that the two endogenous lysines are susceptible to ubiquitination. By average, RTA^{WT} is ~1.4-fold less toxic than RTA^{0K} (a significant difference; p=0.013 by Student's paired T-test). RTA^{6K}, on the other hand, is ~9.5-fold less toxic than RTA^{WT} (p=0.047 by Student's paired T-test). If the lysines of RTA^{6K} were all equally predisposed to polyubiquitination, a ~3-fold change in toxicity should be observed between the RTA^{WT} and RTA^{6K} variants (as there is a 3-fold difference in lysine complement). Thus, it seems that the four non-native lysines of RTA^{6K} are more accessible to the ubiquitination machinery of the cell than its two native lysines. This may tell us that the two endogenous lysines of RTA are specifically placed to avoid them contributing to cytosolic inactivation of the toxin subunit. Alternatively, the lysines may alter the activity of the protein in some other significant way, such as altering its solubility and retrotranslocation dynamics. However, Deeks *et al*. (2002), did determine that the catalytic activities of these A-chain variants were unaffected when tested *in vitro*.

Figure 3.17 – Increasing the lysine complement of RTA reduces holotoxin cytotoxicity.

a) Shows the IC_{50} determined for each preparation of reassociated holotoxin. b) Shows dose-response curves for reassociated holotoxins comprising RTB reassociated to recombinant:

- ○ RTA^{0K}
- ● RTA^{WT}
- ● RTA^{6K}

Example assays are shown from sets of three independent experiments. Error bars show SEM.

a. IC_{50} values (n=3)

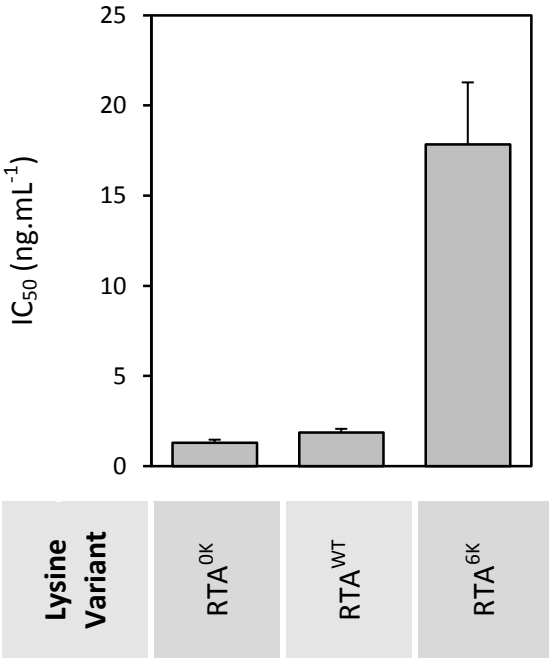

b. Dose-response curves

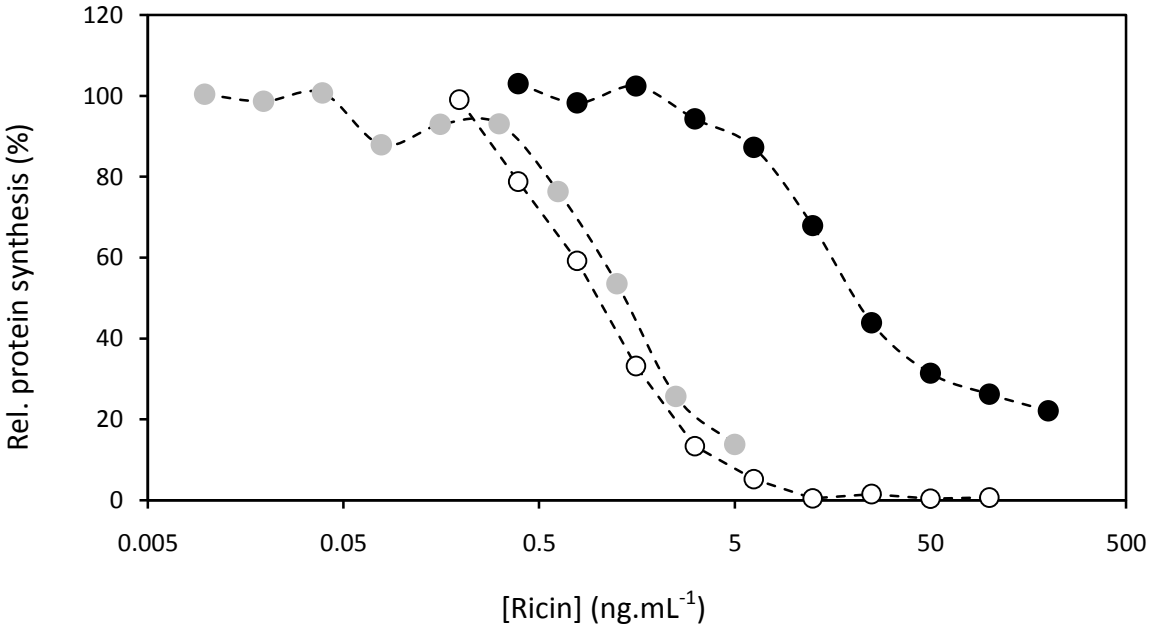

3.6.4 The effects of radicicol upon the potency of three holotoxins with varying lysine complements

The potency of the three reassociated holotoxins was examined in the presence and absence of 1μM RA (Figure 3.18). In the case of RTA^{WT} and RTA^{6K}, radicicol is convincingly sensitising. The toxicity of RTA^{0K}, however, does not appear to be bolstered by Hsp90 inhibition ($p=0.245$ by Student's paired T-test). The greatest sensitising effect of radicicol was clearly upon holotoxin containing RTA^{6K}. The greater concentration of lysine residues in RTA^{6K} presumably predisposes it to degradation. Radicicol apparently neutralises this predisposition. This result implies that Hsp90 helps to mediate the polyubiquitination of RTA *in vivo*.

Reassuringly, the sensitising effect of radicicol with respect to reassociated holotoxin containing RTA^{WT} is similar in magnitude to wild-type toxin which has not been exposed to the rigours of the reassociation process. Radicicol sensitises cells to reassociated RTA^{WT} 1.71-fold (SD ±0.24; n=3; $p=0.016$ by Student's paired T-test). Equivalent wild-type holotoxin purified from *Ricinus communis* sensitises cells to ricin 1.87-fold (SD ±0.35; n=3).

Finally, it is intriguing that the RTA^{0K}-containing holotoxin was not at all responsive to Hsp90-inhibition. This might suggest that RTA^{0K} simply does not interact with Hsp90, unlike the other variants. RTA^{0K} might be extracted from the ERAD pathway at an earlier stage because of its lack of ubiquitination, preventing a subsequent interaction with Hsp90, for instance. Alternatively, the Hsp90-mediated route to inactivation may be one which requires direct, lysine-ubiquitination of RTA.

Figure 3.18 – Increasing the lysine complement of RTA augments radicicol-induced sensitivity to ricin holotoxin.

The effect of 1 µM radicicol (●) upon the IC_{50} of reassociated ricin holotoxin was determined via cytotoxicity assay. Representative dose-response curves under these conditions are plotted alongside DMSO-treated controls (○). Reassociated holotoxin comprised RTB disulfide-bonded to a) RTA^{0K}, b) RTA^{WT} or c) RTA^{6K}. In each case, the representative curves come from a set of three independent experiments. d) Shows the sensitising effect of radicicol for each holotoxin variant (n=3; error bars show the SEM between the three sets of assays).

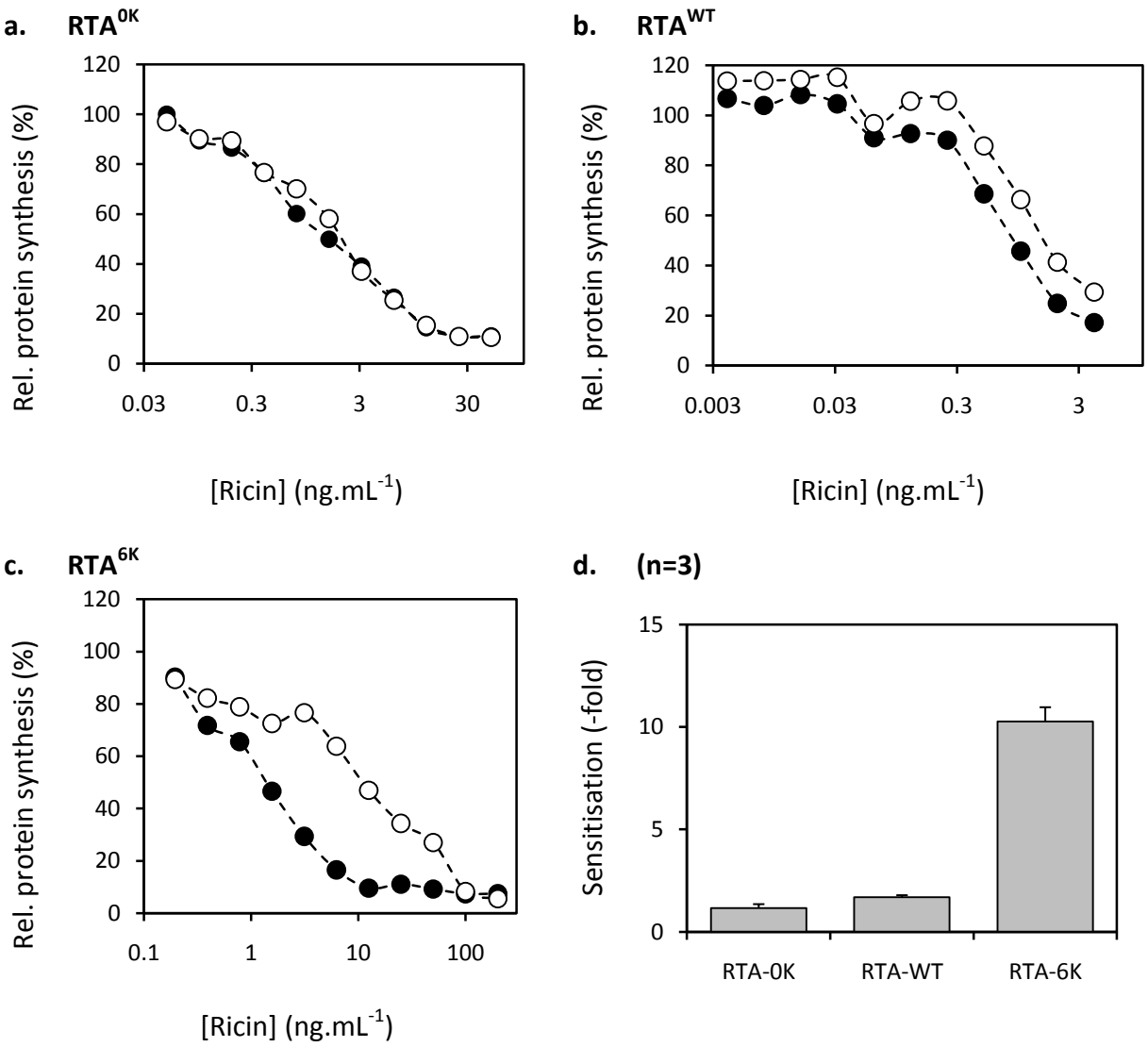

3.7 Discussion

Manipulating the function of chaperones *in vivo* using pharmacological agents changes the sensitivity of the target cell to ricin. The role of the chaperone matrix in the cell is inarguably complex and will control multitudinous cellular functions by promoting the active conformations of various clients (and the degradation of their misfolded forms). Therefore, the effects of inhibiting these chaperones are also likely to be rather complex. However, from the evidence at hand, some tentative models can be proposed.

The role of Hsc70 **-** Inhibition of Hsc70 protects cells. Thus, the uninhibited chaperone somehow helps more active RTA reach, or else survive, in the cytosol (Spooner *et al*., 2008). As DSG does not affect BiP (Brodsky, 1999) and trafficking of ricin through the secretory pathway is unaffected by this treatment, the inhibitory effect appears to be a cytosolic one. That is, Hsc70 effects component involved in intoxication at a stage beyond transport of ricin to the ER. The most direct interpretation of these data is that Hsc70 is responsible for activating cytosolic RTA, potentially by helping it to fold into a catalytically active conformation. Alternatively, Hsc70 might be responsible for maintaining a third party which promotes the toxicity of RTA. For this to be feasible, such a third-party would have to be prone to denature from its native, functional state to a significant extent within a timeframe defined by toxin trafficking. Because of this proviso, the simplest model to adopt is perhaps one of a direct interaction between Hsc70 and RTA (as published in Spooner *et al*., 2008).

The role of Hsp90 & the effect of Hsp90 inhibitors **-** Opposite to Hsc70, inhibition of another key cytosolic chaperone, Hsp90, sensitised cells to ricin. As trafficking times were unaffected by treatment with this inhibitor, it seemed that this was also a cytosolic effect. These findings implied that Hsp90-type chaperones promote inactivation of RTA *in vivo* (published in Spooner *et al*., 2008), or else promoted the existence of a third party which inactivates RTA (again, for this explanation to be feasible, this third-party would have to be prone to denature within a timeframe defined by toxin trafficking).

One obvious candidate for such a third-party might be the proteasomal core, which degrades RTA (Deeks *et al*., 2002). Indeed, Imai *et al*. (2003) shows in yeast that a (much higher) dose of 18µM geldanamycin causes incremental loss of the 26S proteasome and up-regulation of the relative proportion of the uncapped 20S complex after as few as 3 hours of incubation (and progressively moreso to a maximum effect at post 16-hours). In this chapter, however, chronic incubations with radicicol and geldanamycin show that this change

correlates to protection and not sensitisation. Therefore, it seems unlikely that the acute effects of GA/RA or C01 result from an impact upon the proteasome.

On the other hand, the *chronic* effects of GA/RA/C01 in *protecting* cells from ricin intoxication may be associated with loss of the 19S proteasomal cap. Imai *et al.* (2003) showed that, over time, incubation of cells with GA leads to gradual loss of this lid complex. This may be significant, as the proteasomal cap has been posed as a motor driving the extraction of ERAD substrates, including RTA, from the lumen (Lee *et al.*, 2004; Kopito *et al.*, 1997; Li *et al.*, 2010). It may be that chronic treatment with GA/RA reduces the cytosolic concentration of this complex, so reducing the capacity of the cell to retrotranslocate ERAD substrates like RTA, so protecting cells. Alternatively, the difference between acute and chronic Hsp90-inhibition may result from up-regulation of chaperones, e.g. Grp94, or cytosolic chaperones like Hsp70. This might alter the dynamics of ERAD, e.g. retarding retrotranslocation (if caused by Grp94), or cytosolic quality control (if caused by Hsp70).

The role of Hsp90 is dependent upon the lysine content of RTA – Another major finding of this chapter is that the inactivation which Hsp90 apparently coordinates is dependent upon the lysine content of RTA. Introducing additional lysines into the toxin subunit increases the capability of Hsp90 to facilitate deactivation of it. That is, the sensitising effect of RA increases as the lysine complement of RTA does. The toxicity of RTA^{0K}, indeed, is not affected by radicicol. The most forthright interpretation for these observations is that direct, exclusively lysine-targeted polyubiquitination of RTA is involved in this interaction. Two simple models to explain this observation are as follow:

(1) Hsp90 helps target RTA for ubiquitination by interfacing with a co-factor such as CHIP. This co-chaperone is an E3 ligase that binds to Hsp90 and is able to catalyse the formation and extension of polyubiquitin chains upon bound clients (Connell *et al.*, 2001); or,
(2) Hsp90 is responsible for maintaining the structural integrity of another complex which ubiquitinates RTA, e.g. a membrane-integral E3 ubiquitin ligase (but which must be structurally labile enough for a significant population to be disrupted by Hsp90 inhibition in the time taken for toxin trafficking).
(3) Hsp90 might be responsible for inactivating RTA which is already ubiquitinated – perhaps by bridging its interaction to the proteasome.

If RTA is a direct client of Hsp90, and is ubiquitinated by it, it seems at odds with *bona fide* clients of the chaperone: for instance the oncoprotein, src (Whitesell *et al.*, 1994), and firefly luciferase (Schneider *et al.*, 1996). If the association of these substrates with Hsp90 is disrupted with GA/RA, it results in their loss of function. Yet, for RTA, disruption of Hsp90 results in more of its catalytic activity in the cytosol. This contrast may highlight how the interaction of RTA with Hsp90 is a superfluous one.

Hsc70 and Hsp90 seem to work in a sequential triage of RTA - The effect of dually-inhibiting Hsc70 and Hsp90 with DSG/RA implies that there may be an ordered sequence to the action of Hsc70/Hsp90. The effects of Hsp90 inhibition are abrogated by inhibition of Hsc70. This result implies that the Hsp90 interaction may be dependent upon a preceding one with Hsc70 (as published in Spooner *et al*., 2008). This mirrors the folding pathways of numerous other substrates of these chaperones (Young *et al*., 2001).

Lumenal Grp94 may participate in directing RTA toward retrotranslocation - In the ER lumen there exists a homologue of Hsp90-type chaperones, Grp94, which might also be the source of the effects observed with GA/RA/C01. However, this possibility is refuted by the protective effect of the Grp94-specific inhibitor, NECA. If anything, therefore, Grp94 seems to have a role opposite that of the Hsp90s of the cytosol with respect to toxicity (as published in Spooner *et al*., 2009). Eletto *et al*. (2010) shows that Grp94 may help present certain substrates to the Hrd1-associated retrotranslocation complex. It may function in this way for RTA. However, for RTA, Grp94 does not seem to be an absolute requirement for the retrotranslocation process, as GA/RA and C01 affect Hsp90 as well as Grp94. Hypothetically, multiple routes directing RTA to the retrotranslocation machinery may well exist (e.g. one dictated by EDEM, as proposed by Slominska-Wojewodzcka *et al*., 2006).

Differential treatment of RTA by Hsc70 and Hsp70 - The data presented in this chapter are suggestive of different roles for inducible Hsp70 and constitutively-expressed Hsc70 in the intoxication process. This seems so because inhibition of Hsc70 (and putative down-regulation using 4-phenylbutyrate treatment) leads to protection from ricin. Conversely, up-regulation of Hsp70 (by chronic Hsp90 inhibition) correlates with protection from ricin. Inhibition of Hsp90 with GA/RA is likely to have pleiotropic effects upon the cell, as discussed earlier. However, if this transition to protection results from Hsp70 up-regulation, it could be that the dynamics of this chaperone's interaction with RTA are different from Hsc70's. For example, Hsp70 reportedly binds to hydrophobic stretches more strongly than

Hsc70 (Callahan *et al*., 2002). This difference might result in degradation rather than activation for RTA. Hsc70 and Hsp70 have similarly opposite effects upon the expression of other proteins, e.g. the functional maturation of epithelial sodium channels (Goldfarb *et al.*, 2006). Therefore, functional differentiation of Hsc70 and Hsp70 would be consistent.

Further exploration of these findings **-** Multiple lines of evidence imply an *in vivo* role for Hsc70 and Hsp90 in the cytotoxicity of ricin. However, it remains obscure whether these effects result from a direct interaction of the chaperones with RTA, or because these chaperones are required for the functionality of other factors. Indeed, it may be possible that unknown, off-target effects of the inhibitors used could be the source of the effects observed. To clarify whether these pharmacological effects result from direct interactions between RTA and Hsc70/Hsp90 is the objective of the succeeding chapters. The succeeding chapters take an *in vitro* approach, using purified proteins, ensuring there are fewer factors obscuring the interpretation of the results.

Fundamental conclusions **–** The fundamental findings of this chapter imply that Hsp90 has a role in assigning cytosolic RTA for inactivation via a lysine-dependent mechanism. On the other hand, Hsc70 appears to aid the activity of the toxin in the cytosol. In context of the hypotheses laid out at the beginning of this chapter, it could be that Hsc70 participates in the sequence of interactions that RTA makes in the cytosol after or during retrotranslocational. This interaction with Hsc70 could give partially-unfolded, nascently retrotranslocated RTA the chance to re-fold into a state which is regarded as native in the context of the cytosol. By this mechanism, RTA might then simply exit the latter stages of ERAD, i.e. degradation, by merit of simply no longer being recognised as a worthy candidate for degradation. In this model, Hsc70 provides an 'escape hatch' from events that would otherwise lead to degradation.

CHAPTER 4:

An *in vitro* assay for determining factors affecting the solubility of RTA

4.0 How a direct interaction between Hsc70 and RTA could be important

It has been hypothesised that RTA exploits Hsc70 at some point proximal to its retrotranslocation of the ER membrane. RTA putatively uses this interaction to increase the yield of successfully reactivated toxin in the cytosol. A subsequent recurrent, transient interaction of RTA with Hsc70 after having acquired a cytosolic localisation might also significantly extend its toxic half-life therein, enabling the toxin subunit to deactivate more ribosomes than it would be able to otherwise. Often, if a client has a persistent association with Hsc70 it would result in its degradation via polyubiquitination (McDonough & Patterson, 2003; Jiang *et al.*, 2001), but as RTA has a dearth of lysines this side-effect of the interaction might be diminished (Deeks *et al*., 2002).

As an alternative suggestion for the observations of the previous chapter, Hsc70 could contribute to the mechanism by which the retrotranslocation step itself occurs. This would not be without analogous precedents in the cell, as Hsc70-type chaperones are required in the post-translational import of polypeptides across a variety of organelle membranes (Höhfeld & Hartl, 1994; Plath & Rapoport, 2000; Young *et al*., 2003). In such post-translational import pathways, cytosolic Hsc70 binds to clients on the *cis*-side of the membrane being crossed, typically before the cargo polypeptide has completely folded. This interaction ensures that the polypeptide is kept in a conformationally-malleable, transport-competent state (Corsi & Schekman, 1996). Arguably more interesting to this study, however, Hsc70-type chaperones are also thought to act as motors operating upon the *trans*-side of the membrane being crossed (Tomkiewicz *et al*., 2007). In this position they are the hypothesised mediators of "Brownian ratchet" or "power-stroke" mechanisms which are linked to the ATPase cycle of the chaperone, and which effectively help to pull the translocating protein through the pore in the target membrane (Tomkiewicz *et al*., 2007; De Los Rios *et al*., 2006). In mammals, a mitochondrial Hsp70 and the ER-localised BiP have both been proposed to operate in this way (Jehnsen & Johnson, 1999; Tomkiewicz *et al*., 2007). It is therefore a consideration that the cytosolic counterpart of BiP and mitochondrial Hsp70, i.e. cytosolic Hsc70, could exhibit such a function in the dislocation of RTA into the cytosol.

If cytosolic Hsc70 does help drive extraction of RTA from the ER membrane, it would be an unusual mechanism by which an otherwise ERAD-like pathway is resolved. For many *bona fide* ERAD substrates, including ApoB and $CFTR^{\Delta F508}$, the AAA protein-containing 19S proteasomal cap and the p97-containing complex are thought to drive extraction (reviewed in Meusser *et al*., 2005; for ApoB see Fisher *et al*., 2008; and see Carlson *et al.*, 2006, for $CFTR^{\Delta F508}$). Unlike RTA, however, the typical substrates of these putative translocation motors become polyubiquitinated during their ERAD, a modification which is thought to provide a physical anchor which may be bound and pulled upon (Meusser *et al*., 2005). The results of Deeks *et al*. (2002), Li *et al*., (2010) and the previous chapter, however, clearly illustrate that canonical lysine-ubiquitination is not necessary for the retrotranslocation process that RTA undertakes. Previously, Marshall *et al.* (2008) showed that the p97-homologue in *Nicotiana tabacum* (known as Cdc48), can facilitate extraction of RTA^{0K} from the ER of tobacco protoplasts. However, Li *et al*. (2010) showed that this was not the case in yeast. Speculatively, if RTA^{WT} is extracted by p97 in mammals, its retarded polyubiquitination might diminish the avidity with which it is bound. This attenuated interaction might permit chaperones like Hsc70 to displace otherwise typical mediators of ERAD.

If any of the mechanisms hypothesised above were true, then a demonstrable interaction between RTA and Hsc70 should exist. This chapter, therefore, ultimately aims to investigate whether Hsc70 interacts with RTA in a direct and functional way.

4.1 Experimental approach

As described in the previous chapter, a co-immunoprecipitation approach to this investigation was precluded because of the low cytosolic concentrations of RTA that are found during intoxication. Instead, this chapter describes the development of a method to test for an interaction of Hsc70 with RTA *in vitro*. Ideally, this assay would be facile, reliable and able to show a functional association between Hsc70 and RTA amid a myriad of other proteins and chemicals.

In seminal experiments expounding the function of Hsc70, Minami *et al*. (1996) compared the degree to which luciferase irreversibly aggregated in conditions with or without chaperones. They demonstrated that Hsc70 and its loading co-factor, Hsp40, could prevent the aggregation of thermally-denatured luciferase during a 42°C heat-treatment *in vitro*, a feat that was maximally effective in the presence of ATP. They observed this by two methods:

(1) In real-time, by measuring the dynamic light scattering from particles of aggregated luciferase.
(2) By separating an incubation of luciferase and chaperones by centrifugation and analysing the relative distribution of protein between pellet and soluble fractions.

If such assays could be recapitulated with RTA, it would provide evidence for a direct interaction between the two proteins – with RTA as client and Hsc70 functioning as a *bona fide* chaperone. These observations could then help to reconcile the *in vivo* effects of chaperone inhibition. With this intention, this chapter describes a series of experiments investigating whether the general parameters known to govern protein stability lead to measurable changes in the assays mentioned above, and whether these changes are consistent with what would be expected of a good assay for measuring protein folding.

The parameters tested to this end included: pH, temperature, electrolyte concentration, macromolecular crowding and the effect of a small molecule chaperone. With this foundation in place, assays which examined the influence of the Hsc70/Hsp40 chaperone pathway were later introduced.

Mimicking the retrotranslocating or post-retrotranslocation state - As it is hypothesised that RTA interacts with Hsc70/Hsp40 in at least a partially-unfolded state after it has crossed the ER membrane, thermal denaturation was enlisted as a tool to denature RTA (as per Argent *et al*., 2000). This would render RTA in a state more representative of a post-retrotranslocation conformation (i.e. in which significant hydrophobic stretches may be solvent-exposed). It is worth mentioning, however, that this is not the physiological mechanism by which RTA is unfolded during intoxication. Rather, it is thought that factors in the ER environment promote the toxin subunit's change in conformation, e.g. negatively-charged phospholipids of the ER membrane. Liposomes comprising such phospholipid induce measurable changes to RTA's secondary structure when they are co-incubated *in vitro* (Day *et al*., 2002). This same effect is thought to promote co-option of the toxin subunit onto an ERAD-like pathway *in vivo* (Day *et al*., 2002; Mayerhofer *et al*., 2009).

Thermal versus lipid-based denaturation - Importantly for the interpretation of data presented in this chapter and the next, the ways in which thermal denaturation and interaction with negatively-charged phospholipids influence the structure of RTA are certain to be qualitatively different. Thermal denaturation forces the polypeptide chain into a higher-energy state. This breaks non-covalent, intra-chain bonds by increasing the kinetic energy of

the polypeptide backbone and its side-chains, expanding the diversity of conformations the protein population will inhabit. On the other hand, phospholipid-based disruption of the secondary structure would presumably replace non-covalent intra-peptide bonds with non-covalent phospholipid interactions instead. This promotes the partial insertion of RTA into liposomes *in vitro* (Mayerhofer *et al*., 2009). This insertion of RTA into the ER membrane might constrain the polypeptide into a relatively narrower array of conformations, promoting a correspondingly finer set of folding outcomes. These differences may alter the nature of the interactions that so-treated RTA can thereafter make in the cell when the polypeptide emerges on the cytoplasmic side of the membrane (such as with Hsc70). This physiologically relevant point is given consideration in the development of the assay and in the discussion of the results.

Screens for factors contributing to both unfolding and folding of RTA **-** Lastly, the folding state of RTA is deemed critical to the events which govern both co-option onto an ERAD-like pathway in the ER and subsequent success of the toxin subunit in the cytosol (Beaumelle *et al.*, 2002; Argent *et al.*, 1994; Mayerhofer *et al*., 2009). As such, it was a secondary hypothesis that RTA may have evolved to exploit qualities of the lumenal and cytosolic environments to maximise the success of its retrotranslocation and subsequent reactivation. Therefore, a final objective of this chapter was to use the developed assay to screen for factors which might contribute to instability of RTA in the ER lumen (promoting co-option onto an ERAD pathway), and which might support its relative stability in the cytosol (extending its catalytic half-life therein).

4.2 The temperature dependence of RTA aggregation

To determine the temperature dependence of RTA aggregation may seem a simplistic initial foray, but as the assays proposed were as yet untested for the toxin subunit, it was important to determine that the same rules applied to it as had been determined for other experimental systems (e.g. Minami *et al*., 1996; Van den Berg *et al*., 1999). A straightforward prediction preceded these experiments: at higher temperatures, RTA would misfold, aggregate and so lose solubility. This experiment also tests whether a consistent temperature-dependent threshold for RTA unfolding, of around 42°C (as determined by circular dichroism – Argent *et al*. 2000) could be resolved.

As a subunit of the ricin holotoxin, which is laid down in the endosperm of the developing seeds of the castor bean plant (*Ricinus communis*), RTA is stable over a wide range of

temperature (from lows of 0°C in native northern India to highs of 42°C in Kenya – Casey, 2007). During trafficking from the plasma membrane to the ER of a target cell as part of the holotoxin, it also remains stable at a relatively constant physiological temperature of 37°C. Conversely, as an orphan subunit in the ER of target cells, RTA must acquire characteristics at this physiological temperature that ensure it is recognised as misfolded, but which are not so severe so as to prevent it from being irreversibly degraded or terminally inactivated.

Correspondingly, orphaned RTA has been shown to approach a threshold for unfolding arguably close to the physiological temperature of 37°C. Argent *et al.* (2000) showed that the secondary structure of monomeric RTA becomes significantly destabilised at temperatures in excess of 42°C *in vitro* (homologous RIPs, such as saporin, are stable at much higher temperatures). Upon a subsequent increase to 45°C, they observed that a molten globule-like state could be induced, although the precise threshold was batch-dependent.[11] Mayerhofer *et al*. (2009) described another relevant temperature-threshold, showing that, at temperatures lower than 37°C RTA inserts less efficiently into a reconstitution of the membrane it crosses *in vivo*.

With these observations in mind, an initial array of temperatures was investigated: 37, 45 and 95°C. Figure 4.1 shows that RTA which has been incubated at these temperatures for 15 minutes can be split into pellet and soluble fractions after a 10 minute, 16000 $\times g$ centrifugation. At 37°C, RTA was mostly soluble, although much was observed in the pellet. At 45°C, a greater proportion was observed in the pellet fraction. After incubation at 95°C, relatively all of the RTA was found in the pellet. However, the absolute signal size from the combined intensity of pellet and soluble bands was diminished, suggesting loss of RTA from the experimental system (Figure 4.1a & d). To determine how RTA was being lost, a more comprehensive array of temperatures was first examined.

[11] Buffer conditions: 20mM sodium phosphate, pH7.0, with 2mM DTT (Day *et al*., 2002).

Figure 4.1 – RTA can be heated and then split into soluble and aggregated fractions

500ng RTA in a total volume of 20µL (0.8µM) was incubated in an Eppendorf tube at the indicated temperature for 15 minutes (in a buffered solution of 10mM MOPS / 50mM KCl, pH7.2). Samples were then separated into pellet (P) and soluble (S) fractions by centrifugation at 16000 ×*g* for 10 minutes. Both fractions were subsequently dissolved in loading buffer and separated in parallel by SDS-PAGE. a) RTA bands (grey arrowhead) were developed via silver stain. Vertical grey and black lines have been added to help demarcate adjacent pellet/soluble pairs. b) Pellet and soluble RTA bands were quantified relative to one another (using TotalLab). c) Plots the average intensity of bands derived from pellet (●) and soluble fractions (○). d) Plots the average total intensity of the pellet band added to the soluble band for each temperature (●). Note loss of signal at 95°C.

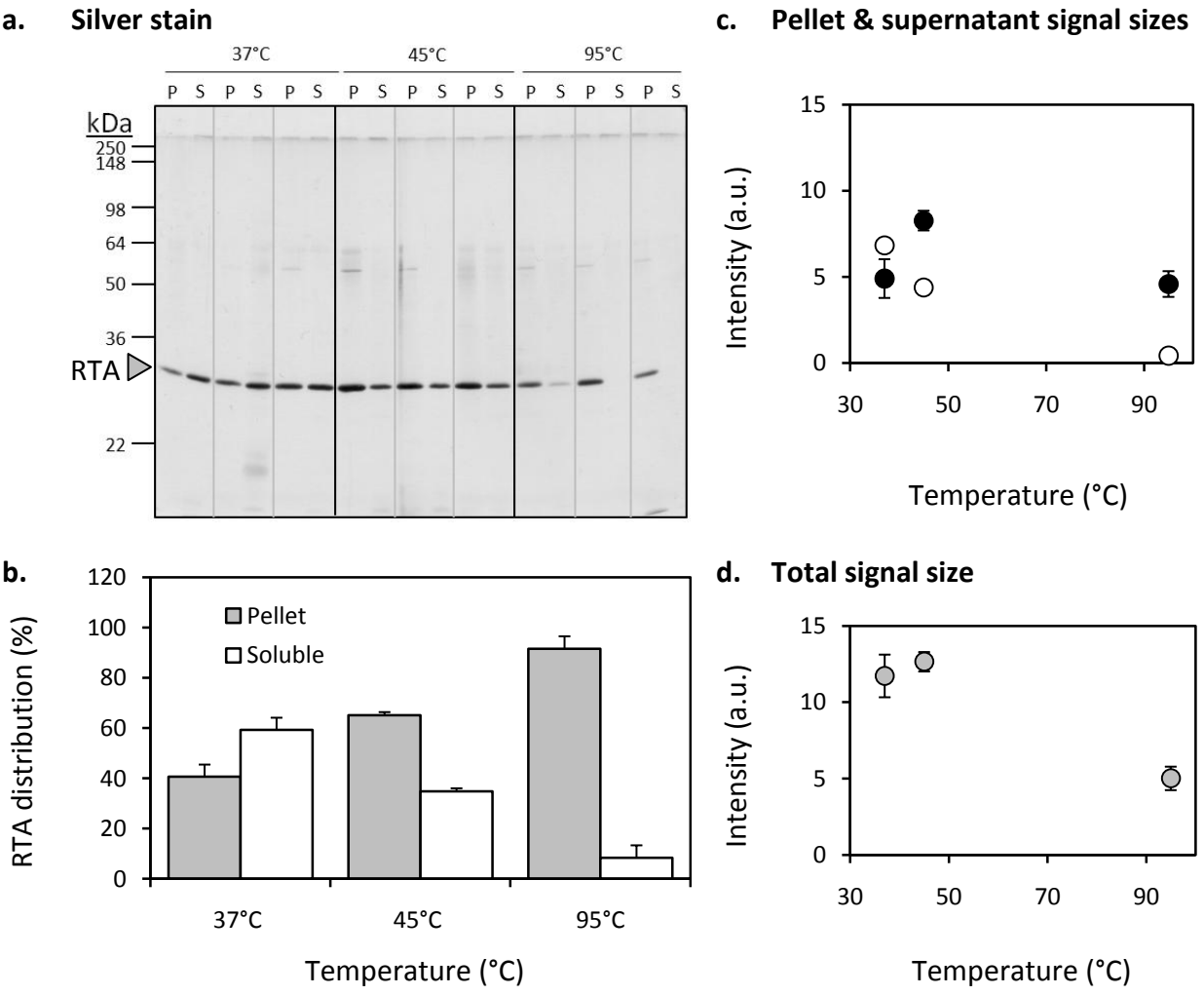

The effect of increasing temperature in gradual increments from 24°C to 55°C can be observed in Figure 4.2a & b. At temperatures of 37°C and below, RTA is quite uniformly divided between pellet and soluble fractions, although there is a marginal decrease in solubility as the temperature increases. This starkly contrasts to a sharp threshold between 37°C and 45°C. At this transition, there is a dramatic loss of RTA from the soluble fraction. The larger error-bars for the 45°C dataset reflect how this is likely to be near an important transition temperature, where small changes in temperature result in relatively gross changes in solubility. Encouragingly, these data mirror the 42-45°C threshold observed by Argent *et al*. (2000).

Just as observed in Figure 4.1, the total amount of RTA in Figure 4.2a & b visibly decreases at elevated temperatures, rather than merely shifting from soluble to pellet fractions as expected. It was possible that this might be because of a protease contaminating the incubation, the activity of which upon RTA was greatly increased above 45°C. Such a protease could have been co-purified with RTA at low concentrations, or could have otherwise contaminated the buffer (although no fragmentation of RTA was observed – Figure 4.1). To test this, RTA was incubated at 55°C with or without Complete protease inhibitor tablets (Roche; used at the manufacturer's recommended concentration). Figure 4.2c shows no difference in the solubility of RTA when the inhibitors are present (quantified in Figure 4.2d), suggesting that loss of signal does not result from the activity of a protease.

If not lost to a protease, then two alternative explanations can be proposed for this phenomenon:

(1) When heated, unfolded RTA has a greater propensity to adhere to the side of the reaction vessel in which it is incubated (the vessel being made of hydrophobic polypropylene).
(2) If, even at low temperatures, the quantity of RTA in the pellet is already saturated with silver-stain, then redistribution of previously soluble matter to this fraction will be masked at higher temperatures.

In either scenario, the results still show the same, informative trend: a relative decrease in solubility at higher temperatures, which is consistent with unfolding.

Figure 4.2 – Relative intensity of RTA from the pellet increases with temperature

a) 500ng RTA in a total volume of 20µL (0.8µM) was incubated at the indicated temperature for 15 minutes, and b) the pellet/soluble fractions quantified. Grey vertical lines demarcate pairs of pellet (P) and soluble (S) fractions. b) Shows quantification of RTA band distribution (using TotalLab). c) RTA was incubated for 15 min at 55°C, with or without Complete protease inhibitors ("CPI" - Roche). Samples were split as before and analysed by silver stain. d) Pellet and soluble RTA bands were quantified as before. In all cases, error bars show the SEM between three independent sets of assays.

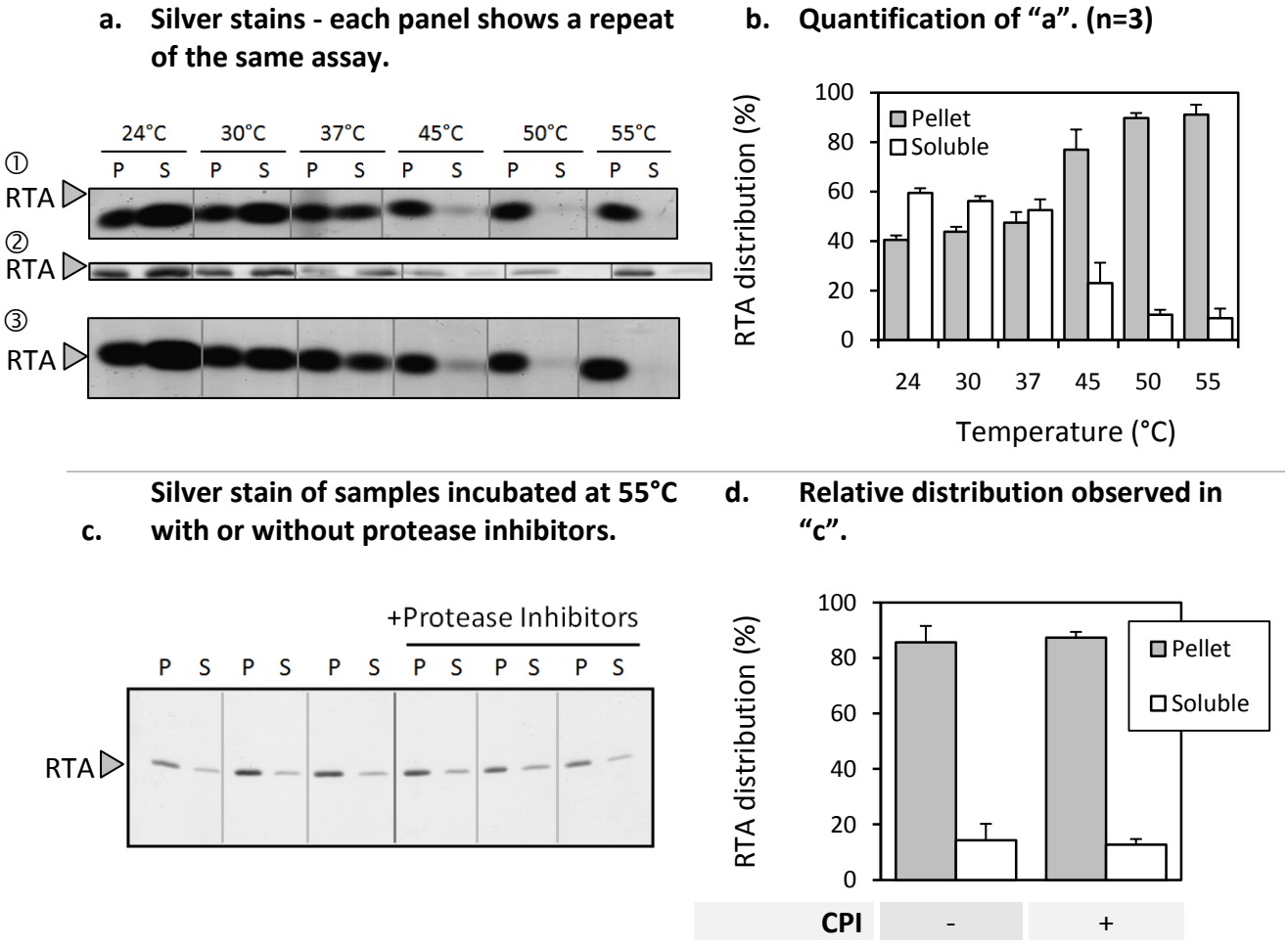

4.2.1 A comparison of the stability of RTA with saporin at 45°C

As a comparison to RTA, saporin (a type I RIP homologous with RTA) does not aggregate with the same distribution between pellet and soluble fractions at 45°C (Figure 4.3). Testament to their similarity, the C_α backbones of these proteins can be superimposed upon one another to a high degree (Fermani *et al*., 2009) and their sequence identity is in the region of 30% (Vago *et al.*, 2005). However, saporin lacks the hydrophobic C-terminus that is implicated in the cytotoxicity of RTA (Day *et al*., 2002). Saporin also has more lysine residues. Correspondingly, the pI of saporin is 9.5, whilst RTA itself has a pI of 7.3 (Li *et al.*, 1992; Vago *et al*., 2005). As the buffer used in the solubility assay is pH7.2, these conditions would favour the solubility of saporin.

From these comparisons it may be inferred that the relative instability of RTA in the soluble phase may be associated with both the hydrophobic C-terminus of the toxin subunit and even its reduced lysine content. This difference in stability is interesting given that saporin is not thought to co-opt an ERAD pathway to enter the cytosol (Vago *et al*., 2005). RTA, on the other hand, seems to have paid a conformational penalty to exploit this route, manifested here in its relatively low solubility. Coincidentally, therefore, evolutionary loss of lysine residues to avoid polyubiquitination may have also contributed to the candidacy of RTA as an ERAD substrate. Putatively, both of these factors may have contributed to the selective pressure which resulted in RTA's substitution of lysine residues.

Also unlike saporin, RTA spends much of its lifetime as the subunit of a holotoxin. As part of this complex, RTA is stabilised by a disulfide linkage to RTB (Day *et al*., 2002). This association conceals the hydrophobic C-terminus of the A-chain from the solvent (Day *et al*., 2002) and ensures that the complex remains stable during vesicular trafficking. This stability persists until the ER is reached, wherein PDI reduces the dimer (Spooner *et al*., 2004). Thus, only in the ER is monomeric RTA liberated. This mechanism ensures that the "conformational penalty" highlighted here becomes significant only when it will also be of use for the toxin in helping it to cross the ER membrane. Once in the cytosol, however, this otherwise latent instability may well persist. This reinforces why cytosolic chaperones are expected to provide a valuable interaction for the toxin subunit.

Figure 4.3 – Solubility of saporin after incubation for 15 minutes at 45°C.

In this assay 500ng saporin (0.8µM) was substituted for RTA in the incubation volume of 20µL, but the protocol was otherwise as before. a) Shows quantification of the saporin distribution between pellet (P) and soluble (S) fractions (the data for RTA in this chart is that from Figure 4.2b). Error bars show SEM. b) Quantification was derived from this set of three independent silver stains. Grey arrowheads indicate the saporin band.

a. Quantification (n=3)

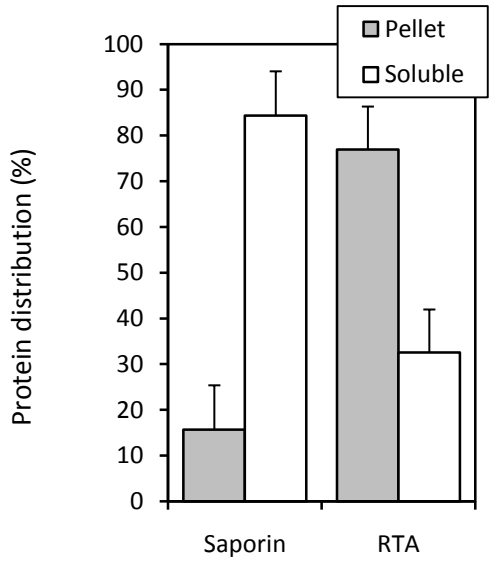

b. Silver stains – each panel shows a repeat of the same assay.

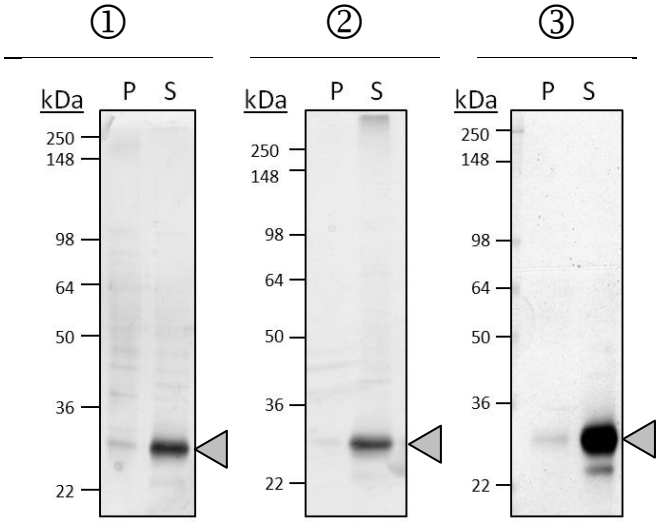

4.3 A turbidity assay can be used to measure aggregation of RTA over time

The assay described to this point only measures the aggregation of RTA at an arbitrary end-point (in all cases described, a 15 minute incubation). Similar assays measuring the dynamic aggregation of RTA over time can also be conducted, for instance by measuring the light scattering from a heated sample (Minami *et al*., 1996). Such experiments were conducted; please see the appendix (Figure 8.2). Unfortunately, this approach was prohibited from being used more extensively in this chapter because of the lack of reliable, accurate temperature controls on the spectrophotometers available. Moreover, limited space available in the sampling chambers of these machines precluded the incorporation of parallel controls. In an ideal situation where these were not problems, this method would have been opted for in preference to the solubility assay, as it would have permitted the acquisition of more comprehensive data.

4.4 Solubility correlates with enzymatic activity

It was important to determine that the quality measured by this assay – solubility – correlated with the enzymatic activity of RTA. Otherwise, it would be less relevant to an *in vivo* reactivation process. The assay typically used to determine the catalytic activity of RTA visualises the depurination of ribosomal RNA by the toxin (Endo *et al.*, 1987). In this assay, RTA-treated ribosomes are exposed to acetic-aniline (pH4.5), which causes the phosphodiester backbone of the 26s rRNA to be cleaved at the site where the toxin subunit has been specifically depurinated. The proportion of this aniline fragment can then be quantified by its apparent intensity on a denaturing formamide:agarose gel relative to the intensity of an rRNA that remains unaffected by the treatment (in this case 5.8S rRNA). The formula for relating fragment intensity to relative depurination is shown in Equation 1, and accounts for the comparative staining of each fragment according to its base pair length. Background from the gel can be removed from this value by subtracting a similar figure derived from intact controls which have not been treated with RTA (or, alternatively, which have not been treated with aniline).

RTA was heated to 45°C for 15 minutes and then assayed for catalytic activity by this method. Figure 4.4a shows that RTA which has been heat-treated has little obvious depurinating activity (no aniline fragment can be observed in these assays, although TotalLab analysis suggests some activity may persist). As a control, untreated RTA possessed observable activity (the aniline fragment can be seen in these assays). Similar experiments

published in Spooner *et al*. (2008) show that the soluble fraction (16000 ×*g*) of heat-treated RTA has less enzymatic activity than does an equivalent soluble fraction from untreated RTA (reprinted in Figure 4.4b). The assays in Spooner *et al.* (2008) also show that the soluble fraction of heat-treated RTA does possess enzymatic activity; at least some material which is soluble at this temperature retains catalytic activity.

Admittedly, it would have been preferable to consistently couple the results of each solubility assay in this chapter with an experiment to confirm the relationship of enzymatic activity to the size of the soluble fraction. However, this RNA-based technique is subject to difficulties owing to the complexity of the protocol and the vulnerability of both the ribosomal RNA and aniline fragment to contaminant RNases. These technical difficulties made a more comprehensive approach unfeasible, especially as the complex mixes which are used later in this chapter potentially contain significant quantities of contaminant RNase.

$$[\mathbf{Relative\ depurination}]_{\%} = \frac{[\mathbf{AnilineFragment}]_{\mathbf{Intensity}}}{[\mathbf{5.8S\ rRNA}]_{\mathbf{Intensity}}} \times \frac{\mathbf{160}}{\mathbf{369}} \times \mathbf{100}$$

Equation 1 – Depurination formula.

For calculating relative depurination from the relative intensity of aniline-fragment and uncleaved 5.8S rRNA bands, as visualised by ethidium-bromide staining after denaturing electrophoresis. The values “160” and “369” account for the different lengths of each fragment, which attract different staining intensities.

Figure 4.4 - Solubility of RTA correlates to enzymatic activity

500ng RTA in a total volume of 20µL (0.8µM) was incubated at either 37°C or 45°C for 15 minutes, as before. The indicated mass was then added to yeast ribosomes for a total period of 2 hours at 30°C. Depurination was then measured by treating the ribosomal rRNA with acetic aniline and observing the intensity of the drop-out band. a) Shows electrophoresis of rRNA under denaturing conditions (1.2% agarose; 50% formamide). Gels were stained with ethidium bromide. b) Shows quantification of the relative depurination caused by RTA in each of the incubations, as calculated by Equation 1. Relative depurination was normalised to the aniline-untreated background. Error bars show the range between the two repeats shown in "a". c) Shows results published in Spooner *et al*. (2008) produced by R.A. Spooner. Here, 16000 ×*g* soluble fractions from 375ng of 45°C-treated RTA (or untreated RTA) were added, in the indicated dilution, to the aniline reactions. d) Shows quantification of the relative depurination in each of the incubations shown in "c". Relative depurination was normalised according to RTA-untreated background.

(Figures displayed on subsequent page.)

(Figure 4.4 – continued.)

a. **Results of Electrophoresis: Heat-treated RTA vs. untreated RTA. The separate panels show repeats of the same experiment.**

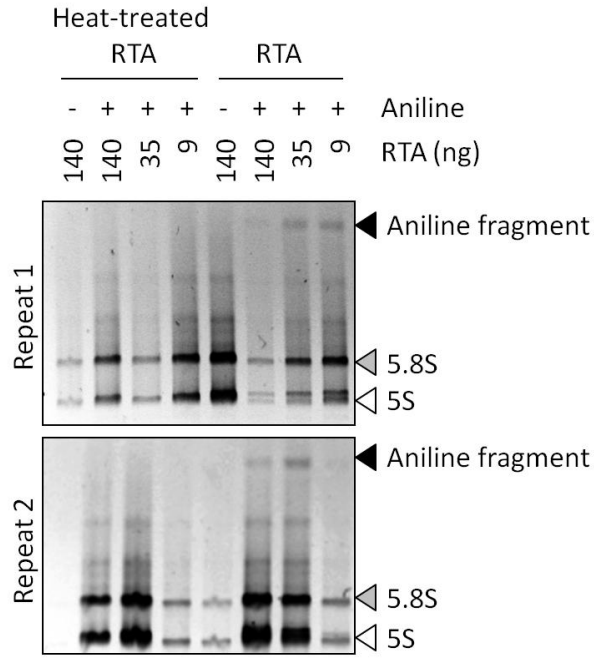

b. **Quantification of "a" (n=2)**

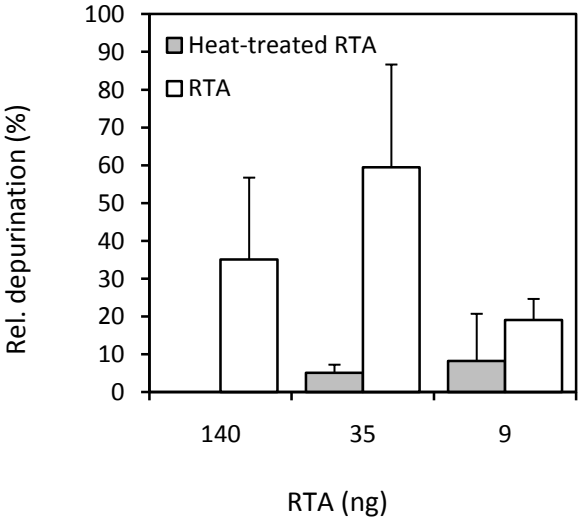

c. **<u>Data from Spooner *et al*. (2008)</u> Comparison of soluble fractions from heat-treated RTA and untreated RTA.**

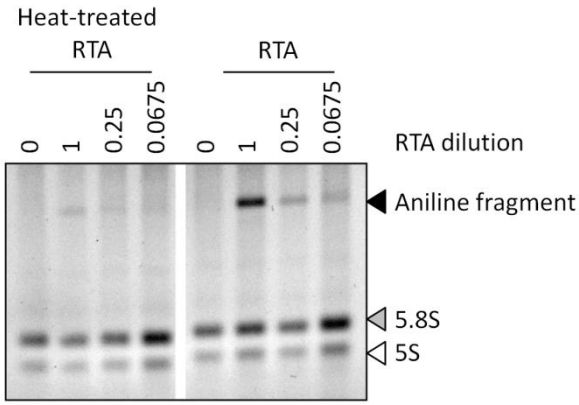

d. **Quantification of "c" (n=1)**

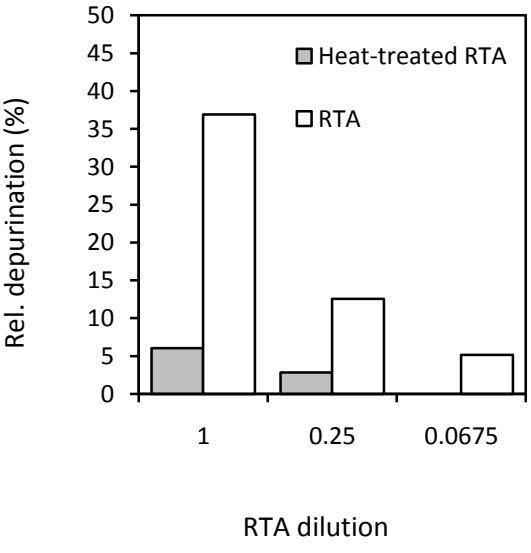

4.5 The effects of macromolecular crowding, pH, electrolyte concentration and a small molecular chaperone

4.5.1 Macromolecular crowding

In vivo, macromolecular crowding imposes limits upon the conformational rearrangements a polypeptide can make. Such crowding effects have not been mimicked in this assays shown so far. Notably, the ER lumen is less crowded than the cytosol, as measured by the diffusion rates of GFP after photobleaching (Swaminathan *et al*., 1997; Marguet *et al*., 1999). In both compartments, however, crowding will putatively increase the chances of RTA interacting aberrantly with adjacent polypeptides. Furthermore, because of spatial confinement, the speed of re-folding interactions is also increased under such conditions (Van den Berg *et al.*, 1999). As such, crowding would be expected to hinder the solubility of RTA.

A highly-branched polymer of neutrally-charged polysaccharide, Ficoll-70, was enlisted to emulate volume-excluding effects (Van den Berg *et al.*, 1999). When RTA was incubated with 200g.L^{-1} of this crowding agent, little change in solubility was observed at 45°C (Figure 4.5a & b) and no change was observed at 37°C (Figure 4.5a & c).[12] Why Ficoll-70 has little or no apparent effect upon solubility is curious. At 37°C, RTA would not be expected to unfold significantly (Argent *et al*., 2000). Therefore, it may be that crowding from Ficoll-70 cannot subsequently augment inter-chain interactions, and so cannot promote a loss of solubility. However, at 45ºC, RTA would be expected to assume a molten globule-like state (Argent *et al*., 2000), where it would presumably be more prone to making inter-chain associations. It seems that some other effect already saturates the propensity of RTA to lose solubility when the toxin subunit unfolds at this temperature (45°C). Speculatively, this could be an interaction between the functionally-important hydrophobic C-terminus of the toxin subunit (Day *et al*., 2002; Simpson *et al*., 1995) and the abundant hydrophobic surface which may be adsorbed to during the incubation (the polypropylene Eppendorf).

[12] N.B., Figure 4.5 shows little difference between the pellet/soluble distribution at 37°C compared to 45°C, unlike has previously been shown (*cf.* Figure 4.1 and Figure 4.2). This is because the RTA used for experiments at 37°C and 45°C comes from different stocks. This highlights the batch dependence reported by Argent *et al.*, (2000) and how it is crucial to use RTA from the same stock for data which are to be compared. As Ficoll-70 was the factor under scrutiny here, however, it was less important to ensure a similar stock was used at both 37°C and 45°C.

Figure 4.5 – The effect of macromolecular crowding upon RTA aggregation at 45°C and 37°C

500ng RTA (concentration and buffer as before) was incubated in an Eppendorf tube at the indicated temperature for 15 minutes, but with or without 200g.L^{-1} of Ficoll-70. Samples were collected and divided, as before, into pellet (P) and soluble (S) fractions before being analysed in parallel by SDS-PAGE. a) Shows resultant silver stains. Vertical grey lines demarcate pellet and supernatant pairs. b) Shows quantification of RTA band distribution at 45°C (using TotalLab). c) Shows quantification from experiments conducted at 37°C. Error bars derived from the standard deviation of the three repeats shown in c). In all cases, error bars show SEM.

a. Silver stains – upper panel shows assays at 37°C, lower panel 45°C.

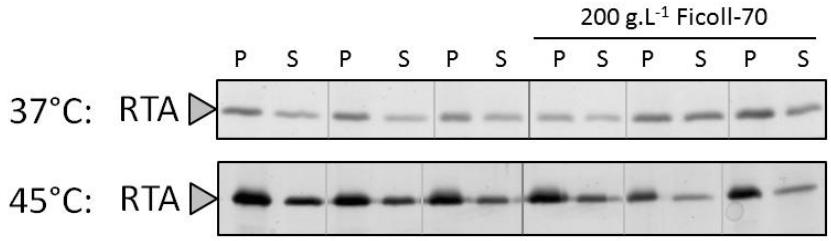

b. 45°C quantification (n=3)

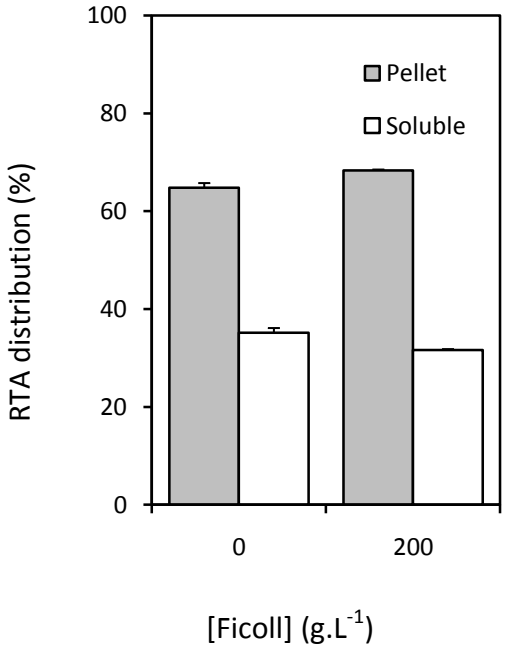

c. 37°C quantification (n=3)

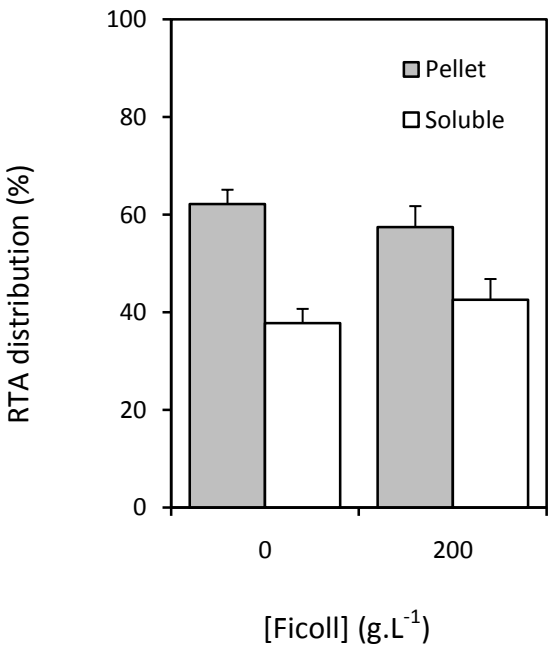

4.5.2 The effect of electrolyte concentration

Unlike crowding from Ficoll-70, the solubility of RTA was found to respond to the electrolyte concentration of the incubation buffer. Solubility was increased in heat-treated incubations which contained more NaCl (Figure 4.6). Hu *et al*. (2009) hypothesise that increased electrolyte concentration stabilises the solvent structure, making hydration of an extended polypeptide backbone less favourable. This effect would inhibit unfolding by causing tight-packing of the protein.

Previously, the secondary structure of RTA has been shown to be destabilised by an interaction with negatively-charged liposomes (Day *et al*., 2002; Mayerhofer *et al*., 2009). As the pI of RTA is reportedly 7.3 (Li *et al*., 1992), and the buffer used to demonstrate the liposome interaction *in vitro* was of pH7.1, the toxin subunit would be positively charged under those conditions. Negatively-charged phospholipid and RTA, therefore, would bear charges complementary to their mutual binding *in vitro* as well as *in vivo*, where pH approaches 7.1 to 7.2 (Van Anken & Braakman, 2005). As introduced earlier, this interaction of RTA with negatively charged lipids is thought to be physiologically significant in promoting retrotranslocation (Day *et al*., 2002; Mayerhofer *et al*., 2009). In the model supported by these papers, RTA is reductively cleaved from RTB in the ER lumen by PDI (Spooner *et al*., 2004). Monomeric RTA subsequently interacts with the lipid environment of the ER, leading to a conformational change that is permissive of both its recognition as an ERAD substrate and retrotranslocation (Day *et al*., 2002; Mayerhofer *et al*., 2009).

Pertinent to the stabilising effect of electrolyte, Day *et al*. (2002) observed that the initial stages of RTA's interaction with liposomes can be prevented at increased concentrations of NaCl. Conversely, pre-formed complexes of RTA and liposomes cannot be disrupted with NaCl. Day *et al.* (2002) concluded that the initial stages dictating the unfolding of RTA were caused by electrostatic interactions with which the electrolyte competed. Thereafter, their model suggests RTA embeds itself in the membrane in a hydrophobic manner, producing an interaction with which electrolyte cannot compete. In addition to these hypotheses, it could be added that high concentrations of NaCl restrains the "thermal breathing" of RTA by stabilisation of the water structure (Hu *et al*., 2009). This would constrain the initial unfolding events which lead to embedding in the liposome. Adding NaCl subsequent to the interaction could thus also hinder unfolding events that would allow the two species to subsequently separate.

Figure 4.6 – The effect of [NaCl] upon RTA aggregation at 45°C

500ng RTA was incubated as before for 15 minutes at 45°C with the indicated concentration of $NaCl_{(aq)}$. Pellet (P) and soluble (S) fractions were collected as previous and analysed in parallel by SDS-PAGE. a) Shows resultant silver stains. b) Shows the quantification of RTA band distribution (using TotalLab). Error bars show SEM.

a. Silver stains – each panel represents an independent assay.

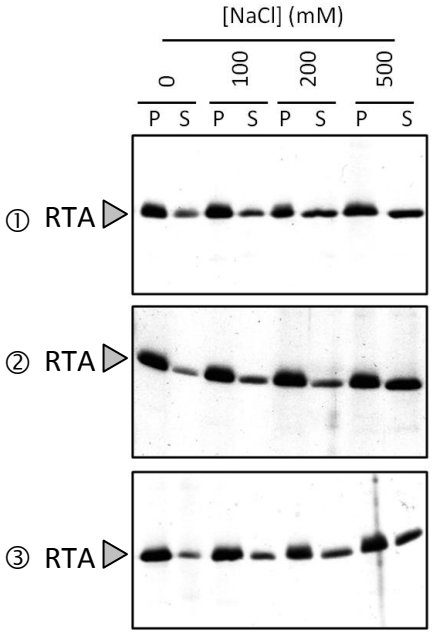

b. Quantification (n=3)

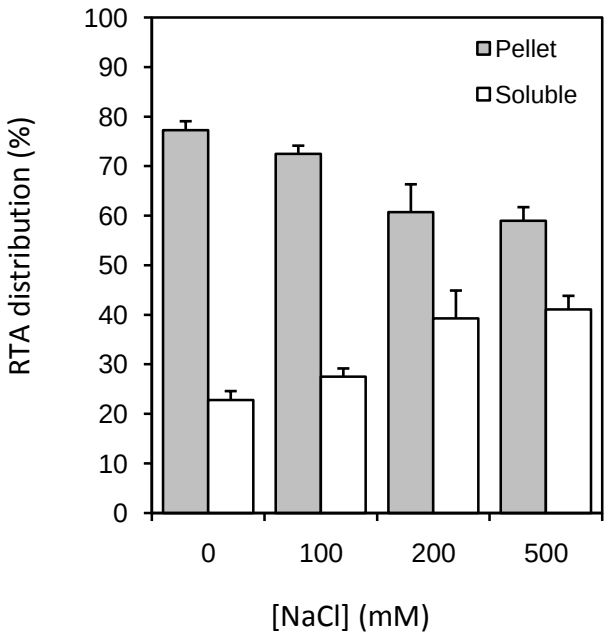

4.5.2.1 The effect of ionic calcium on the solubility of RTA

Unlike sodium ions, there is a heavily-polarised difference in the concentration of calcium ions between the ER and the cytosol (Van Anken & Braakman, 2005). This results from the activity of the sarcoplasmic / endoplasmic reticulum Ca^{2+} ATPase (SERCA) pump (Van Anken & Braakman, 2005). As RTA must cross the membrane which divides these compartments in a process that is conformation-dependent, the effect of electrolyte concentration on the solubility of RTA might pose some mechanistic significance.

Being technically difficult to measure, the total [Ca^{2+}] of the mammalian ER has been estimated very broadly to be between 0.3mM and 50mM by (comprehensively reviewed in Meldolesi & Pozzan, 1998). This additional calcium is sequestered and buffered largely by the protein matrix, the function of which it modulates (Van Anken & Braakman, 2005). Unsequestered [Ca^{2+}] in the ER is even more widely estimated to be between 1μM and 3mM depending on the tissue examined and the experimental technique used, reflecting its more dynamic nature. For HeLa in particular, an ER concentration of 1.5mM to 3mM unsequestered Ca^{2+} has been shown (Meldolesi & Pozzan, 1998). From the kinetics of the SERCA pump, the gradient to the cytosol is expected to involve a difference of around 10^5 units (Meldolesi & Pozzan, 1998).

The effect of [Ca^{2+}] concentration upon the solubility of RTA was examined *in vitro* (Figure 4.7). At 45°C, only the highest concentration of $Ca^{2+}_{(aq)}$ (10mM) visibly stabilises RTA in the soluble fraction. At lower concentrations, little soluble RTA is apparent (Meldolesi & Pozzan, 1998). This is at odds with a preceding hypothesis regarding what ER and cytosolic conditions would promote, which was: RTA would be more soluble in conditions equivalent to the cytosol (to extend its toxic lifetime), whilst in the ER it would be less so (so as to be recognised for ERAD). It would therefore seem that other factors in the ER environment dominate the acquisition of ERAD-permissive traits.

To extend these studies, the experimenter has access to both thapsigargin (which inhibits the SERCA pumps responsible for the gradient) and ionomycin (which is used to neutralise Δ[Ca^{2+}] across biological membranes). However, both of these commonly used agents also affect the endocytosis and trafficking of ricin through the secretory pathway (Llorente *et al*., 2000; Lauvrak *et al*., 2002), likely complicating the interpretation of their effects. Therefore, the use of these reagents has not been pursued herein.

Figure 4.7 – The effect of [$CaCl_2$] upon RTA aggregation at 45°C

500ng RTA was incubated, as before, at 45°C with the indicated concentration of $CaCl_{2(aq)}$. Pellet (P) and soluble (S) fractions were collected as before and analysed in parallel by SDS-PAGE. a) Shows silver stains with vertical grey lines demarcating pellet/soluble pairs; b) shows the quantification of RTA band distribution (using TotalLab). Pellet intensity is shown in grey, with soluble band intensity shown in white. Error bars show SEM.

a. Silver stains – each panel represents an independent assay.

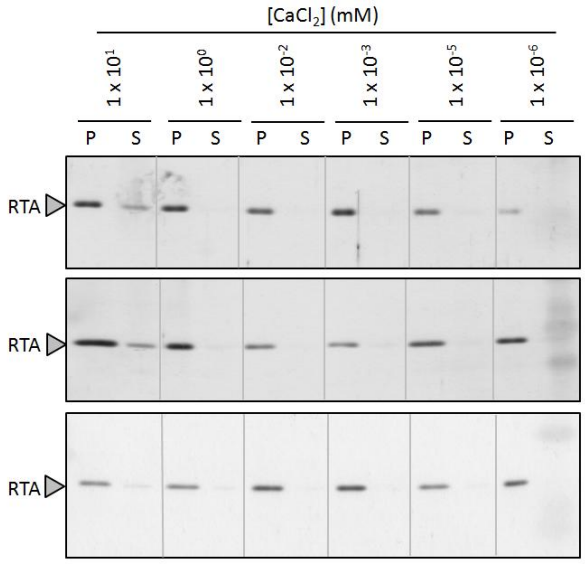

b. Quantification (n=3)

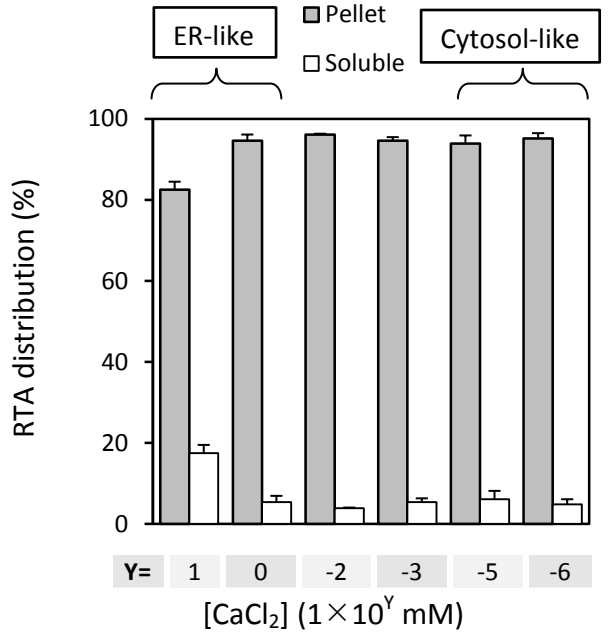

4.5.3 The effect of pH

The effect of different pH buffers on the solubility of RTA was examined (Figure 4.8). Buffers ranging from pH6.4 to 8.0 were tested, centred upon pH 7.2 (the pH otherwise used in all solubility assays throughout this thesis, and also as used by Minami *et al*., 1996). Under these conditions, RTA was most prone to lose solubility at pH 7.0-7.4. This is as predicted from recombinant RTA's pI of 7.3 (Li *et al*., 1992).[13] Around this pH, the net charge of RTA would be neutralised and it would thus become less hydrophilic, accounting for its loss of solubility.

Although RTA is evidently unstable at pH7.2, this was the default pH for other solubility assays undertaken throughout this thesis. Significantly, it is at this pH that Hsc70 and Hsp40 are observed to optimally protect luciferase from thermal denaturation (Minami *et al.*, 1996). It is also a fair approximation of the pH in the ER and cytosol of HeLa cells (Kim *et al*., 1998; Llopis *et al*., 1998; Van Anken & Braakman, 2005). Coincidentally, these findings highlight the importance of storing RTA at a pH that is removed from the physiological norm. Indeed, in our laboratory RTA is stored at pH6.4 to limit aggregation.

The inherent instability of RTA at the physiological pH consistently highlights how RTA is finely-tuned to unfold during its lifetime as an orphan subunit. This is a feature that will likely promote its candidacy as an ERAD substrate. However, as there is no difference in the cytosolic and ER pH (Anken & Braakman, 2005), the same instability would persist after the toxin subunit has gained access to the cytosol. A stabilising factor such as a cytosolic chaperone, might provide a beneficial interaction for the toxin.

[13] Curiously, the pI of recombinant RTA is spuriously reported to be between 6.1 and 6.5 using a variety of bioinformatic approaches (Kozlowski, 2008; Gasteiger *et al*., 2005).

Figure 4.8 – The effect of pH upon RTA aggregation at 37°C

500ng RTA was incubated, as before, at the indicated temperature with the buffer adjusted to the indicated pH. Pellet (P) and soluble (S) fractions were collected as before and analysed in parallel by SDS-PAGE. a) Shows silver stains with vertical grey lines demarcating pellet/soluble pairs; shown are three representative gels from a series of six total; b) shows the quantification of RTA band distribution (using TotalLab). Error bars show SEM.

a. Silver stains – each panel represents an independent assay.

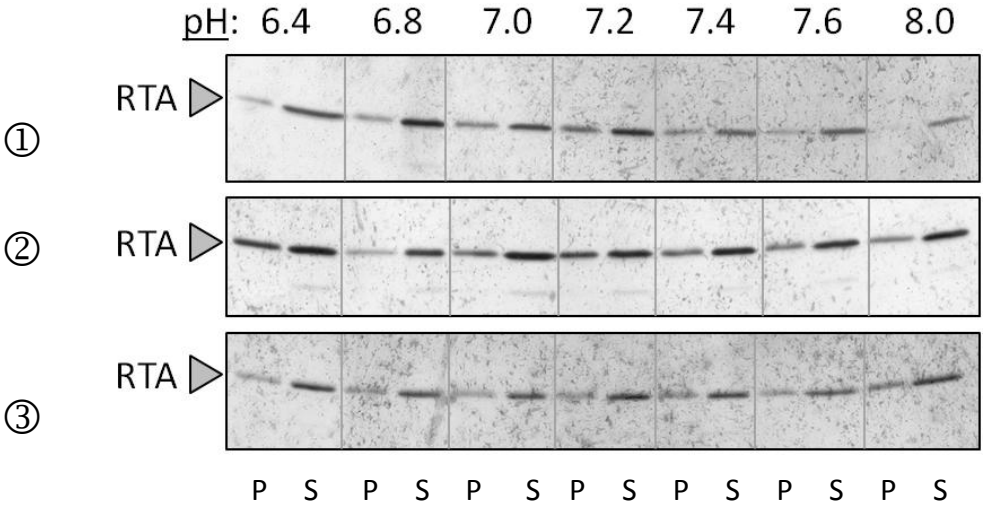

b. Quantification (n=6)

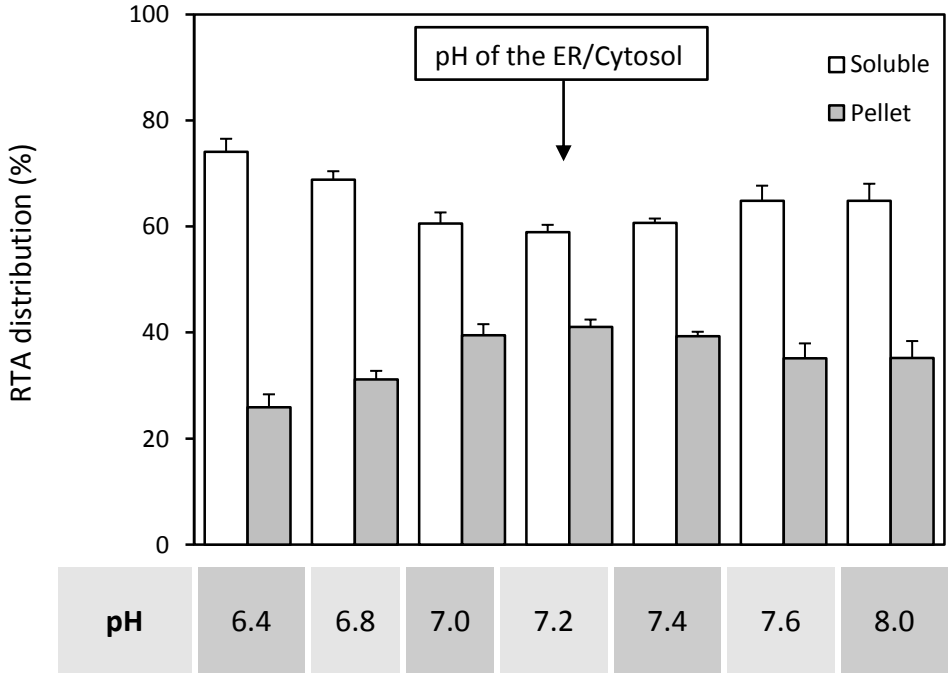

4.6 Glycerol improves the solubility of RTA

Numerous so-called 'small molecular chaperones' promote the solubility of proteins like RTA by inhibiting the unfolding that leads to their aggregation (Van den Berg *et al*., 1999). Glycerol is one such chemical, able to prevent RTA from aggregating at both 37°C and 45°C (Figure 4.9a & b). Peek *et al*. (2006) showed that this was by increasing the midpoint thermal transition temperature for unfolding (as determined by measuring changes in intrinsic tryptophan fluorescence with or without glycerol) rather than by sites that would propagate aggregation. For this reason, glycerol is often supplemented into the buffer in which RTA is stored to promote long-term solubility.

Figure 4.9 – The effect of glycerol on the solubility of RTA

0.3µM RTA was incubated in 10mM MOPS / 50mM KCl (pH7.2) for 15 minutes at the temperature indicated with the shown concentration of glycerol (w/v). Pellet (P) and soluble (S) fractions were then collected and quantified as before. a) Shows silver stains. b) Shows quantifications made using TotalLab, with error bars showing the SEM.

a. Silver stains – each panel represents a separate assay, 3 at each temperature.

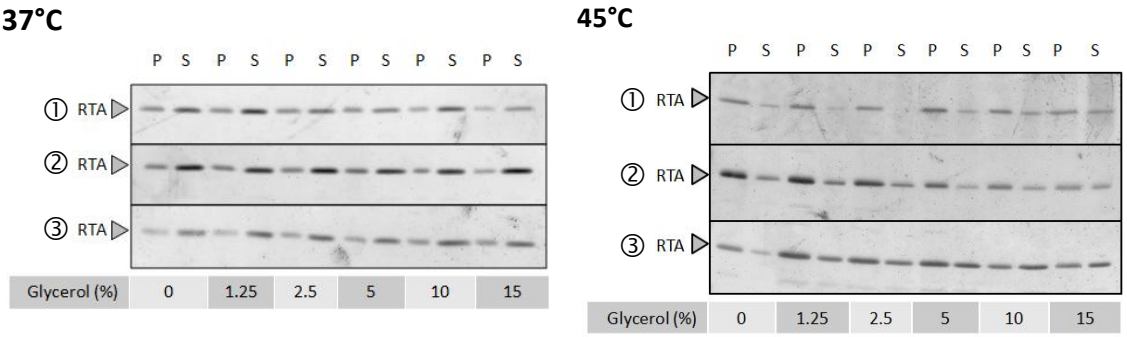

b. Quantification (n=3)

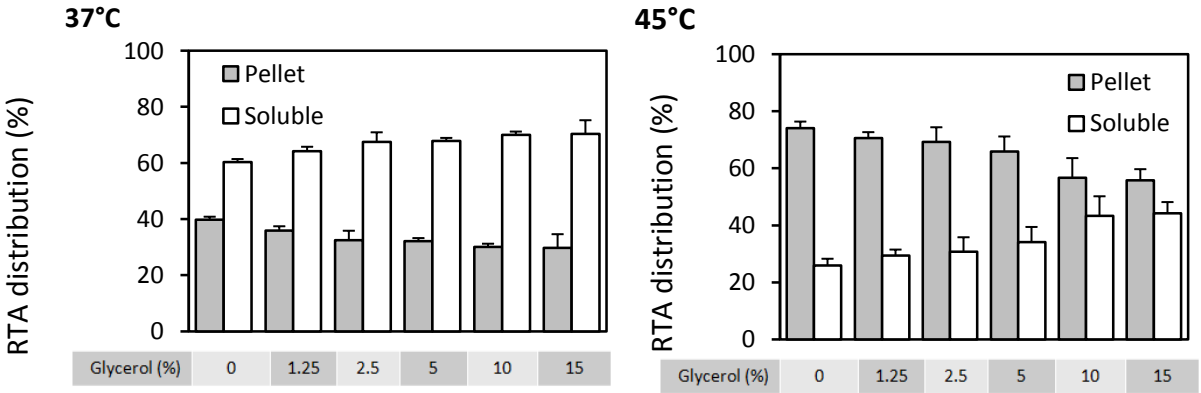

4.6.1 Glycerol reduces the cytotoxicity of ricin

It was introduced earlier that impediments to the unfolding of RTA such as additional disulfide bonds (Argent *et al.*, 1994) or the conjugation of tightly-folded species like DHFR (Beaumelle *et al*., 2002) reduce its cytotoxicity. Therefore, it was predicted that treatment of cells with a small molecular chaperone such as glycerol might also inhibit toxicity, stabilising RTA in the ER lumen. Cells were incubated with or without 10% glycerol (w/v) and the IC_{50} of ricin was determined in each context (Figure 4.10a & b). This treatment protected cells 8.96-fold (SD ±1.45; n=3), a similar effect to that reported by Sandvig *et al.* (1984), who used a concentration of 9.2% (w/v) glycerol in experiments using Vero cells. Contrastingly, Sandvig *et al*., (1984) hypothesised that this effect was because glycerol increased the rigidity of the target ER membrane, prohibiting insertion of RTA into it, rather than from affecting RTA directly.

Figure 4.10 – The effect of glycerol on the cytotoxicity of ricin

HeLa cells were treated with 10% glycerol coeval to ricin-treatment and then examined for the IC_{50} with respect to ricin, as has been shown before. Control cells did not include glycerol in the incubation. a) A typical set of dose-response curves from a total of three independent experiments, comparing cells treated with medium containing no glycerol (○) to medium laden with 10% glycerol at the time of toxin application (w/v) (●). b) This yielded an 8.96-fold protection (SD: ±1.45; n=3) compared to untreated controls. Error bars show SEM.

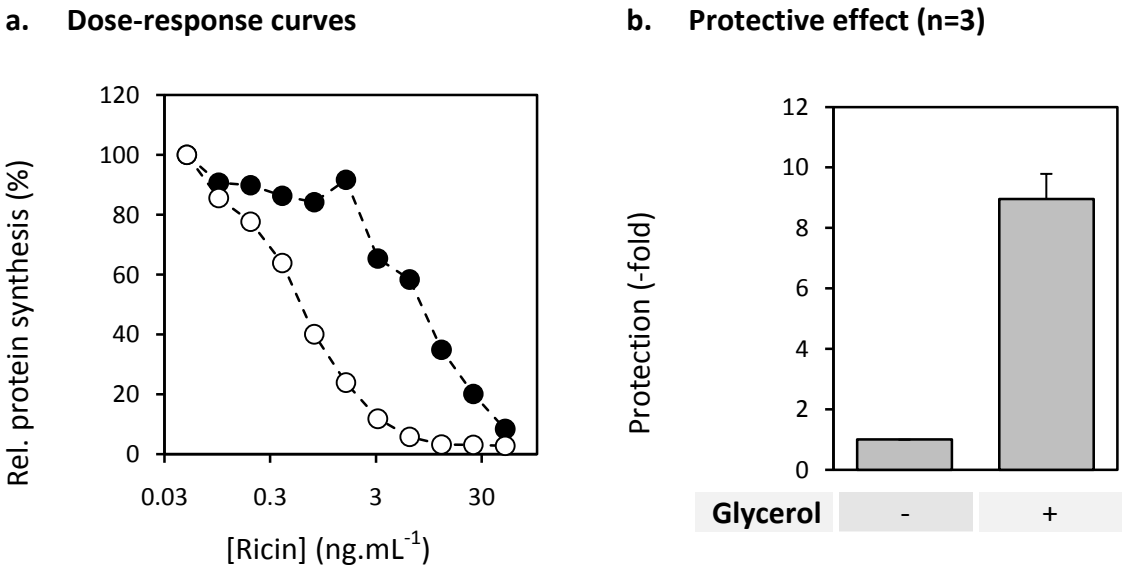

4.6.2 Glycerol increases the lag observed before the cytotoxicity of ricin is exhibited

Sandvig *et al*. (1984) showed that glycerol treatment did not interfere with endocytosis nor binding of the holotoxin to the cell surface. However, they did not exclude any other interaction beyond this stage of holotoxin trafficking. As such, time-response assays were conducted to determine whether the effect of glycerol resided at a stage before entry of RTA into the retrotranslocation-competent compartment (Figure 4.11a & b). The results of these assays confirm that, in incubations with glycerol, there is an increase in trafficking time before the log-linear portion of the profile is reached.[14] According to the regression of these log-linear profiles (Hudson & Neville, 1987), the relative lag before the first signs of toxicity is increased by an average of 57% (SD ±5%; n=3). Furthermore, the rate of delivery after this point is reached is much lower, as shown by the gentler slope of the log-linear region.

These data clarify that glycerol delays the entry of RTA into the cytosol in an active state. To determine whether glycerol could interfere with the interaction of RTA and the ER membrane, so also preventing co-option of the toxin subunit onto an ERAD pathway, was one of the objectives of the next section.

[14] This also provides a positive example of this particular assay being used to measure a factor retarding delivery of the toxin to the cytosol. This was not demonstrated previously as none of the factors tested had an effect.

Figure 4.11 – The effect of glycerol on the trafficking time of ricin

The protocol used to produce this figure was similar to trafficking assays in the previous chapter. However, cells were treated (at time nought) with medium containing 10% glycerol (w/v), or with medium containing no glyercol. Data was interpreted as before: protein synthesis at each timepoint was normalised to controls not treated with ricin (100% protein synthesis). Lines of best fit were then drawn through the exponential phase of the datasets and regressed (Microsoft Excel). The time at which this equation satisfied 100% synthesis for each series was then used to compare control and glycerol-treated cells. c) Shows time-response curves comparing cells treated with medium containing no glycerol (○) to cells treated with medium laden with 10% glycerol (w/v) (●). d) Shows trafficking times relative to controls (n=3; error bars show SEM).

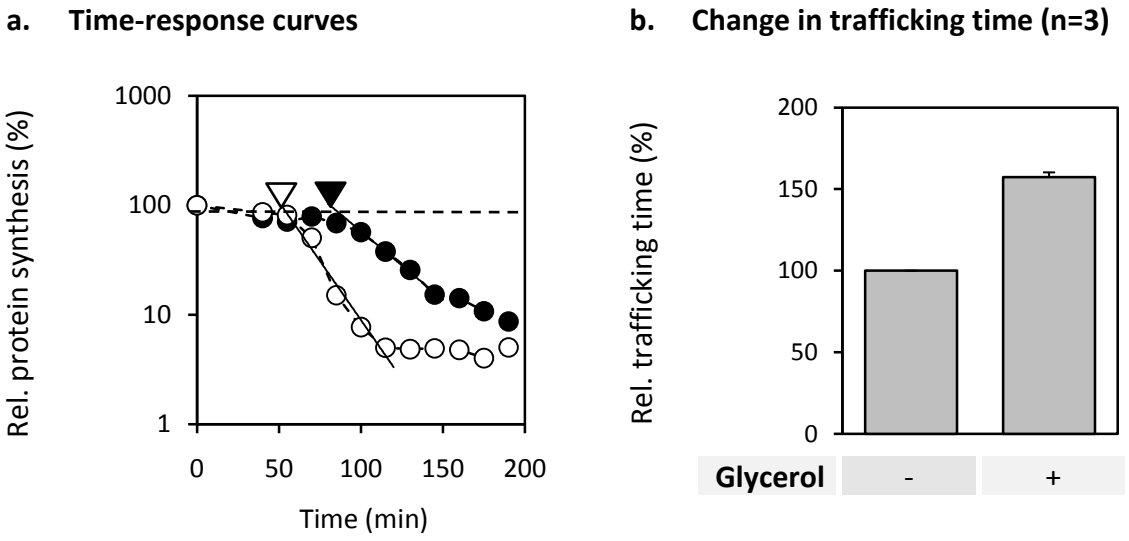

4.6.2 The effect of POPS liposomes on the solubility of RTA

In vivo, it is thought that the interaction of RTA with the ER membrane is initiated by negatively-charged phospholipids such as 1-palmitoyl-2-oleoyl-*sn*-glycero-3-phosphoserine, POPS. This phospholipid is native to the bilayer (Zachowski, 1993). Its interaction with RTA is hypothesised to promote the co-option of the toxin subunit onto an ERAD-like pathway (Mayerhofer *et al.*, 2002), or else to promote the acquisition of a conformational state which permits retrotranslocation. As of yet, few data exist to confirm that this is a significant process *in vivo*. The hypotheses of Sandvig *et al*. (1984) and those of the previous sections posit that glycerol inhibits the toxicity of ricin by interfering with this interaction. A series of experiments were conducted to investigate the following possibilities:

(1) whether a liposomal interaction could be observed by a change in solubility *in vitro*;
(2) whether this could be interfered with by glycerol.

POPS liposomes induce a dramatic loss of solubility **-** RTA was incubated with or without negatively-charged POPS liposomes for 15 minutes at 37°C. These were constructed in the same manner as that used by Heuck *et al*. (2003). The relative distribution of RTA between insoluble and soluble fractions was then analysed by silver-stain (Figure 4.12). Incubation of RTA with negatively-charged liposomes evidently caused a large shift of RTA to the pellet fraction (compare pellet/soluble pairs 1 & 2).

To test whether this loss of solubility was caused by RTA merely adhering to the surface of sedimentable liposomes, detergent was added after the incubation to see whether dissolution of the phospholipid vesicles would restore solubility. Comparing assays with liposomes alone to those where triton had been added afterward, it is apparent that the tendency of RTA to sediment persists even after the liposomes causing it have been disrupted (*cf.* pairs 2 and 3 of Figure 4.12a & b). This would imply that their interaction with RTA results in an irreversible series of structural changes that result in sedimentation, consistent with a process that leads to aggregation. Two explanations could be suggested for this collection of observations:

(1) Interaction with POPS leads to outright aggregation in both cases (i.e. with or without triton), so increasing the pellet fraction.

(2) Alternatively, the interaction leads to embedding of RTA in the liposomes, causing it to sediment with them (without triton). When the liposomes are dissolved by the addition of triton, these structural changes might then cause irreversible aggregation (as hydrophobic regions of polypeptide otherwise solvated by lipid become exposed and subsequently self-associate).

As an essential control, incubation of RTA with triton alone had little effect on the solubility of RTA (*cf.* pairs 1 and 4 of Figure 4.12).

Glycerol does not prevent the interaction **-** To continue investigation of the hypotheses made in the previous section, 10% glycerol (w/v) was added to the incubation before the liposomes were added. These experiments show that this small molecule chaperone has no effect upon the interaction under the conditions of this assay (*cf.* pairs 3 with 5, & 2 with 6).

These effects are just as pronounced at 45°C **-** When these assays were repeated at 45°C, incubation with the liposomes caused a similar shift to the pellet fraction (Figure 4.12c & d). Just as at 37°C, the reduction in solubility was not negated by dissolving the liposomes afterward with detergent, and glycerol could not prevent the interaction. It is also more apparent in these assays that glycerol functions as a small molecule chaperone under these conditions, promoting the solubility of RTA in isolation (*cf.* pairs 1 and 7 of Figure 4.12c & d).

Taken as a whole, these results are of interest because they corroborate the conclusion that the interaction of RTA with negatively-charge liposomes is more than a superficial one (Mayerhofer *et al*., 2009; and Day *et al*., 2002). In this case, it causes structural rearrangement resulting in loss of solubility even if the liposomes are subsequently dissolved with triton. Importantly, however, the physiological membrane will bear significant differences from the liposomes used in this assay (such as protein content and the presence of other lipids, which will dilute POPS). Therefore, *in vivo*, glycerol might still compete with such an interaction.

Figure 4.12 – The effect of POPS liposomes upon the solubility of RTA

500ng RTA was incubated in 10mM MOPS / 50mM KCl (pH7.2) buffer for 15 minutes at 37°C with or without 7.5µM POPS liposomes and 10% (w/v) glycerol. After this incubation, mixtures were transferred to ice for 5 minutes and then 10% (w/v) Triton-X100 detergent (or an equivalent volume of water) was added as indicated. All samples were then incubated on ice for a further 10 minutes before separation into pellet and supernatant fractions at 16000 × *g* for 10 minutes. a) Pellet and soluble fraction were then run in parallel on SDS-PAGE (pairs are demarcated by grey lines) and b) Quantified by TotalLab. Error bars show the standard deviation between 9 independent experiments. c) and d) Shows equivalents to a) and b) respectively, but where the temperature of incubation was 45°C.

a. Silver stains – each panel represents an independent assay conducted at 37°C

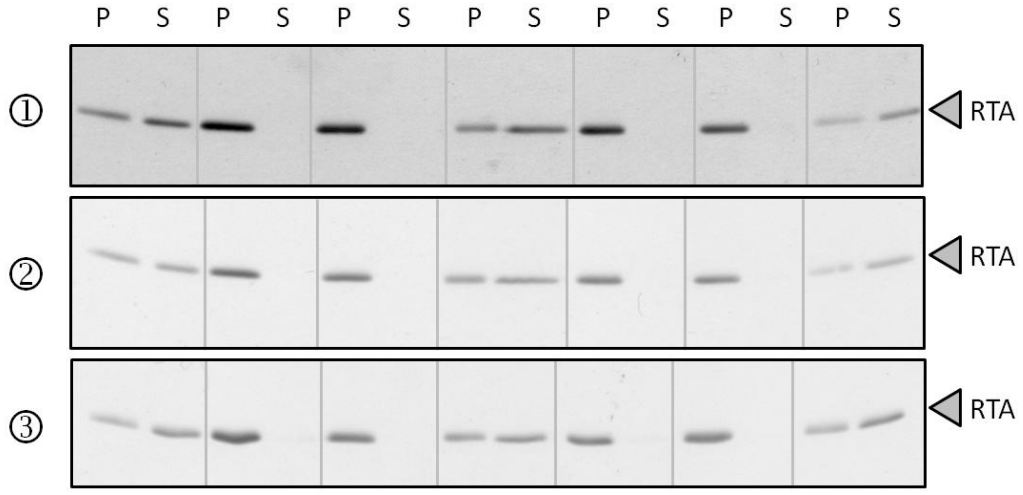

POPS	-	+	+	-	+	+	-
Triton	-	-	+	+	+	-	-
Glycerol	-	-	-	-	+	+	+
Pair	**1**	**2**	**3**	**4**	**5**	**6**	**7**

b. Quantification of assays conducted at 37°C (n=9)

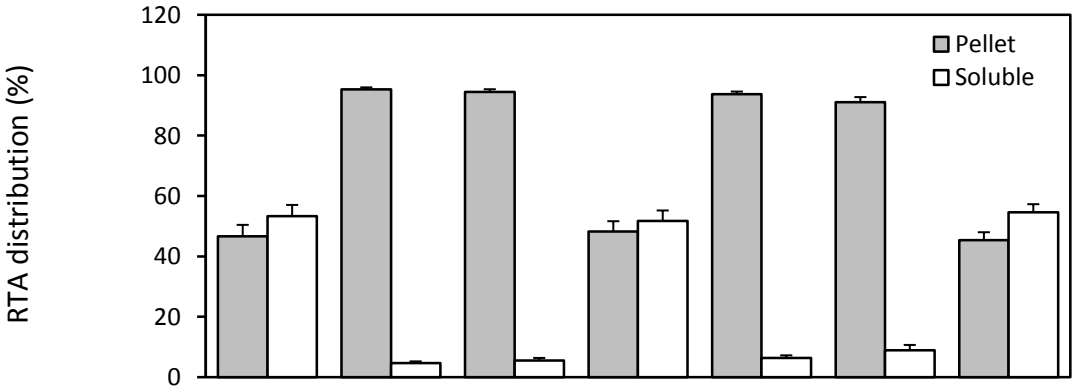

POPS	-	+	+	-	+	+	-
Triton	-	-	+	+	+	-	-
Glycerol	-	-	-	-	+	+	+
Lane	**1**	**2**	**3**	**4**	**5**	**6**	**7**

(Figure 4.12 – continued.)

c. Silver stains – each panel represents an independent assay conducted at 45°C.

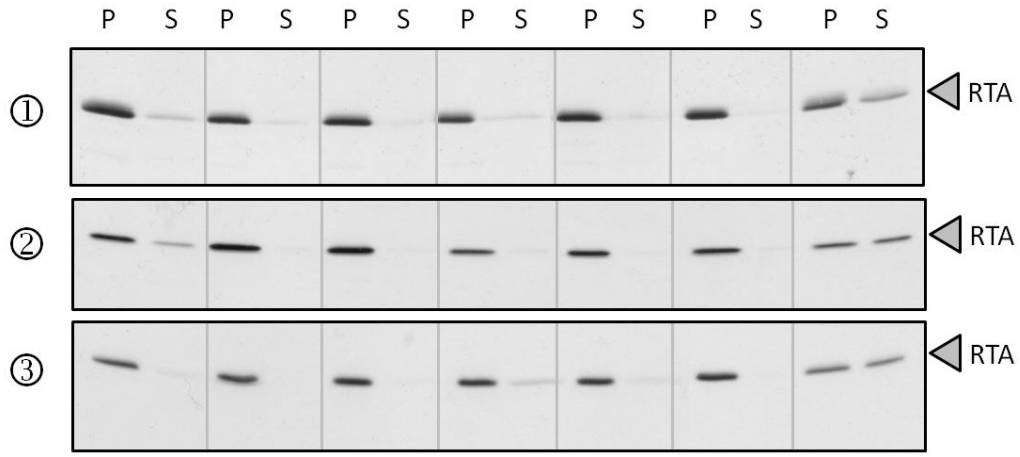

POPS	-	+	+	-	+	+	-
Triton	-	-	+	+	+	-	-
Glycerol	-	-	-	-	+	+	+
Pair	**1**	**2**	**3**	**4**	**5**	**6**	**7**

d. Quantification of assays conducted at 45°C (n=6)

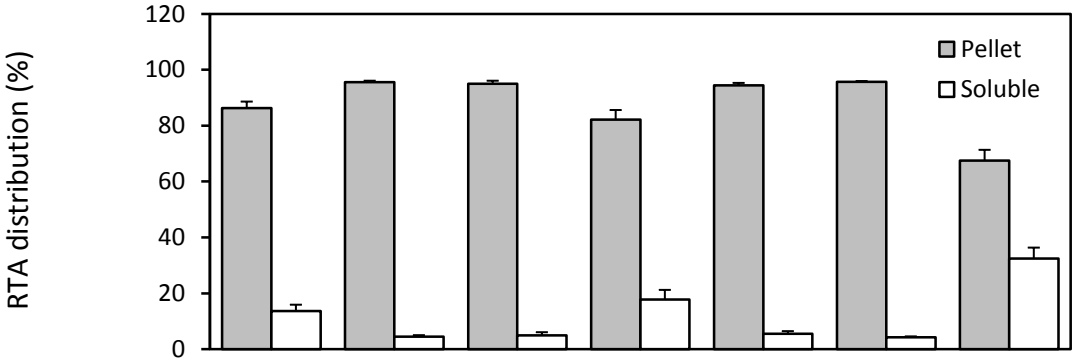

POPS	-	+	+	-	+	+	-
Triton	-	-	+	+	+	-	-
Glycerol	-	-	-	-	+	+	+
Pair	**1**	**2**	**3**	**4**	**5**	**6**	**7**

4.6.3 Neutrally-charged liposomes have little effect on the solubility of RTA

Mayerhofer *et al*. (2009) and Day *et al*. (2002) showed that it was specifically negatively-charged phospholipid which disrupted the secondary structure of RTA and which accommodated the insertion of the toxin subunit into the bilayer. To clarify that this observation was reflected in these assays, further experiments were undertaken using the neutral phospholipid, 1-palmitoyl-2-oleoyl-*sn*-glycero-3-phosphocysteine (POPC; Figure 4.13). POPC liposomes displayed strikingly different effects in the assay. At both 37°C and 45°C POPC induced little loss of solubility (*cf.* pairs 1 & 2); the error-bars between treatments overlap. However, unlike with POPS, where glycerol is present, there is noticeably more soluble RTA at *both* 37°C and 45°C (*cf.* pairs 2 & 6).

Therefore it appears that the negatively-charged character of POPS-containing liposomes is crucial to the dramatic loss of solubility they induce in co-incubated RTA. Contrasting to POPS, in the context of POPC, glycerol can also stabilise RTA from losing solubility. Therefore, *in vivo*, where negatively-charged phospholipids of the ER membrane like POPS will be diluted by POPC and other bilayer constituents, glycerol may be able to prevent the membrane interaction.

Figure 4.13 – The effect of POPC liposomes upon the solubility of RTA

500ng RTA was incubated in 10mM MOPS / 50mM KCl (pH7.2) buffer for 15 minutes at 37°C with or without 7.5µM POPC liposomes and 10% (w/v) glycerol. Samples were otherwise treated as before. a) Three representative silver stains from a set of 6 independent). b) Quantification derived from the silver stains (TotalLab). Error bars show the standard deviation between the 6 experiments. c) and d) Shows equivalents to a) and b) respectively, but where the temperature of incubation was 45°C.

a. Silver stains – each panel represents an independent assay conducted at 37°C.

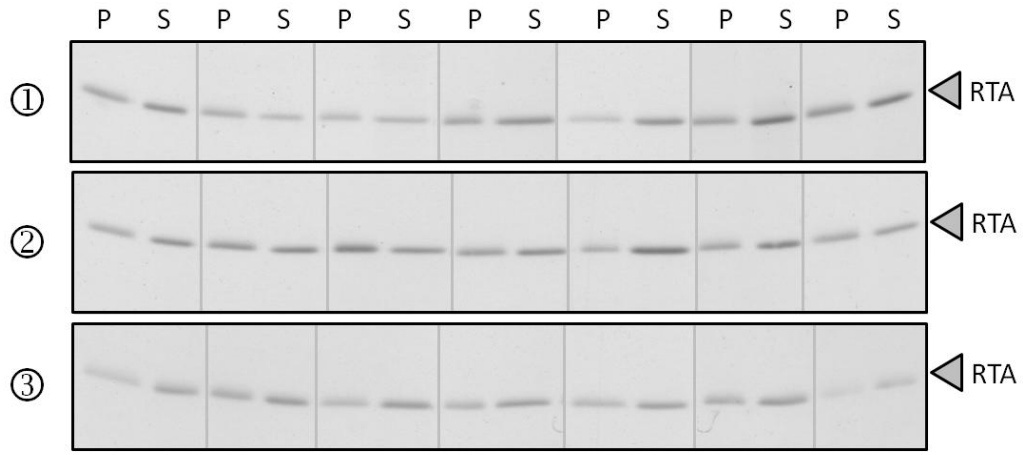

POPC	-	+	+	-	+	+	-
Triton	-	-	+	+	+	-	-
Glycerol	-	-	-	-	+	+	+
Pair	**1**	**2**	**3**	**4**	**5**	**6**	**7**

b. Quantification (n=6)

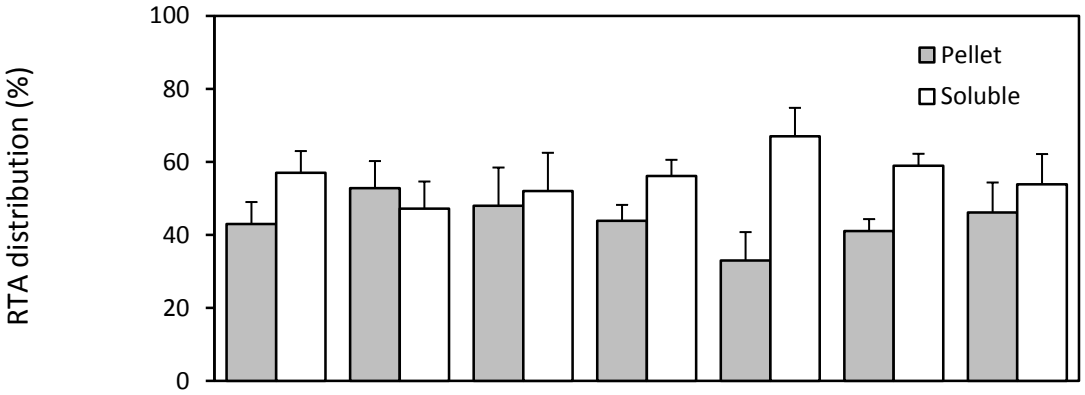

POPC	-	+	+	-	+	+	-
Triton	-	-	+	+	+	-	-
Glycerol	-	-	-	-	+	+	+
Lane	**1**	**2**	**3**	**4**	**5**	**6**	**7**

(Figure 4.13 – continued.)

c. Silver stains – each panel represents an independent assay conducted at 45°C.

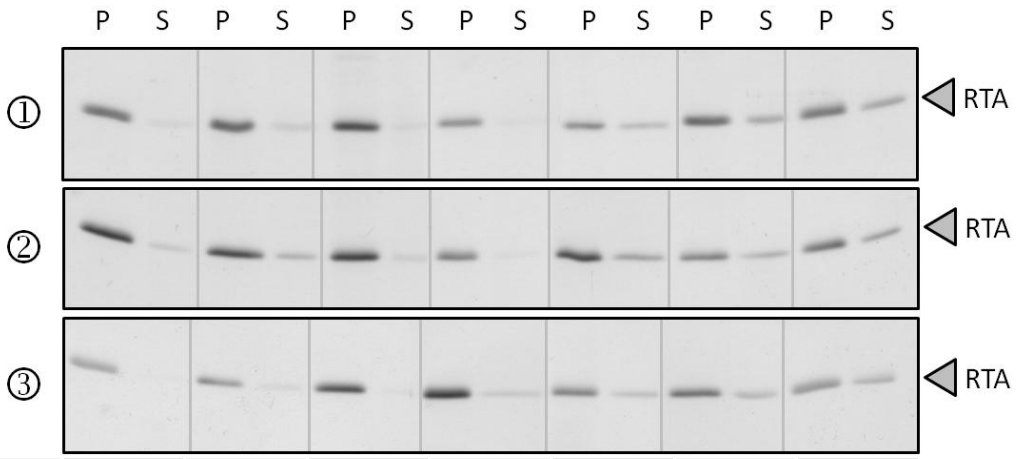

POPC	-	+	+	-	+	+	-
Triton	-	-	+	+	+	-	-
Glycerol	-	-	-	-	+	+	+
Pair	**1**	**2**	**3**	**4**	**5**	**6**	**7**

d. Quantification (n=3)

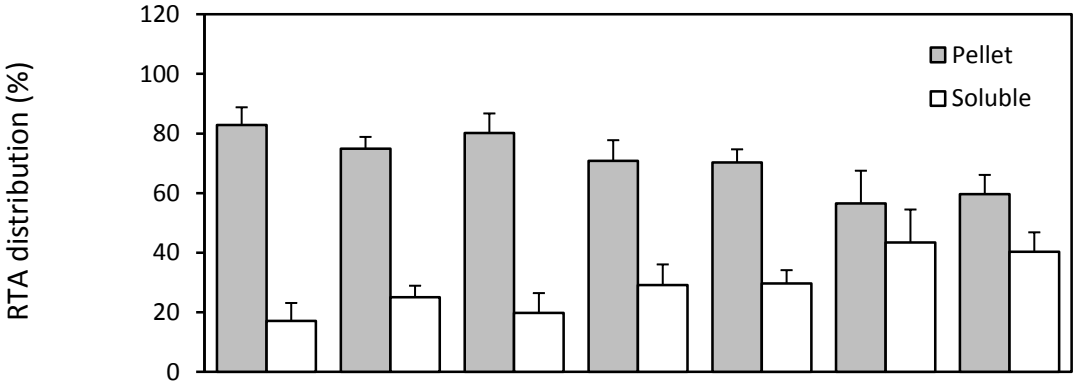

POPC	-	+	+	-	+	+	-
Triton	-	-	+	+	+	-	-
Glycerol	-	-	-	-	+	+	+
Pair	**1**	**2**	**3**	**4**	**5**	**6**	**7**

4.7 The effect of Hsc70/Hsp40 upon the thermal denaturation of RTA

The experiments conducted to this point persuade us that the effect of factors which are expected to influence protein aggregation and misfolding can be observed by measuring the solubility of RTA. The observations made can be reconciled with documented phenomena:

(1) Increased salt concentration salvages RTA from unfolding events that lead to reduced solubility, much as it rescues RTA from initiating interactions with negatively-charged liposomes (Day *et al*., 2002).

(2) A threshold around 45°C delimits a marked change in RTA solubility, unlike for the homologous toxin, saporin, which does not co-opt an ERAD-like pathway. This results from differences between the two toxins, for example the hydrophobic C-terminus of RTA and its lesser lysine content (Vago *et al*., 2005).

(3) Volume-excluding effects by Ficoll-70 do not hinder solubility at 37°C nor 45°C, showing that some other factor dominates loss of solubility rather than crowding from a hydrophilic crowding agent. Again, this may potentially be the C-terminus of RTA.

(4) RTA is predictably least soluble in buffers of pH7.0 to 7.4, a range straddling its reported pI of 7.3 (Li *et al*., 1992).

(5) A small molecule chaperone, glycerol, can rescue RTA from losing solubility during heat-treatment.

(6) Liposomes composed of negatively-charged POPS induce conformational changes in RTA that lead to a loss of solubility (corroborating changes to secondary structure observed under similar treatments - Mayerhofer *et al*., 2009; Day *et al*., 2002). This phenomenon may be interfered with *in vivo* by the small molecule chaperone, glycerol, where strongly-denaturing POPS will be diluted by neutral phospholipids like POPC (Zachowski, 1993) and other membrane components.

As these trends could be explained rationally and related well to earlier literature accounts, it seemed likely that any solubilising activity of chaperones like Hsp40/Hsc70 might also be observed in a meaningful way by this assay. As such, the next section of this chapter discusses the effects of Hsp40/Hsc70 on the solubility of RTA.

4.7.1 Purification of Hsp40

A précis of the Hsp40 purification procedure is given here for ease of reference. A more comprehensive review of the protocol can be found in Chapter 2. Hsp40 was over-expressed in an *E. coli* BL21 culture using an IPTG-inducible system. The culture was then centrifuged and cells resuspended in 20mM KCl / 20mM MOPS-HCl pH7.2 buffer, before sonication. This sonicate was clarified by centrifugation, and Hsp40 was purified in a two-step process via column chromatography. A DEAE-Sepharose column was used first (GE Healthcare). Fractions were eluted from this column with buffer containing increasing concentrations of KCl (up to 100mM). Sequential fractions from this elution were analysed by SDS-PAGE and stained with Coomassie Blue (Figure 4.14a). Those fractions containing fewest impurities were pooled and loaded onto a Source 30S column (GE Healthcare). This column was then eluted with a graduated buffer containing from 100mM to 300mM KCl. Serial fractions were, again, collected and compared via Coomassie staining after SDS-PAGE (Figure 4.14b). Fractions containing Hsp40 and the fewest impurities were pooled and quantified by silver stain, where they were compared to standards of known Hsp40 concentration to determine their protein content per unit volume (Figure 4.14c).

Figure 4.14 – Purification of Hsp40.

Clarified sonicates from *E. coli* containing over-expressed Hsp40 were purified via sequential DEAE Sepharose and 30S source columns. a) Shows the fractions collected from the DEAE Sepharose column. The lane marked A shows 15 µL of the sonicate loaded onto the column. Numbered lanes represent 15L of consecutive fractions from the column as it was eluted. Fractions 1-3 were pooled and loaded onto a 30S source column. B) Shows fractions collected after 30S source column chromatography. Enumerated are consecutive elutions. The lane marked A shows 15 µL of the partially purified Hsp40 from the previous DEAE column. Of the enumerated fractions, 2-4 were pooled. C) Shows the quantification of the resultant solutions by silver stain. 0.875µg of Hsp40, a kind gift from Jörg Höhfeld (Institute for Cell Biology, Bonn) was loaded alongside 10, 5 & 1µL of the Hsp40 purification. The relative intensity of Hsp40 bands were quantified by TotalLab.

a. DEAE-Sepharose fractions (stained with Coomassie Blue)

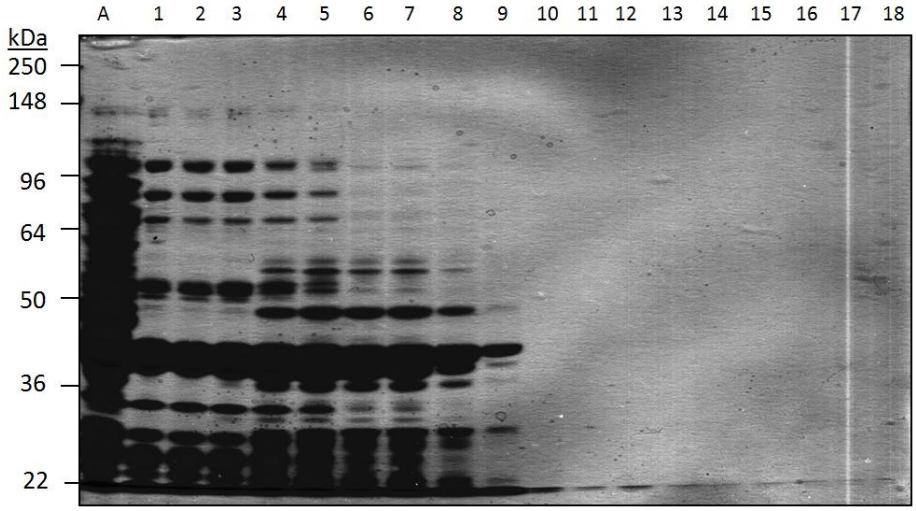

b. Source 30S fractions (stained with Coomassie Blue)

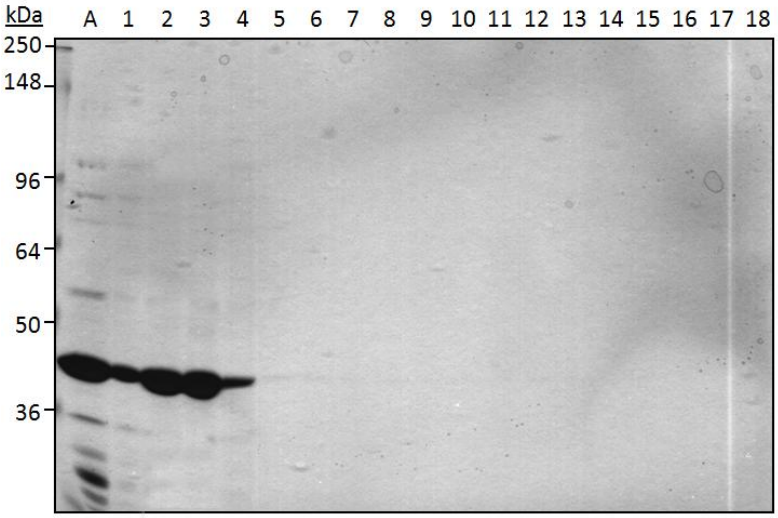

c. Quantification

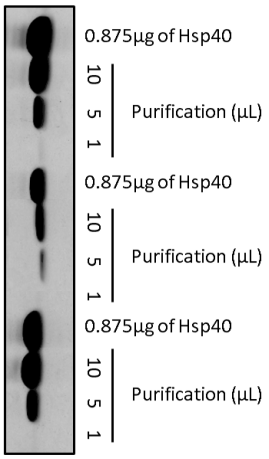

4.7.2 Purification of Hsc70

SF9 (insect) cells were transformed with a plasmid encoding Hsc70 using a baculovirus vector. After infection and incubation, cultures were induced with IPTG and centrifuged. The cell aggregate was lysed using a buffer containing 1% triton X-100. Lysates were then fractionated, in order, with: a DEAE-Sepharose column (GE Healthcare; eluted with increasing concentrations of KCl), then an ATP-agarose column (Sigma-Aldrich; eluted with up to 2mM ATP) and finally a Source 30Q column (from GE Healthcare, which was also eluted with up to 1M KCl). As fractions were eluted from each column, the A_{280} was observed. Those fractions showing absorbance in excess of the buffer alone were pooled, separated by SDS-PAGE and analysed by Coomassie staining for Hsc70 content (Figure 4.15). Only those fractions containing the 70kDa Hsc70 band were collected and transferred to a subsequent column.[15] After the Source 30Q column, the purified fractions were concentrated using Centricons (Millipore).

Please note that in Figure 4.15b, an impurity can be seen at 60kDa. This is a breakdown product of Hsc70, where the C-terminus has been cleaved off. This is often observed in the purification of the chaperone, and it lacks any regulatory modulation owing to the C-terminal EEVD motif which is usually bound by co-chaperones and inhibitors like DSG (Höhfeld J. – personal communication). Importantly, Figure 4.15c shows that there is no remnant of this moiety in the final Hsc70 preparation. Thus, it is not interfering in the assay hereafter.

[15] For the DEAE-Sepharose column, fractions from which were analysed for Hsc70 content by determining peaks in A_{280} absorbance alone.

Figure 4.15 – Purification of Hsc70

Hsc70 was purified by a three-stage process. The Coomassie analyses of the latter two of these stages are shown here. a) The pooled fractions from the DEAE-Sepharose column (10µL of which was loaded in the lane marked "A") were loaded onto an ATP-agarose column. The column was then washed extensively before Hsc70 was eluted with a buffer containing ATP. Sequential fractions were collected and analysed by SDS-PAGE and Coomassie staining. All those fractions containing Hsc70 and no impurities were then loaded onto a Source 30Q column. 10µL of these pooled fractions is loaded in lane "A" of b), which shows the fractions were eluted using a gradient of KCl. Fractions containing only the 70kDa band were collected (numbers 4 through 6) and concentrated by centricon. c) Shows 2µg of the final Hsc70 preparation per lane, as determined by biorad. Grey arrowheads mark the Hsc70 band. White arrowheads mark a 60kDa C-terminally truncated Hsc70, lacking the EEVD regulatory motif. All gels are stained with Coomassie blue.

a. Fractions from ATP-agarose column

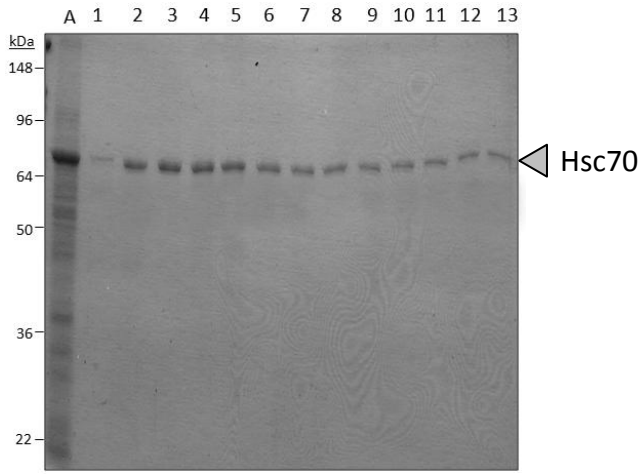

b. Fractions from Source 30Q column

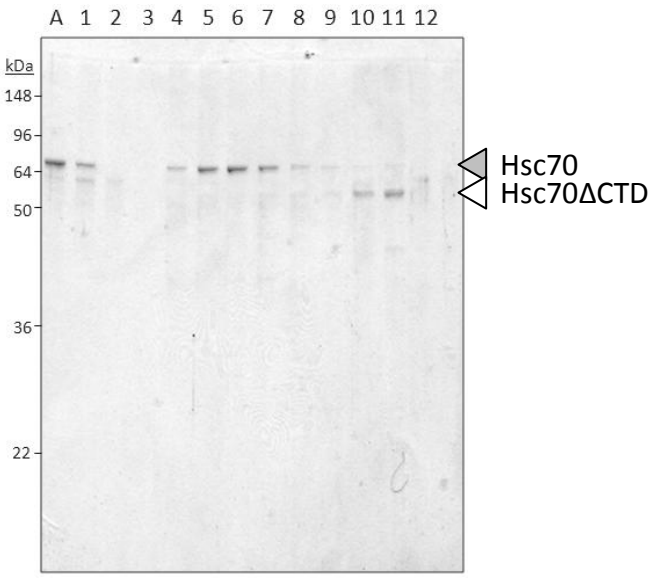

c. Assessment of purity

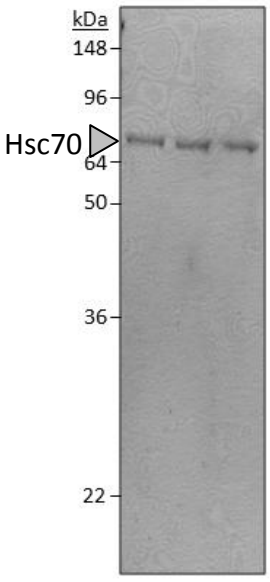

4.7.3 Hsc70/Hsp40 bolster the solubility of RTA

After purification, Hsc70 and Hsp40 could be tested for their effect upon the solubility of RTA, which would help to determine:

(1) Whether they could form a complex.
(2) Whether they had a predictably functional association.

The effects of Hsc70/Hsp40 at 45°C - RTA was heated to 45°C and incubated for 15 minutes with or without Hsc70, Hsp40 and ATP in the indicated combinations (Figure 4.16). The pellet and soluble distribution of RTA was then analysed by silver-stain after a 10 minute centrifugation at 16000 $\times g$. Figure 4.16a shows that including Hsc70 in the incubation during the heat treatment boosts the solubility of RTA. Presumably, this is because the chaperone reversibly masks regions of transiently-exposed hydrophobic polypeptide during the heat-treatment, preventing aggregation between neighbouring RTA molecules.

Minami *et al*. (1996) observed an obvious synergy between Hsp40 and Hsc70 in keeping luciferase from aggregating. However, this is not strongly shown in the case of RTA, where there is no significant additional increase in solubility in Hsp40-containing incubations compared to assays containing Hsc70 alone. However, assays shown in Spooner, *et al*. (2008) clearly do show the cooperation of Hsp40 and Hsc70 in keeping RTA soluble. This disparity may reflect batch-dependent differences in the conformational stability of RTA, or the activity of Hsp40 (all other things being the same between these assays). Results published in Spooner *et al*. (2008) also clearly show that chaperone-stabilised RTA retains catalytic activity with respect to ribosomal RNA, whereas heat-treated RTA does not.

Importantly, the inclusion of ATP in similar incubations increased the ability of Hsc70 and Hsp40 to maintain the solubility of RTA, by average (Figure 4.16a). This demonstrates the ATP-dependence of Hsc70 (Beissinger & Buchner, 1998) and that the ATPase cycle of the chaperone contributes to the optimal preservation of solubility. This provides more convincing evidence that RTA can be actively bound by the chaperone, in a functional way.

It should be recalled that DSG, which was used *in vivo* in the previous chapter, stimulates the ATPase activity of Hsc70 *in vitro*, perturbing the chaperone's normal association with clients (Brodsky, 1999; Nadler *et al*., 1998). As rescue of RTA from aggregation *in vitro* seems to be at least partially ATP-dependent, interfering with the ATPase cycle of Hsc70 *in vivo* may affect the same process.

The effects of Hsc70/Hsp40 at 37°C – To check whether the interaction observed at 45°C resulted from attributes of thermally-denatured RTA, rather than some attribute of the native polypeptide, the above assays were repeated at 37°C (Figure 4.16b). At this temperature, an unexpectedly similar effect of the chaperones upon the solubility of RTA was observed, with a less pronounced difference between assays with and without ATP. The relatively large error bars correspond to differences in solubility between the batches of RTA used in independent assays rather than to variability in the effects of Hsc70/Hsp40.

According to Argent *et al*. (2000), the secondary structure of RTA is relatively intact until a temperature threshold of 42°C is reached. Therefore, it would seem that at 37°C there is some feature of the native RTA monomer that Hsc70 and Hsp40 can have an effect upon to render it more soluble. A pre-eminent candidate for this is the hydrophobic C-terminus of the toxin subunit. This hydrophobic domain is solvent-exposed (Mayerhofer *et al*., 2009). Therefore it is also exposed to the hydrophobic surface of the polypropylene incubation vessel, to which it might adsorb. Hsc70 could bind to this domain at 37°C, masking it.

Arguably, this apparent effect of Hsc70 and Hsp40 on the solubility of RTA at 37°C could result from a phenomenon which is independent of direct binding to the toxin subunit. Interactions made between RTA and the hydrophobic surface of the incubation vessel might instead be displaced by the chaperones, which cling to the tube instead. The immediate question to answer, then, is: do the chaperones displace Hsc70 from binding to the incubation vessel by binding to RTA directly, or do they block binding by themselves saturating the hydrophobic surface of the incubation vessel? To clarify this issue, a series of experiments were conducted in which BSA was included instead of the chaperone complex.

Figure 4.16 – The effect of Hsc70 and Hsp40 upon the solubility of RTA after incubations at 45°C and 37°C

500ng RTA (0.8µM) was incubated at a) 45°C or b) 37°C, but otherwise as before, with the indicated mixture of chaperones and ATP. Gels were silver-stained and quantified (using TotalLab). RTA bands are highlighted with a grey arrowhead and Hsc70 is highlighted with an asterisk. Hsp40 is only present in catalytic quantities and is thus not clearly visible. Error bars show SEM in all cases.

Concentration of the chaperone components were as follows: 4.7µM Hsc70; 3.2µM Hsp40. Where used, ATP was included at a concentration of 5mM. (In all cases the standard 10mM MOPS / 50mM KCl buffer of pH7.2 was supplemented with 5mM $MgCl_2$ to ensure solubility of the ATP.)

a. Assays conducted at 45°C (panel shows a representative assay)

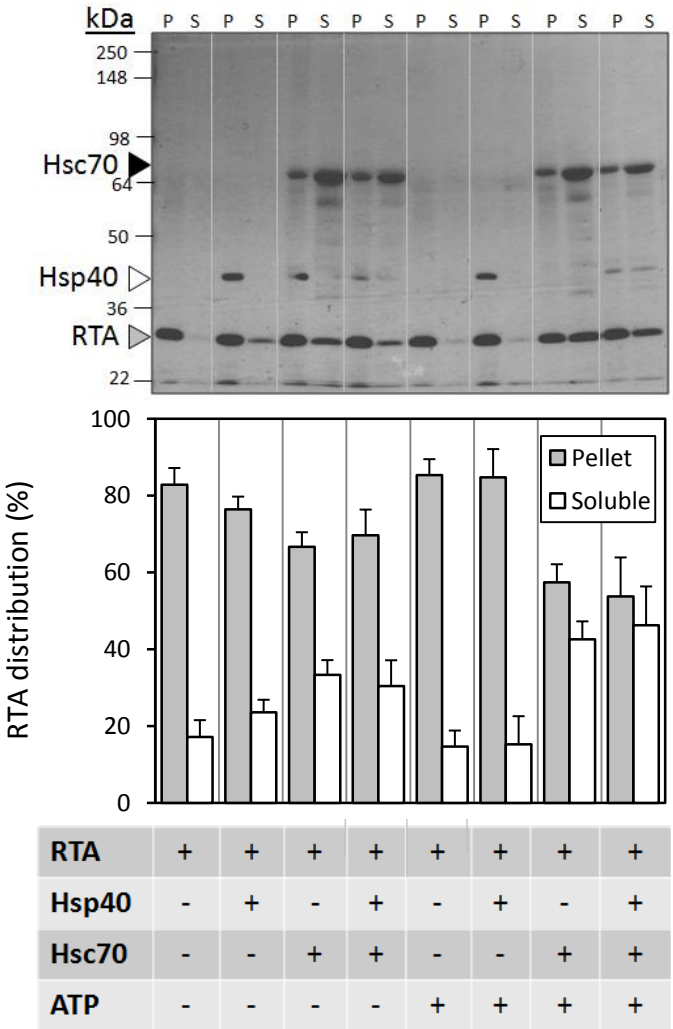

(Figure 4.16 – continued.)

b. Assays conducted at 37°C (panels show a representative assay)

i. Without ATP **ii. With ATP**

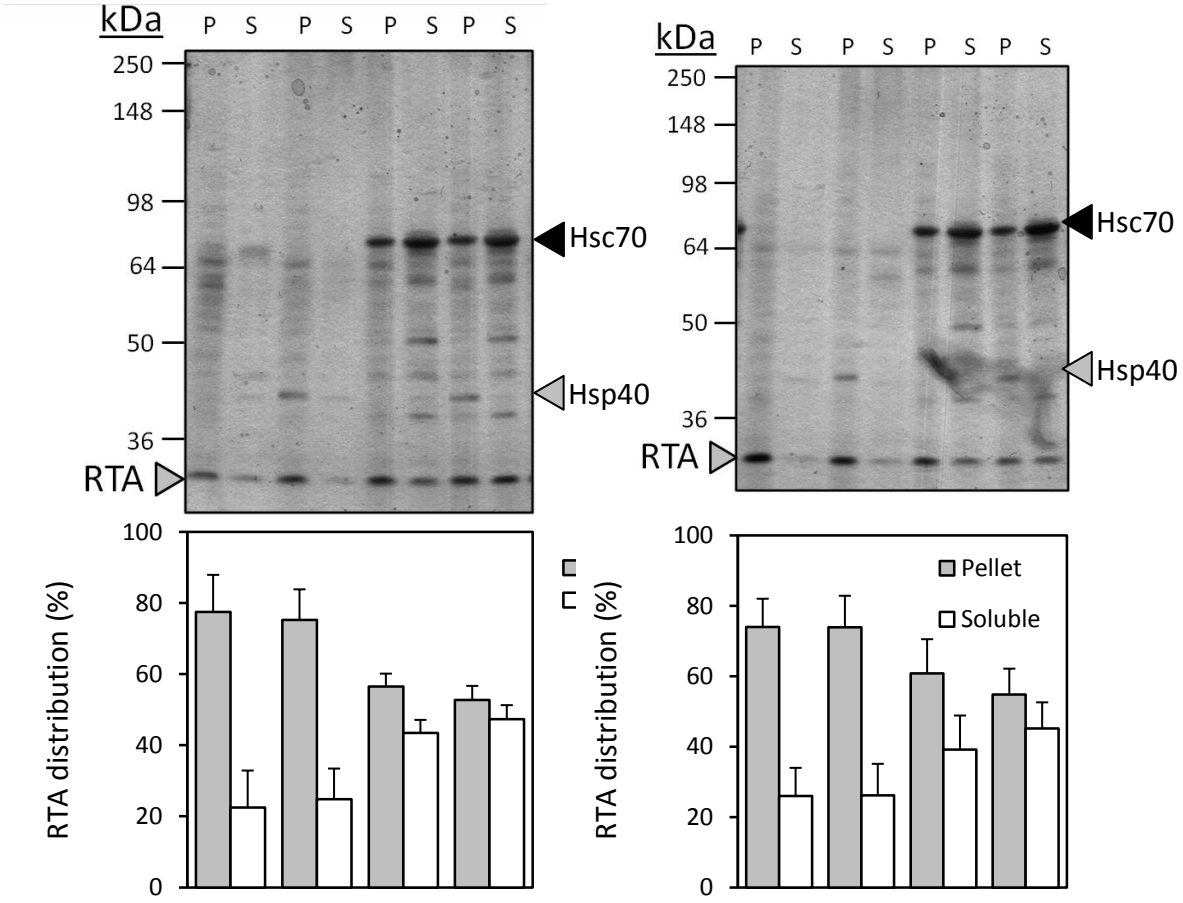

RTA	+	+	+	+
Hsp40	-	+	-	+
Hsc70	-	-	+	+
ATP	-	-	-	-

RTA	+	+	+	+
Hsp40	-	+	-	+
Hsc70	-	-	+	+
ATP	+	+	+	+

4.8 The effect of BSA upon the solubility assay

To determine whether Hsc70 and Hsp40 were simply binding to the reaction vessel and so displacing RTA from doing the same, BSA was used as a comparison. RTA was incubated with a range of BSA concentrations rather than with the chaperones. The assays presented in Figure 4.17 show that increasing the concentration of co-incubated BSA resulted in an apparent increase in the relative solubility of RTA. The maximal effect of this occurs at approximately 2.5 $mg.mL^{-1}$ of BSA. This suggested that BSA itself may block RTA from adhering to the side of the Eppendorf tube in which it is incubated. Thus, at least some of the effect of Hsc70/Hsp40 may result from a non-specific blocking phenomenon.

Table 4.1 - Conversion of chaperone molarity into absolute concentration

In previous assays with chaperones, the concentration of each was stated in terms of molarity. The following table shows the equivalent concentration in $mg.mL^{-1}$, using a molecular weight of 40kDa for Hsp40 and 70kDa for Hsc70.

	Concentration	
Protein	**µM** (2s.f.)	**$mg.mL^{-1}$** (2d.p.)
Hsc70	4.7	0.34
Hsp40	3.2	0.13
Total	N/A	0.47

In earlier assays containing chaperones (shown in Figure 4.16a & b) the maximum concentration of protein other than RTA was ~$0.47mg.mL^{-1}$. This chaperone mixture contributed to an increase in solubility of 31% at 45°C and of 23% at 37°C (by average) compared to incubations without chaperones. On the other hand, a $0.63mg.mL^{-1}$ concentration of BSA results in an increase to solubility of only 5% at 37°C (by average, Figure 4.17b). Indeed, at this concentration of BSA there is significantly less solubilising effect (Figure 4.17c; $p<0.001$ using an unpaired Student's T-test). Moreover, by average the *maximal* contribution of BSA to the solubility of RTA is a mere 11% at 37°C. Thus, unless Hsc70 and Hsp40 have greater preference for the side of the incubation vessel than does

BSA, their solubilising effect seems attributable to a different activity. It seems reasonable to suggest that this is a direct interaction between RTA (as client) and Hsc70 (as chaperone).

Importantly, if the relative increase in pellet fraction at temperatures higher than 37°C is because of RTA merely sticking to the edge of the incubation vessel, it is important to ask whether this assay is at all measuring protein aggregation or misfolding. In answer, the side of the tube is a hydrophobic material. An otherwise soluble protein would therefore bind to this surface only if it, too, had exposed hydrophobic regions. Otherwise, it would be repelled, being solvated by water molecules in preference. As the exposure of hydrophobic domains will be determined by factors affecting protein folding, this assay still seems appropriate to qualify them. To refine this protocol, however, the reaction vessel could be pre-treated by washing with low concentrations of an inert protein to block the binding of RTA. As the availability of purified Hsc70 was limiting, however, it has not yet been possible to do so.

Figure 4.17 – Effect of low BSA concentrations on the distribution of RTA between pellet and soluble fractions.

500ng RTA was incubated as before at a) 37°C or b) 45°C and then separated into pellet (P) and soluble (S) fractions, separated by SDS-PAGE. Bands were developed by a silver-stain protocol. Included in the incubation was the indicated concentration of BSA. Grey arrowheads mark RTA bands, black arrowheads mark BSA bands. c) Shows the average pro-solubility effect of the concentration of BSA tested (0.63 $mg.mL^{-1}$) which was closest to the absolute concentration of chaperones used in Figure 4.16 (0.47 $mg.mL^{-1}$). To attain the percentage 'pro-solubility' effect, the P/S distribution of RTA was compared in BSA and chaperones treatments to the P/S distribution of RTA in buffer alone. Error-bars show the SEM in all cases.

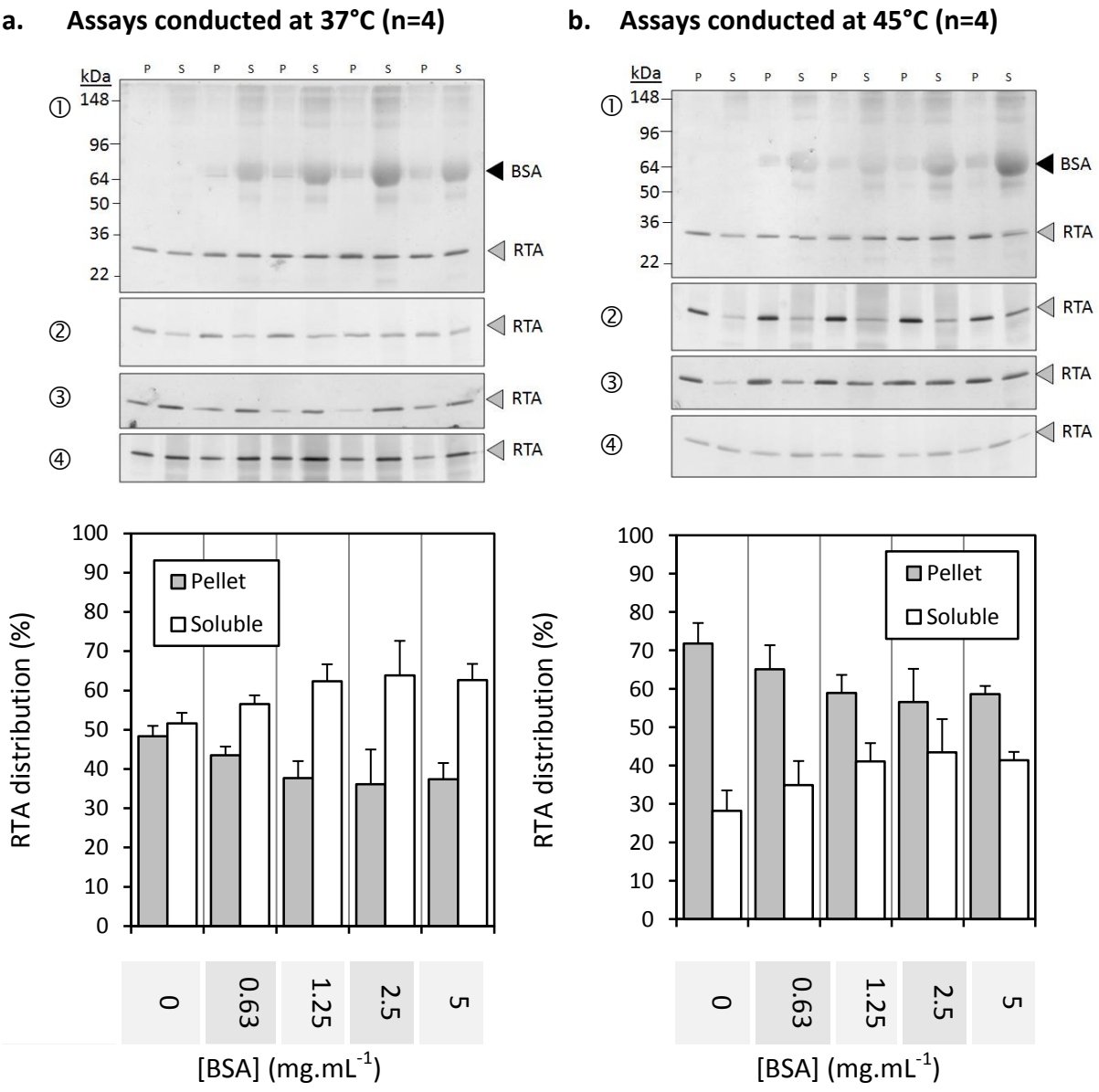

(Figure 4.17 - continued.)

c. Average pro-solubility effect of BSA and Hsc70/Hsp40 from different experiments conducted at 37°C (n=3)

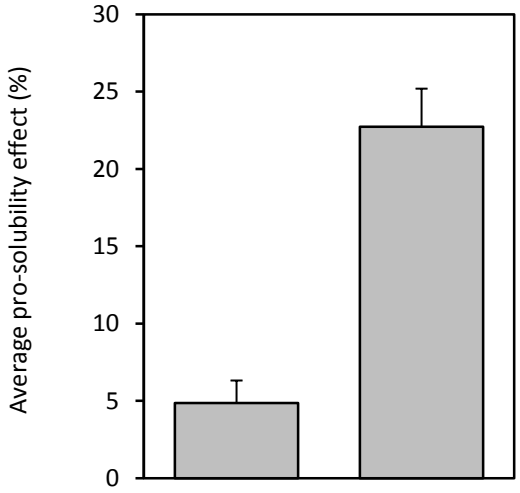

Protein	BSA	Hsc70/Hsp40
mg.mL^{-1}	0.63	0.47

4.8.1 The effect of concentrated BSA upon the solubility assay

Low concentrations of BSA convincingly promoted the solubility of RTA, potentially by displacing it from binding to the reaction vessel. However, at higher concentrations it was expected that BSA might have the opposite effect, promoting misfolding, aggregation and loss of solubility by crowding effects (Van den Berg *et al*., 1996). This was hinted at in the previous section, where the maximal solubilising effect of BSA peaks at 2.5mg.mL^{-1}, by average.

The effect of crowding from a polar macromolecule was already tested with the use of Ficoll-70. This uncharged, polar molecule had little effect upon solubility, even at high concentrations. However, Van den Berg *et al.* (1999) observed differential effects of Ficoll-70 and BSA upon the folding of lysozyme *in vitro*. Thus, it was possible that higher concentrations of BSA might produce a crowding effect that was detrimental to solubility. To this end, RTA was incubated with a range of much higher BSA concentrations than previously tested (Figure 4.18). As the concentration of BSA was increased beyond 5mg.mL^{-1}, the solubility of RTA was shown to decrease.

Van den Berg *et al*. (1999) note that the pI of BSA is 4.9. At the incubation pH of 7.2 BSA would be negatively-charged and might provide an interaction analogous to that provided by negatively-charged POPS liposomes (i.e. where a charged exterior leads RTA to interact with a hydrophobic interior, leading to loss of solubility).

Figure 4.18 – Higher concentrations of BSA inhibit the solubility of RTA

500ng RTA was incubated, as before, at 37°C with a higher concentration of BSA. Pellet (P) and soluble (S) fractions were then analysed in parallel by SDS-PAGE, silver stain and quantification in TotalLab. Grey arrowheads mark RTA bands. Error bars show the SEM.

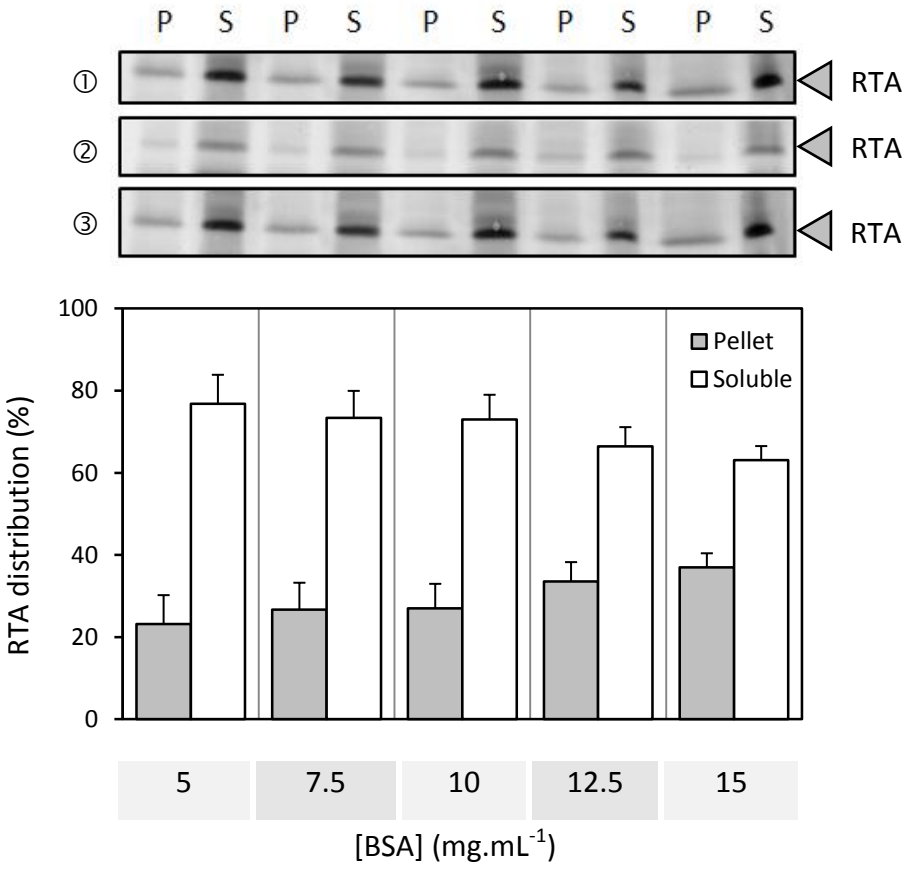

4.9 The effect of DSG upon the ability of Hsc70 to keep RTA soluble

The effect of Hsc70 and Hsp40 upon the solubility of RTA during heat-treatment *in vitro* was shown to be more than that of an arbitrary protein, BSA. Furthermore, the optimal conditions were dependent upon the presence of ATP (*cf.* Figure 4.16). To help link the effect of inhibiting Hsc70 *in vivo* to the activity of Hsc70 *in vitro*, the influence of an Hsc70 inhibitor (DSG) upon this rescue of soluble RTA was examined. To this end, RTA was incubated with Hsc70/Hsp40 and a concentration of DSG equivalent to that used *in vivo* was added.

As DSG was packaged with a lactose excipient, it was important to provide controls which showed this chemical was not responsible for any change in solubility the incubation showed (Figure 4.19c, *cf.* pairs 1 & 2). These data show that lactose increases the solubility of RTA. Likewise, DSG also promotes solubility in isolation from the chaperone complex (*cf.* pairs 1 & 3). These properties have to be accounted for when looking at their effects upon the chaperone complex. With this in mind, the most appropriate comparison to discern the effects of DSG upon the chaperone complex are incubations which include DSG/lactose/Hsc70/Hsp40/RTA and identical incubations which simply lack DSG (Figure 4.19c, *cf.* pairs 4 & 6). For convenience, these datasets have been outlined with red.

Inclusion of DSG apparently abrogates some of the effect that Hsc70/Hsp40 have upon solubility. The magnitude of this effect is, by average, a ~22% relative shift of RTA to the pellet fraction (Figure 4.19c, pairs 4 & 6). This is an unexpectedly large value given the total effect of the chaperones was, by average, a ~31% shift (Figure 4.16a). Moreover, some of this solubilising effect will be caused by non-specific blocking of RTA from binding to the Eppendorf's interior surface. Coupled to this, DSG would also have an antagonistic role to any explicitly inhibitory effect upon Hsc70, as it itself promotes solubility (Figure 4.19a & c, pairs 2 & 3). Therefore, the effect of DSG upon Hsc70 may actually be larger than the ~22% shift observed, but is obscured by these complexities.

Very unexpectedly, the magnitude of this effect is also clearly larger than any ATP-dependent chaperoning effect of the chaperone (Figure 4.16), suggesting that this chemical also interferes with a passive ability of the chaperone in promoting solubility. DSG could be operating in this fashion *in vivo*, and by this mechanism protect cells from ricin.

Figure 4.19 – Silver-stained gels showing the effect of DSG upon the ability of Hsc70 and Hsp40 to prevent aggregation of RTA.

500ng RTA was incubated with the indicated mixture of chaperones, 50µg.mL^{-1} DSG, 100µg.mL^{-1} lactose and 5mM ATP for 15 minutes at 45°C. Pellet (P) and soluble (S) fractions were collected as before and analysed by SDS-PAGE. a) & b) Resultant gels were silver-stained. Shown below are experiments demonstrating the effect of DSG and lactose upon both RTA aggregation and upon the ability of Hsc70/Hsp40 to prevent that aggregation. c) Shows quantification via TotalLab, incorporating data displayed in Figure . Outlined more boldly are the datasets which, when compared, best describe the effect of DSG upon the ability of Hsc70 and Hsp40 to rescue RTA from aggregation at 45 °C. Black arrowheads mark bands which owe to staining of Hsc70. All assays presented in this figure contain ATP.

Concentration of the chaperone components were as follows: 4.7µM Hsc70; 3.2µM Hsp40. Where used, ATP was included at a concentration of 5mM. (In all cases the standard 10mM MOPS / 50mM KCl buffer of pH7.2 was supplemented with 5mM $MgCl_2$ to ensure solubility of the ATP.)

a. Effect of DSG (separate panels show repeats of the same assay).

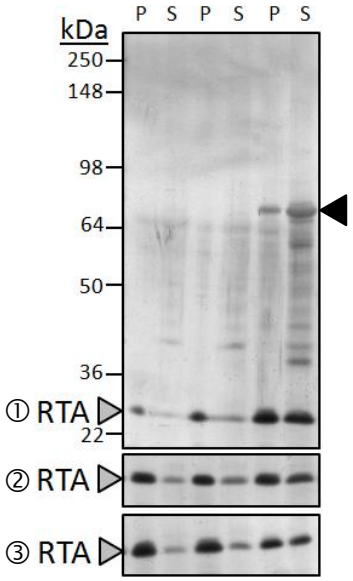

RTA	+	+	+
ATP	+	+	+
Lactose	+	+	+
DSG	-	+	+
Hsc70	-	-	+
Hsp40	-	-	+

b. Effect of lactose (separate panels show repeats of the same assay).

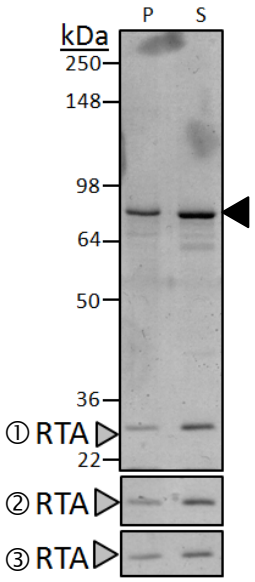

RTA	+
ATP	+
Lactose	+
DSG	-
Hsc70	+
Hsp40	+

(Figure 4.19 – continued.)

c. Quantification (n=3). This figure quantifies a & b and displays it alongside data from Figure 4.16.

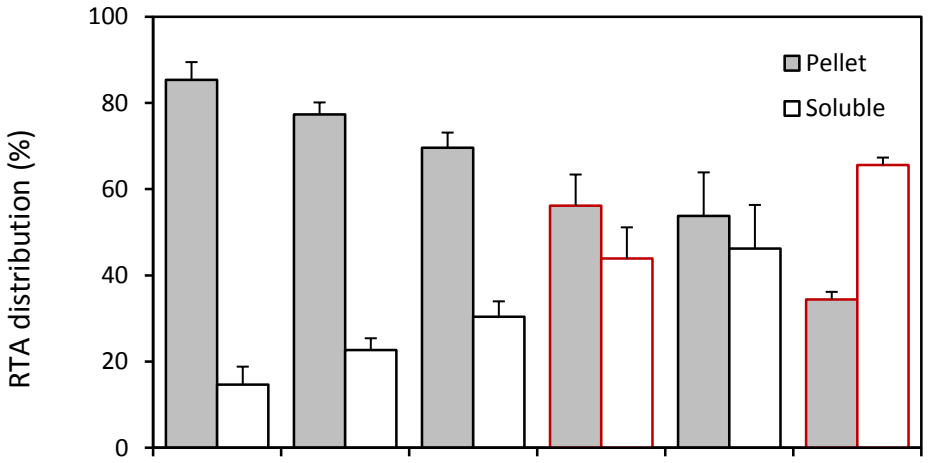

RTA	+	+	+	+	+	+
Lactose	-	+	+	+	-	+
DSG	-	-	+	+	-	-
Hsc70/Hsp40	-	-	-	+	+	+
Pairs	**1**	**2**	**3**	**4**	**5**	**6**

4.10 The effect of chaperones upon saporin

To show that Hsc70 and Hsp40 are passive species which do not interact with clients unless they show some degree of non-native character, an abridgement of the assay above was created with saporin. As previously determined, saporin is not prone to lose solubility at 45°C. In Figure 4.20, it is shown that Hsc70, Hsp40 and DSG do not affect the distribution of saporin between pellet and soluble fractions after incubation at 45°C. However, as the dynamic range of this assay is likely to be small (i.e. already ~90% of the saporin is soluble), any effect may be beyond the scope of reliable determination.

Figure 4.20 - The effect of chaperones upon saporin

In identical assay to those conducted with RTA (conducted at 45°C, 500ng saporin was incubated with lactose, DSG and Hsc70/Hsp40 in the indicated combinations. All reactions also contained ATP. Concentration of the chaperone components were as follows: 4.7µM Hsc70; 3.2µM Hsp40. Where used, ATP was included at a concentration of 5mM. (In all cases the standard 10mM MOPS / 50mM KCl buffer of pH7.2 was supplemented with 5mM $MgCl_2$ to ensure solubility of the ATP.)

a. Silver-stains - separate panels show repeats of the same assay.

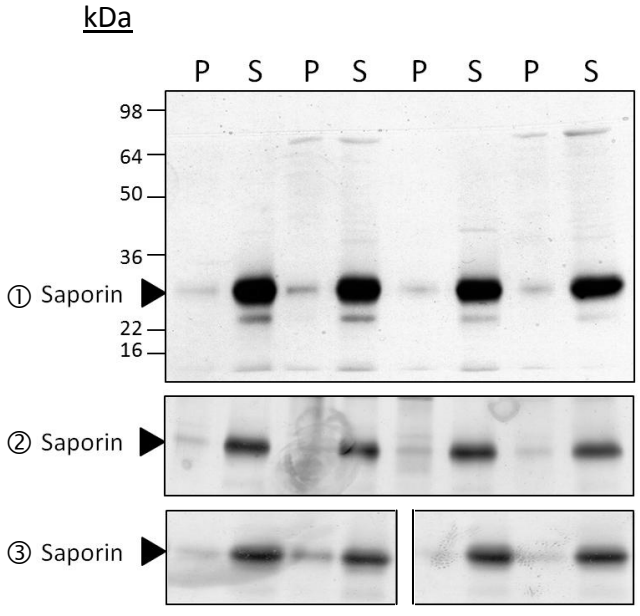

Lactose	+	+	+	+
DSG	-	-	+	+
Hsc70	-	+	-	+
Hsp40	-	+	-	+

b. Quantification (n=3)

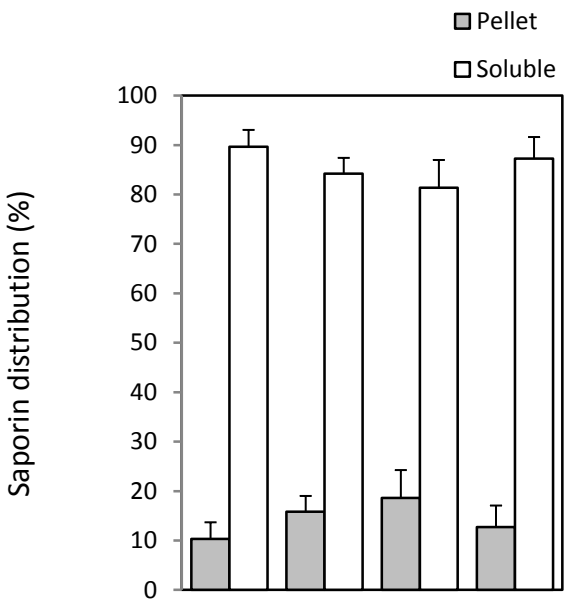

Lactose	+	+	+	+
DSG	-	-	+	+
Hsc70	-	+	-	+
Hsp40	-	+	-	+

4.11 Effect of cytosol on the aggregation of RTA

Each of the solubility assays to this point has examined the effect of *purified* constituents upon the solubility of RTA. It was possible a more complex incubation could recapitulate the phenomena observed in isolation, showing that the effect of Hsc70 could be manifest amid a mixture of other proteins, e.g. a cytosolic extract. It was thought that a cytosolic extract might be observed to:

(1) Displace RTA from annealing to the side of the incubation vessel, as the cytosol would have a variety of proteins which might compete with RTA in doing so.
(2) Have crowding effects – a cytosolic extract would be densely populated by proteins and other macromolecules.
(3) Prevent RTA from being thermally denatured – a cytosolic extract would include chaperones which might cause this effect.
(4) If point 3 were demonstrated, then those effects might be interfered with by Hsc70 inhibitors like DSG, or even Hsp90 inhibitors like GA, RA and C01.

Production of a cytosolic extract **-** A cytosolic extract was prepared from a monolayer of HeLa cells. The monolayer was incubated with trypsin solution and then resuspended in 10mM MOPS / 50mM KCl pH7.2 with Complete protease inhibitors (Roche). Cells were then lysed by grinding with metal ball bearings.[16] The resulting lysate was clarified of remaining membrane-bound material by centrifugation at 120000 $\times g$ for an hour at 4°C. This clarified lysate was then dialysed against 10mM MOPS / 50mM KCl pH7.2 buffer overnight to remove small molecules. Samples were then snap-frozen on dry ice and stored at -80°C. Aliquots of the extract were compared, via silver stain, to a separate extract made with a buffer containing 1% triton X-100 (Figure 4.21a). In the mechanically lysed extract, there is a reduction of bands at most molecular weights, and particularly at molecular masses above 64kDa relative to detergent-lysed extracts. This preferential loss of higher-molecular weight species suggests the release of lytic enzymes (resulting in universally lower molecular weight fragments). Some membrane-bound protein content may have also been removed after being sedimented at 120000 $\times g$ as well, putatively including lumenal chaperones (e.g. Grp94 & BiP).

[16] The use of detergent as the mode of lysis was precluded since detergents might also interfere significantly with protein interactions affecting the solubility assay.

It was planned that RTA would be incubated with increasing concentrations of this extract at 45°C and that the resultant solubility of RTA would be assayed by the distribution of protein between pellet and soluble fractions. Initially, an immunostain method was used to visualise the distribution of RTA between soluble and pellet fractions, but this approach was abandoned as it did not yield reliable results (data not shown). A silver stain approach was opted for instead. Figure 4.21b shows cytosolic extracts stained in this manner, compared in parallel to RTA. This shows that the RTA band appears in a region of the gel that is *relatively* free of obscuring bands. This is just as true when the cytosol incubation is heated to 45°C for 15 minutes and split into pellet and supernatant fractions. Therefore, it seemed that a silver-stain approach might return an interpretable set of data, as the intensity of the RTA band could be determined with relatively little background interference.

Figure 4.21 – Production of cytosol from HeLa cells

a) Cellular extracts were separated by SDS-PAGE and silver-stained. Lanes marked "mechanically lysed" show the extracts generated from the method discussed in the text. Lanes marked "lysed by detergent" were lysed in a buffer containing 1% Triton X-100 and were not clarified of membrane content. c) 500ng RTA was loaded into the lane marked "RTA". The lane marked "Cytosol" was loaded with 10µL of the cytosolic extract as well as 500ng RTA. Lanes followed by "(P)" or "(S)" are the products of heating the indicated mixture of 10µL cytosol and 500ng RTA (in a total volume of 20µL) at 45°C for 15 minutes followed by 16000 ×*g* fractionation into pellet and soluble fractions.

a. Silver-stain of cytosolic extracts

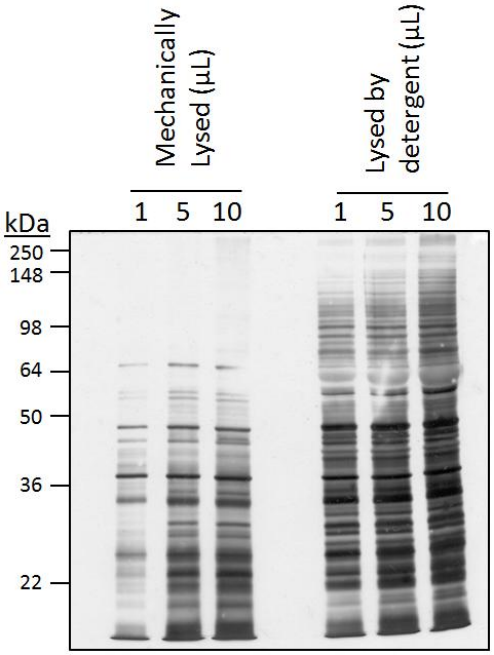

b. Where RTA falls in the cytosol ladder

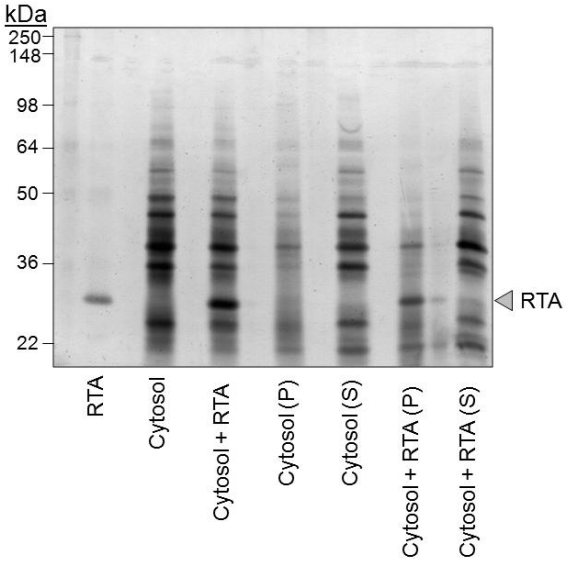

Testing the effect of the cytosolic extract on the solubility of RTA **-** RTA was incubated with increasing concentrations of the cytosolic extract. The quantification of each data-point was carefully normalised to a background value. This background value corresponded to the intensity of silver-staining by an equivalent concentration of cytosol alone (at the position where RTA would have otherwise migrated to in the protein ladder). The results of this analysis and the silver stains from which they are derived are presented in Figure 4.22a (RTA bands are marked with asterisks).

As the concentrations of cytosol increases above 5%, the total signal size from RTA bands decreases (Figure 4.22b). This trend does not appear to be because the background negation is over-compensating, but probably results from proteolytic activity (which persists despite Complete protease inhibitors being used in generation of the extract). Encouragingly, incubation with lower concentrations of cytosol (5-10%) appears to conserve the solubility of RTA. However, at a cytosol concentration of 25% the solubilising effect diminishes and a greater proportion of the RTA is found in the pellet. Unfortunately, the total signal size also diminishes under these conditions, which makes interpretation difficult: the decrease in the soluble fraction may be because of an increase in crowding effects, or the preference for any endogenous protease to cleave soluble RTA rather than aggregated RTA of the pellet.

Figure 4.22 - The effect of a cytosolic extract upon the aggregation of RTA

500ng RTA was incubated at 45°C for 15 minutes with ATP and increasing concentrations of the mechanically-lysed cytosol extract. After this incubation, it was separated into 16000 ×*g* supernatant and pellet. These were analysed in parallel via SDS-PAGE. Bands were visualised by silver-staining, and are shown below, in a). The concentration of cytosol is given arbitrarily, as a percentage of the extract relative to the entire incubation volume. A 25% concentration, therefore, is equivalent to 25% of the incubation mixture: 5µL of the cytosol preparation in a total volume of 20µL. Marked with both the grey arrowheads and asterisks are RTA bands. b) Shows quantification of the entire signal size from both pellet and soluble bands, as determined by TotalLab, and normalised arbitrarily to the most intense pair. c) Shows relative quantification of pellet and soluble bands. The pellet is in gray and the soluble fraction is in white. d) The pellet and soluble signal sizes of RTA relative to the maximum total signal size from both. Error bars on all charts show the standard deviation between the three sets of experiments shown in a). Note that the signals from the RTA bands are normalised to the background shown in lanes which include cytosol alone.

a. Silver stains - separate panels show independent repeats of the same experiment.

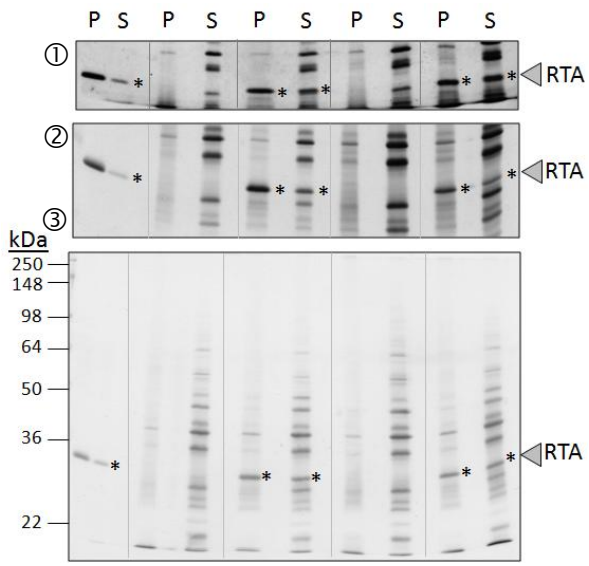

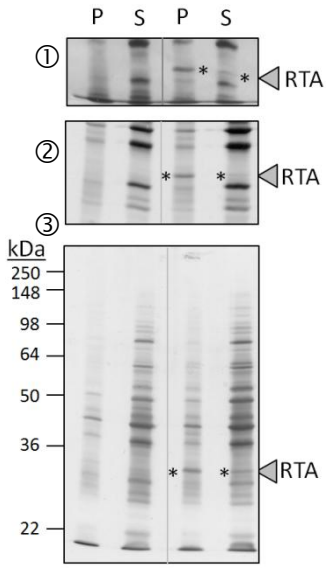

RTA	+	-	+	-	+
Cytosol (%)	0	5	5	10	10

RTA	-	+
Cytosol (%)	25	25

(Figure 4.22 – continued.)

b. Total signal size

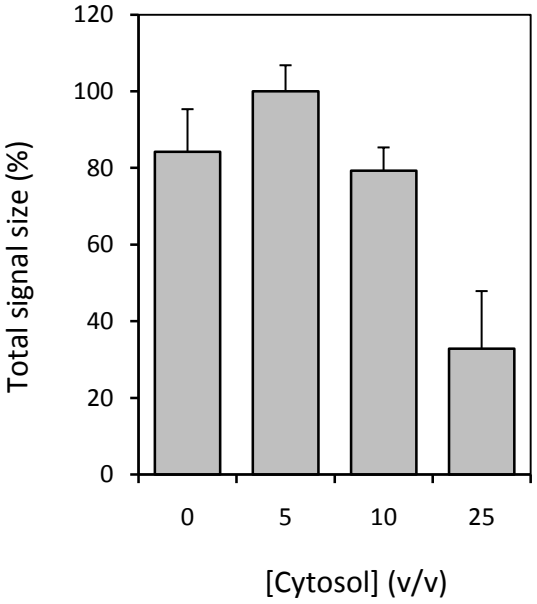

c. RTA distribution

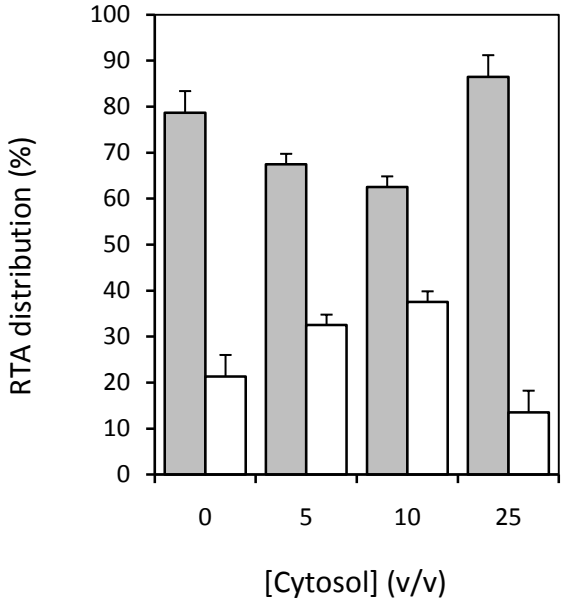

d. Absolute pellet signal size

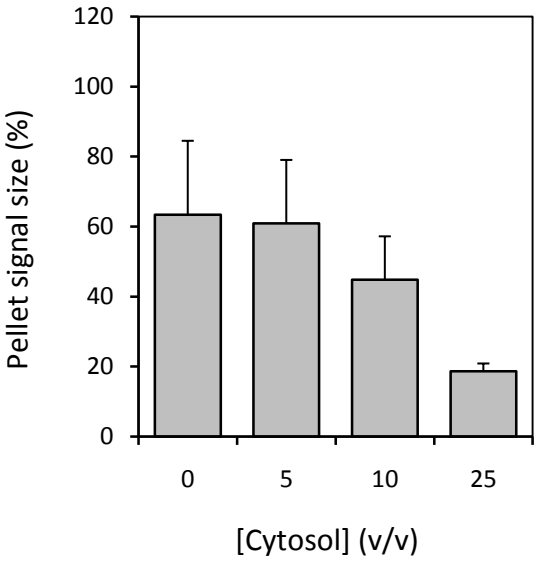

e. Absolute soluble signal size

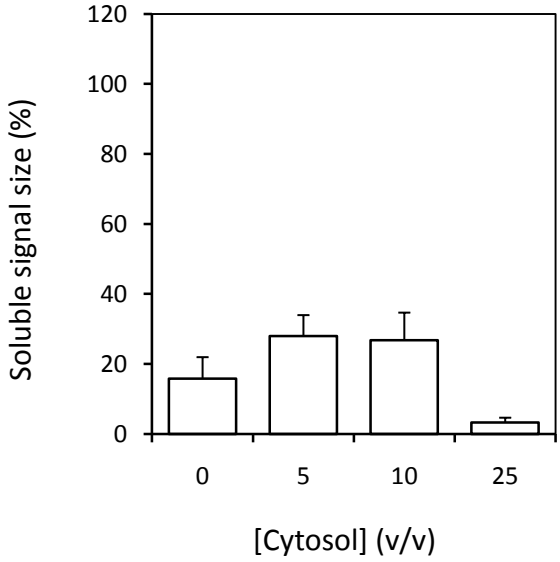

4.11.1 The effect of Hsc70 and Hsp90 inhibitors upon the properties of cytosol

If the effect of cytosol at concentrations of 5-10% was because of the activity of chaperones therein, then that activity would be inhibited by the pharmacological agents used in Chapter 3. To this end, the effects of DSG and C01 upon 10% cytosol were tested (Figure 4.23c & d). Unfortunately, in these assays cytosol alone had no significant effect upon the pellet/soluble distribution of RTA. It is possible that the extract, although frozen in individual aliquots at minus 80°C, may have lost some of its potency during protracted storage. Alternatively, the inclusion of DMSO or lactose in the assay may have disrupted pro-solubility interactions which would otherwise occur.

Incidentally, these results seem to vouch against the idea that the increased solubility which earlier correlated to concentrations of 5-10% cytosol (Figure 4.22) results from non-specific binding of the protein to the incubation vessel (which would displace RTA from doing the same). Such a phenomenon would likely be a consistent feature of the extract, irrespective of an activity that could be degraded by a protease upon storage. Figure 4.23d, however, shows that the effect has disappeared upon storage.

Figure 4.23 - The effect of C01 and DSG upon the rescue of soluble RTA by cytosol.

a) 500ng RTA was incubated, as before at 45°C, but with or without 10% cytosol (v/v), and with or without 3.2µM C01 and DMSO. b) Shows quantification of the silver stains in a). Error bars show the standard deviation between the three assays. The intensity coming from RTA bands where cytosol was present was normalised to the background from equivalent assays where RTA was absent. Asterisks help mark RTA bands, for ease of reference. c) & d) Show equivalent assays, but where 50µg.mL^{-1} DSG and the excipient of DSG, 100µg.mL^{-1} lactose have been substituted for C01 and DMSO respectively.

Experiments using the Hsp90 inhibitor, C01018159 (C01)

a. Silver stains - separate panels show independent repeats of the same experiment.

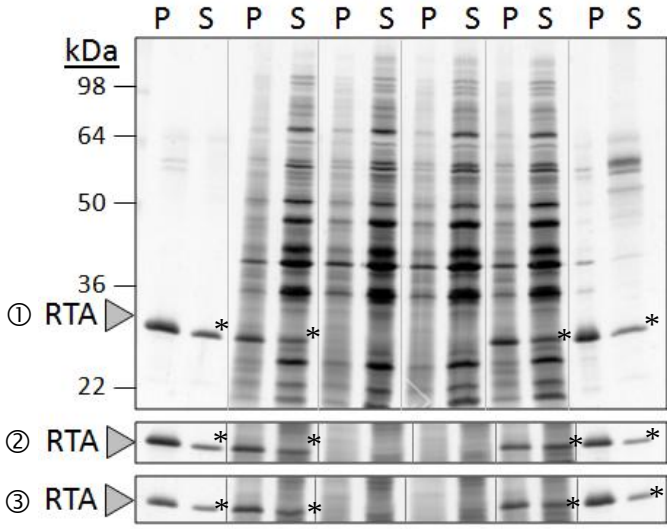

RTA	+	+	-	-	+	+
Cytosol	-	+	+	+	+	-
C01	-	-	-	+	+	+
DMSO	+	+	+	+	+	+

b. Quantification normalised to cytosol background (n=3)

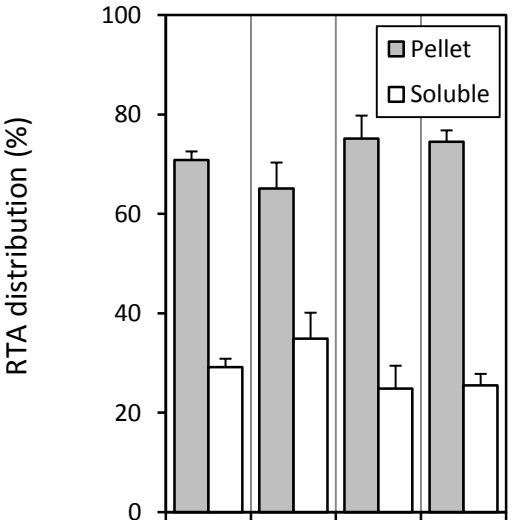

RTA	+	+	+	+
Cytosol	-	+	+	-
C01	-	-	+	+
DMSO	+	+	+	+

(Figure 4.23 – continued.)

Experiments using the Hsc70 inhibitor, deoxyspergualin (DSG)

c. Silver stains - separate panels show independent repeats of the same experiment.

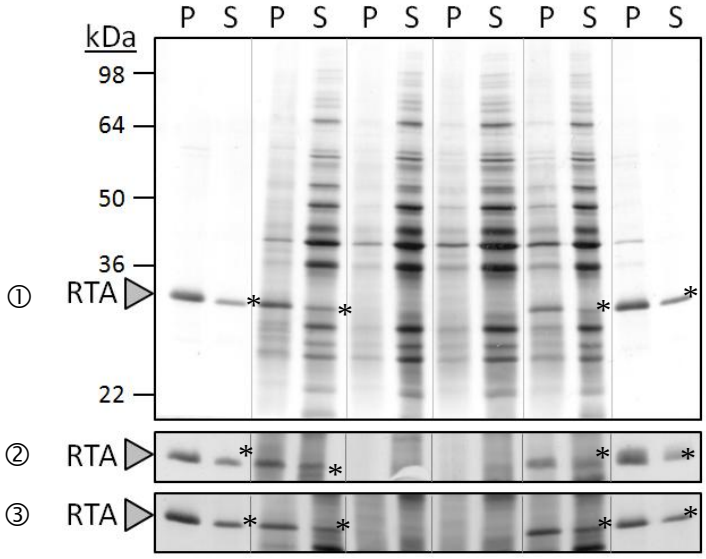

RTA	+	+	-	-	+	+
Cytosol	-	+	+	+	+	-
DSG	-	-	-	+	+	+
Lactose	+	+	+	+	+	+

d. Quantification normalised to cytosol background (n=3)

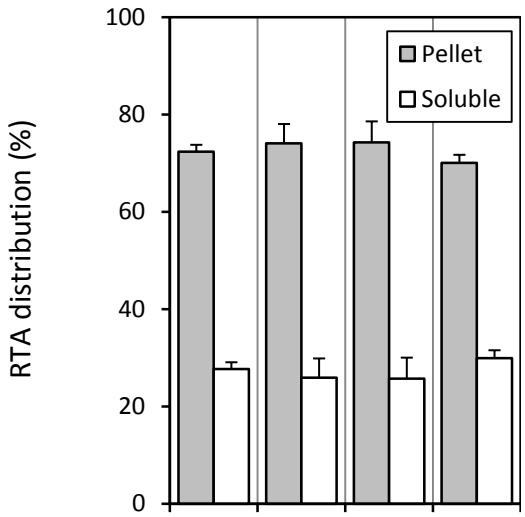

RTA	+	+	+	+
Cytosol	-	+	+	-
DSG	-	-	+	+
Lactose	+	+	+	+

4.12 Discussion

This chapter set out to examine a functional interaction of Hsc70 with RTA *in vitro*. An interaction which resembles such an association has been observed *in vitro*. When RTA is incubated with Hsc70 and Hsp40 at both 37°C and 45°C, more can be found in a soluble condition than in incubations without chaperones. According to the results published in Spooner *et al*. (2008) and data presented in this chapter, this effect occurs maximally when ATP is present, showing that there is an interaction between the two proteins involving the ATPase cycle of the chaperone. In other words, the data in this chapter show that Hsc70 may actively bind to RTA.

Binding of Hsc70 to RTA may contribute to the solubility of the toxin subunit by two mechanisms, as determined by the effects of the chaperone at both 37°C and 45°C:

(1) By masking transiently-exposed hydrophobic regions of RTA that otherwise promote loss of solubility by aggregation and association with the incubation vessel (accounting for the increased pro-solubility effect of Hsc70 at 45°C).
(2) By masking the hydrophobic C-terminus of the toxin subunit, which seems to promote adherence of the protein to the incubation vessel (accounting for unexpected effects at 37°C, at which the protein is not thought to unfold to a significant extent – Argent *et al*., 2000).

An interaction of Hsc70 with non-native RTA - At 45°C, it was anticipated that Hsc70 and RTA would interact. This is because RTA would be prone to unfold at this temperature (Argent *et al.*, 2000), a treatment which would mimic the substantially-unfolded state in which RTA is suspected to enter the cytosol (Beaumelle *et al.*, 2002; Argent *et al.*, 1994). Fittingly, at this temperature, Hsc70 had the greatest effect in promoting solubility. Just after retrotranslocation a transient Hsc70·RTA complex similar to that which evidently occurs at 45°C may exist, helping the toxin subunit thereafter reach an active conformation in the cytosol. Alternatively, Hsc70 might interact with RTA while the toxin subunit is still partially-enclosed by the membrane (or the membrane pore it uses). In this case, Hsc70 could help promote extraction (akin to roles proposed for homologous BiP and mitochondrial Hsc70 during other translocation processes – Tomkiewicz *et al*., 2007).

DSG inhibits passive and active effects of Hsc70 - The observation that DSG protects cells against ricin intoxication has also been paralleled in this *in vitro* system. DSG inhibits Hsc70

from keeping RTA soluble, and apparently beyond perturbation of the chaperone's ATPase cycle. *In vivo*, the same effect of this inhibitor may be dominant, interrupting an Hsc70·RTA complex. This would abandon the polypeptide to an increased likelihood of misfolding, or to a longer period embedded in the membrane, potentially permitting other ERAD machinery the chance to facilitate its degradation.

Interestingly, DSG itself was shown to be a small molecule chaperone which promoted the solubility of RTA. Confusingly, *in vivo* this might cause a partial stabilisation of RTA in the ER lumen of target cells. This could putatively interfere with membrane translocation (and so result in a portion of the protection it bestows *in vivo* against ricin, *cf.* glycerol). However, DSG's inhibitory effect upon Hsc70 results in a ~22% decrease in the pellet/soluble distribution of RTA. On the other hand, its isolated, positive effect upon RTA solubility is a mere ~8% (Figure 4.19c). Thus its greater function, at least *in vitro*, seems to be inhibition of Hsc70 rather than as a pro-solubility factor. Nevertheless, such composite effects should be considered.

An interaction of native RTA with Hsc70 - At 37°C, a temperature at which RTA is thought to be largely "native" (Argent *et al*., 2000), it was anticipated that Hsc70 would not have an effect upon solubility. However, Hsc70 did have a solubilising effect at this temperature. As an equivalent concentration of an arbitrary protein (BSA) produced a much smaller solubilising effect, it seemed that the effects of Hsc70 resulted at least partially from its activity as a chaperone. The eminent quality of the native toxin subunit which could cause such an interaction at 37°C seems to be RTA's solvent-exposed, hydrophobic C-terminus.

The hydrophobic C-terminus of native RTA may promote an Hsc70 interaction - That the C-terminus might be responsible for chaperone interactions with native RTA during a 37°C incubation seems a reasonable connection to make. In this chapter it was shown that saporin – which lacks this domain but is otherwise very similar to RTA (Vago *et al*., 2005) – does not interact with chaperones in the same way as RTA does. This is interesting as the unique hydrophobic C-terminus of RTA is important for its toxicity (Simpson *et al*., 1995). *In vitro* it has been postulated to embed into the hydrophobic core of negatively-charged liposomes (Day *et al*., 2002; Mayerhofer *et al*., 2009). Therefore, that this portion of the protein might lead to a hydrophobic series of interactions *in vitro* resulting in loss of solubility seems congruent.

Regardless of which domain of RTA is responsible for the interaction of RTA with Hsc70 at 37°C, it does seem that even the native toxin subunit is recognised by the chaperone. Therefore, this result might indicate refolded RTA would be subjected to continuous surveillance by Hsc70 in the cytosol of target cells. That is unless its native quality is altered in some fashion by events surrounding retrotranslocation.

The effects of the cytosolic extract - Unfortunately, it proved difficult to determine whether the inhibitory effects of DSG and the Hsp90 inhibitor, C01, could be recapitulated in a cytosolic extract. While it was shown that low concentrations of cytosol might have a pro-solubility effect, assays where higher concentrations of cytosol were used proved un-interpretable. This was because of a putative proteolytic activity in the extract. Repeat assays were prevented due to the quickly-fading activity of the cytosolic preparation in maintaining the solubility of RTA (potentially owing to the same proteolytic activity). Repetition with fresh cytosol preparations would also skew the comparability of the data, owing to batch-variability in generating the extract.

Other influences upon the solubility of RTA - When other aspects that could govern protein-folding were tested, it was evident that charged species affected the unfolding of RTA, whereas polar species did not. Increasing concentration of aqueous $CaCl_2$ and NaCl resulted in the greater stability of soluble RTA conformers. This effect may result from stabilisation of the solvent structure, which would constrain the polypeptide from unfolding and so promoting aggregation (Hu *et al.*, 2009). On the other hand, incubation with a charged protein, BSA, and liposomes constructed from negatively-charged POPS led to *loss* of solubility. Much like Day *et al*. (2002) report: initially electrostatic interactions may lead to progressively more hydrophobic ones.

Consistently, neutral liposomes and high concentrations of the polar crowding agent, Ficoll-70, did not have a large effect at either 37°C or 45°C. It seems that electrostatic interactions dominate the threshold temperature at which RTA unfolds. As Ficoll-70 had no effect even at 45°C, it seems that when RTA does unfold, another feature (other than crowding) dominates loss of solubility. This could be a combination of the hydrophobic C-terminus of the protein and the abundance of a surface to which the protein can be adsorbed (i.e. the reaction vessel; or, in other cases, the hydrophobic cores of POPS liposomes and BSA molecules).

A sharp temperature-dependent threshold for unfolding between 37°C and 45°C was also shown. This threshold coincides with the observations of Argent *et al*. (2000) who pinpointed the threshold more precisely to 42-45°C. At this threshold secondary structure becomes significantly perturbed (although the authors stipulate a batch variation to this threshold). This starkly contrasts to the structurally-related toxin, saporin, which is stable at equivalent temperatures and does not undertake an ERAD-like route to achieve toxicity (Vago *et al*., 2005). This relatively low threshold highlights the conformational malleability RTA has attained to exploit ERAD.

Similarly, RTA seems to be most prone to misfold, losing solubility, near a physiological threshold of pH. Over a range of pH6.4 to 8.0, soluble RTA was found to be least stable around pH7.0 to 7.4. Such as latent instability, which is masked by the stabilising effect of RTB until the ER of the target cell is reached (Argent *et al*., 2000; Spooner *et al*., 2004), might contribute to the co-option of RTA onto an ERAD pathway.

Incidentally, although recombinant RTA does have a pI that is very close to the physiological pH, Di Cola *et al*. (2001) showed that RTA isolated from *Ricinus communis* has a relatively raised pI. This results from glycosylation in its wild-type host. An increased pI would make the protein more soluble in the ER. In the mammalian cytosol, where RTA would likely be subjected to de-glycosylation (as it is in yeast – Li *et al*., 2007), its pI would subsequently be reduced to a level akin to recombinant RTA, making it less soluble. This example, therefore, does not conform to a preceding hypothesis: that various inherent qualities of RTA in response to physiological conditions might favour stability in the cytosol and instability in the ER lumen.

The effect of negatively-charged liposomes – As predicted from the observations of Day *et al*. (2002) and Mayerhofer *et al*. (2009), the solubility assay showed that RTA could interact with negatively-charged liposomes *in vitro*. This interaction caused a loss of solubility which was not restored after the liposomes were dissolved with a detergent. This suggested that RTA underwent structural changes after binding which resulted in an irreversible loss of solubility. After initial electrostatic contacts are made between lipid and RTA, hydrophobic interactions take over as the toxin subunit embeds itself into the liposome (Day *et al*., 2002). This putatively leads to a state which irreversibly aggregates or else irreversibly adheres to the reaction vessel after the detergent treatment disperses the liposome.

This same loss of solubility is not observed when RTA is incubated with neutrally-charged liposomes. Furthermore, any effect of POPC upon the solubility of RTA which does occur is dominated by the presence of a small molecule chaperone, glycerol, which is not the case for negatively-charged lipid. This reiterates that the charge of the lipid used to construct the liposome is essential in inducing the structural rearrangements observed. This corroborates other trends observed in this chapter: i.e. charged species like BSA, pH and electrolyte concentration affect solubility, whereas neutral, polar Ficoll-70 – and now POPC – do not.

4.12.1 Improving upon this assay & potential future uses

Pre-blocking of the incubation vessel **-** If these *in vitro* findings were to be extended, it would be advisable to block binding to the incubation vessel beforehand by flushing it with low concentrations of a relatively inert protein (Van den Berg *et al.*, 1999). Alternatively, a material which provides a polar rather than a hydrophobic surface could be chosen for the incubation vessel. This would increase the proportion observable in the soluble fraction under untreated conditions and would increase the dynamic range of the assay. This would enable material which has truly aggregated to be distinguished from material which has adhered to the reaction vessel. Without such blocking, the assay used in this chapter measures both of these phenomena.

The observation of this tendency of RTA to adhere to hydrophobic surfaces, however, is not without meaningful application. The results presented in this chapter have indicated that the C-terminus of RTA is likely to be responsible for this binding and may also interact with Hsc70 while the toxin subunit is in its native conformation. This may well result in an ongoing interaction with Hsc70 long after membrane retrotranslocation. As the C-terminus is functionally implicated in the toxicity of RTA (Simpson *et al*., 1995), judicious experiments using unblocked tubes might provide an experimental system useful in its investigation.

Screening for destabilising ER factors and stabilising cytosolic factors **–** If a systematic way for producing the cytosolic extract could be established which also maintained long-term solubilising activity, it would be a useful tool. The extract could be fractionated and screened for proteins with solubilising or pro-aggregation activity. Fractionation could be repeated iteratively (with progressive refinement) until isolated protein species with significant effects were identified. These species could then be identified by mass spectrometry. By such a method, a whole host of other "pro-solubility" or "pro-aggregation" factors could be discovered which might be significant interacting partners of RTA *in vivo*.

It might be expected that the toxin subunit has evolved to exploit the physiological conditions of the ER and cytosolic compartments in different ways, tailored to its toxic motives. Unfortunately, the complexity of these compartments is difficult to meaningfully disassemble using the solubility assay – especially for broadly important factors like calcium ion concentration (*cf.* section 4.5.2.1). Synergy between one aspect and another in the more complex system that undeniably exists *in vivo* will likely drastically alter otherwise simplistically-observed trends. For instance: the overlaid functionality of the protein matrix in response to these chemical factors. The concentration of calcium in the ER – as a particular example – modulates the ERAD of many secretory proteins (Van Anken & Braakman, 2005). So, too, do changes in redox levels and the pH (Sevier & Kaiser, 2008). To provide a more exhaustive study of any physiologically relevant chemical factors that might affect the conformational stability of RTA, however, would be intriguing. The most obvious candidates for future investigation would be the lipid environment and a comparison of the chaperone complements of both the ER and cytosol.

Screening for antagonism of the negatively-charged liposome interaction – The interaction of RTA with liposomes constructed from exclusively POPS could not be countered simply with the use of a small molecular chaperone (as predicted from the hypotheses of Sandvig *et al*., 1984). However, glycerol might be able to compete against liposomes where POPS has been diluted with neutral lipid. Identification of other factors which could counter this interaction would be particularly interesting to study. This is because no such factor has yet been proposed to suggest how RTA would be prevented from interacting with the cytosolic leaflet of the ER membrane, just as it is proposed to in the ER (Mayerhofer *et al*., 2009). This problem is highlighted by reports that lipid distribution between the two leaflets of the ER membrane is highly symmetrical (Pomorski & Menon, 2006). This precludes the enrichment of negatively-charged phospholipids in the ER-leaflet being the mechanism. It is a possibility that chaperones like Hsc70 might be responsible for sustaining the cytosolic solubility of RTA and preventing such a regressive membrane interaction. Intriguingly, interactions with the membrane are thought to be caused by the C-terminus of RTA (Mayerhofer *et al*., 2009). That Hsc70 seems to bind this region at 37°C and prevent it from associating with a hydrophobic surface *in vitro* may be an analogous feat.

Alternatively, the solubility assay could be used to determine if RTA can be removed from a liposome-bound state after having already been allowed to interact. RTA and liposomes could be incubated together, and factors added to see if they could subsequently disengage

such a complex. If the supply of Hsc70 had not been limiting, experiments like this would have been undertaken to test this possibility. Other factors that would have been interesting to study in this regard include the regulatory 19S proteasomal caps and p97-containing complexes, which have a similar role during ERAD (Meusser *et al*., 2005).

Identification of potential storage excipients **-** Incidentally, the methods demonstrated in this chapter could also be used as a tool to study potential excipients with which RTA may be stored for long periods of time. Such a study is of special interest to those who wish to develop and store vaccines (Peek *et al*., 2006). Currently, our laboratory stores RTA in a pH6.4, sodium phosphate buffer – often containing KCl or glycerol, which stabilises the solubility of RTA. These conditions could be optimised, using this assay to maximise the chronic solubility of RTA. Peek *et al*. (2006) used a similar assay, where they studied the effect of candidate chemicals on the turbidity of a dilute solution of RTA over time. However, they discovered this assay was inappropriate in the case of chemicals which themselves contributed to turbidity. The techniques used herein would not be affected in this way and so might prove complementary.

Alternative assays – Other assays for determining the interaction of two proteins (such as Hsc70 with RTA) do exist. For instance: analytical ultra-centrifugation, gel filtration, fluorescence resonance energy transfer (FRET) and surface plasmon resonance. If the experimenter wished to support the data herein, those assays might prove a useful supplement to those used herein. For the interaction of factors such as salt, glycerol and pH, fluorescence could even be measured.

4.12.2 Pursuing the chaperone interaction further

As Chapter 3 showed, inhibition of Hsc70 protects cells – thus, this chaperone seems responsible for providing an interaction which leads to activation of the toxin subunit in the cytosol. Evidence for the potential mechanism by which Hsc70 can aid the toxin has been posed by this chapter. Hsc70 can interact functionally with both thermally-denatured RTA and, surprisingly, with non-denatured toxin. Therefore, Hsc70 may have relevance both during the retrotranslocation step and afterward during the toxin subunit's lifetime in the cytosol. It may both prevent it from losing catalytic activity by aggregating and prevent it from re-engaging with the leaflet of the membrane that envelops the cytosol.

Earlier in Chapter 3 it was shown that inhibition of Hsp90 *sensitised* target cells to ricin in a way which responded to the lysine content of the toxin subunit. Thus, Hsp90 seems to be responsible for hindering the toxin in a way which involves lysine-polyubiquitination. A proteasomal route may be the most forthright explanation for such a lysine-dependent effect, much as Deeks *et al*. (2002) theorised. However, mechanisms for how Hsp90 might inactivate RTA or facilitate its polyubiquitination have not yet been investigated. The next chapter continues these studies by examining how such chaperone-mediated routes may be executed, with the aid of co-chaperones.

CHAPTER 5:

Co-factors of Hsc70 and Hsp90 modulate their *in vitro* and *in vivo* activities

5.0 How co-chaperones may determine the outcome of RTA's interaction with Hsp70 or Hsp90

Hsc70 and Hsp90 have vital roles in the mammalian cell (Whitesell & Lindquist, 2005). To optimise their function, they require external modulation, tailoring their activities to the diverse array of clients a eukaryotic cell possesses. This external modulation is provided by the co-chaperone environment of the cytosol. Members of this diverse population of co-factors provide bespoke 'folding pathways' for certain subsets of client (Young *et al*., 2004). Some of these co-chaperones change the role of the chaperone·client interaction from a nurturing complex to one which actively targets the client for proteolysis (Höhfeld *et al*., 2001). Whilst data presented so far in this thesis indicate that Hsc70 might aid retrotranslocated RTA gain an active conformation in the cytosol, it shows that other chaperones may hinder toxicity, such as Hsp90 appears to. An extension of this hypothesis is that the native balance of co-chaperones in the cytosol contributes to these different roles.

If cytosolic chaperones *can* mediate the inactivation of RTA, this facet of the cytosolic triage poses an extremely interesting topic of study. Hsp90 may be involved in a route by which RTA is proteolytically inactivated. As would be implied from the lysine-dependent effect of Hsp90 inhibition upon the cytotoxicity of ricin, the interaction of Hsp90 could convey RTA to the proteasome, or bring it into contact with an E3 ubiquitin ligase. An eminent candidate for this E3 ligase would be the chaperone-dependent co-factor, CHIP (Alberti *et al.*, 2004). Such a mechanism could account for the two-thirds of cytosolic RTA^{WT} that is apparently degraded by proteasomes during intoxication (Deeks *et al*., 2002; Wesche *et al*., 1999).

In addition to an explicitly pro-destruction role such as polyubiquitination, the balance of co-chaperones in the cytosol could also alter the longevity of a putative RTA·Hsc70 or RTA·Hsp90 complex. In this fashion they could alter the likelihood that chaperone-bound RTA successfully finds a native state – by prolonging or shortening residency in the binding site of each chaperone. On one hand, prolonged binding might contribute to the success of folding by preventing aggregation. Conversely, it might also increase the chances of a subsequent interaction with a co-factor that promotes degradation. Thus, a co-chaperone may not be destructive in the same explicit way that the E3 ubiquitin ligase, CHIP, is, but may still

contribute to an environment which promotes degradation (or inactivation) of chaperone-bound material. Table 5.1 notes co-chaperones of Hsc70; Table 5.2 (on the subsequent page) reviews co-chaperones of Hsp90. In brief, these co-factors exert their effects by:

- Stimulating chaperone nucleotide exchange or ATPase activity, so altering the affinity of the chaperone towards its clients.
- Interacting with clients directly, as anti-aggregation factors.
- Bringing other cytosolic machinery into close proximity with the client·chaperone complex (e.g. the proteasome).
- Acting as recruitment factors to certain cellular locations.
- In the case of the Hsp90 co-chaperone, prolyl peptidyl isomerise (PPI), performing *cis*/*trans* isomerisation of client prolyl residues.

This thesis maintains that genetically interfering with Hsc70 and Hsp90 is a difficult experimental approach because of their vital nature, high concentration and multiple cytosolic paralogues (as reviewed in Whitesell & Lindquist, 2005). The cytosolic concentrations of their co-chaperones, however, are relatively minor. For example, while Hsp90 represents 1-2% of dry cell mass and is one of the most abundant proteins of the cell (Csermely *et al.*, 1998), CHIP and HspBP1 each represent only 0.05% of this total (Alberti *et al.*, 2004). This arguably renders experimentally significant changes in their cytosolic concentration more attainable. Thus, the co-chaperones of Hsc70 and Hsp90 provide practical targets to experimentally target.

Table 5.1 - Co-chaperones of Hsc70.

Their functions, mode of binding, and some example substrates. The column labelled "Hsp90" shows whether the co-chaperone has a potential interaction with Hsp90 as well. Ticks indicate a definite interaction. Question-marks denote a suspected, or else unclear one. This list is not exhaustive, but indicative.

Co-factor	Hsp90	Binding Domain	Known functions
CHIP	✓	TPR	• Hsc70/Hsp90-dependent E3 ligase (Murata *et al.*, 2001) • Stabilises Hsc70·ATP, enhancing *in vivo* refolding of luciferase (Kampinga *et al.*, 2003) • Conflicting reports suggest CHIP inhibits Hsc70-mediated luciferase refolding *in vitro* (Ballinger *et al.*, 1999)
Hsp40		J-domain	• Stimulates the ATPase activity of Hsc70 • Binds clients and has an independent anti-aggregation activity • Binds clients and loads them onto Hsc70
HspBP1		TPR	• Nucleotide exchange factor of Hsc70 (Kabani *et al.*, 2002) • Inhibits refolding of luciferase in reticulocyte lysate (McLellan *et al.*, 2003) • Inhibits CHIP, stimulating maturation of $CFTR^{\Delta F508}$ *in vivo* (Alberti *et al.*, 2004)
HIP		TPR	• Stabilises ADP-bound form of Hsc70 (Höhfeld *et al.*, 1995) • *In vitro,* isolated HIP inhibits refolding (Bruce & Churchich, 1997) • Promotes steroid hormone receptor maturation *in vivo* (Prapapanich *et al.*, 1998)
BAG-1		BAG	• Nucleotide exchange factor of Hsc70 (Alberti *et al.*, 2003) • Inhibits Hsc70-mediated refolding of β-galactosidase *in vitro* (Takayama *et al.*, 1997) • Associates Hsc70·client complexes with the proteasome (Lüders *et al.*, 2000) • Promotes Tau protein levels *in vivo* by aiding folding (Elliott *et al.*, 2007)
BAG-2		BAG	• Nucleotide exchange factor of Hsc70 (Takayama & Reed, 2001) • Inhibits CHIP, and stimulates maturation of CFTRΔF508 (Arndt *et al.*, 2005) • Possesses its own anti-aggregation activity for CFTRΔF508 (Arndt *et al.*, 2005)
BAG-5		BAG	• Nucleotide exchange factor of Hsc70 (Takayama & Reed, 2001) • Inhibits Hsc70-mediated refolding of luciferase *in vivo* (Kalia *et al.*, 2004) • Inhibits the chaperone-dependent activity of the E3 ligase, Parkin (Kalia *et al.*, 2004)
HOP	✓	TPR	• Binds and stabilises Hsp90·ADP (Johnson *et al.*, 1998) • Hsp90·HOP binds Hsc70·client complexes (Hernández *et al.*, 2002) • Stimulates Hsc70 nucleotide exchange (Gross & Hessefort, 1996). • Promotes *in vivo* maturation of steroid hormone receptors & various kinases (Murphy *et al.*, 2003) • Required for optimal Hsc70/Hsp90-mediated refolding of luciferase *in vivo* (Johnson *et al.*, 1998).

Table 5.2 - Co-chaperones of Hsp90.

Their functions, mode of binding, and some example substrates. The column labelled "Hsc70" indicates whether the co-chaperone has a potential interaction with Hsc70 as well. Ticks indicate a definite interaction. Question-marks denote a suspected, or else unclear one. This list is not exhaustive, but indicative.

Co-factor	Hsc70	Binding Domain	Known functions
HOP	✓	TPR	• As previous table. Also notable, as reviewed by Prodromou & Pearl (2003): • Interacts with Hsp90 early in its ATPase cycle, • Inhibits the ATPase activity of Hsp90, • Stabilises a conformation of Hsp90 that is open to clients.
p50 / Cdc37		No family	As reviewed by Prodromou & Pearl (2003): • Interacts with Hsp90 early in its ATPase cycle, • Inhibits the ATPase activity of Hsp90, • Stabilises a conformation of Hsp90 that is open to clients.
p23		No family	As reviewed by Felts & Toft (2003): • Stabilises mature client·Hsp90·ATP complexes • Promotes maturation of steroid-like hormone receptors, but is not essential • Isolated p23 prevents aggregation of citrate synthase *in vitro*.
Aha1		No family	• Activates the ATPase activity of Hsp90 (Prodromou & Pearl, 2003) • Stimulates client release (Koulov *et al.*, 2010) • Stimulates kinase and hormone receptor maturation *in vivo* (Harst *et al.*, 2005) • Contrastingly, down-regulation stimulates CFTRΔF508 maturation (Wang *et al.*, 2006)
CHIP	✓	TPR	• As previous table.
Cyclo- / immuno-philins	?	TPR	• Bear peptidyl prolyl isomerise activity (Fischer et *al.*, 1984) • Cpr6 activates the ATPase cycle of Hsp90 (Prodromou & Pearl, 2006) • Cyclophilin 40 may also bind to Hsc70 (Carrello *et al.*, 2004) • Cyclophilin 40 binds non-native proteins, preserving their folding competent state (Freeman *et al.*, 1996)

Of course, Hsc70 and Hsp90 are not always in direct physical contact with these co-chaperones. Their respective interactions typically occur at different stages in the chaperone's client binding cycle, and in different combinations (*cf.* Figure 1.6b, for instance). The nature of their interaction will depend on the substrate protein itself, and perhaps the distinct conformational character of a given instance of that client. The binding of some co-chaperones are also mutually exclusive (e.g. BAG-2 and BAG-1), and can lead to opposite fates for similar substrates (e.g. CFTR, see Arndt *et al.*, 2005). The decision of Hsc70/Hsp90 to aid folding or to promote degradation, therefore, is pivotally determined by the relative concentration of cytosolic co-chaperones, as well as by the apparent qualities of the client itself.

There are very obvious differences in the conformational qualities defining clients of Hsc70 and Hsp90. Hsc70 preferentially associates with extended, unfolded sequences of hydrophobic polypeptide (Landry *et al.*, 1992). On the other hand, Hsp90 is thought to bind to the surface of partially-folded proteins, promoting "subtler" changes in conformation (Prodromou & Pearl, 2006). This differentiation is reflected by data presented in this thesis – i.e. the distinctly opposite effects of these chaperones upon ricin cytotoxicity. Their different binding specificities are also reflected in the hierarchical order in which they interact with substrates like kinases and steroid hormone receptors. As the conformational adjustments a folding client makes become more refined approaching the native state from the unfolded one, the client's tenure shifts from binding Hsc70 to binding Hsp90 (Murphy *et al.*, 2003). This sequential interaction also seems to exist for the cytosolic triage of RTA (as Hsc70 inhibitor effects dominate Hsp90 inhibitor effects – *cf.* Chapter 3, Figure 3.12).

As these kinds of pathway are augmented by a client-dependent co-ordinate of co-chaperones, it might be expected that a specific subset of these factors is responsible for the activation of retrotranslocated RTA in the cytosol. Owing to the differing effects of Hsc70/Hsp90 inhibition on ricin intoxication, it is anticipated that a cohort of pro-folding co-chaperones might dominate the interaction of Hsc70 with RTA. On the other hand, a pro-destruction cohort of co-chaperones might dominate the interaction of Hsp90 with RTA. This chapter aims to investigate these balances.

5.1 Experimental approach

First, this chapter investigates whether CHIP can polyubiquitinate RTA in a chaperone-dependent fashion. The method uses an *in vitro* reconstitution of purified chaperones and components of the ubiquitination cascade to test conditions under which a client is ubiquitinated (as described by Murata *et al.*, 2001). This would show whether it was *feasible* that RTA could become ubiquitinated during a chaperone audit, which would aid interpretation of the observations made *in vivo* so far. The results of this experiment would also provide additional evidence for whether RTA is bound by these chaperones directly, given this is requisite for CHIP-mediated ubiquitination (Murata *et al*., 2001).

Second, this chapter used a synthesis of approaches already described in this thesis to investigate the role of other co-chaperones in the intoxication of a cell by RTA. That is, by studying:

(1) The effect of the co-chaperone BAG-5 on the solubility of RTA.
(2) The effect of over-expressing select co-chaperones on the cytotoxicity of ricin.

5.2 An introduction to CHIP, a co-chaperone of Hsc70 and Hsp90

The inactivation of cytosolic RTA by Hsp90 is lysine-dependent (*cf.* Chapter 3, Figure 3.18). It was suggested CHIP could polyubiquitinate Hsp90-bound RTA, which would target it to the 26S proteasome. Inhibition of Hsp90 with radicicol could putatively disrupt this interaction, preventing the exposure of RTA to this E3 ligase. This seemed a reasonable hypothesis, given radicicol-induced dissociation of client·Hsp90 complexes is reported for many substrates (Sharma *et al.*, 1998; Schneider *et al.*, 1996; Whitesell *et al.*, 1994; Whitesell & Cook, 1996).

As Table 5.1 and Table 5.2 detail, CHIP is a co-factor of *both* Hsc70 and Hsp90. It associates with these chaperones via its three TPR domains, which bind the C-terminal tetrapeptide, 'EEVD', of both chaperones (Ballinger *et al.*, 1999; Kundrat & Regan, 2010). This permits CHIP to ubiquitinate bound clients and inhibits the Hsp40-stimulated ATPase activity of Hsc70, antagonising Hsc70-mediated refolding of clients *in vitro* (Ballinger *et al.*, 1999). Curiously, this interaction appears to be a beneficial one for the Hsc70-mediated refolding of some clients *in vivo*. For instance, cells over-expressing CHIP are better able to restore the activity of luciferase after heat denaturation (Kampinga *et al.*, 2003). However, it is quite possible that the situation is more complex. For example, the degradation promoted

by CHIP might clear the chaperone machinery of terminally-misfolded substrates, permitting Hsc70 to handle denatured luciferase in a more beneficial way. Interestingly, CHIP can also polyubiquitinate Hsc70/Hsp90, leading to the proteasomal degradation of the targeted chaperone (Qian *et al.*, 2006) and of its bound client. Thus, direct ubiquitination of a client is not necessarily required to promote its degradation (Urushitani *et al.*, 2004; Jiang *et al.*, 2001). For a client such as RTA, which has few lysines, this is a potentially significant point of information.

Importantly, the quality of the chain which an E3 ligase makes is vital to the network of interactions the polyubiquitin attachment fosters in the cell (Kim *et al.*, 2007). The qualities in which an ubiquitin chain may vary include:

(1) The number of ubiquitin monomers attached.
(2) Whether or not these are in a contiguous chain.
(3) Which lysine (of the possible seven in ubiquitin) is used to propagate the chain.

Table 5.3 provides a summary of the various polyubiquitin linkages that exist and their ascribed functions in cells.

Table 5.3 - Ubiquitination and its various cellular roles.

The linkage types are listed in approximate order of abundance (as described in Li & Ye, 2009). The reported effects of mono-ubiquitination are described in the final row, but its position does not reflect its relative abundance.

Diminishing relative abundance.

Type	Processes involving this linkage type	References
Lys48 *(Most abundant.)*	• Promotion of proteasomal degradation • Transcriptional regulation (deactivation of Met4 in *S. cerevisiae*) • Stimulation of p97 "segregase" activity	Kim *et al.,* 2007 Li & Ye, 2008
Lys63	• Promotion of proteasomal degradation • Promotion of autophagy • Promotion of endocytosis • DNA repair • Transcriptional regulation & signal transduction	Kim *et al.,* 2007 Li & Ye, 2009 Hochstrasser, 2006
Lys11	• Promotion of proteasomal degradation	Kim *et al.,* 2007
Lys33	• Inhibition of AMPK-related kinase activity	Li & Ye, 2009
Lys27	• Remodelling of ubiquitination complexes	Hatakeyama *et al.*, 2001
Lys6	• Stabilisation of the BRCA1 complex (an E3 ligase) • Remodelling ubiquitination complexes	Li & Ye, 2009 Hatakeyama *et al.*, 2001
Lys29 *(Scarcest.)*	• Promotion of lysosomal degradation (of Notch signalling modulator, DTX) • Inhibition of AMPK-related kinase activity	Li & Ye, 2009
Mono	• Promotion of receptor internalisation • Vesicle sorting • DNA repair • Gene silencing	Sun & Chen, 2004

It has been shown that the ubiquitin linkages produced by CHIP in a minimal reconstitution *in vitro* are not exclusively those which lead to proteasomal recognition. Kim *et al.* (2007) observed that CHIP produces highly-branching polyubiquitin chains wherein each of the seven possible isopeptide linkages is present.[17] Substrates linked with these highly-branching chains are resistant to degradation by purified proteasomes (Kim *et al.*, 2007). Thus, to assay whether a substrate of interest (such as RTA, in this case) is targeted to the proteasome by this system, the quality of the polyubiquitination observed is also an important consideration.

At odds with these *in vitro* observations, the CHIP-dependent degradation of clients *in vivo* has been convincingly linked to multiple disease-states. In amyotrophic lateral sclerosis, ubiquitination of Hsc70 contributes to the degradation of SOD1 in motor neurons. This predisposes neurons to damage by oxidative stress (Urushitani *et al.*, 2004). Another example is cystic fibrosis, where CHIP is responsible for the premature degradation of aberrant, ER-localised $CFTR^{\Delta F508}$ (Albert *et al.*, 2004; Dickey *et al.*, 2007). CHIP has also been shown to contribute to the polyubiquitination of densely-tangled microtubule-associated Tau protein aggregates in moribund neurons. This ubiquitination is thought to be involved in the aetiology of Alzheimer's disease, and occurs via both Hsc70- (Shimura *et al.*, 2004) and Hsp90-dependent routes (Dickey *et al.*, 2007). Reports suggest that up-regulation of CHIP *in vivo* attenuates the formation of these Tau protein tangles, alleviating neurotoxicity by increasing their degradation (Sahara *et al.*, 2005; Shimura *et al.*, 2004).

This schism between the *in vitro* quality of CHIP ubiquitination and the *in vivo* role of CHIP in client degradation highlights how its E3 ligase activity will be subjected to complex layers of regulation in the cytosol. These layers of regulation have not been fully elucidated. However, Kim *et al.* (2009) recently showed that a soluble ubiquitin-binding protein of the yeast 26S proteasome complex, s5a/Rpn10, can temper the linkages made by CHIP *in vitro*. Regardless of the quality of the ubiquitination CHIP might bestow, if it could be shown to ubiquitinate RTA *in vitro*, it would nevertheless elaborate upon the diversity of fates a chaperone triage could impose upon RTA. Indeed, showing any ubiquitination at all would be an important observation as there were significant doubts that ubiquitination of RTA would be possible by any method *in vivo* or *in vitro*.

[17] The linkage types are predominantly Lys^{11}, Lys^{48} and Lys^{63}. All of these linkages, at least in homogeneous chain-types, have been implicated in the increased proteasomal degradation of substrates bearing them (reviewed in Kim *et al.*, 2007).

The reasons for these doubts were: first, RTA^{WT} has only two lysines upon which to anchor a polyubiquitin chain, which is a small number for a polypeptide of its length (Deeks *et al.*, 2002). Furthermore, Chapter 3 reported that the sensitising effect of radicicol did not vary greatly between holotoxins containing RTA^{WT} and RTA^{0K}, whereas it was disproportionately increased for RTA^{6K}. This indicated that the two endogenous lysines of RTA were not pliant candidates for a putative Hsp90-dependent inactivation, if they were at all. Finally, as a polypeptide which has evolved to possess relatively few lysines, it might be that RTA has experienced selective pressure that has promoted the acquisition of other adaptations to evade the proteasome. Precedents for such evasion exist, for example the transcription factor Met4, which possesses a novel ubiquitin-binding domain responsible for *cis*-regulating chain length (Flick *et al.*, 2006). Another example is the co-chaperone BAG-2, which escapes CHIP-mediated ubiquitination altogether by binding to Hsc70 in an orientation that prohibits it being target (Arndt *et al.*, 2005). It may be that RTA has a novel activity in this regard.

5.2.1 Ubiquitination of chaperone-bound clients by CHIP

Initially, the Hsc70-dependent activity of CHIP was studied rather than the Hsp90-dependent activity. Importantly, our expectations of Hsc70 differ from Hsp90, owing to the fact that Hsc70 apparently aids activation of cytosolic RTA *in vivo*, whereas Hsp90 hinders it. Because of this observation, it might be predicted that Hsc70 promotes less CHIP-mediated ubiquitination of RTA than Hsp90 does, or even none. However, as the co-chaperone make-up of the cytosol is complex and many co-factors are mutually antagonistic, the functionality of Hsc70 in a reduced system was unknown. Factors which would suppress (or else remove) this ubiquitination *in vivo* would presumably be absent. If Hsc70/CHIP could ubiquitinate RTA in this reduced system, it would therefore pose more interesting questions about the complexities of the co-chaperone environment *in vivo*.

Hsc70 and Hsp40 were purified as has previously been described. Ubiquitin was purchased commercially (Sigma-Aldrich). CHIP, E1 and E2 (UbcH5b) were kind gifts of Jörg Höhfeld (University of Bonn). So, too, were two example substrates: human microtubule-associated Tau protein and firefly luciferase. The latter two proteins were used to determine that the purified components of the ubiquitination cascade and the chaperones were functioning as expected after their purification.

5.2.1.1 Ubiquitination of a native client

One client of Hsc70/CHIP which does not have to be unfolded (via thermal denaturation or chaotropes) to become ubiquitinated is Tau protein (Petrucelli *et al*., 2005). Tau proteins are a family of polypeptides which bind to and stabilise microtubules. The folded, monomeric Tau polypeptide displays hydrophobic side chains to the solvent which would otherwise be hidden by binding to tubulin. These exposed hydrophobic side-chains interact with Hsc70 (Sarkar *et al.*, 2008). This permits ubiquitination if CHIP is also present (Petrucelli *et al.*, 2004). Indeed, these qualities of Tau make it analogous to a monomeric, cytosolic RTA, which also has an exposed hydrophobic patch that is masked for most of the protein's lifetime (by RTB).

Tau protein was incubated with Hsp40, Hsc70, ATP and components of the ubiquitin cascade for two hours at 30°C (Figure 5.1). In the immunostain for Hsc70, a ladder of oligo-ubiquitinated Hsc70 is observed only in the complete incubation, showing the requirement for each of the components added (E1, E2, CHIP and Hsp40/Hsc70). In this lane no ubiquitin-free Hsc70 is detectable at 70kDa, showing that all observable Hsc70 has been subjected to the modification. Similarly, ubiquitination of the client, Tau, is only observed in the final lane, where all components of the cascade and chaperone system are added. In this lane the intensity of the un-ubiquitinated Tau band also decreases, showing the ladder of slower-migrating material is derived from it.[18] Approximately 6 distinctly-ubiquitinated species can be observed. According to Thrower *et al.* (2000), 4 consecutive lys^{48}-linked ubiquitin monomers is the minimum chain length required for proteasomal degradation. Thus, at least the number of ubiquitin attachments observed here is sufficient for "canonical" proteasomal degradation.

This assay demonstrates that the purified components can efficiently label a substrate with polyubiquitin, under conditions like those described by Murata *et al*. (2001). Thus, these components remained functional after their purification. Furthermore, a protein with a solvent-exposed hydrophobic patch could be bound by Hsc70. This binding evidently enables convincing ubiquitination by CHIP without a prior denaturation step.

[18] Notably, the intensity of the un-ubiquitinated Tau band also drops in lanes without Hsc70/Hsp40. This may result from a loss of solubility where these chaperones are absent.

Figure 5.1 – Hsc70, Hsp40 and CHIP can target native clients for ubiquitination.

3µM Hsc70, 3µM Hsp40, 3µM CHIP, 0.1µM E1 and 0.4µM E2 (UbcH5b) were incubated in the indicated combinations with 0.3µM of Tau protein, 10mM DTT, 5mM ATP, 5mM $MgCl_2$, and 2 $mg.mL^{-1}$ ubiquitin in 20mM MOPS / 100mM KCl buffer, pH7.2. They were then incubated for 2 hours at 30°C before the addition of SDS-containing loading buffer ahead of SDS-PAGE. Samples were split into two equal volumes, electrophoresed on separate gels, blotted onto nitrocellulose and finally immunostained for Hsc70 and Tau protein respectively. Grey arrowhead indicates un-ubiquitinated Tau protein; Hsc70 is indicated by the black arrowhead.

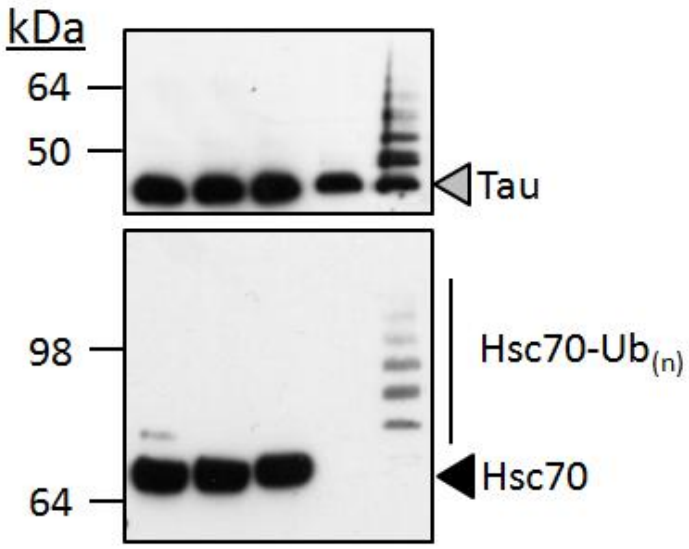

E1	-	+	+	+	+
E2	+	-	+	+	+
CHIP	+	+	-	+	+
Hsc70/Hsp40	+	+	+	-	+

5.2.1.2 Ubiquitination of a thermally-denatured client

The ability of CHIP to polyubiquitinate thermally-denatured clients of Hsc70 can also be examined. A client polypeptide in a conformationally-perturbed state is expected to resemble the state in which RTA is thought to emerge from the ER membrane. That is, it will display extended stretches of hydrophobic polypeptide to the cytosol, and so to the binding site of Hsc70 as well. In this case, firefly luciferase was used as the client (Figure 5.2). Luciferase was heated with or without both Hsc70 and Hsp40 (for 15 minutes at 45ºC). The components of the ubiquitination cascade were then added (in combinations as indicated) for a further 2 hours at 30°C. Under these conditions, there is a pronounced ubiquitin ladder for both luciferase and Hsc70 in reactions where all components of the cascade were provided. Curiously, polyubiquitination upon Hsc70 is not as extensive as it is for the substrate, implying the client is preferentially targeted in this instance. Hsc70 might also auto-regulate its ubiquitination.

The polyubiquitination of luciferase clusters predominantly at molecular weights between 250 and 148kDa. Loss of the un-ubiquitinated luciferase band in the final lane, where the reaction is complete, corroborates that this material is derived from it. The contiguous ladder bridging the two regions of the stain is also consistent with this interpretation. Under similar conditions, Kim *et al.* (2007) show that only one lysine of luciferase is targeted by CHIP, and that the polyubiquitin chain formed upon it is highly branching.[19] Therefore the two lysines of RTA may also be all that is needed for an extensive chain. Luciferase can also become ubiquitinated by CHIP in the absence of Hsc70/Hsp40 (*cf.* fourth lane, Figure 5.2). This happens to a small degree for particularly susceptible substrates, as CHIP itself has a slight affinity for misfolded clients (McClellan *et al*., 2005).

Darkly-stained species can be seen at high molecular weights on the immunostain for luciferase (Figure 5.2), even when the ubiquitination cascade is incomplete. These are therefore unlikely to be polyubiquitinated species, especially given their uneven distribution (Murata *et al.*, 2001). They may be multimers of luciferase. Some of these bands (between 148kDa and 98kDa), can be seen more faintly in preceding lanes where Hsc70/Hsp40 are present. It they are multimers, it seems that Hsc70/Hsp40 may prevent their formation.

[19] Resulting in a loss of electrophoretic mobility under SDS-PAGE that responds disproportionately to molecular weight; thus, the precise number of attached ubiquitin residues cannot be estimated.

Figure 5.2 – Hsc70, Hsp40 and CHIP targets denatured clients for ubiquitination.

0.3µM of luciferase was incubated with 3µM Hsc70 and 3µM Hsp40 in 20mM MOPS / 100mM KCl buffer, pH7.2 for 15 minutes at 45 °C. After this incubation, 3µM CHIP, 0.1µM E1, 0.4µM E2 (UbcH5b) and BAG-5 were added in the indicated combinations along with 10mM DTT, 5mM ATP, 5mM $MgCl_2$, and 2 $mg.mL^{-1}$ ubiquitin. A further 2 hour incubation at 30°C was then conducted. Samples were then analysed, as before, by immunostaining (for luciferase and BAG-5).

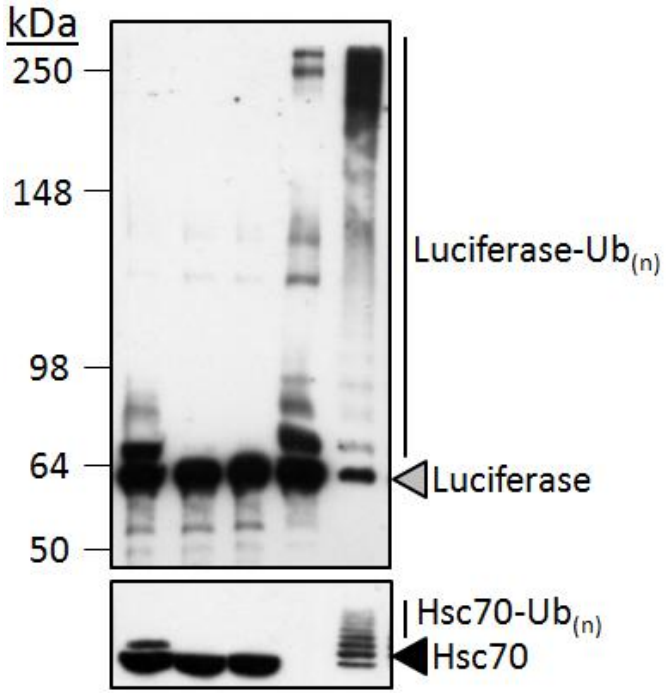

E1	-	+	+	+	+
E2	+	-	+	+	+
CHIP	+	+	-	+	+
Hsc70/Hsp40	+	+	+	-	+

The two substrates examined at this point are ubiquitinated in strikingly different ways. The denatured protein, luciferase, attracts far more ubiquitination than the native one, Tau. This supports the observations of Murata *et al.* (2001), who showed that thermally-denatured luciferase is ubiquitinated more efficiently than native luciferase. This is elicited by the higher affinity of Hsc70 to the solvent-exposed hydrophobic stretches of an unfolded substrate. Indeed, the selectivity of CHIP is thought to be governed by the binding of Hsc70. Thus, denatured clients are selected for ubiquitination, stochastically, by the recurrent binding of Hsc70 (McDonough & Patterson, 2003; Jiang *et al.*, 2001). However, luciferase and tau protein are not homologous and they were not assayed in parallel, so such interpretations should be made cautiously and are only made here in light of prior literature accounts.

By analogy, RTA is likely to be more vulnerable to ubiquitination when unfolded, such as during or directly after membrane transit. Expeditious refolding in the cytosol thereafter would help reduce the risk of degradation, so increasing toxicity. However, the C-terminus of the toxin subunit may promote interaction with Hsc70 even in the toxin subunit's native state (*cf.* Chapter 4 and Tau protein). Therefore, the risk of ubiquitination might never be eliminated entirely.

5.3 Can CHIP ubiquitinate Hsc70-bound RTA?

To clarify whether the above trends were consistent for RTA, the prior assays were repeated using the toxin subunit. Initially, RTA was incubated at 37°C for 2 hours with the Hsc70/Hsp40 chaperone complex and components of the ubiquitination cascade, in combinations as indicated (Figure 5.3a). The higher temperature (37°C rather than 30°C) was adopted to reflect the temperature at which intoxication of a mammalian cell would occur. This is especially important given that RTA has a threshold for unfolding near this temperature (*cf.* Chapter 4, Figure 4.2). In a parallel assay (Figure 5.3b), RTA was first denatured at 45°C for 15 minutes in the presence or absence of Hsc70, ATP and Hsp40. Components of the ubiquitination cascade were added afterward (in combinations as indicated) before subsequent incubation at 37°C for 2 hours.

In both assays, ubiquitination of Hsc70 was observed, which confirms that the ubiquitination cascade is functional at this elevated temperature, *in vitro*. Notably, in Figure 5.3b, a

ubiquitin-free species of Hsc70 cannot be observed.[20] The loss of this band vouches for the extensive ubiquitination of Hsc70 in this particular assay. Contrastingly, no ubiquitin ladder can be observed on immunostains for RTA – irrespective of whether a denaturation step was imposed. Furthermore, the unmodified RTA band does not alter in intensity visibly, implying little or none had been converted into higher molecular-weight species.[21] Under careful examination, the ladder of ubiquitination upon Hsc70 also appears remarkably shortened compared to previous assays.

We expect that Hsc70 interacts with RTA at both 45°C and 37°C. At 37°C because of its hydrophobic patch. It would also be expected to interact strongly at 45°C because of denaturation. Thus, it seems that RTA is not efficiently ubiquitinated by CHIP despite Hsc70 being able to bind it. This would be congruent with the protective effect of the Hsc70 inhibitor, DSG. According to that observation, the normal function of Hsc70 is to aid the toxicity of RTA *in vivo*. Therefore, Hsc70 would not be expected to mediate efficient lysine-ubiquitination of RTA, which would presumably expedite degradation.

[20] Please notice that the fastest-migrating Hsc70 band in the final lane is slightly raised compared to those in preceding lanes.

[21] Importantly, the RTA antibody was polyclonal in nature. This meaning it is relatively unlikely that a crucial immuno-reactive epitope was masked by the ubiquitination process, which might otherwise obscure the staining of a ubiquitin ladder.

Figure 5.3 – RTA as a substrate of the Hsc70 / CHIP complex

3µM Hsc70, 0.3µM Hsp40, 3µM CHIP, 0.1µM E1 and 0.4µM E2 (Ubc5hb) were incubated in the indicated combinations with 0.3µM RTA, 10mM DTT, 5mM ATP, 5mM $MgCl_2$, and 2 $mg.mL^{-1}$ ubiquitin in 20mM MOPS / 100mM KCl buffer, pH7.2. They were then incubated for 2 hours before the addition of SDS-containing loading buffer ahead of SDS-PAGE. Samples were split into two equal volumes, electrophoresed on separate gels, blotted onto nitrocellulose and finally immunostained for Hsc70 and RTA. a) Shows immunostains from experiments conducted at 37°C. b) Shows immunostains from an assay where RTA was first heated to 45°C for 15 minutes with 3µM Hsc70, 5mM ATP and 3µM of Hsp40. After this incubation, the remaining components were added (as before) and incubated for 2 hours at the normal temperature of 37°C.

a. RTA^{WT}

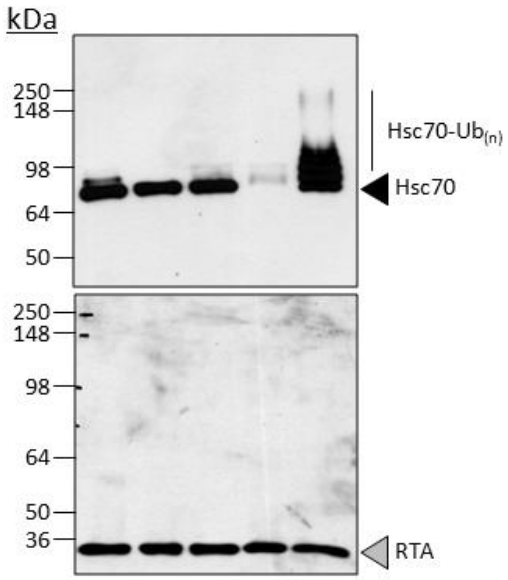

E1	-	+	+	+	+
E2 (UbcH5b)	+	-	+	+	+
E3 (CHIP)	+	+	-	+	+
Hsc70/Hsp40	+	+	+	-	+

b. RTA^{WT} denatured at 45°C

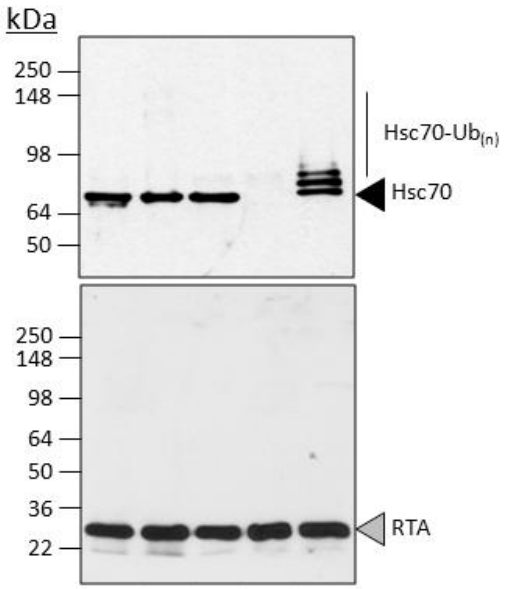

E1	-	+	+	+	+
E2 (UbcH5b)	+	-	+	+	+
E3 (CHIP)	+	+	-	+	+
Hsc70/Hsp40	+	+	+	-	+

5.3.1 Does altered lysine content alter the candidacy of RTA as substrate of CHIP?

To clarify whether the lack of ubiquitination resulted from RTA's dearth of lysines (Deeks *et al.*, 2002), or some other feature of the polypeptide, the lysine variants used in Chapter 3 were re-enlisted: RTA^{0K} and RTA^{6K}. These were incubated, parallel with RTA^{WT}, at 45°C with Hsc70/Hsp40 for 15 minutes. The components of the ubiquitination cascade were then added and the incubation extended for another 2 hours at 37°C. The results from this assay can be seen below (Figure 5.4).

Where all the components of the cascade were included, Hsc70 was observably polyubiquitinated and the intensity of the unmodified band was correspondingly reduced. This was true in the context of each RTA variant. In contrast, in no case was any RTA variant detectably ubiquitinated. It was expected that at least RTA^{6K} would be ubiquitinated because of its increased lysine content. From these results, it would seem that RTA escapes ubiquitination whilst bound to Hsc70 by a method that is independent of lysine content.[22]

If such a method for evading ubiquitination does exist, it would be unexpected that this quality persists even when the secondary structure of RTA is disrupted by a 45°C thermal treatment. It is possible that Hsc70 has a higher affinity for a portion of the polypeptide which orientates the lysines of RTA away from CHIP. Figure 5.5a shows the relative positioning of the two native lysine residues with respect to one another in the primary polypeptide sequence. They occupy opposite ends of the polypeptide. This distance is mirrored in the fully-folded 3D structure, where they occupy diametrically opposed positions (Figure 5.5b). Therefore, both are unlikely to be masked from CHIP by the binding of a single Hsc70.

Again, it is noticeable that the range of the polyubiquitinated Hsc70 ladder is reduced compared to what is the case in the context of the test substrates in the prior sections. If this ubiquitination is used as a measure of reaction efficiency (Höhfeld J., personal communication), it seems that the reaction is not functioning as well in these assays. This may contribute to why no ubiquitinated RTA is observed.

[22] This is certainly in contrast to what is expected of the toxin subunit's interaction with Hsp90, given the lysine-dependent sensitising effect Hsp90 inhibition has (*cf.* Chapter 3, Figure 3.18*)*.

Figure 5.4 – The effect of lysine content upon ubiquitination of RTA by the Hsc70 / CHIP complex

RTA variants were heated to 45°C for 15 minutes before addition of the rest of the ubiquitination apparatus (to the same concentrations as used before). From some reactions E1 was omitted and from others, Hsc70 and Hsp40 were omitted. Three different RTA variants were compared: RTA^{0K}, RTA^{WT} and RTA^{6K}. Samples were then incubated for 2 hours at 37°C. Afterward, each was split into two equal volumes, electrophoresed on separate gels, blotted onto nitrocellulose and finally immunostained for Hsc70 and RTA.

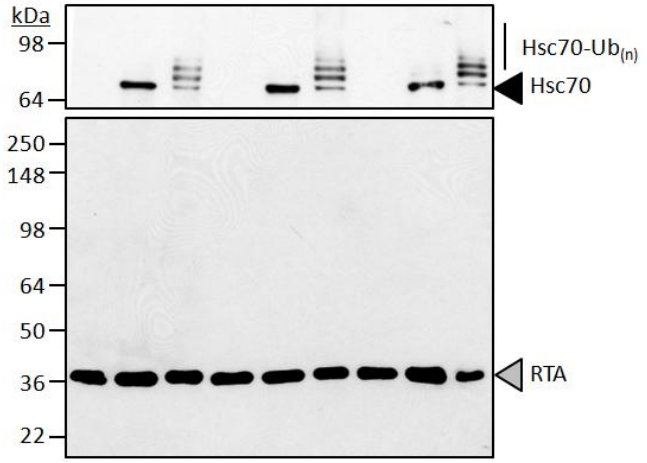

E1	-	-	+	-	-	+	-	-	+
E2, E3, Hsp40/Hsc70	-	+	+	-	+	+	-	+	+
RTA^{0K}	+	+	+	-	-	-	-	-	-
RTA^{WT}	-	-	-	+	+	+	-	-	-
RTA^{6K}	-	-	-	-	-	-	+	+	+

Figure 5.5 - Sequence of Ricin A Chain highlighting the relative positions of the native lysines

The accession number of the sequence used (Pubmed) is AAA72820. a) The primary sequence of RTA. Lysine residues are highlighted in yellow. The ordinal position of the first amino acid in each line of the printed sequence (relative to its situation in the entire polypeptide) is indicated by the number on the left-hand side. b) A ribbon diagram of RTA showing the opposite distribution of the native lysines in three dimensional structure of the polypeptide. Generated using Chimera (University of California). The structure is rainbow-coloured so that the C-terminus is red and the N-terminus is blue, with relative position along the polypeptide indicated by changes in colour. Lysine residues are ringed in red; their position in the polypeptide backbone is indicated by black shading; a written label indicates their ordinal position within the polypeptide.

a. Primary sequence

```
1       mifpkqypii nfttagatvq sytnfiravr grlttgadvr heipvlpnrv glpinqrfil
61      velsnhaels vtlaldvtna yvvgyragns ayffhpdnqe daeaithlft dvqnrytfaf
121     ggnydrleql agnlreniel gngpleeais alyyystggt qlptlarsfi iciqmiseaa
181     rfqyiegemr trirynrrsa pdpsvitlen swgrlstaiq esnqgafasp iqlqrrngsk
241     fsvydvsili piialmvyrc apppssqf
```

b. 3D structure

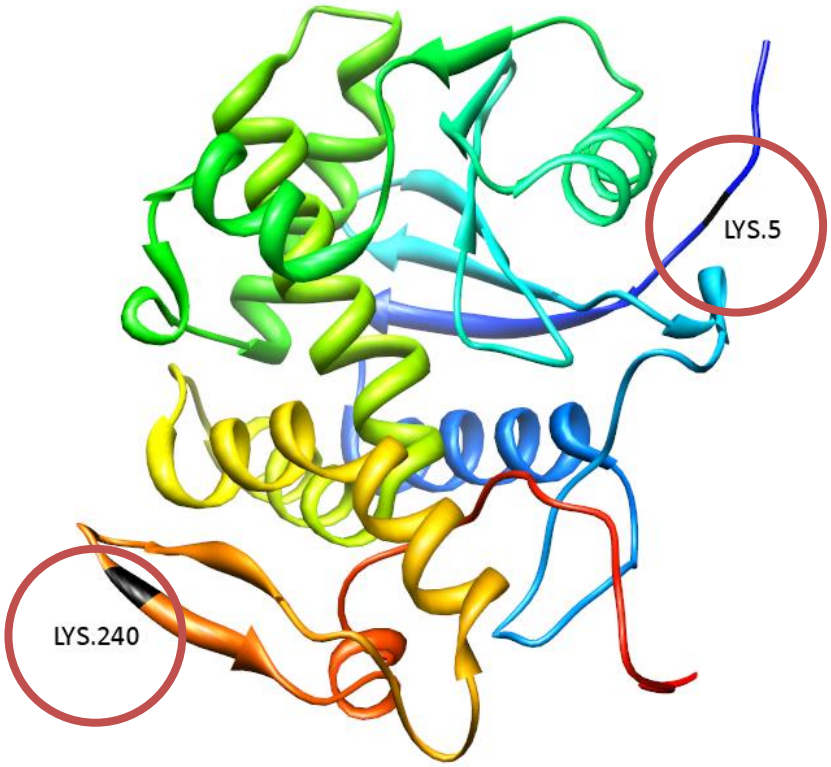

Contrastingly, when colleagues performed similar experiments to those above, slight ubiquitination of RTA^{WT} was demonstrated (Spooner *et al.*, 2008). However, this was only noticeable after very prolonged film exposures. For ease of reference, this figure has been reprinted below (Figure 5.6a). Nevertheless, the ratio of ubiquitinated to un-ubiquitinated RTA recorded by this immunostain remains very slight (note the concentration of RTA in these experiments was also relatively increased: 0.8μM rather than 0.3μM). Indeed, the intensity of the unmodified RTA band is approximately equivalent in all lanes. This contrasts to the positive controls enlisted earlier: Hsc70, microtubule associated Tau and firefly luciferase (*cf.* Figure 5.1 & Figure 5.2).

Encouragingly, Spooner *et al.* (2008) also showed, using similarly extended film exposures, that the degree to which RTA^{6K} was ubiquitinated under these conditions was increased relative to RTA^{WT} (Figure 5.6b). However, the relative proportion of the ubiquitinated population still seemed small. The range of the polyubiquitin ladder observed upon RTA^{6K} is also not as extensive as for the test substrates, with chains of only up to three ubiquitins being visible. This value is thought to be insufficient for efficient proteasomal degradation, even if they are linked in a way which is canonically associated with efficient proteasomal degradation (Thrower *et al.*, 2000). Taken together, these data are not so contrasting to the other data presented in this thesis. They, too, imply that the toxin subunit is not an ideal candidate for ubiquitination by the Hsc70/CHIP complex. Furthermore, the additional lysines of RTA^{6K} seem insufficient to render RTA as pliant a substrate of Hsc70/CHIP as denatured luciferase or native Tau protein evidently are (*cf.* Figures 5.6c).

The low level of ubiquitination observed in all assays may invite another explanation: perhaps RTA has an unpredicted, explicitly inhibitory effect upon the ubiquitin reaction in excess of its few lysines? A repeat of these assays with parallel controls where RTA is absent would have been useful in clarifying this point. However, resources were very limiting.

Figure 5.6 – Hsc70/CHIP-mediated ubiquitination of RTA^{WT} and RTA^{6K}

N.B. Assays a) and b) in this figure were performed by Robert Spooner (University of Warwick)

a) 0.8µM RTA was incubated, "complete", with Hsp40, Hsc70, E1, E2 and CHIP for 15 minutes at 45°C (at concentrations as used before at this temperature in this thesis). Parallel incubations lacked E1, E2, CHIP or Hsp40/Hsc70 (as indicated). The ubiquitination cascade was then activated with the addition of ATP and the reducing agent required to initiate the cascade, DTT. Reactions were then incubated for a further 2 hours at 37°C. b) Shows similar experiments (with a simplified set of controls), comparing the ubiquitination of RTA^{6K} ("6K") to RTA^{WT} ("2K") in parallel experiments. In both a) & b), reactions were split into equal volumes, analysed by SDS-PAGE and stained separately for the proteins indicated. c) Equivalent "complete" lanes from Figure 5.1 and 5.2.

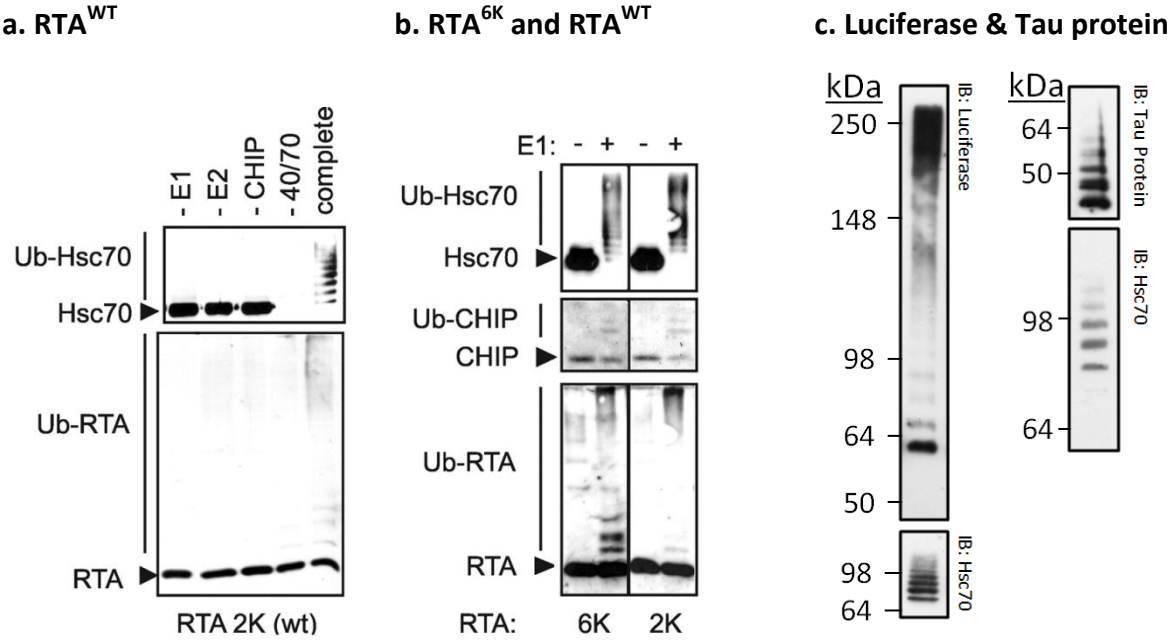

5.3.2 Pre-treatment with POPS liposomes promotes the ubiquitination of RTA

During the retrotranslocation process from the ER into the cytosol, RTA is thought to be denatured by the phospholipid membrane (Mayerhofer *et al*., 2009). It is feasible that specific features of this denaturation persist until it egresses into the cytosol and refolds. The ways in which thermal denaturation and the way in which RTA might unfold *in vivo* are certainly qualitatively different, leading to possible differences in the network of interactions subsequently made in the cell. One of these differences could be the nature of RTA's interaction with Hsc70 and CHIP. Liposome-bound RTA might simply be oriented in a more (or less) vulnerable way, altering the efficacy of CHIP-mediated ubiquitination.

To test whether treatment of RTA with liposomes had an effect upon the propensity of the toxin subunit to become ubiquitinated, RTA was incubated with both Hsc70/Hsp40 and with (or without) liposomes made of POPS for 15 minutes at 37°C. Subsequent to this, components of the ubiquitination cascade were added and the incubation was extended for another 2 hours at 37°C.

Figure 5.7a shows that Hsc70 is ubiquitinated to an equivalent extent in the presence and absence of POPS liposomes. This indicates that the liposomes have no inhibitory effect upon the efficiency of the ubiquitination cascade itself. Figure 5.7b, on the other hand, shows that RTA is more heavily ubiquitinated when it has first been incubated with liposomes. In the first exposure, an obvious reduction in the non-ubiquitinated RTA band can be seen in the final lane (where the ubiquitination cascade is complete and liposome-treatment has been provided). Ubiquitination of RTA in the parallel assay, free of liposomes, also occurs (note a faint band directly above the non-ubiquitinated RTA band in exposures 1 & 2; if this is too faint to observe in print, please see the digital copy of this thesis). This also informs us that RTA can be ubiquitinated without prior denaturation at the physiological temperature of 37°C. However, it is still not to an extent which would be canonically associated with proteasomal recognition (Thrower *et al*., 2001).

These observations may seem counter-intuitive: how would becoming embedded in the membrane increase the chances of RTA becoming ubiquitinated? The presence of the liposome membrane might hinder the interaction of RTA with Hsc70, sterically blocking sites the chaperone could bind to, so reducing the exposure of the polypeptide to CHIP. In answer: first, the secondary structure of RTA will be disrupted by the interaction (Day *et al*., 2002). This would putative increase the number of exposed hydrophobic regions to which

Hsc70 could bind. Second, circular dichroism and fluorescence data suggests that the interaction of RTA with liposomes occurs in a predictable, reproducible way, with certain residues of the C-terminal tail directing the hydrophobic interactions which occur (Mayerhofer *et al*., 2009; unpublished data of Cook J.C., University of Warwick). It may be that this directs Hsc70 to interact with RTA in a limited, reproducible array of orientations which happen to predispose the interaction to an outcome resulting in ubiquitination. Conversely, native RTA would have just one, dominant site for Hsc70-binding: the hydrophobic C-terminal tail (*cf.* Chapter 4), which might restrict ubiquitination. Incubation with liposomes may hide this domain from Hsc70, by embedding it in the hydrophobic core (Mayerhofer *et al*., 2009). This might permit Hsc70 to bind the toxin subunit in an ubiquitination-permissive orientation.

It is interesting to speculate that a low level of ubiquitination could help mediate extraction of the toxin subunit from the ER membrane rather than degradation, but evidence would indicate otherwise given that lysine-dependent ubiquitination is not required for this step in plant and yeast cells (Di Cola *et al*., 2005; Li *et al*., 2010). Moreover, RTA^{0K} is marginally more toxic than RTA^{WT} in mammals (*cf.* Figure 3.17 and Deeks *et al*., 2002).

To extend this finding, it would be interesting to determine whether neutrally-charged liposomes have the same effect upon the ubiquitination process. This would help to clarify whether the effects observed here result from the known effects of negatively-charged POPS upon RTA (Mayerhofer *et al*., 2009; Day *et al*., 2002), or some other effect of the phosopholipid.

Figure 5.7 – The effect of negatively charged POPS liposomes upon the susceptibility of RTA to CHIP-mediated ubiquitination.

0.3µM of RTA was incubated with 3µM Hsc70 and 0.3µM Hsp40 in 20mM MOPS / 100mM KCl buffer, pH7.2 for 15 minutes at 37°C with or without a concentration of 7.5µM POPS liposomes. After this incubation, 3µM CHIP, 0.4µM E2 (UbcH5b) and BAG-5 were added along with 10mM DTT, 5mM ATP, 5mM $MgCl_2$, and 2 $mg.mL^{-1}$ ubiquitin. Lanes contained 0.1µM E1 to complete the ubiquitination cascade where indicated. These mixtures were then incubated for 2 hours at 30°C before the addition of SDS-containing loading buffer. Samples were split into two equal volumes, electrophoresed on separate gels, blotted onto nitrocellulose and finally immunostained for a) Hsc70, (Hsc70 is indicated by the black arrowhead.) and b) RTA. Grey arrowheads indicate un-ubiquitinated RTA. ①, ② and ③ are separate exposures of the same blot (at consecutively increasing times after adding the developer solution).

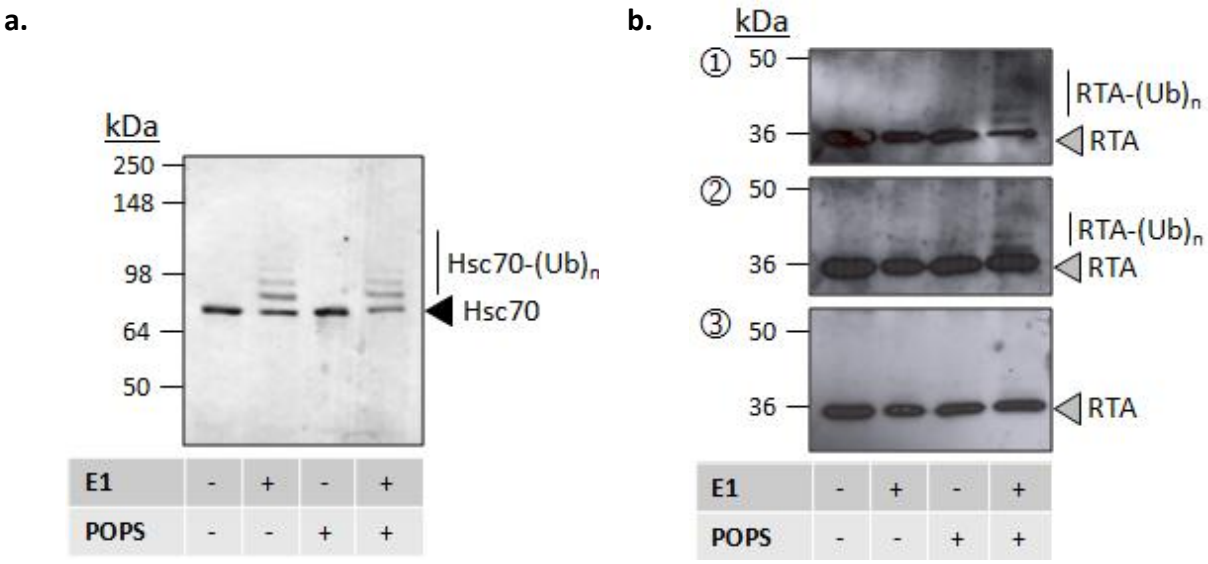

5.4 Hsp90-dependent ubiquitination of RTA

In vivo and *in vitro*, Hsc70 can be held in proximity to Hsp90 by a TPR-bearing co-factor called HOP. HOP preferentially binds to ADP-bound Hsp90 in the cytosol (Johnson *et al*., 1998). This association stalls the chaperone in its ADP-bound state, when it is most receptive to client binding (Johnson *et al*., 1998). Furthermore, in this Hsp90-bound form, HOP acquires a greater affinity for client-bound Hsc70, causing the formation of a ternary complex containing Hsp90, HOP, Hsc70 and client (Hernández *et al.*, 2002). In this complex, HOP stimulates Hsc70 to undergo nucleotide exchange, permitting release of bound clients (Gross & Hessefort, 1996). This concerted, sequential mode of action means HOP directs clients from binding Hsc70 to Hsp90, as has been shown to be the case in the conformational maturation of steroid hormone receptors, various kinases (Murphy *et al.*, 2003) and in the optimal refolding pathway of substrates like firefly luciferase (Johnson *et al.*, 1998). A sequential triage of RTA like this is thought to occur *in vivo* because Hsc70 inhibition dominates the sensitisation caused by Hsp90 inhibition *in vivo* when cells are intoxicated with ricin (*cf.* Figure 3.12).

In results that are published in Spooner *et al.* (2008) a sequential triage was recreated *in vitro* (using purified Hsp40, Hsc70, HOP and Hsp90). When all of these components were provided, along with CHIP, an increase in the ubiquitination of RTA was observed relative to incubations excluding Hsp90 or Hsc70 (Figure 5.8). Consistent with the concept of a sequential triage, these results also show that Hsp90 cannot ubiquitinate RTA without Hsc70 in the reconstitution. It appears that co-operation of Hsc70 and Hsp90 allots more RTA to the proteasome than either would independently. In the incubation where Hsc70, HOP and Hsp90 are present, CHIP is given two opportunities to act upon RTA.

Curiously, Spooner *et al.* (2008) also showed that, in isolation from Hsc70, Hsp90 has an apparent solubilising effect upon RTA at 45°C, but none at all at 37°C. This contrasts to Hsc70, which has an effect in this experimental system at both temperatures. Therefore, unlike Hsc70, Hsp90 might be able to bind to a substantially-unfolded state of RTA, but not to the native protein. Thus, if RTA can quickly fold in the cytosol to a state that is no longer recognised by Hsp90, it may also no longer endure the threat of polyubiquitination by Hsp90-dependent CHIP. This helps contribute to the case for Hsc70 being called an "escape-hatch" from a cytosolic chaperone triage.

Figure 5.8 – Increased CHIP-mediated ubiquitination of RTA^{WT} in the presence of Hsc70 and Hsp90, as published by Spooner *et al.* (2008).

N.B. The experiment in this figure was performed by Robert Spooner (University of Warwick)

RTA was incubated with combinations of CHIP/Hsc70/Hsp40/E1/E2 as in the previous figure. Where indicated, HOP and Hsp90 were also added. Samples were subjected to SDS-PAGE and blotting, as before, and were immunostained for RTA and HOP. Hsc70 and Hsp90 were visualised by silver-staining. The asterisk indicates a cross-reacting band on the RTA immunostain.

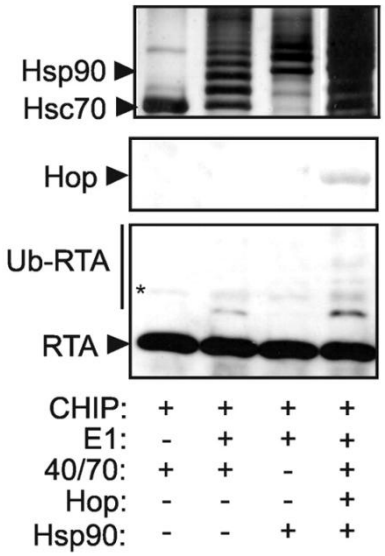

5.5 Incubation in a cytosolic extract does not lead to observable polyubiquitination of RTA

If RTA could be ubiquitinated *in vitro* by Hsp90/Hsc70, it might also be ubiquitinated in a more complex scenario where components of the ubiquitination cascade have been provided by a cytosolic extract. As such, RTA was incubated at 45°C for 15 minutes with Hsc70 and Hsp40 (concentrations as before). This would denature the toxin subunit, but keep it soluble. Subsequent to this, cytosolic extract was added (produced as before, as in Chapter 4), which would supply a co-chaperone environment analogous to what would be present during the intoxication process *in vivo*. Controls where the proteasome inhibitor, ALLN, was included were also produced in case any ubiquitinated RTA was degraded. Samples were then incubated at 37°C for the time indicated. These reactions were separated by SDS-PAGE, blotted onto nitrocellulose and immunostained for RTA (Figure 5.9a).

No ubiquitinated band can be observed in any of the incubations with cytosol. The intensity of a cross-reacting smear from the RTA preparation decreases especially in the presence of cytosol (and less so when cytosol and ALLN are incubated together). It is also noticeable that the intensity of the unmodified RTA band decreases over time in incubations with cytosol, and that this appears to be rescued by the inclusion of ALLN. The ratio of signal intensity from RTA in lanes containing cytosol and ALLN to lanes containing cytosol alone was plotted against time (Figure 5.9b), giving an indication of the level of this degradation over time. This effect presumably results from inhibition of the proteasome, or else cathepsins and calpains of the cytosolic extract, which ALLN also affects (Sasaki *et al*., 1990).

Unfortunately, it is not obvious whether this degradation is ubiquitin-dependent. The lack of observably ubiquitinated bands in lanes containing ALLN would imply that it is not. However, in lanes where ALLN is present, it is possible that DUBs might subsequently remove any ubiquitination, given degradation of the substrate has been retarded. To clarify this issue, ubiquitin-aldehyde might be employed in future experiments. This modified ubiquitin would stabilise putative ubiquitin-conjugates from the hydrolytic action of DUBs (Hershko & Rose, 1987).

Figure 5.9 - The effect of cytosol on RTA

a) RTA was denatured at 45°C for 15 minutes with Hsc70 and Hsp40, as before for ubiquitination experiments, with 5mM ATP. Reactions were then incubated at 37°C with or without 10% ($v_{\%}$/v) cytosol and 100nM ALLN for the indicated length of time. At the timepoint indicated, samples were placed on ice and mixed with SDS-PAGE loading buffer. Samples were then electrophoresed and immunostained via the Odyssey system for RTA (grey arrowhead). †Shows lower molecular weight species than RTA which are putatively degradation products of the protein during storage. ‡ Marks species of higher molecular weight from the RTA preparation which may be cross-reacting impurities. b) Shows quantification of the putative degradation – it plots the ratio of signal intensity from RTA in lanes containing cytosol and ALLN to lanes containing cytosol alone over time.

a. Immunostain

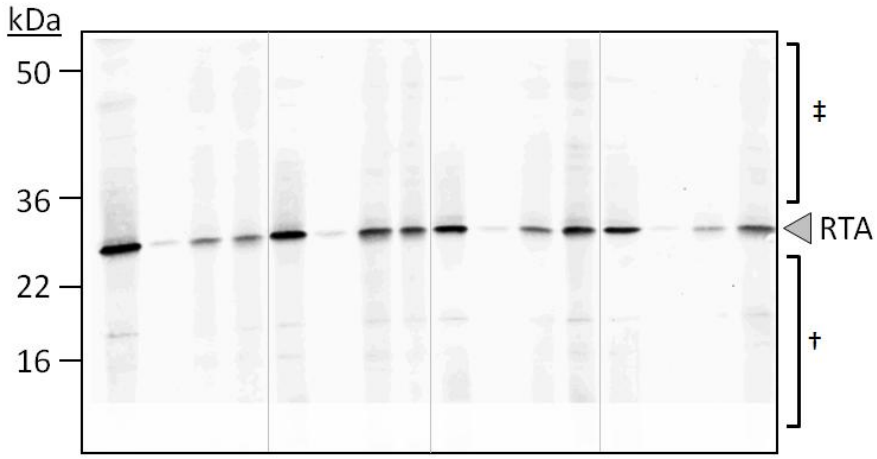

RTA	+	-	+	+	+	-	+	+	+	-	+	+	+	-	+	+
ALLN	-	-	-	+	-	-	-	+	-	-	-	+	-	-	-	+
Cytosol	-	+	+	+	-	+	+	+	-	+	+	+	-	+	+	+
Time (min)	15				30				60				120			

b. Relative degradation of RTA in the cytosol preparation. N=1.

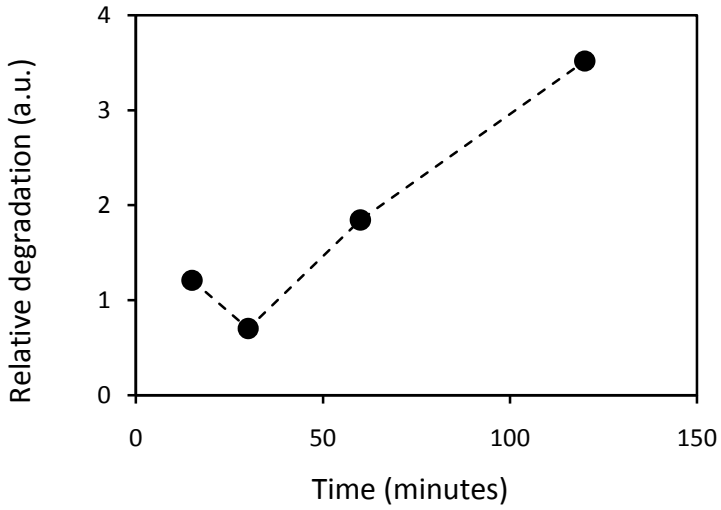

5.6 Polyubiquitination by CHIP is antagonised by other cytosolic co-chaperones

Polyubiquitination of Hsc70 and Hsp90 clients by CHIP is affected by the concentration of other co-chaperones in the cytosol. For Hsc70, these include co-factors like HspBP1 and BAG-2. These co-factors bind to Hsc70 alongside CHIP, non-competitively masking the client protein from ubiquitination (Arndt *et al.*, 2005; Alberti *et al*., 2003 & 2005). BAG-1 and HspBP1 also promote Hsc70 nucleotide exchange, shifting the chaperone into an open conformation that allows a client to dissociate if it is able to refold (Arndt *et al.*, 2005; Alberti *et al.*, 2004).

To test whether a co-chaperone could influence the polyubiquitination of RTA *in vitro*, Jörg Höhfeld kindly provided a preparation BAG-5. This co-chaperone has four repeats of the BAG domain, which is the definitive motif of the eponymous family of proteins (schematically compared in Figure 5.10). Other BAG-domain proteins stimulate Hsc70 nucleotide exchange (Alberti *et al.*, 2001) and act as bridging factors from Hsc70 to other proteins (Takayama and Reed, 2001). Thus, BAG-5 is anticipated to have similar functionality. Like BAG-2, BAG-5 might also inhibit CHIP from ubiquitinating chaperone-bound clients (Arndt *et al.*, 2005).

It is thought that the unusual multiplicity of BAG-5's Hsc70 interacting domains helps assemble a "work-bench" of chaperones and co-factors with a tailored stoichiometry (Jörg Höhfeld, personal communication). If each BAG domain interacts separately with an instance of Hsc70, this would increase the local concentration of Hsc70 and might result in a more processive series of interactions with a given client. This might ensure substrates do not escape triage prematurely. Alternatively, the multiplicity of the BAG-domains might ensure the co-factor, itself, has a more processive series of interactions with Hsc70, more strongly promoting the release of clients. In one of the only studies published at the time of writing, Kalia *et al.* (2004) showed that BAG-5 inhibits Hsc70 from aiding client refolding. They also showed that BAG-5 inhibited another of Hsc70's dependent E3 ligases, Parkin. They hypothesise that this might contribute to the accumulation of cytotoxic aggregates in neuronal models of Parkinson's Disease.

Figure 5.10 - A comparison of the domain architecture of human BAG domain proteins.

Shown below are the relative domain organisations of BAG-family proteins. The BAG-domain, which interacts with Hsc70, is usually at the C-terminus of the protein. However, in BAG-5, these are spread throughout the protein. Other domains are also highlighted, e.g. ubiquitin-like (UBL) domains, nuclear localization signal (NLS), the WW domain, TXSEEX repeat and PXXP motifs.

N.B. This figure is from Takayama & Reed, 2001.

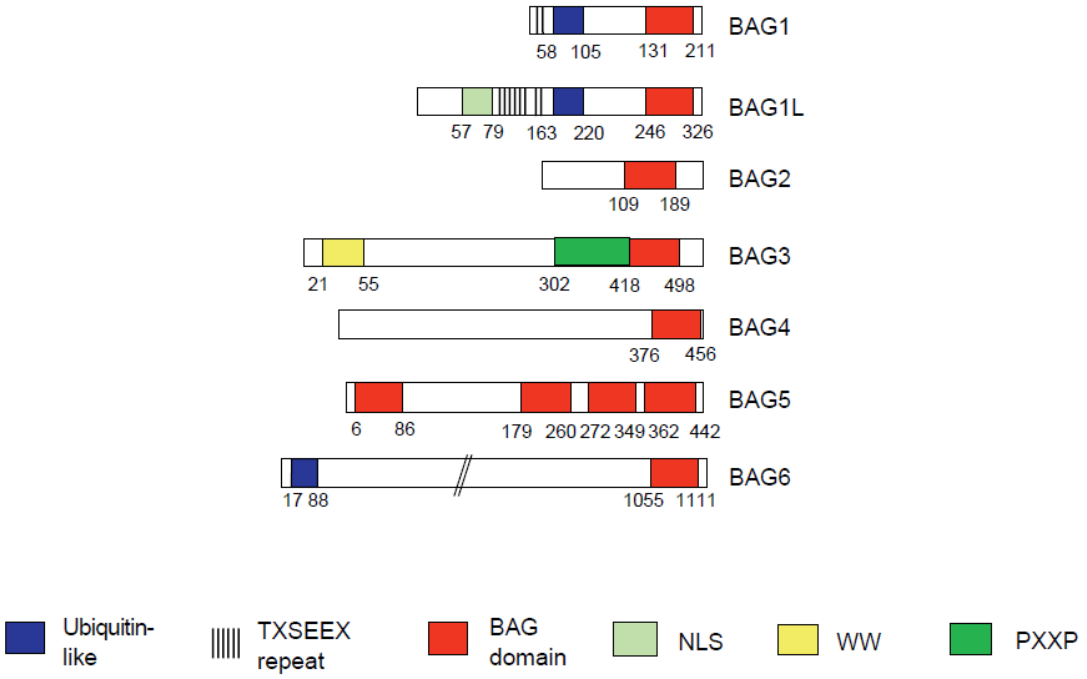

With the above data in mind, the effect of BAG-5 upon the CHIP/Hsc70-mediated ubiquitination of two previously introduced substrates – Tau protein and luciferase – was investigated. In both cases (Figure 5.11), the ubiquitination of Tau protein and luciferase is decreased when the BAG-5 concentration is increased.

Curiously, the mono-ubiquitinated Tau band comprises two distinct species which did not separate by 8.6kDa (the molecular weight of ubiquitin). It is possible that they represent mono-ubiquitination at two disparate sites upon the protein, which result in disproportionate changes in electrophoretic mobility. However, these distinct species might alternatively owe to heterogeneity in the original Tau protein preparation.

It was important to clarify that the apparent inhibition of ubiquitination was not by competition of BAG-5 with Tau protein or luciferase as substrate of CHIP/Hsc70. This is shown by Figure 5.11, as BAG-5 is not ubiquitinated like a client of Hsc70 is. This is much as is reported for the related co-chaperone, BAG-2 (Arndt *et al.*, 2005) which binds to Hsc70 independently of the client peptide-binding domain of the chaperone (Takayama *et al.*, 1997). This provides evidence that the inhibitory effect of BAG-5 is a specific effect of the co-factor, and gives another example of a protein that can evade ubiquitination by mechanisms other than a dearth of lysines.

Hsc70 is ubiquitinated in all reactions shown in Figure 5.11. However, the extent to which this ubiquitination responds to the concentration of BAG-5 is not as dramatic as it is for the substrate. The simplest explanation would be that BAG-5 does not effectively mask the regions which CHIP targets upon Hsc70.

Figure 5.11 - BAG-5 inhibits the Hsc70/CHIP-mediated ubiquitination of clients

a) Tau protein was incubated, as before, at 30°C for 2 hours with Hsc70, Hsp40, the components of the ubiquitination cascade and the indicated concentration of BAG-5 protein. b) Luciferase was pre-incubated at 45°C with Hsc70 and Hsp40 before the incubation with the components of the ubiquitination cascade. Then these components were added and the rest of the protocol was as before. In each case, the incubation mixtures were split into three equal volumes and immunostained for BAG-5, the substrate in question, and Hsc70. Asterisks mark a band which may be mono-ubiquitination of BAG-5, but is thought to be a cross-reacting species in the BAG-5 preparation.

a. Tau protein

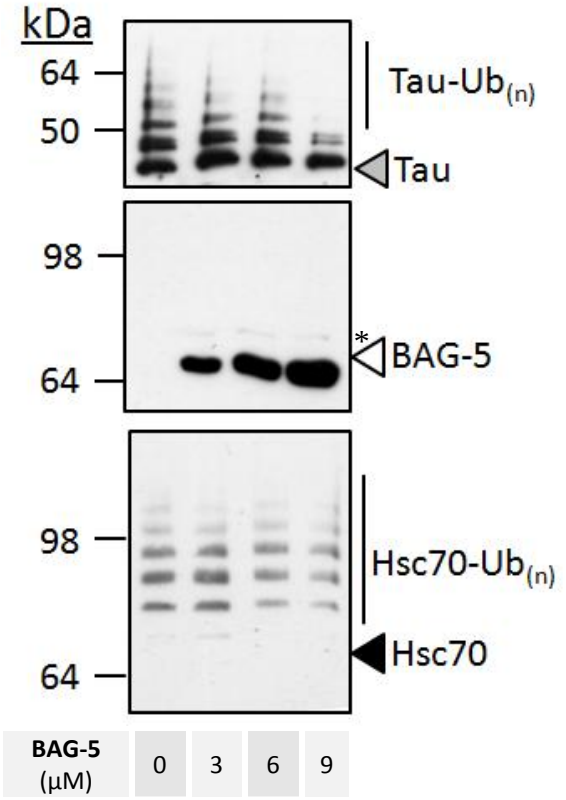

b. Luciferase

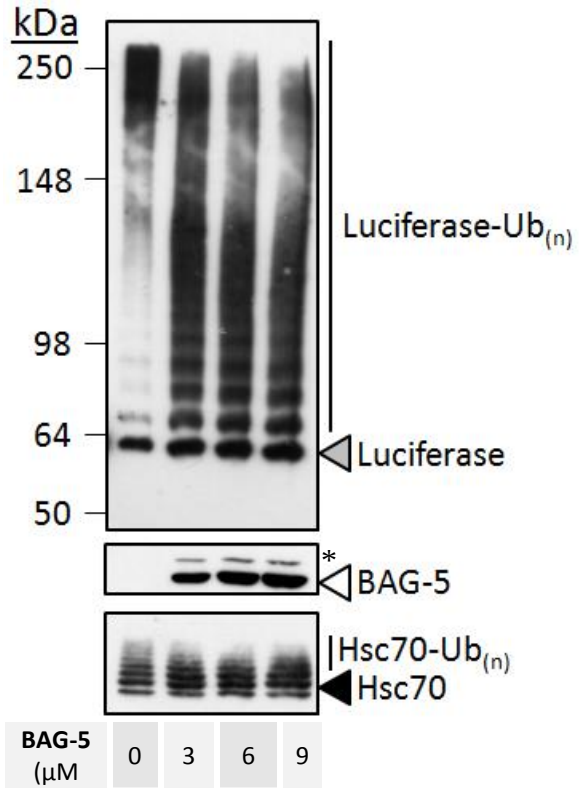

5.7 Effect of BAG-5 upon the Hsc70/CHIP-mediated ubiquitination of RTA

RTA has already been shown to be a weak candidate for the Hsc70/CHIP complex (*cf.* Figure 5.3 and Spooner *et al.*, 2008). It was hypothesised that co-chaperones of the cytosol might further reduce ubiquitination by CHIP. As such, similar experiments to those above were repeated with RTA. A Ponceau S stain of nitrocellulose blots made of this experiment is presented in Figure 5.12, alongside an immunostain for Hsc70.

If the Ponceau S stain is examined first (Figure 5.12a), an extensive protein ladder can be observed in incubations where all the usual components of the cascade have been provided (E1, E2, CHIP, Hsc70 & Hsp40). The formation of this ladder is coincident with the reduction in intensity of lower molecular weight bands which are present in prior lanes, showing the ladder is derived from these species (e.g. CHIP, Hsc70) rather than from contaminants. When BAG-5 is introduced into the complete incubation, the general intensity and range of the protein ladder diminishes as the concentration of BAG-5 increases. The titrated dose of BAG-5 is shown by a band corresponding to a molecular weight of 51kDa (Kalia *et al.*, 2004), which is marked with a white arrowhead.

The reduction of the putative ubiquitination ladder by the addition of BAG-5 is accompanied by the congruent increase of non-ubiquitinated progenitor bands, such as Hsc70 (black arrowhead) and CHIP (stripy arrowhead). Interestingly, CHIP appears to be ubiquitinated even in controls where Hsc70 and Hsp40 are absent (note a reduction in the intensity of this band where the upstream components of the cascade have been provided). This shows it can interact with the E2 conjugating enzyme in the absence of Hsc70. However, its ligating ability remains largely localised to itself in these instances (much as in Murata *et al.*, 2001; *cf.* Figure 5.2 as well).

In Figure 5.12b, a very striking, dose-dependent inhibition of Hsc70 ubiquitination by BAG-5 can be observed (note that this immunostain is derived from the blot printed in Figure 5.12a). Indeed, the reduction of the ladder observed in Figure 5.12a may result, largely, from this effect upon Hsc70. This stark inhibition of Hsc70-ubiquitination contrasts to Figure 5.11, where Tau protein and luciferase were used as substrates. In the case of these substrates, the ubiquitination of Hsc70 did not seem as strongly affected by the dose of BAG-5.

Figure 5.12 - The effect of BAG-5 upon ubiquitination by Hsc70/CHIP

RTA was pre-incubated at 45°C with Hsc70 and Hsp40 before components of the ubiquitination cascade were added for a subsequent 2 hour incubation at 37°C. The rest of the protocol was as before. In each case, the incubation mixture was split into two equal volumes and immunostained. a) Shows a Ponceau S stain of the blot which was eventually used for b), the Hsc70 immunostain.

a. Ponceau stain

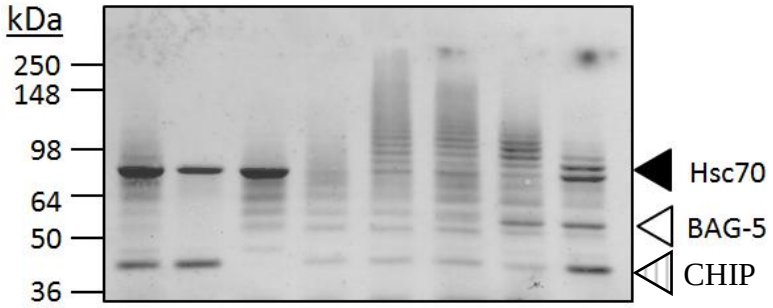

E1	-	+	+	+	+	+	+	+
E2 (UbcH5b)	+	-	+	+	+	+	+	+
E3 (CHIP)	+	+	-	+	+	+	+	+
Hsc70/Hsp40	+	+	+	-	+	+	+	+
BAG-5 (μM)	0	0	0	0	0	3	6	9

b. Hsc70 immunostain

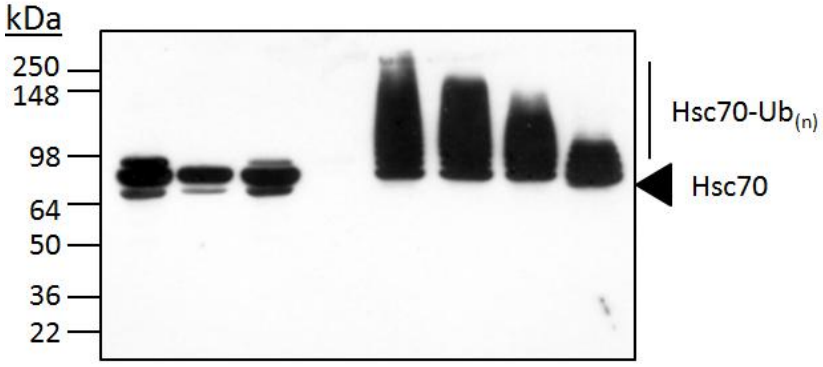

E1	-	+	+	+	+	+	+	+
E2 (UbcH5b)	+	-	+	+	+	+	+	+
E3 (CHIP)	+	+	-	+	+	+	+	+
Hsc70/Hsp40	+	+	+	-	+	+	+	+
BAG-5 (μM)	0	0	0	0	0	3	6	9

Unfortunately, the immunoblots for RTA from the same reactions have a great deal of background (Figure 5.13a, exposures 1 & 2). Curiously, prior applications of the same antibodies yielded noise-free blots (*cf.* Figure 5.4). It may be that the development procedure in this particular assay worked fortuitously well, highlighting dilute species. Alternatively, the stock of RTA may have formed multimers after repeated freeze/thaw cycles.

Nonetheless, an attempt at interpretation has been made. In incubations where the complete ubiquitination cascade is provided, putative mono-, di- and tri-ubiquitination of RTA can be observed. Consistent with an inhibitory effect of BAG-5, the intensity of some of these bands responds negatively to its increasing concentration. Fittingly, the intensity of the un-ubiquitinated RTA band is weakest in incubations without Hsc70/Hsp40 and in reactions where the ubiquitination cascade is completed. Where Hsc70/Hsp40 are absent, this would be caused by a loss of solubility. When the ubiquitination cascade is completed, this would be because of conversion into slower migrating, ubiquitinated species.

From the second exposure, it can be seen that the high molecular weight smear results from ubiquitination. It is observably laddered and most intense in incubations where all components of the cascade have been provided. This ladder is likely not derived from the RTA band at 33kDa, as no contiguous array of bands bridges the two zones upon the immuno-blot. Instead, the smear may be derived from a multimer of RTA at 98kDa. Contamination of incomplete incubations (with small concentrations of the indicated missing catalytic enzymes) may have caused the ubiquitination observed in these lanes, accounting for the weaker ladders observed therein.

Importantly, the BAG-5 preparation possesses impurities (marked by asterisks in Figure 5.13b). Jörg Höhfeld maintains that partial purification of recombinant protein from a prokaryotic host is appropriate for testing the inhibitory effects of co-factors upon CHIP-mediated ubiquitination (personal communication).[23] Unfortunately, such contaminant species might compete with the probed substrate (for ubiquitination, or Hsc70 binding), obscuring an inhibitory effect of BAG-5. However, as BAG-5 inhibits the chaperone-dependent E3 ligase, Parkin (Kalia *et al*., 2004), and is related to BAG-2, which inhibits CHIP (Arndt *et al.*, 2005), it does not seem unreasonable that this may be a true inhibition rather than a competition effect.

[23] As prokaryotes do not possess endogenous components of the ubiquitination cascade which could interfere with the activation and ligation of ubiquitin to a substrate protein.

Figure 5.13 - The effect of BAG-5 upon ubiquitination of RTA by Hsc70/CHIP

RTA was pre-incubated at 45°C with Hsc70 and Hsp40 before components of the ubiquitination cascade were added for a subsequent 2 hour incubation at 37°C. Then these components were added and the rest of the protocol was as before. In each case, the incubation mixture was split into two equal volumes and immunostained. a) Shows the immunostain for RTA. Two separate exposures. b) A silver stain of the BAG-5 preparation and the RTA preparation in parallel (the masses of protein used are equivalent to those loaded on the gels in a).

a. RTA immunostain (separate panels show different exposures).

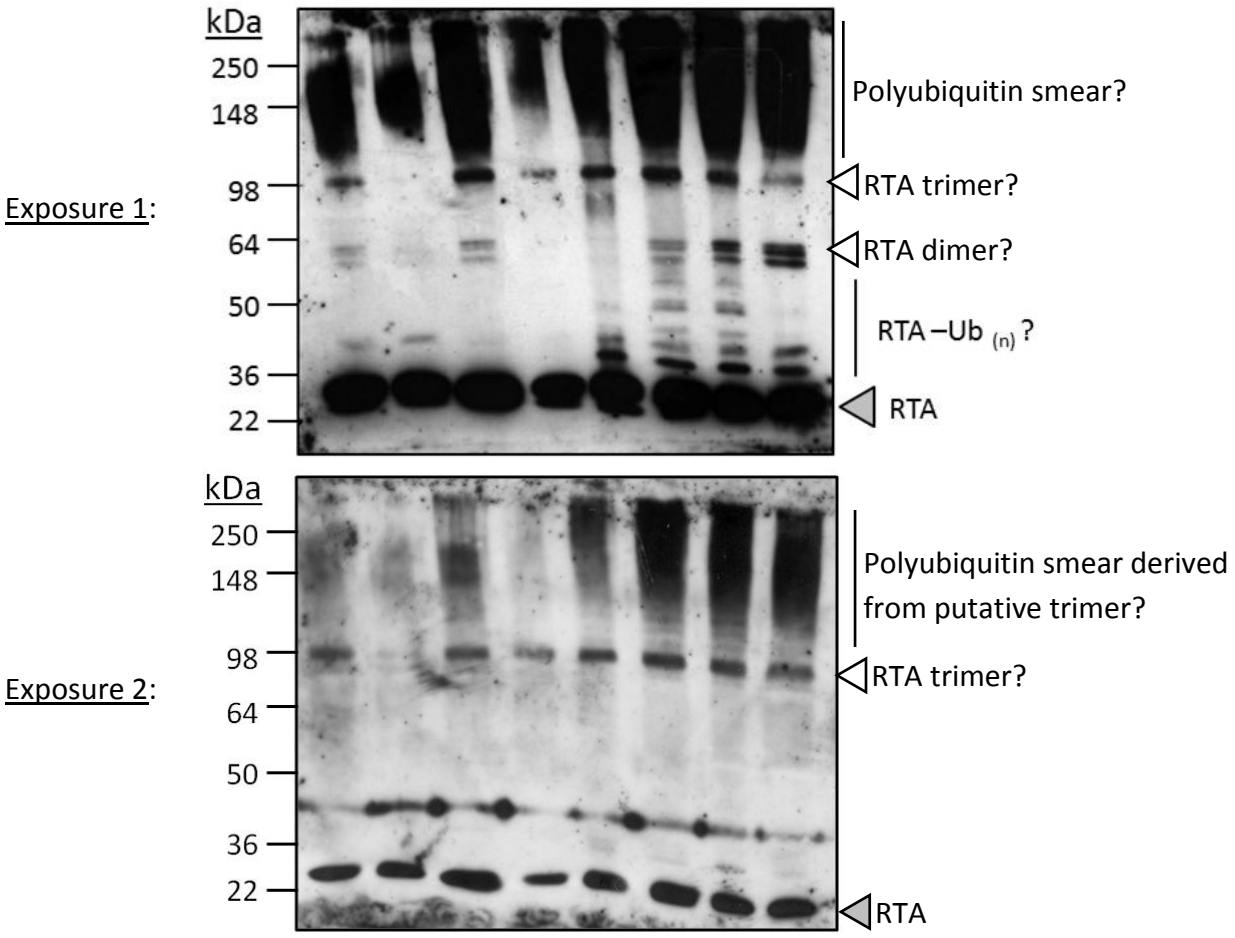

Lane	1	2	3	4	5	6	7	8
E1	-	+	+	+	+	+	+	+
E2 (UbcH5b)	+	-	+	+	+	+	+	+
E3 (CHIP)	+	+	-	+	+	+	+	+
Hsc70/Hsp40	+	+	+	-	+	+	+	+
BAG-5 (μM)	0	0	0	0		3	6	9

(Figure 5.13 – continued.)

b. Silver stain showing contaminants in the BAG-5 preparation

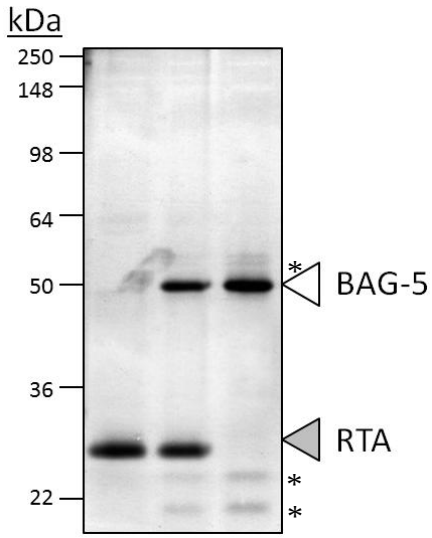

BAG-5	-	+	+
RTA	+	+	-

5.8 The effect of BAG-5 upon RTA solubility

BAG-5 may have effects other than inhibiting CHIP-mediated ubiquitination. The related co-factor, BAG-2, inhibits the chaperoning effect of Hsc70 upon some substrates and has, itself, anti-aggregation properties (Arndt *et al*., 2005). In a similar fashion, BAG-5 could provide an additional regulatory overlay upon Hsc70 activity *in vivo*. To test this, BAG-5 was supplemented into the solubility assay from the previous chapter to determine whether it augmented or interfered with the effect of Hsc70 (Figure 5.14).

The effects of BAG-5 upon Hsc70/Hsp40 **-** The apparent effects of BAG-5 upon solubility are reasonably consistent. In these assays the solubilising properties of Hsc70 and Hsp40 alone can be seen (*cf.* pairs 1 & 2). Without ATP in the incubations, BAG-5 alone has a solubilising effect equivalent to that of Hsc70 in the parallel assay (compare pairs 2 & 3). Thus, both seem to act passively as pro-solubility factors. However, Hsc70 has a greater effect than BAG-5, by average, when ATP is present (compare pairs 8 & 9). This seems to support that Hsc70 has an ATP-dependent mechanism for promoting solubility under these conditions in addition to a passive effect. BAG-5 does not have an equivalent ATP-dependent mechanism.

In assays without ATP, BAG-5 does not have much of an effect upon Hsc70's solubilising effect (at a concentration of 3μM BAG-5 – *cf.* pairs 2 & 4). In reactions containing ATP, it appears that including 3μM BAG-5 partially abrogates the solubilising effect of Hsc70 (*cf.* pairs 8 & 10). This shows that the co-chaperone has an effect on the ATP-dependent solubilising activity of Hsc70. In light of what is known about these two factors, it could be hypothesised that the following justifies these trends:

(1) BAG-5 and Hsc70 both have pro-solubility activities independent of ATP;
(2) Hsc70, alone, has an additional pro-solubility activity dependent on ATP;
(3) BAG-5 inhibits the ATP-dependent activity of Hsc70.

An effect of BAG-5 on the ATP-dependent chaperoning activity of Hsc70 would not be unexpected, given BAG-5 is a putative nucleotide exchange factor of the chaperone (Takayama & Reed, 2001). Furthermore, Kalia *et al.* (2004) report that BAG-5 negatively affects the Hsc70-mediated refolding of thermally-denatured luciferase *in vivo*, so a negative influence upon Hsc70 is also not unexpected. Nevertheless, before making such conclusions, it is important to remember that the BAG-5 preparation was only "partially purified" from

E.coli, and so possesses some contaminants (as in Figure 5.13b). As these contaminants are added during the 45°C denaturation, impurities will compete with RTA for tenure in the peptide binding domain of Hsc70 if they denature. If anything, however, this competition would be expected to further hinder solubility as the dose of BAG-5 (and contaminants) was increased, rather than to promote it as they are titrated into the incubation.

The effect of BAG-5 in isolation from Hsc70/Hsp40 - To simplify the previous experiment, BAG-5 was incubated with RTA at increasing concentrations without accompanying chaperones (Figure 5.15a & b). In all cases, increasing the dose of BAG-5 increased the solubility of RTA. This effect may be slightly increased when ATP is present. However, given that the nucleotide has a slight solubilising effect itself, the effect of BAG-5 appears to be more or less the same in both contexts.

If the change in solubility as a factor of protein concentration is considered, the effects of the BAG-5 preparation are greater than that of BSA, and equivalent to Hsc70/Hsp40 under similar conditions. 9μM BAG-5 (0.46mg.mL^{-1}) results in a ~23% shift in solubility. Under similar conditions, BSA caused only a ~5% shift at a marginally higher concentration of 0.63mg.mL^{-1} (*cf.* Figure 4.17; for ease of reference the shifts caused by BAG-5, BSA and Hsc70/Hsp40 are compared in Figure 5.15c). Thus, it appears that the BAG-5 preparation is able to promote solubility of RTA. This effect may be contributed to by a blocking effect like BSA. However, its effect is in excess of that of BSA, suggesting an additional mechanism: e.g. by stabilising soluble conformations of RTA or by blocking the sites which could propagate aggregation.

Figure 5.14 – The effect of BAG-5 upon the ability of Hsc70 / Hsp40 to keep RTA soluble at 45°C.

RTA was mixed with varying concentrations of BAG-5 and chaperones, with concentrations and buffers as in other solubility assays. "40/70" indicates a concentration of Hsp40 and Hsc70 as previously used in the solubility assay. Pellet / supernatant distributions of RTA were then analysed as normal. a) Shows experiments conducted without ATP alongside the relative quantification of pellet/soluble bands; b) Shows the equivalents, but with 5mM ATP. Asterisks indicate a contaminant band from the BAG-5 preparation, particularly visible in the final lane. In all cases error bars show SEM.

a. Without ATP (each panel shows an independent assay).

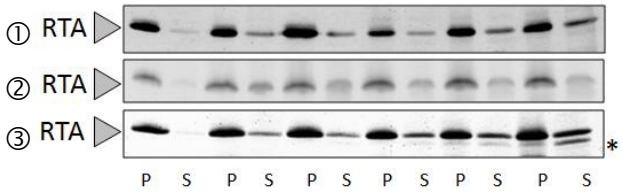

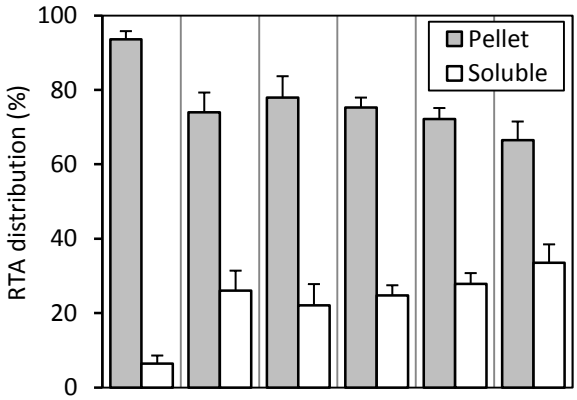

40/70	-	+	-	+	+	+
BAG-5	0	0	3	3	6	9
ATP	-	-	-	-	-	-
Pair	1	2	3	4	5	6

b. With ATP (each panel shows an independent assay).

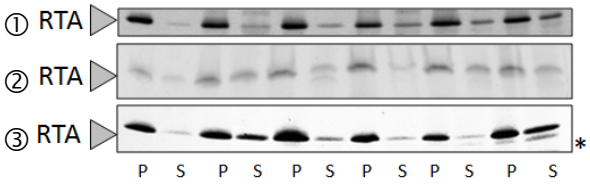

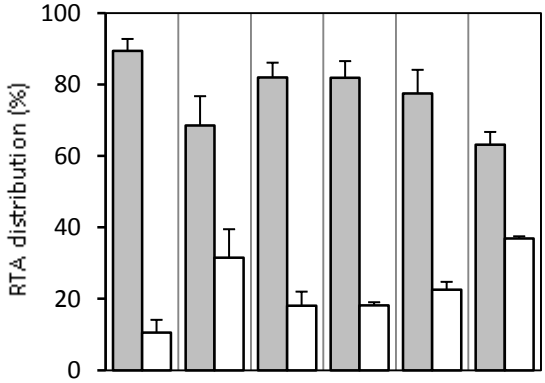

40/70	-	+	-	+	+	+
BAG-5	0	0	3	3	6	9
ATP	+	+	+	+	+	+
Pair	7	8	9	10	11	12

Figure 5.15 – The effect of BAG-5 alone upon the aggregation of RTA at 45°C.

RTA was mixed with varying concentrations of BAG-5, with or without 5mM ATP (as indicated). The solubility of RTA was then compared at each concentration. a) Shows silver stains and relative pellet/soluble quantification. b) Shows the relative absolute signal size between lanes. Asterisk shows a contaminant band from the BAG-5 preparation. c) Compares the average pro-solubility effects of BSA, Hsc70/Hsp40 and BAG-5 compared to independent controls of RTA in buffer alone. In all cases error bars show SEM.

a. Silver stains and quantification (each panel shows a separate assay).

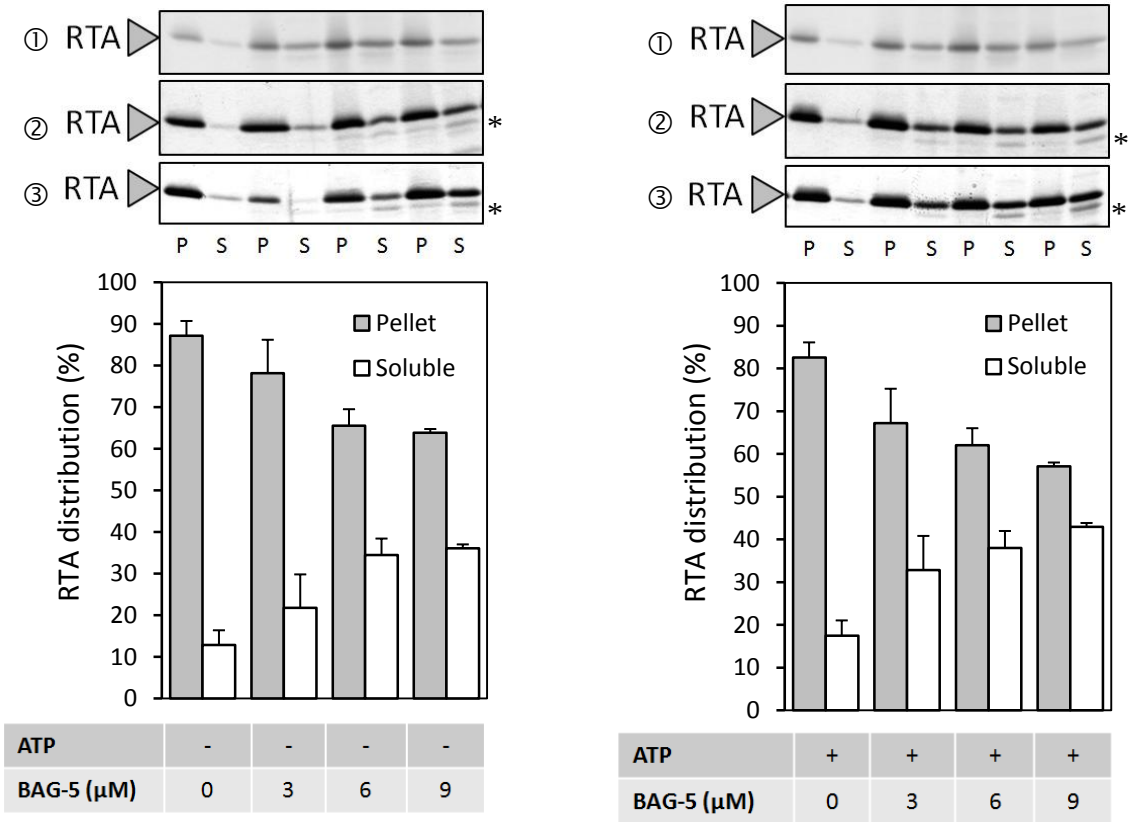

(Figure 5.15 - continued.)

b. Absolute pellet and soluble signal sizes (n=3)

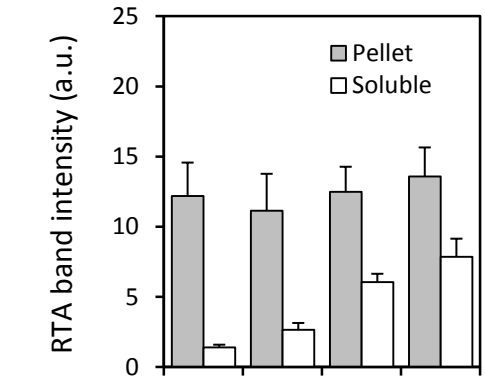

ATP	-	-	-	-
BAG-5 (µM)	0	3	6	9

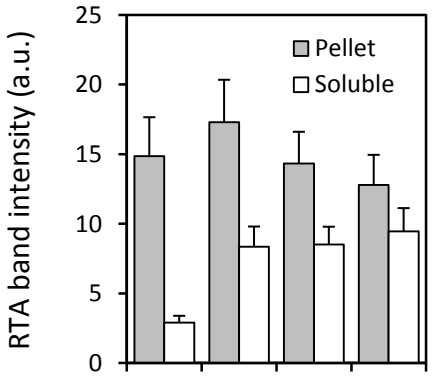

ATP	+	+	+	+
BAG-5 (µM)	0	3	6	9

c. Average pro-solubility effect of BSA, Hsc70/Hsp40 and BAG-5 from different experiments conducted at 37°C (n=3)

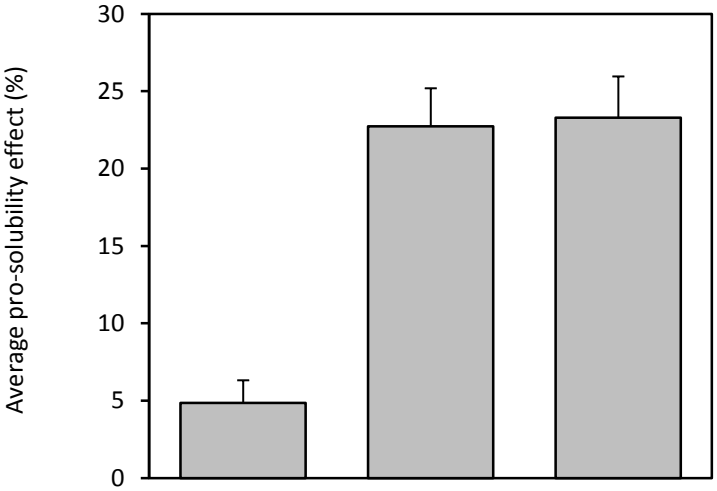

Protein	BSA	Hsc70/Hsp40	BAG-5 (9µM)
mg.mL^{-1}	0.63	0.47	0.46
See Figure	4.17	4.16	5.15a

5.9 Over-expression of Hsc70 co-factors

To extend these findings, the *in vivo* effect of over-expressing co-chaperones upon ricin toxicity was studied. This would provide evidence for whether the balance of co-chaperones in the cytosol contributed to the fate of RTA *in vivo*.

5.9.2 Targeted over-expression of Hsc70 co-chaperones

Jörg Höhfeld kindly provided plasmid vectors for the over-expression of the co-chaperones HIP, BAG-1, BAG-2, BAG-5 and HOP in mammalian cells.

5.9.2.1 Optimisation of over-expression conditions

HeLa cells were transfected using the lipofectamine protocol (Invitrogen) under a variety of conditions. A plasmid for the over-expression of HOP was used as a standard to optimise this process as an antibody for this protein was available. Figure 5.16 shows that the intensity of HOP immunostaining increases with both the mass of vector and the volume of Lipofectamine reagent used for the transfection. However, HOP over-expression is not so convincingly seen in total lysates examined by silver stain. There is a heavily-stained band at a similar molecular weight (marked with an asterisk) which possibly dwarfs any staining attributable to HOP. Examination of a band (marked with a black arrowhead) slightly above the asterisk-marked one shows a slight rise in intensity as mass of plasmid is increased. This seems a good candidate for HOP. Reassuringly, the silver stains do show that there are no dramatic changes in the remaining protein content of transfected cells. This is a useful observation, as it informs us that the transfection procedure will have relatively few off-target effects.

R.A. Spooner (University of Warwick) previously optimised the transfection efficiency of this procedure for the same cell line, reporting that 0.7μg was a sufficient quantity of plasmid to use (which is why the plasmid was added in multiples of 0.7μg, Figure 5.16). Using an identical vector for over-expressing cytosolic GFP, it was estimated that, when ~0.7μg of plasmid was transfected with 3μL of transfection reagent, ~30% of cells showed clear GFP fluorescence when viewed by epifluorescence microscopy (R.A. Spooner, unpublished data). This relatively low level may explain why HOP cannot be seen so strongly in the silver-stains presented.

Figure 5.16 – Optimisation of over-expression conditions

HeLa cells were plated at a density of 2.5 × 10^4 cells per well of a 6-well plate and transfected with the indicated mass of plasmid DNA (for over-expression of HOP). Cells were then grown in normal medium over a period of 72 hours. Detergent soluble lysates were then collected and assayed for protein content. a) Shows transfections using 3µL of lipofectamine (label: "lipofect"). b) Shows parallel transfections using 6µL of the reagent. In each case, an immunostain for HOP was made (upper panel) alongside a silver stain (lower panel) showing even loading of 10µg of protein/lane. Grey arrowheads mark HOP bands. Asterisk indicates a heavily staining band of slightly increased electrophoretic mobility relative to HOP, obscuring interpretation.

a. 3µL of lipofectamine

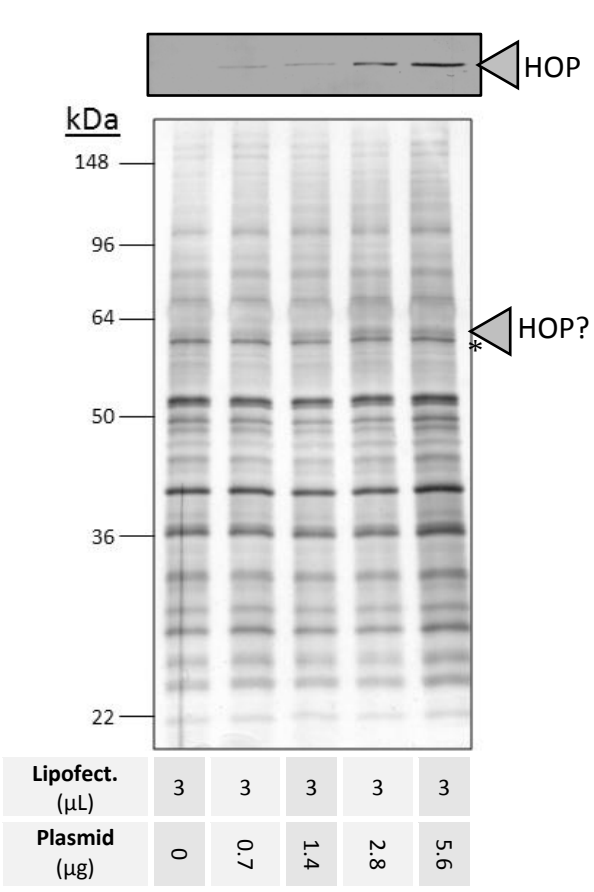

Lipofect. (µL)	3	3	3	3	3
Plasmid (µg)	0	0.7	1.4	2.8	5.6

b. 6µL of lipofectamine

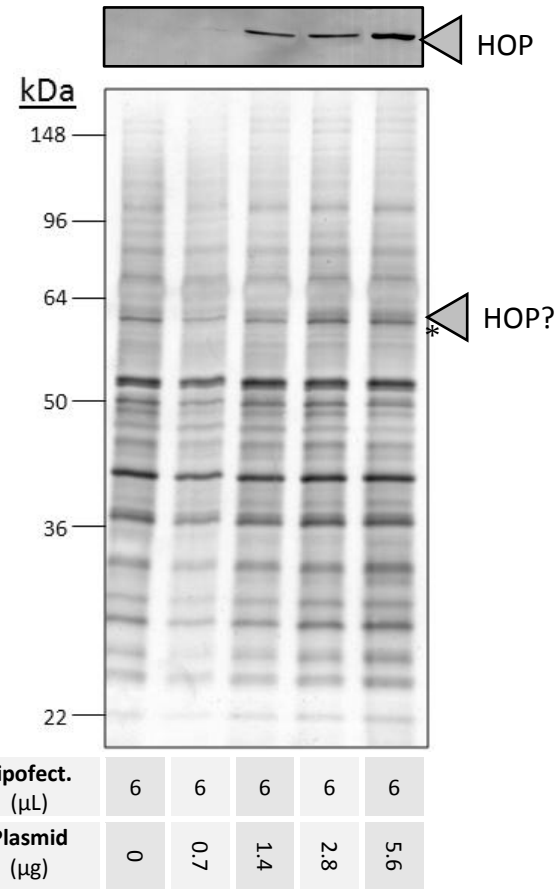

Lipofect. (µL)	6	6	6	6	6
Plasmid (µg)	0	0.7	1.4	2.8	5.6

5.9.3 The effect of over-expressing HOP on ricin intoxication

As an increase in HOP was observed via immunostaining at a ratio of 0.7μg plasmid to 3μL of lipofectamine, this ratio was used in subsequent assays. Such a minimal approach would reduce stress responses associated with high doses of lipid-based transfection reagents (Calvin *et al.*, 2006) which might not have been obvious from the silver stains in the previous figure.

After 48 hours of incubation, HOP-transfected cells and mock-transfected cells (transfected with empty vector) were re-plated into 96-well plates so their sensitivity to ricin could be compared after an overnight incubation. The IC_{50} of such cells with respect to ricin was determined using the cytotoxicity assay (Figure 5.17a). Because the size of the protective effect was small, this assay was repeated multiple times (Figure 5.17b), showing a high degree of reproducibility. A consistently protective effect was observed. These results are published in Spooner *et al.* (2008), where there is also published a dose-response to the HOP plasmid. This suggests the recorded effect result from the DNA of the vector rather than to an off-target effect of the lipid-based transfection reagent.

As discussed previously (*cf.* Table 5.1 and section 5.4), HOP increases the processivity of the Hsc70/Hsp90 triage, aiding transfer of clients from Hsc70 to Hsp90 (Johnson *et al.*, 1998; Hernández *et al.*, 2002; Gross & Hessefort, 1996; Murphy *et al.*, 2003). Over-expressing HOP, then, would be expected to increase transfer of clients from Hsc70 to Hsp90. In such a context, any RTA that encounters and binds to Hsc70 would be more likely to subsequently interact with Hsp90. Therefore, increasing the level of this co-chaperone would be predicted to be protective, as interactions with Hsp90 have already been shown to inactivate RTA (*cf.* Chapter 3 and Spooner *et al.*, 2008). Furthermore, as a stimulator of Hsc70 nucleotide exchange, HOP over-expression might contribute to premature release of RTA from Hsc70, which might disrupt the otherwise beneficial effect that Hsc70 has upon the cytosolic reactivation of the toxin subunit. Notably, the protective effect of over-expressing HOP is also consistent with the observation that dual Hsc70/Hsp90 inhibition results in a net protection. Both results vouch for the sequential order of an Hsc70/Hsp90 triage, with an interaction of RTA and Hsc70 occurring first.

Figure 5.17 – Over-expression of HOP protects cell from ricin

HeLa cells were plated at a density of 2.5 × 10^4 cells per well and transfected with 0.7µg of vector (either empty. "mock" or encoding HOP). Cells were then grown in normal medium over a period of 48 hours. These cells were trypsinised and re-divided equally into 96-well plates and grown for a further 24 hours. The efficacy of ricin was then studied via cytotoxicity assay. a) Shows example dose-response curves from each over-expression, with the HOP over-expressing dataset represented by "●" and mock-transfected dataset by "○". b) The IC_{50} value for cells over-expressing HOP was then compared to the IC_{50} value of cells which were mock-transfected. Error bars show the SEM between sets of independent experiments (n=8).

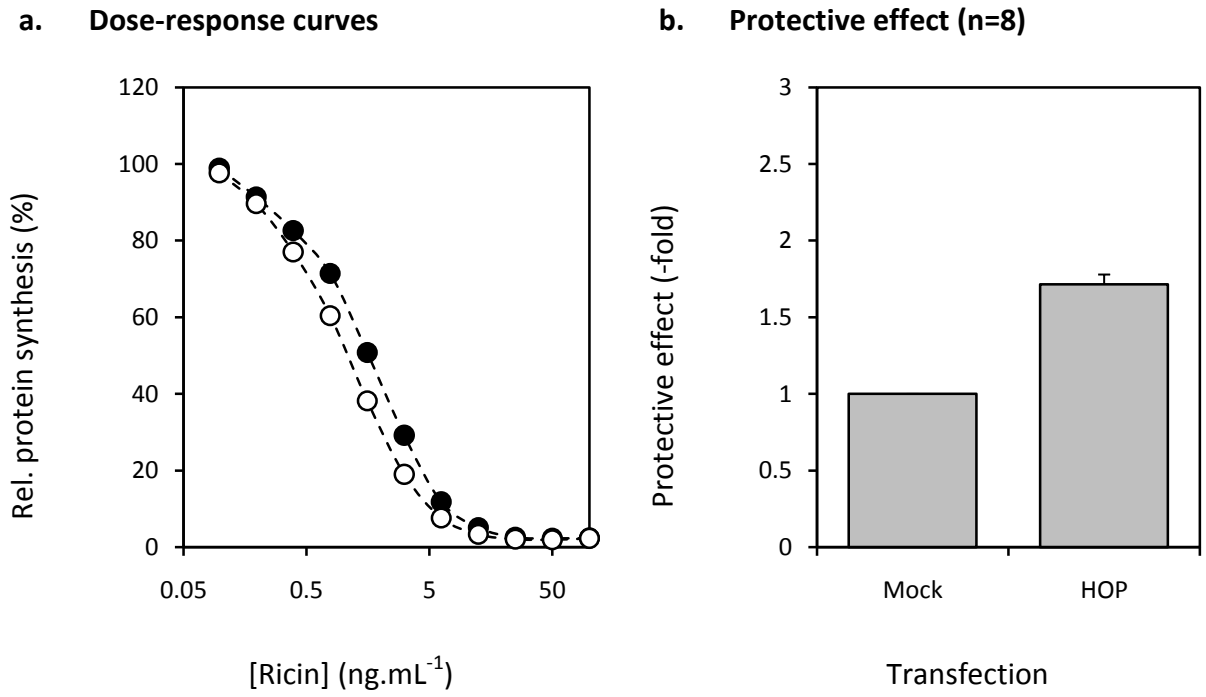

5.9.4 Other co-factors

Vectors for over-expression of the co-chaperones BAG-1, BAG-5, CHIP, HIP and BAG-2 were each transfected independently into HeLa cells, as before. Each of these treatments was found to have an effect upon ricin intoxication. However, they varied as to whether they were sensitising or protective.

5.9.4.1 Protective co-factors

Over-expression of BAG-1 **–** protected cells from ricin (Figure 5.18b & e). Lysates from mock-transfected and BAG-1 transfected cells were compared via silver stain after being separated in parallel on SDS-PAGE (Figure 5.18f). In the lysate from BAG-1 transfected cells, there is a relatively diffuse band centred on a molecular weight of 33kDa, as would be anticipated for this protein. This staining is much more intense than was ever the case for HOP.

Interactions of BAG-1 with both Hsc70 and the proteasome are well-elaborated, an association which is thought to promote degradation of Hsc70-bound clients (Alberti *et al.*, 2001 & 2002). BAG-1 is also ubiquitinated by CHIP in an Hsc70-dependent manner, which synergistically augments the affinity of a client·chaperone complex for the proteasome (Alberti *et al.*, 2001 & 2002). Fittingly, over-expression of BAG-1 increases the degradation of Hsc70-bound clients like the glucocorticoid receptor *in vivo* (Demand *et al.*, 2001). However, reports do exist of proteins which are stabilised *in vivo* by the over-expression of BAG-1, e.g. microtubule-dissociated Tau protein, although the mechanism by which this occurs is unclear (Elliott *et al.*, 2007).

From these results it would be hypothesised that, when RTA enters the cytosol from the ER, any subsequent interaction with Hsc70 will be more likely to result in inactivation of the toxin subunit if the complex encounters BAG-1. This effect may be executed ultimately by proteasomal degradation. Alternatively, the co-chaperone might interfere with the mechanism by which Hsc70 keeps RTA soluble (by acting as a nucleotide exchange factor), much as was demonstrated for BAG-5 *in vitro*.

Over-expression of BAG-5 **–** protected cells against ricin intoxication (Figure 5.18c & e). Lysates from BAG-5-transfected and mock-transfected cells can be seen in Figure 5.18f, where they have been run in parallel by SDS-PAGE and silver-stained. The BAG-5

transfected lysate possesses an additional band at 51kDa, just underlying a very bold band at ~52kDa.

This protective effect is unexpected given the inhibitory effect of BAG-5 upon CHIP-mediated ubiquitination *in vitro*, and its apparent pro-solubility activity. On the other hand, BAG-5 has been shown to have an inhibitory effect upon the chaperoning effect of Hsc70 (*cf.* Figure 5.14 and Kalia *et al.*, 2004). It seems that this inhibitory effect upon Hsc70 may be the dominant function of the co-chaperone *in vivo*, as the other effects would sensitise if they were dominant.

***Over-expression of CHIP* –** is also protective against ricin intoxication (Figure 5.18d & e). Lysates from CHIP-transfected and mock-transfected cells can be seen in Figure 5.18f, where they have been separated in parallel by SDS-PAGE and silver-stained. At the expected molecular weight for CHIP, ~36kDa – there is bleaching of a band which is intensely stained in the control. This bleaching seems to owe to exclusion of the stain by the over-expressed CHIP. This staining phenomenon is not without precedent; Chuba & Palchaudhuri (1986) note the differential colour-staining of proteins based on cysteine content (as well as other, unidentified, attributes).

Previously in this thesis it was shown that CHIP can ubiquitinate Hsc70, Hsp90 and client RTA in a manner which can be titrated against inhibitory co-factors *in vitro* (see also Arndt *et al.*, 2004 & 2005). Given that over-expressing CHIP would change this balance in the cell, a congruent increase in degradation of chaperone clients, including RTA, would be expected. This is the case for other clients *in vivo*, such as CFTR (Meacham *et al.*, 2001) and microtubule-dissociated Tau protein (Shimura *et al.*, 2004). Even if RTA is not directly ubiquitinated, then the chances of it being carried to the proteasome by ubiquitinated Hsc70 (Urushitani *et al.*, 2004; Jiang *et al.*, 2001) would presumably be increased under conditions of CHIP over-expression.

Figure 5.18 – Over-expression of HOP, BAG-1, BAG-5, and CHIP sensitises cells to ricin treatment.

HeLa cells were treated as before, but an array of co-factors was studied independently. Shown below are exemplar dose-response curves from the over-expression of a) HOP and putative over-expression of b) BAG-1 c) BAG-5 and d) CHIP. In each case "●" denotes the co-chaperone over-expressing datasets and "○" denotes the mock-transfected datasets. e) Shows the protective effect of each co-chaperone relative to the mock-transfected cells at the IC_{50}. Data for HOP displayed here is identical to that in the previous figure and has been transferred here for comparative purposes. Error bars show the SEM. f) Shows silver stains from cells which have been transfected in the same fashion, but which have instead been lysed in a detergent-containing buffer and analysed by SDS-PAGE (10µg of protein loaded per lane).

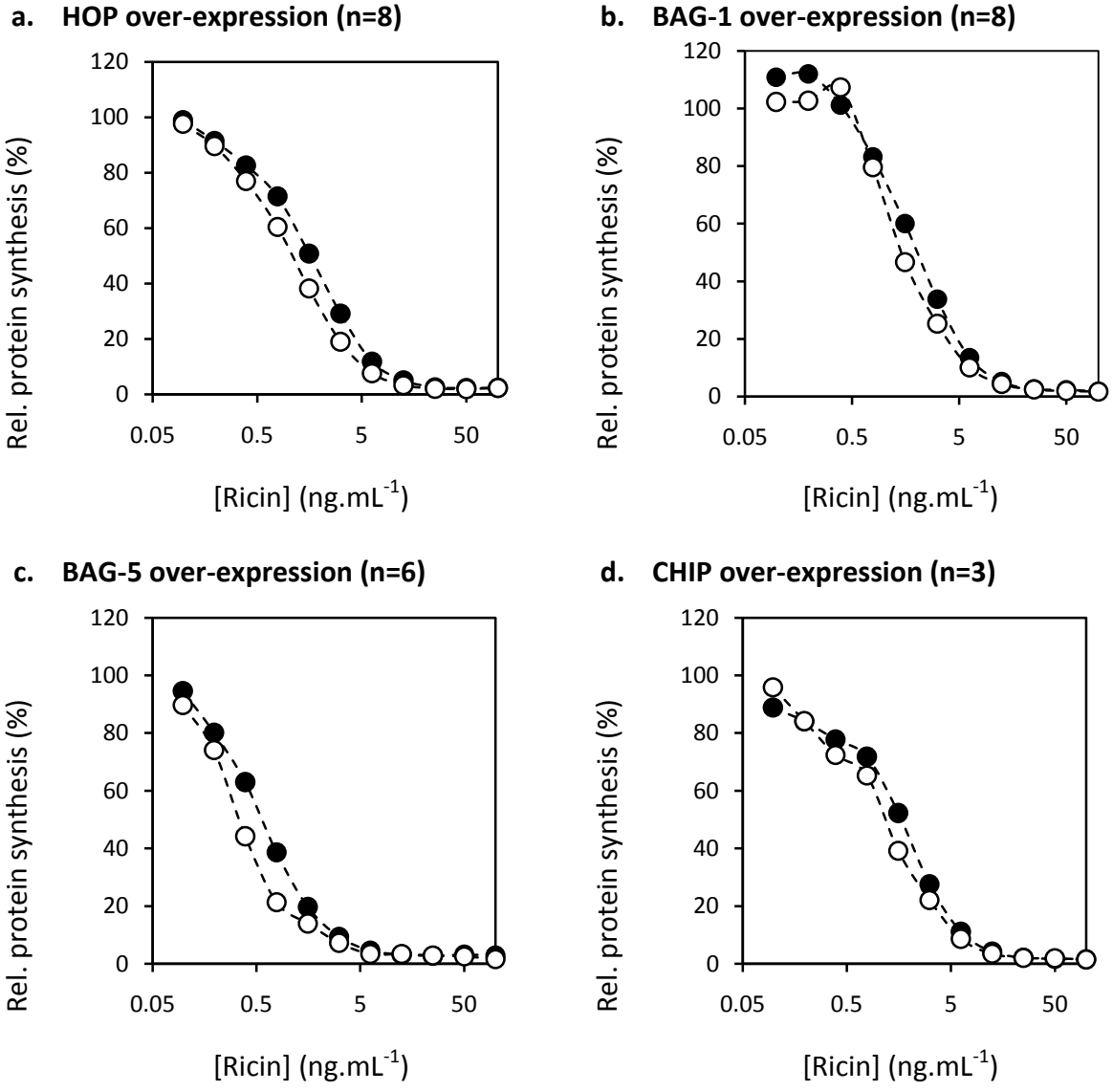

(Figure 5.18 – continued.)

e. The protective effects of over-expressing HOP (n=8), BAG-1 (n=8), BAG-5 (n=6) and CHIP (n=3).

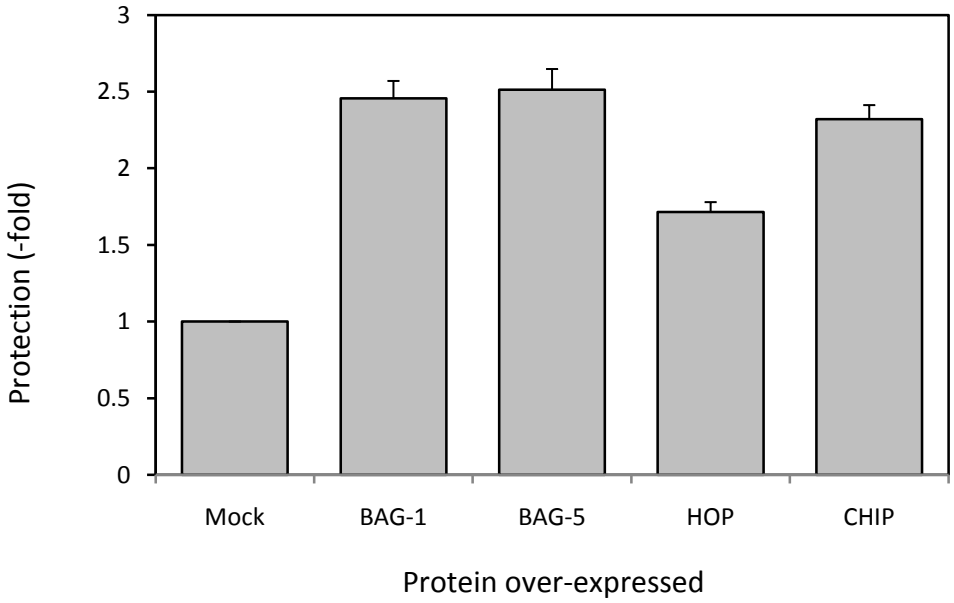

f. Silver-stains of transfected and mock-transfected lysates

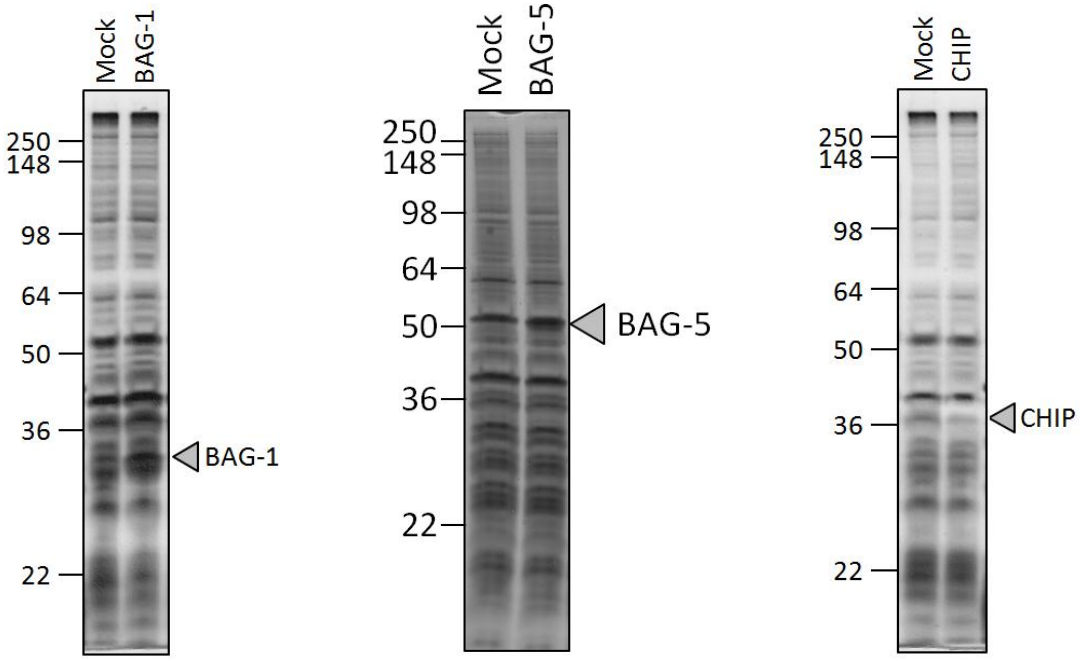

5.9.4.2 Sensitising co-factors

Over-expression of BAG-2 – sensitised cells to intoxication by ricin (Figure 5.19a & b). Over-expression of BAG-2 under the same conditions can be visualised by the appearance of a new band at around the expected molecular weight of 24kDa (Figure 5.19d). Unlike BAG-1, BAG-2 possesses no ubiquitin-like domain for proteasome binding (Arndt *et al.*, 2005). BAG-2 is also known to inhibit ubiquitination by CHIP and to exclude the binding of BAG-1 to Hsc70 (Arndt *et al.*, 2005). As such, BAG-2 will compete against the activity of these other co-chaperones (and likely BAG-5 as well).

Precisely why there is a difference between the effects of over-expressing BAG-2 and BAG-5 is unknown, given that they differ mainly by virtue of the multiplicity of the BAG-domain they both possess. It might result from the altered stoichiometries these two co-chaperones are likely to promote in the folding complexes they interact with, or the localised concentration of nucleotide exchange factor activity, or some as yet unidentified property of either protein.

Over-expression of HIP – also sensitised cells to ricin (Figure 5.19b & c). Evidence of the over-expression of HIP under these transfection conditions can be seen in the silver stain, where a narrow band appears at ~43kDa which is not observable in the control (Figure 5.19d). HIP over-expression might induce sensitisation by promoting the refolding of Hsc70-bound RTA, much as this chaperone promotes refolding of thermally-denatured luciferase *in vivo* (Nollen *et al.*, 2001). HIP stabilises the ADP-bound conformation of Hsc70 (Höhfeld *et al.*, 1995), which increases its affinity for bound clients by inducing conformational changes which occlude client exit from the peptide binding domain.

Unlike BAG-2, then, HIP would cause tight association between RTA and Hsc70. Whilst their effects upon a putative Hsc70·RTA complex are therefore different, both of these chaperones displace, or else inhibit destructive co-factors like CHIP and BAG-1 (Höhfeld *et al.*, 1995). HIP, like BAG-2, also possesses an anti-aggregation activity independent of Hsc70 (Nollen *et al.*, 2001). This may also help to sensitise the cell to ricin intoxication, by directly stabilising retrotranslocated RTA.

It can also be noticed that the error-bars for BAG-2 and HIP are rather large, covering most of the effect. This is quite unlike those co-factors which were found to be protective. The error-bars describing those data were markedly smaller. It is difficult to suggest why this

might be. It could be that promotion of folding might be more weakly determined by co-factors than is promotion of degradation. Alternatively, greater variability in the transfection efficiency of these constructs might be the cause.

Figure 5.19 – Over-expressing BAG-2 and HIP sensitise cells to ricin treatment.

Hela cells were transfected, as before, and assayed for their sensitivity to ricin. a) The IC_{50} value for cells over-expressing co-chaperone was compared to the IC_{50} value of mock-transfected cells. Error bars show the SEM between sets of independent experiments. b) & c) show example dose-response curves from each over-expression, with co-chaperone over-expressing datasets represented by "●" and mock-transfected datasets by "○". d) Shows silver stains from cells which have been transfected in the same fashion, but which have instead been lysed in a detergent-containing buffer and analysed by SDS-PAGE (10µg of protein loaded per lane).

a. The sensitising effects of BAG-2 (n=3) and HIP (n=6).

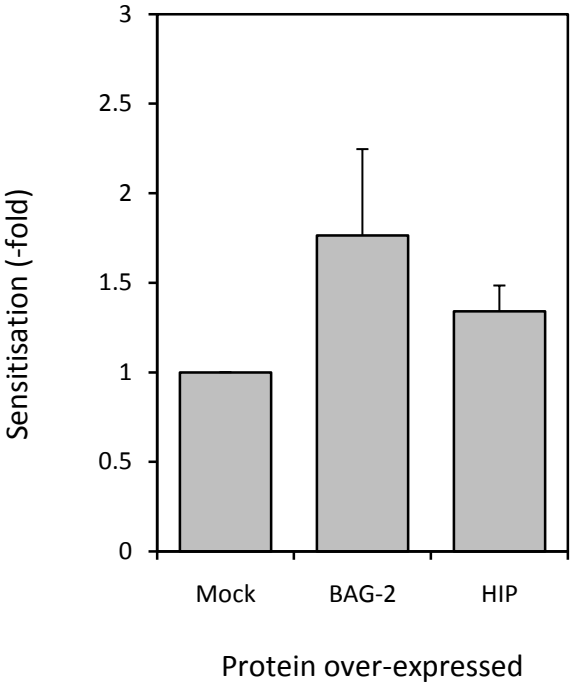

b. BAG-2 over-expression

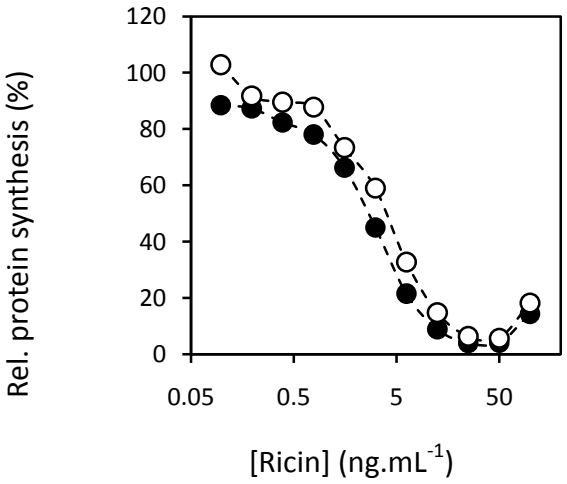

c. HIP over-expression

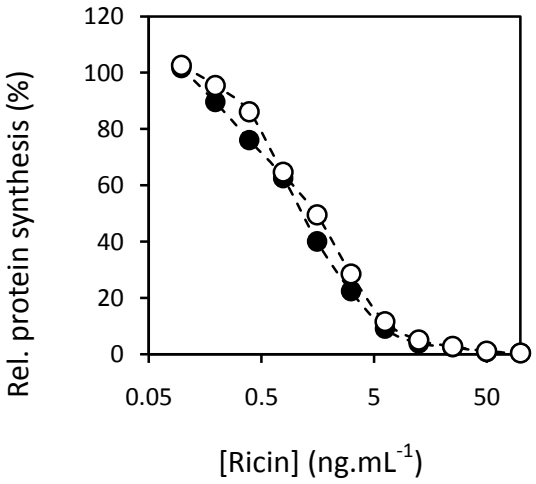

(Figure 5.19 – continued.)

d. Silver-stains of transfected and mock-transfected lysates

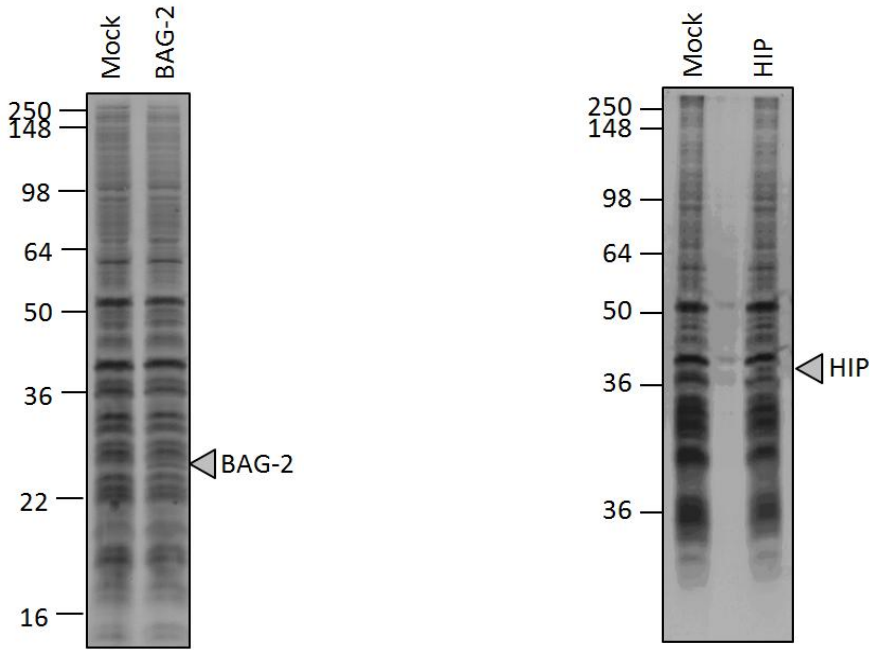

5.9.5 Transfections with LacZ have no effect

It was possible that over-expressing any arbitrary protein had an effect upon the intoxication of cells by ricin. For example, over-expression of a protein might lead to cellular aggregates which could alter the dynamics of the cytosolic chaperone complement, or upon trafficking. To account for this possibility, HeLa cells were tested for whether the over-expression of LacZ affected ricin intoxication (Figure 5.20). Although the over-expression of LacZ has not been confirmed by silver stain, this assay shows there is no difference in IC_{50} between transfected and mock-transfected cells. This starkly contrasts to the results observed when over-expressing co-chaperones, suggesting their effect is more specific.

Figure 5.20 – Putative over-expression of an arbitrary protein, LacZ, does not affect ricin sensitivity.

Hela cells were transfected, with empty vector or vector for over-expression of LacZ and assayed for their sensitivity to ricin. a) Shows a single assay from a total of three independent experiments. "●" Indicates the LacZ transfected dataset. The empty vector transfected dataset is indicated by "○". b) The IC_{50} value for cells over-expressing co-chaperone was compared to the IC_{50} value of mock-transfected cells. Error bars show the SEM between three sets of independent experiments.

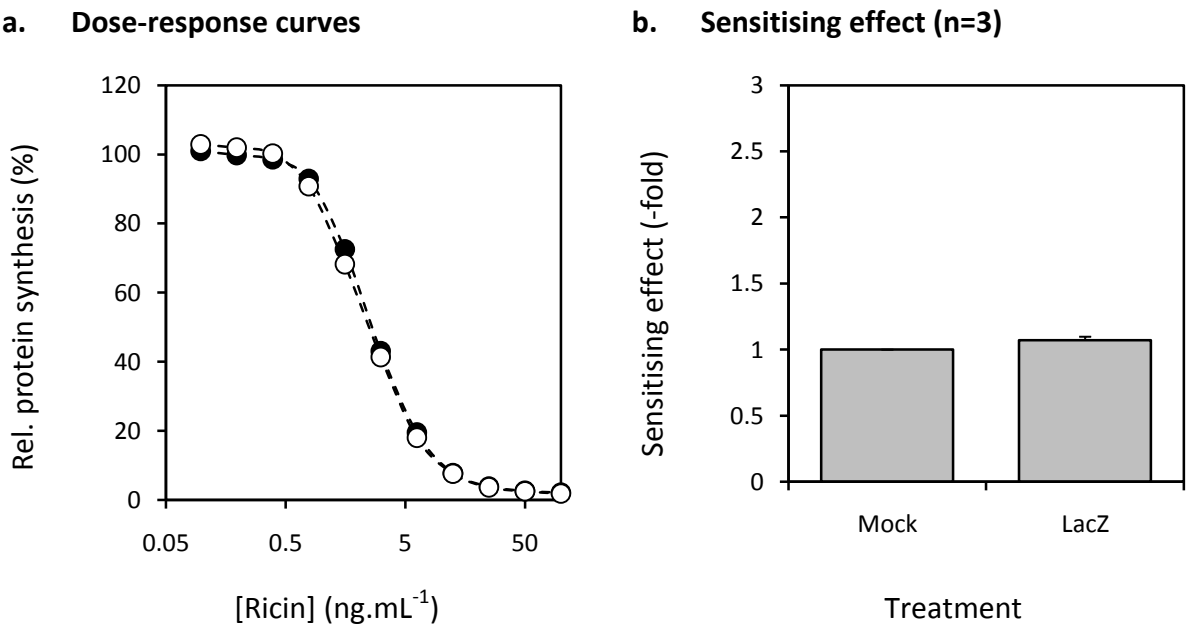

5.10 Over-expression of a J-domain protein during viral infection

It is known that some viruses possess in their capsids, or else encode in their genetic material, proteins which modulate the functionality of the chaperone matrix for the benefit of their life cycle (Brodsky & Pipas, 1998). Such viruses include Simian vacuolating virus 40 (SV40). The circular DNA genome of this virus encodes a protein, Large T Antigen (TAg; DeCaprio *et al.*, 1997). TAg inhibits homologues of the retinoblastoma tumour suppressor (Rb) and the pro-apoptotic protein, p53 (DeCaprio *et al.*, 1997). More specifically, TAg possesses an N-terminal J-domain motif, similar to that of Hsp40, which stimulates the ATPase of Hsc70 (Genevaux *et al.*, 2003). It is thought that this co-chaperone activity is required for its effects upon p53 and Rb, preferentially engendering interactions of these proteins and their complexes with Hsc70 (Genevaux *et al.*, 2003; Brodsky & Pipas, 1998).

As such, it was predicted that infection of HeLa cells with SV40 virus would result in modulation of Hsc70 function in the cytosol, so altering the dynamics of an RTA triage by it. The infection process itself provided a convenient vector for the over-expression of the protein, which was one motivation for the experiment. To this end, cells were infected with SV40 virus (K.N. Leppard, University of Warwick), lysed and examined for immunoreactivity to TAg. From Figure 5.21a it can be seen that a ~96kDa species appears after 24 hours of infection, peaking at 48 hours. This is as expected for TAg protein (K.N. Leppard – personal communication; Stubdal *et al.*, 1996).

The IC_{50} of ricin toward cells expressing TAg versus untreated cells was then compared in parallel assays. It appeared that cells treated with virus for 48 hours were protected from ricin intoxication (Figure 5.21b). It remains unclear whether this is because the virus might have an effect on trafficking, or because of another viral protein or a separate function of TAg aside from its Hsc70-interaction. However, it is interesting to speculate that this "viral co-chaperone" interferes with the normal interaction of RTA with Hsc70. Intriguingly, Kampinga *et al.* (2003) show that over-expressing a cytosolic J-domain protein, Hsp40, locks Hsc70 onto clients. This depletes the pool available to help thermally-denatured luciferase if the protein is *subsequently* added to the mix. This explanation correlates well to what is observed here: TAg might decrease the population of Hsc70 available to bind (and thus rescue) RTA as it emerges from the ER membrane. Hsc70 would be locked onto other (endogenous) clients. However, because of the number of potential off-target effects, the interpretation of this result must be treated with caution.

Figure 5.21 – The effect of SV40 virus infection upon the sensitivity of cells to ricin.

a) Hela cells were plated out at a density of 2.4 $\times$ 10^4 cells per well in a 6-well plate and infected with SV40 at a multiplicity of infection (MOI) of 10. At time-points afterward, detergent-soluble extracts were taken and run in parallel through SDS-PAGE at a concentration of 10µg of protein per lane. The gel was blotted onto nitrocellulose and immunostained for large tumour antigen (black arrowhead; TAg) and γ-tubulin (white arrowhead), which were visualised with an alkaline phosphatase development. γ-Tubulin was stained to provide a loading control. DOI: duration of infection. M: markers. b) Shows dose-response curves comparing cells which have been pre-infected for 48 hours versus cells which have not been treated with virus. "●" represents infected and "○" represents negative-control cells. c) Shows the protective effect of both these treatments. Error bars (which are very small) plot the SEM of three independent assays.

a. Immunostain

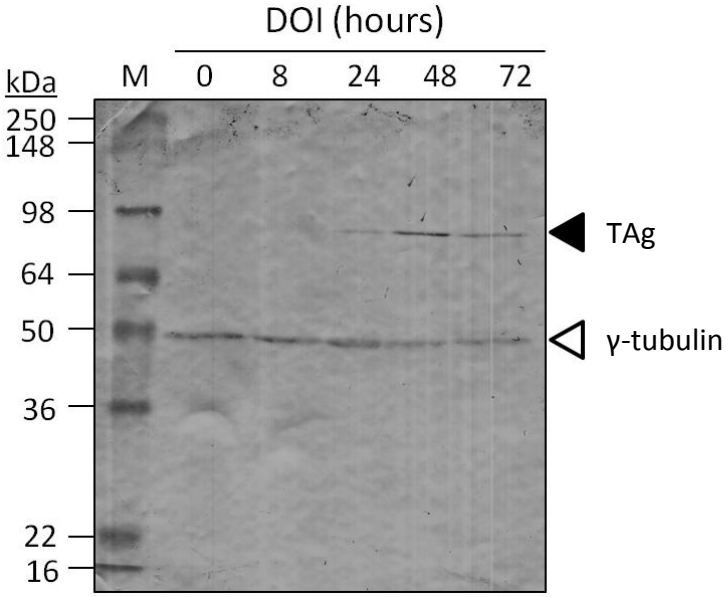

b. Dose response at 48 hours post-infection

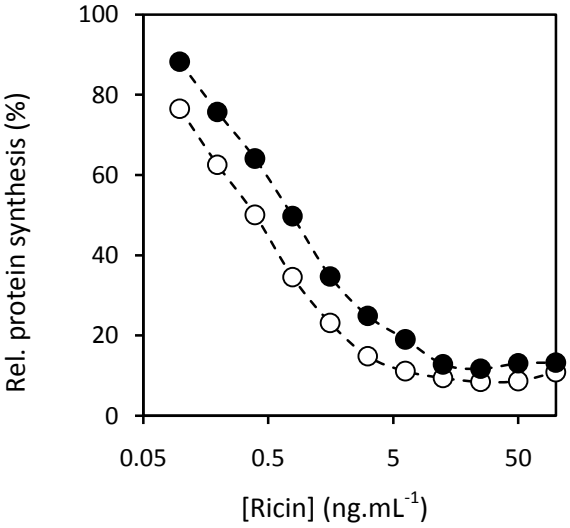

c. Protective effect (n=3)

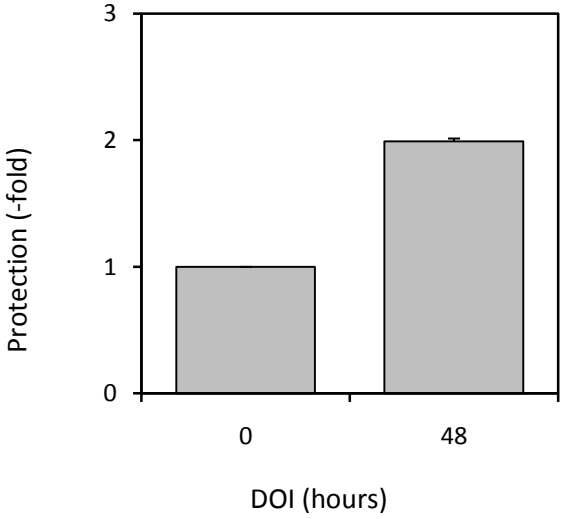

5.11 Conclusions

This chapter has attempted to consolidate a model for the division of fates a chaperone triage might impose upon retrotranslocated RTA. As determined in the previous chapter, the solubility of RTA can be stabilised by chaperones. On the other hand, as presented by this chapter, RTA might be allotted for degradation by their interaction – via polyubiquitination, for instance. The propensity of either of these processes to occur appears to be dictated by the balance of co-factors in the cytosol. The outcome Hsc70 and Hsp90 tend to promote will be a composite of the chaperone's inherent properties, the conformational state of a given instance of the client in question, and the relative abundance of their co-factors.

5.11.1 Chaperones may promote degradation of RTA by coordinating with CHIP

It has been shown that CHIP can polyubiquitinate chaperone-bound RTA *in vitro*, which provides evidence for the destructive fate that might result from the chaperone audit. In this reconstitution, ubiquitination can occur via either Hsc70 or Hsp90 (published in Spooner *et al*., 2008). However, ubiquitination via Hsp90/CHIP requires Hsc70 and HOP to deliver RTA to it first (Spooner *et al*., 2008). In both of these contexts it has not been possible to positively detect species of RTA with more than three conjoined ubiquitin attachments. This is significant because a length of four contiguous ubiquitin attachments is regarded necessary to fulfil the criteria of a "canonical" proteasomal signal – as defined by Thrower *et al*. (2000). However, a definition of the "canonical signal" should be treated with caution because of the diversifying array of co-factors that are being shown to supplement catalysis of – and response to – these processes *in vivo* (Kim *et al*., 2007 & 2009). For instance, accessory factors *in vivo* could promote the extension of the chain into – or else interpretation of the chain as – a *bona fide* proteasomal signal. Regardless, the findings herein suggest that RTA^{WT} *can* become ubiquitinated, which is a novel finding in itself.

A lipid-induced vulnerability of RTA **-** The apparently increased ubiquitination of RTA after treatment with liposomes may pose physiological significance as it may compare to the vulnerability of the toxin subunit during retrotranslocation. Other ER membrane-integral proteins are targeted by Hsc70/CHIP activity (e.g. CFTR – Arndt *et al*., 2005), and so the same may be true of RTA at some point in its retrotranslocation. The cytosolic domains of CFTR which promote this interaction, however, are known to be very large. Whether this is strictly analogous to the condition of RTA whilst it is embedded upon the surface of a liposome is unknown. If such an interaction like this does occur *in vivo*, it appears not to

result in the net-degradation or inactivation of RTA by Hsc70, considering that the chaperone's normal function promotes toxicity (*cf.* Figure 3.2).

***Ratifying a sequential triage by Hsc70/Hsp90* -** It seems likely that there is a sequential order to the triage of RTA by Hsc70/Hsp90. Hsc70 seems to interact first and Hsp90 after, a process which promotes the ability of CHIP to ubiquitinate RTA by giving it two junctures at which it may polyubiquitinate RTA. The sequential nature of the triage has been supported by multiple observations. First, the effect of dually-inhibiting Hsc70 and Hsp90 is almost the same as for inhibiting Hsc70 alone (*cf.* Chapter 3, Figure 3.12). Furthermore, increasing the flow of clients from Hsc70 to Hsp90 (by over-expressing HOP) has a correspondingly protective effect. This suggests that there is transfer from Hsc70 to Hsp90, and that the latter interaction is dependent on the first, and has a negative influence upon the activation of RTA in the cytosol.

At odds with this, perhaps, it has been observed that Hsp90 can rescue the solubility of thermally-denatured RTA *in vitro*, in isolation from Hsc70 (Spooner *et al*., 2008). This would suggest that RTA and Hsp90 can interact outside of the triage. It remains a quandary why Hsp90 can rescue solubility independently, but cannot facilitate ubiquitination by CHIP without Hsc70/HOP present (Spooner *et al*., 2008). It may be that a specific quality that is necessary for ubiquitination is imposed upon RTA by its prior interaction with Hsc70, or by its transit thereafter to Hsp90. This quality could be a conformational cue that forms during the Hsc70 interaction, which results in a more protracted association with Hsp90, or the imposition of a particular binding orientation which renders the lysines of the polypeptide more accessible to Hsp90-mounted CHIP.

5.11.2 The activity of CHIP will be opposed by multiple cytosolic factors *in vivo*

When RTA was incubated with a cytosolic extract, it appeared that some was degraded in an ALLN-sensitive manner, which might suggest the proteasome degrades RTA in this experimental setup. However, in these incubations, ubiquitin-conjugation could not be observed – suggesting that ubiquitination was not necessary for this degradation,[24] or that such modifications are swiftly removed during conditions of proteasomal inhibition (e.g. by

[24] Ubiquitin-independent routes to the 20S proteasome do exist, especially for disordered or especially denatured substrates (Jariel-Encontre *et al*., 2008).

DUBs). This experiment could be improved by including ubiquitin-aldehyde to block the potential de-ubiquitination of RTA, which might thereafter be observed.

As well as de-ubiquitination, other factors in the cytosol would oppose the ubiquitination of RTA by CHIP e.g. HIP (Höhfeld *et al.*, 1995), HspBP1 (Alberti *et al*., 2004) and BAG-2 (Arndt *et al*, 2005). Here, the inhibitory effect of another co-factor, BAG-5, upon CHIP-mediated ubiquitination was shown for the first time *in vitro*. This compares well with Kalia *et al*. (2004), who report that BAG-5 inhibits another Hsc70-dependent E3 ligase, Parkin. Increasing doses of BAG-5 observably prevented CHIP-mediated ubiquitination of Hsc70, RTA and other test substrates. Thus, the already low-level of RTA ubiquitination that might occur during intoxication would be further attenuated *in vivo*. Arguably, there might equally be pro-ubiquitination co-factors *in vivo* (e.g. E4s) which complicate this scenario.

5.11.3 Does RTA have a lysine-independent mode of avoiding ubiquitination during its interaction with Hsc70?

Data presented in this chapter shows that RTA^{6K} and RTA^{WT} are not ubiquitinated efficiently. In similar experiments with longer exposures, Spooner *et al*. (2008) showed that ubiquitination of RTA^{6K} is increased relative to RTA^{WT}. Curiously, the extensive level of Hsc70-ubiquitination in the assays of Spooner *et al.* (2008), reprinted in Figure 5.6, shows the reaction may be working even more efficiently than was the case for the test substrates which were relatively efficiently ubiquitinated (Tau protein and luciferase, Figure 5.1 and 5.2). Thus, despite being supplemented with non-native lysines, the ubiquitination of RTA^{6K} does not approach the level to which positive controls (Tau protein and luciferase) are polyubiquitinated. That RTA^{6K} remains relatively poorly ubiquitinated implies there might be some quality about the toxin subunit, surprisingly regardless of lysine content, which makes it a poor substrate of Hsc70. This was unexpected, especially as it contrasts to the outcome of the interaction of RTA with the Hsp90·CHIP complex, which is strongly lysine-dependent *in vivo* (*cf*. Chapter 3, Figure 3.18).

To clarify this phenomenon, it would be beneficial to produce an experiment analogous to that conducted in Chapter 3 (Figure 3.18). Experiments could be conducted to test whether the protective effect of DSG differed between holotoxins consisting of reconstituted RTA and RTA^{WT}/RTA^{0K}/RTA^{6K}. This would help determine whether lysine content has a bearing on a potential Hsc70/CHIP mediated ubiquitination *in vivo*, or whether some other factor dominates the process (in which case there would be no difference in effect between

holotoxin variants). Unfortunately, DSG has proved difficult to acquire and degrades swiftly in storage (see appendix, Figure 8.1). For completeness, it would also be interesting to see whether RTA^{6K} responds more strongly *in vitro* to Hsp90/CHIP-mediated ubiquitination than it does to that mediated by Hsc70/CHIP.

Other than a shortage of lysines, it could be that denatured RTA simply does not interact with Hsc70 as strongly as denatured luciferase or Tau protein do, thereby reducing CHIP-mediated ubiquitination. It is an enticing notion that evasion of ubiquitination by RTA whilst bound to Hsc70 may owe as much to a shortened residence in the peptide binding domain of the chaperone as to the reduced lysine content of the toxin subunit. It might be that RTA refolds particularly swiftly in the cytosol with the aid of Hsc70 – subsequently escaping candidacy for a protracted triage where it is in a vulnerable state – so as to avoid any negative interaction with co-chaperones.

This hypothesis of "shortened residency", however, is at odds with an earlier observation: that the hydrophobic C-terminal domain of RTA, part of the native structure of the protein, seems enough to promote interactions with Hsc70. This domain was proposed to engender interactions with RTA even without prior denaturation (*cf.* Chapter 4). It could be speculated that the nature of this binding is distinct from the binding that occurs after heat denaturation. It could be that, without prior denaturation, the C-terminal tail defines the orientation in which RTA binds to Hsc70, ensuring polyubiquitination does not occur efficiently. In the case of liposome treatment, this deterministic, protective C-terminal tail would be hidden in the liposomal core (Mayerhofer *et al*., 2009). After heating, other stretches of extended hydrophobic polypeptide would compete with the C-terminal tail. These regions would not impose the same orientation to the interaction with the chaperone complex, and might predispose the toxin subunit to greater ubiquitination. Indeed, Flynn *et al*. (1991) showed that isoleucine and leucine were favoured for binding in the peptide-binding domain of Hsc70. Encouragingly, the hydrophobic C-terminal domain of ricin is defined as (from V_{245} to V_{256}): VSILIPIIALMV (Simpson *et al*., 1995). Curiously, however, the proline residue in the midst of this region is not favourable for binding Hsc70 (Flynn *et al*., 1991). This might contribute to the peculiarity of the association, which would be interesting to investigate, especially given this residue has been implicated as having an important role in toxicity (Simpson *et al*., 1995).

5.11.4 The role of other co-factors in the putative cytosolic triage of RTA

It was shown that those co-factors which have an explicitly destructive role, e.g. BAG-1 and CHIP, protected cells from ricin intoxication. This fits the model generated so far, as the over-expression of these proteins would be expected to increase the chances that an interaction of RTA with Hsc70 would result in degradation. They would thus promote clearance of RTA from the cytosol, reducing its toxic action therein. The co-chaperone, HOP, also protected cells when over-expressed. This is presumably by promoting interactions of RTA with Hsp90, which were shown to be detrimental for the toxin subunit (Figure 3.4).

On the other hand, BAG-2 and HIP sensitised cells to ricin intoxication. Strangely, these two co-chaperones have opposite modes of interaction with regard to the ATPase cycle of Hsc70. Although they are different in this regard, they are united in their ability to inhibit Hsc70-associated CHIP and in displacing BAG-1 (Arndt *et al*., 2005; Höhfeld *et al*., 1995). Thus, it seems to be this commonality which defines their shared sensitising effect. Unexpectedly, although BAG-5 inhibited Hsc70/CHIP-mediated ubiquitination *in vitro* and possessed its own pro-solubility qualities, over-expression of it protected cells from ricin intoxication. Another property that this co-chaperone possesses, which is consistent with these observations, is its inhibitory effect upon the ATP-dependent solubilising activity of Hsc70. This seems the dominant effect of this co-chaperone *in vivo*. As BAG-2 is also a nucleotide exchange factor of Hsc70 (Arndt *et al*., 2005), but has the opposite effect, there must be some central difference between the two proteins. For instance, the multiplicity of BAG-5's interlinked BAG domains may be responsible for the assembly of a folding complex which has a bias toward degrading the RTA the complex encounters.

5.11.5 Summarising

Chaperone-based triage of RTA in the cytosol is modulated by the co-chaperone concentration. These co-chaperones determine client ubiquitination and the solubilising effect of Hsc70. Additionally, co-factors may act independently as pro-solubility factors (e.g. BAG-5). The diversity of fates that may be imposed by the co-chaperone environment reflects the integral housekeeping roles of these proteins in the cytosol. The homeostatic role of the co-chaperone environment is immensely broad: the functional content of the proteome is defined as much by what is kept appropriately folded, or degraded by proteases, as by what is synthesised at the ribosome.

CHAPTER 6:
Final Discussion

6.0 RTA unfolds to retrotranslocate and is inherently unstable to achieve this

The question posed at the start of this thesis was: how does RTA gain a catalytic conformation in the cytosol after retrotranslocating across the ER membrane? Imposing extra unfolding constraints upon the toxin subunit inhibits cytotoxicity, which is interpreted as evidence that RTA has to unfold substantially during the intoxication process (Beaumelle *et al*., 1998; Argent *et al*., 1994). On the other hand, if the stability of RTA is drastically reduced, it results in its irreversible misfolding and its incontrovertible degradation by a *bona fide* ERAD route (Li *et al*., 2010). RTA is therefore finely-tuned: able to be recognised by ERAD, but – critically – also able to resolve itself from the majority of ERAD substrates which are degraded in the cytosol.

This thesis has made observations which, consistently, highlight how RTA is structurally poised to unfold near physiological conditions. This has been demonstrated by observing changes in the toxin subunit's solubility under various, controlled incubations. First, the toxin subunit is prone to lose solubility at the physiological pH of 7.2 (compared to other pH conditions ranging from 6.4 to 8.0). Second, there is a stark threshold between 37°C and 45°C where increases in temperature result in a dramatic loss of solubility. Corroborating this finding, Argent *et al*. (2000) previously pinpointed a batch-dependent threshold of around 45°C (using circular dichroism) at which RTA becomes a molten globule. Small temperature increases beyond this threshold temperature result in a dramatic disruption of the protein's secondary structure and aggregation. Mayerhofer *et al*. (2009) also identified that, at temperatures of 37°C and above, RTA inserts far more efficiently into microsomal membranes. Thus, a temperature threshold may have significance *in vivo* during intoxication, promoting a membrane interaction that could prompt retrotranslocation.

A RIP closely related to RTA, saporin, does not share its temperature-dependent instability. Moreover, it is not thought to exploit an ERAD route (Vago *et al.,* 2005). Two major differences between these proteins are their respective lysine contents and the presence of RTA's hydrophobic C-terminus. These features are likely to be significant during ERAD (Simpson *et al*., 1998; Deeks *et al*., 2002), and to influence solubility. Thus, they may account for their different routes into the cytosol. Curiously, Deeks *et al*. (2002) note that engineering RTA^{WT} to contain more lysines, producing RTA^{6K}, creates a protein which is

7°C more stable than RTA^{WT} (as determined by the midpoint change in intensity of a 208nm peak, measured by circular dichroism). This additional stability could feasibly contribute to differing retrotranslocation dynamics from the ER lumen. Indeed, Deeks *et al*. (2002) showed that RTA^{6K} is 100-fold less toxic than RTA^{WT}. Most of this effect is thought to result from increased lysine-ubiquitination, leading to proteasomal degradation. However, according to Deeks *et al*. (2002), RTA^{6K} is still 2-fold less toxic than RTA^{WT} when the proteasome is inhibited. This difference in toxicity might reflect the stabilising effect of the additional lysines, which perhaps retards the toxin subunit's exit from the lumen.

Whilst the structural instability of RTA does not compare well with the related saporin, it does share similarity with unrelated cholera toxin and pertussis toxin A chains. Both of these toxic A chains dislocate from the ER of target cells via an ERAD-like mechanism and are unstable in isolation from their respective holotoxins (Pande *et al*., 2007 & 2008). It is thought that this instability promotes their ERAD. Thus, this thesis reports that A-chain instability is a consistent feature of multiple ERAD-dislocating toxins. The cholera toxin field, however, does have a competing argument to explain the co-option of CTA1 onto an ERAD route – beyond its inherent instability. Moore *et al*., (2010) suggest that PDI helps to unfold CTA1, passing it thereafter to the retrotranslocation machinery of the Hrd1 complex. Thus, a toxin subunit's inherent instability can be coupled to chaperone recognition in the lumen. No such unfolding interaction of RTA with PDI has been reported, beyond the role of PDI in reducing the holotoxin (Spooner R.A., personal communication; Spooner *et al*., 2004).

Regardless of what factor initiates ERAD in the ER lumen, CTA1 and pertussis toxin A chain are both ultimately stabilised by cytosolic targets. Pertussis toxin A chain is stabilised in the cytosol by nicotinamide adenine dinucleotide, a proton acceptor required for its toxic activity (Pande *et al*., 2008). Cholera toxin A chain (CTA1), on the other hand, is stabilised by binding to ADP-ribosylating factor 6, ARF6 (Pande *et al*., 2007). In the case of RTA, stabilisation may result from a combination of ribosomal binding (Argent *et al*., 2000) and – this thesis reports – the properties of cytosolic chaperones like Hsc70.

6.1 The role of Hsc70

Inhibition of cytosolic Hsc70 using deoxyspergualin (DSG) results in a ~2-fold protection of HeLa cells from ricin. Hsc70 could be responsible for promoting a catalytic conformation of RTA after dislocation from the ER. Reassuringly, DSG does not alter the lag before the first reduction in protein synthesis is observed during intoxication. This is also the case for the

other chaperone inhibitors used in this thesis. Transport to the translocation-competent compartment is deemed the rate-limiting step of ricin's mechanism (Hudson & Neville, 1987). Thus, the effect of these inhibitor compounds (C01, NECA, DSG, GA & RA) occurs at a point subsequent to this stage. That is, the effect of the chaperones they inhibit occurs after access of the toxin subunit to the translocation-competent compartment.

It seems feasible that DSG abrogates a direct, cytosolic interaction between RTA and Hsc70 *in vivo*. First, it was shown that Hsc70 can prevent RTA from losing solubility after heat-treatment (to 45°C). This *in vitro* buffering effect can be prevented with DSG. Colleagues showed that the rescue of solubility also correlated to the increased enzymatic activity of RTA (Spooner *et al*., 2008). This suggests that Hsc70 preserves the toxin subunit in an active conformation as well as a soluble one. Unexpectedly, an interaction between Hsc70 and RTA was even observed at 37°C, at which the structure of RTA is regarded as native under similar conditions (Argent *et al*., 2000). This interaction is putatively associated with the hydrophobic C-terminus of the toxin subunit and could result in a more prolonged interaction with the chaperone. It is well-known that cytosolic Hsc70 interacts with the hydrophobic N-terminal targeting sequences of proteins destined for export to other compartments (Zara *et al*., 2009). Indeed, the hydrophobic C-terminus of RTA is known to bear some structural resemblance to a signal peptide (Chaddock *et al*., 1995). *In vivo*, a persistent or recurrent interaction of RTA with Hsc70 might prevent the regressive interaction of the toxin subunit with the cytosolic leaflet of the ER membrane. Such a function may be important, given it is thought similar interactions of RTA with the lumenal leaflet of the ER membrane promote its ERAD (Mayerhofer *et al*., 2009). In this sense, Hsc70 could perform a role as NAD does for pertussis toxin A chain, or ARF6 does for CTA1 (Pande *et al*., 2007 & 2008).

Notably, DSG has no effect upon the sensitivity of HeLa cells to diphtheria toxin (Spooner *et al*., 2008), which translocates from endosomes into the cytosol. It could be that the stability of diphtheria toxin A chain is simply such that it is not a candidate for being bound by Hsc70 after its translocation. Indeed, it relies upon endosomal acidification to promote its translocation-competent state, qualities of which will be lost after access to the pH7.2 cytosol (Rodnin *et al*., 2010). Alternatively, it may be that a local concentration of certain J-domain containing proteins at the mammalian ER membrane, like ER-associated Ydj1 or Hlj1 in yeast (Beilharz *et al*., 2003), ensures RTA is subjected to the activity of Hsc70.

This thesis also showed that the Hsc70-associated co-factor, CHIP, can ubiquitinate RTA^{WT} at 37°C, with or without a prior 45°C heat treatment (Spooner *et al*., 2008). A maximum of 3-4 ubiquitin tags was the largest detectable chain length using the techniques in this thesis. This contrasts to other CHIP substrates examined herein: Hsc70, firefly luciferase and mictrotubule-associated tau protein. Curiously, addition of further lysines does not restore RTA to a level of ubiquitination as intense as that observed for the other substrates examined (although it does increase the propensity for ubiquitination slightly – Spooner *et al*. 2008). Explaining this, the frequency of lysines in RTA^{6K} remains only 2.4% of residues, compared to 8.4% and 7.3% of Hsc70 and luciferase residues respectively. Thus, compared to these standards, it actually remains lysine-deficient. Nevertheless, for some substrates only one appropriately-placed lysine is necessary for an extensive ubiquitin chain, e.g. luciferase (Kim *et al*., 2007). Therefore, other features might remain significant in reducing Hsc70·CHIP-mediated polyubiquitination. For example, the frequency and quality of sites which may be bound by Hsc70.

Provocatively, the extent of CHIP-mediated ubiquitination can be increased if RTA^{WT} is first pre-incubated with liposomes made from negatively-charged POPS. These liposomes are similar to those which RTA has been shown to insert into, and which disrupts its secondary structure (Mayerhofer *et al*., 2009). If this lipid-based denaturation plays a role in the retrotranslocation of RTA, then it would appear that it also renders the toxin subunit in a conformation that is particularly vulnerable to ubiquitination. Evidently, the extent of ubiquitination under these conditions is still small. Even so, co-factors *in vivo* might modulate the process. Moreover, the tight association of the proteasome to the ER membrane (Ng *et al*., 2007), where RTA will be transiently localised may substitute for an extensive polyubiquitin signal (Janse *et al*., 2004). Nevertheless, this thesis is clear in showing that the net effect of Hsc70 is to promote the toxicity of RTA rather than its degradation.

Even a low level of ubiquitination can have significant physiological functions. In the context of some recipients, these processes include plasma membrane receptor internalisation and the determination of vesicle sorting (Sun & Chen, 2004). More speculatively, Feldman & van der Goot (2009) hypothesise that low levels of ubiquitination may control iterative cycles of ER-associated chaperone binding (reminiscent of the calnexin/calreticulin cycle in the ER lumen). Participation in this chaperone binding cycle would be controlled by competition between de-ubiquitinating enzymes and ubiquitin ligases. The low levels of ubiquitination RTA might apparently bear after interacting with Hsc70·CHIP could even

dictate such events in a fashion which benefits its toxicity. The putative involvement of such factors in ricin intoxication may be a good target for future study. Indeed, many proteins could be fine-tuned to auto-regulate their ubiquitination, optimising their chaperone-binding properties.

6.2 The role of Hsp90

If Hsp90 is inhibited, cells become sensitised to ricin (by ~2-3-fold). Supporting this observation, if the co-chaperone which links Hsc70 and Hsp90 together, HOP, is over-expressed, cells are protected. This is putatively because of the increased transfer of clients from Hsc70 to Hsp90 – clients which could include RTA. The idea of Hsc70 working in a *sequential* triage with Hsp90 is supported by the effects of dual Hsc70/Hsp90 inhibition, which is the same effect as Hsc70 inhibition alone (Spooner *et al*., 2008). An interaction of RTA with Hsp90 *in vivo* may be dependent upon one with Hsc70 first.

The sensitising effect of Hsp90 inhibition is greatly amplified when RTA is engineered to contain additional lysines. Moreover, it is abrogated when it has none. This implies that the effect of Hsp90 is mediated by lysine-ubiquitination. RTA could be ubiquitinated by CHIP in the context of Hsp90 binding. Alternatively, Hsp90 might maintain the stability of a third party, such as an E3 ligase complex, which ubiquitinates RTA. If there is such a third-party complex, it would have to be sufficiently labile to become dysfunctional within a timeframe defined by toxin trafficking (roughly an hour), as sensitisation is observed after coeval application of chaperone inhibitor and toxin. Fitting a direct ubiquitination by Hsp90·CHIP, colleagues have published results showing that, when an incubation of RTA/Hsc70/CHIP (with other, essential, components of the ubiquitination cascade) is supplemented with additional HOP/Hsp90, more efficient ubiquitination ensues (Spooner *et al*., 2008). Hsp90 may direct RTA to degradation by the 26S proteasome.

Unexpectedly, these observations contrast to what is known of the A chain of cholera toxin. CTA1 has been shown to dislocate into the cytosol assisted by a complex containing Hsp90 (Taylor *et al*., 2010). Thus, in the context of CTA1, Hsp90's activity seems to be opposite. CTA1 retrotranslocation is diminished in cells inhibited by geldanamycin and is blocked when Hsp90 is depleted using RNAi (Taylor *et al.*, 2010). Either Hsp90 maintains the stability of a third-party, such as the pore, or else it participates directly in retrotranslocation. This compares well to Giodini & Cresswell's (2008) report that Hsp90 assists the ERAD-like retrotranslocation of exogenous luciferase into the cytosol of dendritic cells. The Hsp90-

regulated routes taken by both RTA and CTA1 contrast to diphtheria toxin. In the case of this endosome-translocating toxin, Hsp90 does not appear to be involved at all, as geldanamycin and radicicol have no effect upon intoxication (Spilsberg *et al*., 2005). Indeed, investigators have shown that diphtheria toxin can dislocate its catalytic activity across reconstituted lipid bilayers independently of cytosolic factors (Ren *et al*., 1999; Oh *et al*., 1999). Conversely, Hsp90 is vital to the translocation of other proteins from endosomes. Ratts *et al*. (2003) show that translocation of a diphtheria toxin and IL-2 construct is assisted by Hsp90. This non-native, engineered construct apparently becomes a candidate for the extracting activity of Hsp90. Another example of an endosome-translocating protein dependent on Hsp90 is HIV-1 *trans*-activating protein, Tat (Vendeville *et al*., 2004). Fibroblast growth factors FGF-1 and FGF-2 also translocate from endosomes into the cytosol and are prevented from doing so by pre-treatment of cells with radicicol and geldanamycin (Wesche *et al*., 2006). Finally, Haug *et al.* (2004) showed that the toxic activities of two AB-toxins from *Clostridium perfringens* (Iota toxin) and *Clostridium difficile* (an ADP-ribosyltransferase) are dependent on Hsp90. They show that radicicol protects cells from toxin-induced apoptosis. These proteins may all become unstable in acidified endosomes, leading to their interaction with the membrane of the compartment and dislocation by an 'endosome-associated degradation' route.

So, why might Hsp90 have such a different, opposite, role in ricin intoxication? First, RTA retrotranslocates from the ER and so the localisation of assisting protein factors will be different from those operating at the endosome. This does not explain the difference between RTA and CTA1, however. Ultimately, it may be that RTA is simply a client which Hsp90 is more likely to recognise as terminally misfolded, perhaps because of the context of a prior triage by Hsc70. RTA may have evolved to exploit Hsc70 instead of Hsp90. Alternatively, CTA1 may, itself, be particular in requiring Hsp90 to orientate its assembly into a stable complex with cytosolic ARF6 (Pande *et al*., 2007).

6.3 Long term Hsp90 inhibition changes the dynamics of cytosolic quality control

When cells were incubated with Hsp90 inhibitors for longer periods of time (up to 16-hour), the effect of the treatment upon ricin intoxication makes a transition from sensitisation to protection. It is unclear what this is caused by, but suggestions can be made, for instance: the up-regulation of inducible Hsp70, or potentially the reconfiguration of the proteasome. Both of these explanations provoke new questions. If the change in effect results from Hsp70 up-

regulation, it would appear that it has a discrete activity from Hsc70 in handling RTA. Such a difference would not be without precedent, such as in the case of epithelial sodium channels (Goldfarb *et al.*, 2006). If this is the case, it seems Hsc70 is a positive regulator of RTA activity, whilst Hsp70 is a negative regulator. On the other hand, the protective effect could result from reduction in the steady-state level of the proteasomal cap, which is coincident with chronic Hsp90 inhibition (Imai *et al*., 2003). In yeast, of course, the proteasomal cap is thought to facilitate extraction of RTA (Li *et al*., 2010), and therefore this may be evidence of a similar role in mammals. Alternatively, chronic inhibition of Hsp90 may change the dynamics of the laterally-integrated chaperone network in other ways. This could result in diversion of RTA to chaperone machineries which promote inactivation rather than activation.

6.4 A role for Grp94

Inhibition of Grp94 with NECA results in protection of cells from ricin intoxication. However, as with Hsp90, it is not apparent whether this results from a direct interaction. In a direct interaction, Grp94 might keep RTA soluble and *ready* for retrotranslocation, or else direct it to downstream effectors of ERAD. This finding would be consistent with the role ascribed to Grp94 in gating substrate access to Hrd1 complexes (Christianson *et al*., 2008). It would be a pleasing symmetry if lumenal Grp94 recognises RTA as misfolded and directs it to an ERAD pathway (leading to toxicity), whilst Hsp90 recognises RTA as misfolded and directs it to the proteasome (leading to reduction in toxicity). However, this is certainly not necessarily the case: Taylor *et al*. (2010) report that Grp94 has no effect upon the Hsp90-dependent retrotranslocation of CTA1, for instance. As described previously, PDI is thought to have a role in unfolding CTA1 ahead of its ERAD. It could be that Grp94 fulfils or contributes to this role in the context of RTA.

6.5 Manipulation of Hsc70/Hsp90 co-factors alters the dynamics of the triage

Demonstrating the dynamism of the cytosolic chaperone network, manipulating the concentration of Hsc70 and Hsp90's co-factors alters the sensitivity of cells ricin. Over-expressing a chaperone-dependent E3 ubiquitin ligase, CHIP, leads to protection of cells from ricin. Presumably this is because it leads to greater ubiquitination of retrotranslocated RTA, and complexes of chaperones bound to RTA. This would result in the attraction of the proteasome, which could degrade the toxic A chain. Consistently, over-expression of a co-chaperone which co-operates with Hsc70·CHIP to attract the proteasome, BAG-1 (Alberti *et*

al., 2003; Alberti *et al*., 2004), also protects cells from ricin. Over-expressing an antagonist of both BAG-1 and CHIP, BAG-2 (Arndt *et al*., 2005), has an appropriately opposite effect, sensitising cells to ricin. Finally, over-expression of HIP also leads to sensitisation, putatively by prolonging an Hsc70·RTA complex, enhancing the success of the folding it is hypothesised to promote. This is the attributed effect of HIP for Hsc70 clients like the archetypal firefly luciferase (Lüders *et al*., 1998), and so it seems a reasonable suggestion to make.

These results point to the flexibility of the chaperone network, reinforcing the concept that the aetiology of many misfolding diseases will be polygenetic (Csermely, 2001). That is: the severity of a disease phenotype will be based upon the nature of a patient's chaperone network, as well as the nature of the misfolding protein regarded to be at fault. This could be manifest in multiple ways: from overly-stringent degradation to overly-lax recognition of conformational faults. Csermely (2001) also argues that if a chaperone network is too-efficient at masking the faults of a mutated protein, their negative effects could be manifested later at times of stress or old age – producing so-called 'civilisation diseases'.

6.6 Characterisation of BAG-5, a co-chaperone of Hsc70

BAG-5 is one of the least well-studied co-chaperones of the BAG-domain family (Kalia *et al*., 2004). This thesis has demonstrated the inhibitory effect of this protein upon CHIP-mediated ubiquitination. BAG-5 can prevent the ubiquitination of both Hsc70 and client. This effect is much like what is reported for the related protein, BAG-2. In isolation, it appears that BAG-5 also has a pro-solubility effect upon RTA – a function which might translate to other substrates. However, BAG-5 inhibits the ability of Hsc70 to keep RTA soluble. As BAG-5 increases relative to Hsc70, its own ability to maintain the solubility of RTA eclipses this inhibitory effect on Hsc70. BAG-5 may operate like this *in vivo* as a general regulator of Hsc70 function. *In vivo,* however, its concentration will be less than that of the abundant Hsc70.

6.7 Fitting these interactions into a wider context: at what stage would the chaperone interaction with RTA occur?

The results of trafficking assays would imply the effect of chaperone inhibition happens after the entry of the toxin into the ER. Li *et al*. (2010) showed that when RTA is targeted to the cytosol of yeast, without prior import into the ER, it is not degraded to a significant degree.

This suggests that a process is required to render RTA vulnerable to degradation – such as ER retrotranslocation. The unfolding involved in such a process might make RTA vulnerable to Hsp90-mediated inactivation.

With reference to Figure 6.1, RTA may be ubiquitinated to a low degree as it emerges from the ER membrane. This could be facilitated by a core E3 ubiquitin ligase-associated complex from which the toxin subunit might emerge. However, this modification is not efficient enough to ensure all RTA is degraded by the proteasome. Moreover, Li *et al*. (2010) show that lysine-ubiquitination is not necessary for retrotranslocation in yeast. The retarded or attenuated ubiquitination that may result from RTA's resistance to the modification may weaken subsequent interactions of the toxin subunit with both p97 and the proteasome. This may permit de-ubiquitinating enzymes and eventually Hsc70 to intercede instead. A low level of ubiquitination may occur again at this stage (e.g. mediated by CHIP), but this is also not enough to ensure all encountered RTA is sent to the proteasome. Instead, net interactions with Hsc70 permit RTA a greater chance to gain a catalytic conformation. Potentially Hsc70 could also help to pull the protein away from the membrane – by an entropic-pulling mechanism (De Los Rios *et al*., 2006). Thereafter, RTA would be entered into a soluble phase of audit by cytosolic quality control. Alternatively, Hsc70 might capture an unfolded form of RTA that has been released from the membrane by p97 or the proteasomal cap. After RTA folds into its native state, it has been noted that it is strikingly resistant to proteases (Argent *et al*. 2000), which may prevent the protein from being vulnerable to degradation after this stage. Extending this idea, it remains a possibility that RTA folds in a different way after being exposed to a retrotranslocation step. The ER-dislocation of calreticulin into the cytosol from the ER makes an interesting precedent in this regard. Afshar *et al*. (2005) showed that calreticulin becomes strikingly resistant to proteases after dislocation. They also show that this phenomenon was independent of the different calcium concentrations of the ER lumen and the cytosol, suggesting an intrinsic change to the protein was responsible rather than the surrounding environment. A similar phenomenon might be of great benefit to the toxic motive of RTA.

6.8 Broader relevance: escape from ERAD may be a common theme

The wider significance of this recovery pathway potentially extends to substrates beyond RTA. The escape of RTA from ERAD may reflect a more universal antagonism between the degradation of protein and the capability to refold it. Many chaperones of the cytosol have

evolved as generalists, with broad specificity by evolutionary design. Only a few barriers may exist to preserve retrotranslocated ER protein from being 'reactivated' in the cytosol by these cytosolic generalists. One obstruction may be swift degradation by ER-tethered proteasomes (Ng *et al*., 2007). Another may be the packaging of retrotranslocated protein into quality-controlled inclusions whose interface with the cytosolic milieu is carefully controlled (Bagola & Sommer, 2008). Of course, the ultimate barrier will be whether that protein was selected for ERAD because of terminal misfolding (such as caused by mutation and oxidative damage) rather than transient misfolding (in the case of a kinetically-trapped folding intermediate).

RTA happens to represent a unique example where its liberation from a 'masqueraded' misfolded state after retrotranslocation results in a very toxic activity. Thus, it highlights the presence of a normally obscure pathway allowing a protein's escape beyond the barriers mentioned. Multiple routes to reactivation may exist, but one route has been identified: an Hsc70-dependent mechanism. Other retrotranslocated ER proteins with more benign activities may, similarly, be reactivated in the cytosol by Hsc70. Indeed, calreticulin is known to retrotranslocate from the ER into the cytosol in physiologically significant concentrations (Afshar *et al*., 2005). A substrate's success in doing this would be determined by its propensity to become ubiquitinated, to be degraded, to refold, and the cytosolic context of chaperones and co-factors. Although the contribution of these reactivated proteins to the overall composition of the cytosol might be minuscule, this process might not be without essential significance. Needless to say, the role of this process will be especially interesting for proteins with exquisite catalytic activities, like RTA. RTA will remain a very useful toxic probe with which to test these putative pathways.

Figure 6.1 - A model for the triage of RTA by cytosolic chaperones.

The following figure borrows some styling from the Cell Snapshot of Kawaguchi & Davis (2007). It summarises the putative interaction of RTA with tested lumenal and cytosolic chaperones during the retrotranslocation process. In the ER lumen, Grp94 may be responsible for preparing RTA (or the pore) for retrotranslocation. After dislocation, Hsc70 intercepts RTA which is not immediately sent to the proteasome. Hsc70 can potentially do several things to RTA: ubiquitinate it and send it to the proteasome under the auspices of CHIP & BAG-1; release it, folded to the cytosol where it can depurinate ribosomes; or, pass it, via HOP, to Hsp90. Hsp90 may then also help RTA to refold or else send it for degradation via CHIP-mediated ubiquitination. Presumably, lateral co-operation between other chaperones of the cytosol may also operate, allowing audit of RTA by a wide variety of chaperones. Red indicates factors preventing toxicity of RTA; green indicates factors promoting activity. Broad, forking arrows indicate the proposed sequence of interactions.

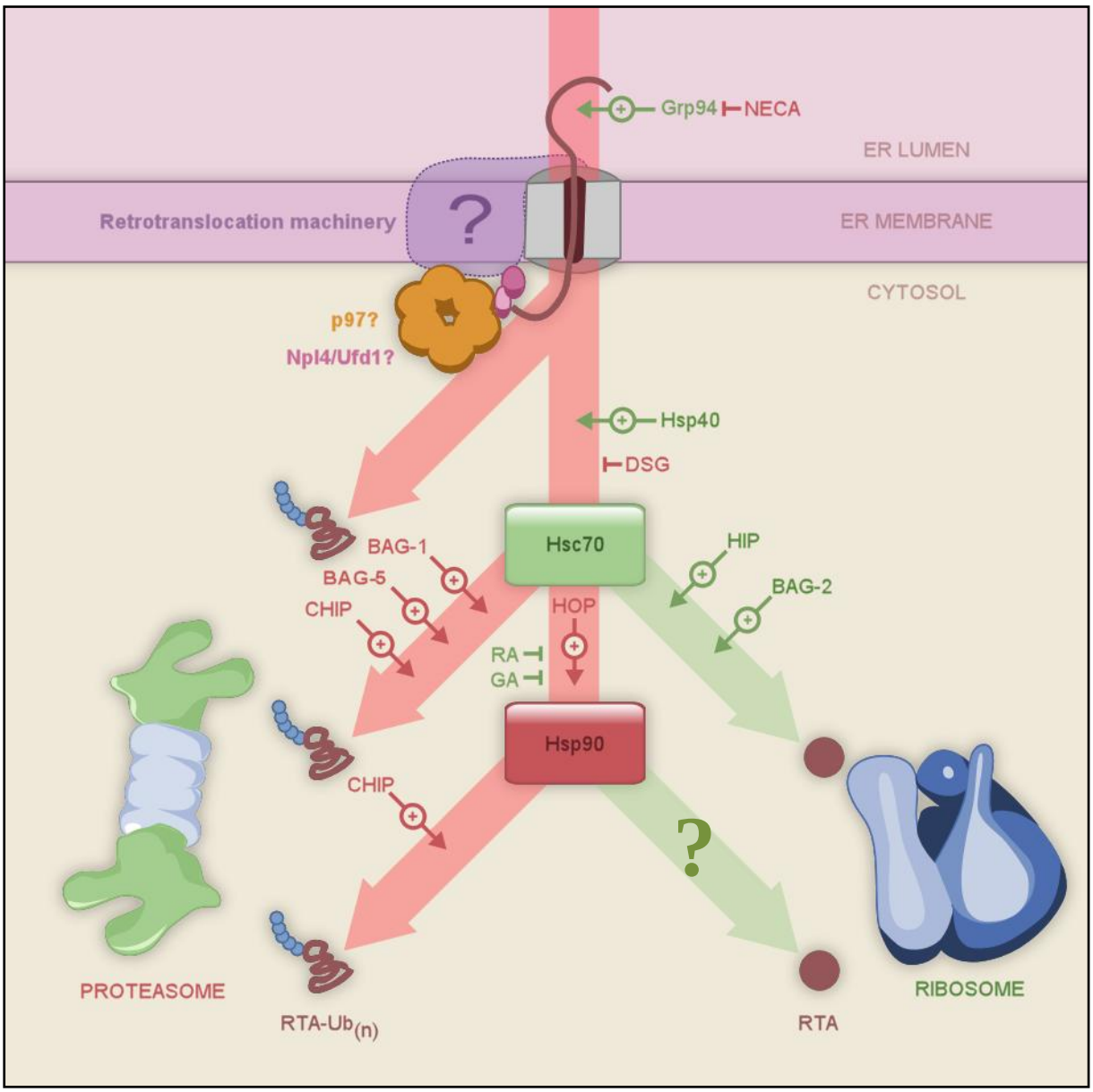

6.9 Further research

Research derived from the findings of this thesis could go in a number of directions. Much of it could pursue further elaboration of the reactivation pathway which RTA undertakes, using different iterations of the inhibitor experiments and targeted manipulation of the chaperone machineries involved (knocking-down with RNAi, for instance). It would be interesting to see whether Hsp90 inhibition is redundant with proteasomal inhibition, which would test whether the chaperone does direct RTA to this proteolytic machine. It would also be interesting to see whether the effect of DSG upon the cytotoxicity of ricin changes according to the lysine content of the holotoxin.

The solubility assay could be refined by pre-blocking reaction tubes with relatively inert protein or silane. This assay could be re-appropriated to screen for pro-solubility (or pro-aggregation) factors by incubating an indicator protein (such as RTA) with fractions of cytosol. Fractions could be subjected to iterative rounds of testing and division, eventually identifying individual factors. Cytosolic extracts could also be made from cultures over-expressing particular co-chaperones. If the method for producing the extract could be made systematic enough, this would allow the cross-comparison of how different co-chaperones (in the context of a cytosolic mix) may influence the solubility of an indicator protein *in vitro.* A similar screening approach could be tailored to examine whether factors of the cytosol could bolster or inhibit ubiquitination of RTA. It would also be interesting to see whether CHIP-ubiquitinated RTA can be degraded *in vitro* by 26S proteasomes and whether cytosolic factors can be identified which augment that process.

Examining whether Hsc70 and Hsp90 play different roles in other organisms and for a variety of toxins would also be an interesting topic of study and would test how universal the pathway is. As yeast is genetically tractable, it would be an interesting platform upon which to base these future experiments. However, redundancy in the chaperone network may mean that the effects of knockouts might not be as convincing as targeting members of the Hrd1 complex (as in Li *et al*., 2010). Moreover, gross qualitative differences might be anticipated. The differential involvement of Cdc48 in yeast and plants in the ERAD of RTA, for example, is a prime example of the disparate retrotranslocation mechanisms than can exist between the kingdoms of life (Li *et al*., 2010; Marshall *et al*., 2008). Essential differentiation would therefore be predicted. The ATPase turnover of mammal Hsp90, for instance, is reportedly

10-fold higher than that of yeast (Vaughan *et al*., 2008) and there is no CHIP in yeast. These disparities would possibly change the dynamics of the reactivation pathway entirely.

This thesis has also discussed the hydrophobic C-terminus of RTA. It would be interesting to determine specifically what roles this domain has *in vivo*. For instance roles in dictating chaperone interactions, dictating ubiquitination and promoting membrane insertion. A therapeutic polypeptide might even be designed which binds to this region of RTA, inhibiting retrotranslocation and even the Hsc70-interaction. Although, given RTA can separate itself from RTB in the lumen (with the help of PDI - Spooner *et al*., 2006), it might similarly separate from such a polypeptide. Lastly, the lumenal homologue of Hsp90, Grp94, has been suggested to work in the lumen to prepare RTA for retrotranslocation. If this is the case, BiP may also be worth investigating – as the lumenal homolog of Hsc70. However, in previous immuno-precipitation attempts with RTA, BiP has not been identified (Day *et al*., 2001). Moreover, BiP and Hsc70 do not complement each other effectively in reconstitutions of ERAD using microsomes (Brodsky *et al*., 1993). Therefore, they may have functionally differentiated in such a way as not to have a symmetrical operation across the membrane.

6.10 A Final Summary

At a stage proximal to its retrotranslocation across the ER membrane, RTA interacts with chaperones in a way that differentiates it from ERAD substrates doomed to degradation. After RTA has unfolded to cross the membrane, an interaction of it with Hsc70 seems to promote its successful cytosolic refolding. The relative balance of Hsc70's cofactors in the cytosol determines the success of this step: whether the protein is ubiquitinated, freed in a folded conformation, or else transferred to Hsp90 (Figure 6.1). Thereafter, Hsp90 seems to promote the toxin subunit being sent to the proteasome, a feat which is reliant upon the lysine-ubiquitination of RTA. This feat may well be indicative of a competition that exists in the cytosol between degradation and refolding for other substrates of the ERAD process. It emphasises the possibility that escapees from ERAD may occur more broadly, given the right substrate qualities and a permissive context of cytosolic chaperones.

CHAPTER 7

References

AFSHAR N., BLACK B.E., PASCHAL B.M., 2005, *Retrotranslocation of the chaperone calreticulin from the endoplasmic reticulum to the cytosol*, Molecular Cell Biology, 25(20):8844-53.

ALBERTI S., BÖHSE K., ARNDT V., SCHMITZ A., HÖHFELD J., 2004, *The cochaperone HspBP1 inhibits the CHIP ubiquitin ligase and stimulates the maturation of the cystic fibrosis transmembrane conductance regulator*. Molecular Biology of the Cell, 15(9):4003-10.

ALBERTI S., DEMAND J., ESSER C., EMMERICH N., SCHILD H., HÖHFELD J., 2002, *Ubiquitylation of BAG-1 suggests a novel regulatory mechanism during the sorting of chaperone substrates to the proteasome*. Journal of Biological Chemistry, 277(48):45920-7.

ALBERT S., ESSER C., HÖHFELD J., 2003, *BAG-1—a nuclear exchange factor of Hsc70 with multiple cellular functions.* Cell Stress Chaperones, 8(3):225-31.

ALEXANDER J., BENFORD D., COCKBURN A., CRAVEDI J.P., DOGLIOTTI A.D., FERNANDEZ-CRUZ M.L., FURST P., FINK-GREMMELS J., LODOVICO G., GRANDJEAN P., GZYL J., HEINEMEYER G., JOHANSSON N., MUTTI A., SCHLATTER J., LEEUWEN R., PETEGHEM C., VERGER P., 2008, *Scientific Opinion of the Panel on Contaminants in the Food Chain on a request from the European Commission on ricin (from Ricinus communis) as undesirable substances in animal feed.* The EFSA
Journal, 726:1-38.

ARGENT R.H., PARROTT A.M., DAY P.J., ROBERTS L.M., STOCKLEY P.G., LORD J.M., RADFORD S.E., 2000, *Ribosome-mediated Folding of Partially Unfolded Ricin A-chain.,* The Journal of Biological Chemistry, 275(13):9263-9269.

ARGENT R.H., ROBERTS L.M., WALES R., ROBERTUS J.D., LORD J.M., 1994, *Introduction of a disulfide bond into ricin A chain decreases the cytotoxicity of the ricin holotoxin*, Journal of Biological Chemistry, 269:26705-26710.

ARNDT V, DANIEL C, NASTAINCZYK W, ALBERTI S, HÖHFELD J., 2005, *BAG-2 acts as an inhibitor of the chaperone-associated ubiquitin ligase CHIP*. Molecular Biology of the Cell, 16(12):5891-900.

AUSTIN C.D., DE MAZIÈRE A.M., PISACANE P.I., VAN DIJK S.M., EIGENBROT C., SLIWKOWSKI M.X., KLUMPERMAN J., SCHELLER R.H., 2004, *Endocytosis and Sorting of ErbB2 and the Site of Action of Cancer Therapeutics Trastuzumab and Geldanamycin*, Molecular Biology of the Cell, 15:5268-82.

BAENZIGER, J.U. AND FIETE, D., 1979, *Structural Determinants of* Ricinus communis *Agglutinin and Toxin Specificity for Oligosaccharides.* The Journal of Biological Chemistry 254(19):9795-9799.

BAGOLA K. & SOMMER T., 2008, *Protein Quality Control: On IPODs and other JUNQ.* Current Biology, 18(21):R1019-R1021.

BALLINGER C.A., CONNELL P., WU Y., HU Z., THOMPSON L.J., YIN L.Y., PATTERSON C., 1999, *Identification of CHIP, a novel tetratricopeptide repeat-containing protein that interacts with heat shock proteins and negatively regulates chaperone functions*. Molecular Cell Biology, 19(6):4535-45.

BARZILAY E., BEN-CALIFA N., SUPINO-ROSIN L., KASHMAN Y., HIRSCHBERG K., ELAZAR Z., NEUMANN D., 2004, *Geldanamycin-associated inhibition of intracellular trafficking is attributed to a co-purified activity.* The Journal of Biological Chemistry, 279(8):6847-6852.

BAZIRGAN O.A. & HAMPTON R.Y., 2008, *Cue1p is an activator of Ubc7p E2 activity in vitro and in vivo*. Journal of Biological Chemistry, 283(19):12797-810.

BEAUMELLE B., TAUPIAC M.P., LORD J.M., ROBERTS L.M., 1997, *Ricin A chain can transport unfolded dihydrofolate reductase into the cytosol.*, Journal of Biological Chemistry, 272(35):22097-102.

BEILHARZ T., EGAN B., SILVER P.A., HOFMANN K., LITHGOW T., *Bipartite signals mediate subcellular targeting of tail-anchored membrane proteins in Saccharomyces cerevisiae*, The Journal of Biological Chemistry, 278(10):8219-23.

BEISSINGER M., BUCHNER J., 1998, *How chaperones fold proteins.* Biological Chemistry, 379(3):245-59.

BERNARDI K.M., FORSTER M.K., LENCER W.I., TSAI B., 2008, *Derlin-1 Facilitates the Retro-Translocation of Cholera Toxin*. Molecular Biology of the Cell, 19(3):877-884.

BERNARDI K.M., WILLIAMS J.M., KIKKERT M., VAN VOORDEN S., WIERTZ E.J., YE Y., TSAI B., 2010, *Molecular Biology of the Cell*, 21(1):140-51.

BORDALLO J. & WOLF D.H., 1999, *A RING-H2 finer motif is essential for the function of Der3/Hrd1 in endoplasmic reticulum associated degradation in the yeast Saccharomyces cerevisiae.* FEBS Letters 448(2-3):244-8.

BRAMBILLA R., CATTABENI F., CERUTI S., BARBIERI D., FRANCESCHI C., KIM Y.C., JACOBSON K.A., KLOTZ K.N., LOHSE M.J., ABBRACCHIO M.P., 2000, *Activation of the A3 adenosine receptor affects cell cycle progression and cell growth.* Naunyn Schmiedebergs Arch Pharmacology, 361(3):225-34.

BRAUWEILER A., LORICK K.L., LEE J.P., TSAI Y.C., CHAN D., WEISSMAN A.M., DRABKIN H.A., GEMMILL R.M., 2007, *RING-dependent tumor suppression and G2/M arrest induced by the TRC8 hereditary kidney cancer gene.* Oncogene, 26(16):2263-71.

BRODSKY J.L., 1999, *Selectivity of the molecular chaperone-specific immunosuppressive agent 15-deoxyspergualin: modulation of Hsc70 ATPase activity without compromising DnaJ chaperone interactions.*, Biochemical Pharmacology, 57(8):877-80.

BRODKSY J.L., 2007, *The protective and destructive roles played by molecular chaperones during ERAD.* Biochemical Journal, 404(3):353-63.

BRODSKY J.L., HAMAMOTO S., FELDHEIM D., SCHEKMAN R., 1993, *Reconstitution of protein translocation from solubilised yeast membranes reveals topologically distinct roles for BiP and cytosolic Hsp70.* Journal of Cell Biology, 120(1):95-102.

BRODSKY J.L., & PIPAS J.M., 1998, *Polyomavirus T Antigens: Molecular Chaperones for Multiprotein Complexes*, Journal of Virology, 72(7):5329-34.

BUCHNER J., 1999, *Hsp90 & Co. – a holding for folding*. TRENDS in Biochemical Science, 24:126-141.

BUKAU B. & HORWICH A.L., 1998, *The Hsp70 and Hsp60 Chaperone Machines*, Cell, 92:351-366.

BURDON R.H., SLATER A., MCMAHON M., CATO A.C.B., 1982, *Hyperthermia and the heat-shock proteins of HeLa cells*. British Journal of Cancer, 45:953-963.

BUTTERWORTH A.G. & LORD J.M., 1983, *Ricin and ricinus communis agglutinin subunits are all derived from a single-sized polypeptide precursor.* European Journal of Biochemistry, 137(1-2):57-65.

CALVIN S., WANG J., EMCH J., PITZ S., JACOBSEN L. 2006, *FuGene 6 HD Transfection Reagent: Choice of a Transfection Reagent with Minimal Off-Target Effect as Analyzed by Microarray Transcriptional Profiling*. Biochemica (Gene Expression), 4:22-25.

CALLAHAN M.K., CHAILLOT D., JACQUIN C., CLARK P.R., MÉNORET A., 2002, *Differential Acquisition of Antigenic Peptides by Hsp70 and Hsc70 under Oxidative Conditions*. The Journal of Biological Chemistry, 277(37):33604-33609.

CAPLAN A.J., 1999, *Hsp90's secrets unfold; new insights from structural and functional studies.* Trends in Cell Biology, 9:262-268.

CARRELLO A., ALLAN R.K., MORGAN S.L., OWEN B.A., MOK D., WARD B.K., MINCHIN R.F., TOFT D.O., RATAJCZAK T., 2004, *Interaction of the Hsp90 cochaperone cyclophilin 40 with Hsc70.* Cell Stress Chaperones, 9(2):167-81.

CARVALHO P., GODER V., RAPOPORT T.A., 2006, *Distinct ubiquitin-ligase complexes define convergent pathways for the degradation of ER proteins*. Cell. 126(2):361-73.

CASEY J., 2007, *World Climate Index*, published at: climate-charts.com, which procedurally compiles data from the World Meteorological Organization (a venture of the United Nations).

CASHIKAR A.G., DUENNWALD M., LINQUIST S., 2005, *A chaperone pathway in protein disaggregation* , The Journal of Biological Chemistry, 280(25):23869-75.

CHADDOCK J.A., ROBERTS L.M., 1993, *Mutagenesis and kinetic analysis of the active site Glu177 of ricin A chain.* Protein Engineering, Design and Selection. 6:425-431.

CHADDOCK J.A., ROBERTS L.M., JUNGNICKEL B., LORD J.M., 1995, *A hydrophobic region of ricin A chain which may have a role in membrane translocation can function as an efficient noncleaved signal peptide.* Biochemical and Biophysical Research Communications, 217(1):68-73.

CHANG Y.S., LEE L.C., SUN F.C., CHAO C.C., FU H.W., LAI Y.K., 2006, *Involvement of calcium in the differential induction of heat shock protein 70 by heat shock protein 90 inhibitors, geldanamycin and radicicol in human non-small cell lung cancer H460 cells. Journal of Cell Biochemistry*, 97(1):156-65.

CHAUDRY G.J., FULTON R.J., DRAPER R.K., 1993, *A Variant of Exotoxin A That Forms Potent and Specific Chemically Conjugated Immunotoxins*, The Journal of Biological Chemistry, 268(13):9437-9441.

CHEN, A., ABUJAROUR, R.J., DRAPER, R.K., 2003, *Evidence that the transport of ricin to the cytoplasm is independent of both Rab6A and COPI*. Journal of Cell Science, 16(17):3503-3510.

CHEN B., PIEL W.H., GUI L., BRUFORD E., MONTEIRO A., 2005, *The Hsp90 family of genes in the human genome: insights into their divergence and evolution*., Genomics, 86(6):627–37.

CHEN C.Y., & BALCH W.E., 2006, *The Hsp90 chaperone complex regulates GDI-dependent Rab recycling.* Molecular Biology of the Cell, 17(8):3494-507.

CHEN C.Z., WHITE R.F., ANTONIW J.F., LIN Q., 1991, *Effect of pokeweed antiviral protein (PAP) on the infection of plant viruses.* Plant Pathology, 40(4):612-620.

CHUBA P.S., PALCHAUDHURI S., 1986, *Requirement for cysteine in the color silver staining of proteins in polyacrylamide gels.* Analytical Biochemistry, 156(1):136-139.

CITORES L., DE BENITO F.M., IGLESIAS R., FERRERAS J.M., ARGUESO P., JIMENEZ P., TESTERA A., CAMAFEITA E., MENDEZ E., GIRBES T., 1996, *Isolation and characterisation of a new non-toxic two-chain ribosome inactivating protein from Fruits of Elder (*Sambucus nigra L.*)*. Journal of Experimental Botany, 47:1577-1585.

CHRISTIANSON J.C., SHALER J.A., TYLER R.E., KOPITO R.R., 2008, *OS-9 and GRP94 deliver mutant α1-antitrypsin to the Hrd1-SEL1L ubiquitin ligase complex for ERAD.* Nature Cell Biology, 10(3):272-282.

CINTRON N.S., TOFT D., 2006, *Defining the Requirements for Hsp40 and Hsp70 in the Hsp90 Chaperone Pathway*, Journal of Biological Chemistry, 28(36):26235-26244.

CLEMENS W.M., Jr., MENETRET J.F., AKEY C.W., RAPOPORT T.A., 2004, *Structural insight into the protein translocation channel.* Current Opinions in Structural Biology, 14:390-396.

CONNELL P., BALLINGER C.A., JIANG J., WU Y., THOMPSON L.J., HÖHFELD J., PATTERSON C., 2001, *The co-chaperone CHIP regulates protein triage decisions mediated by heat-shock proteins.* Nature Cell Biology, 3(1):93-6.

CORSI A.K., SCHEKMAN., R., 1996, *Mechanism of Polypeptide Translocation into the Endoplasmic Reticulum*. Journal of Biological Chemistry, 271:30299-30302.

CSERMELY P., 2001, *Chaperone overload is a possible contributor to 'civilization diseases'*, Trends in Genetics, 17(12):701-704.

CSERMELY P., SCHNAIDER T., SÖTI C., PROHÁSZKA Z., NARDAI G., 1998, *The 90-kDa Molecular Chaperon Family: Structure, Function, and Clinical Applications. A Comprehensive Review.* Pharmacology and Therapeutics. 79(2):129-168.

DAI Q., QIAN S.B., MCDONOUGH H., BORCHERS C., HUANG D., TAKAYAMA S., YOUNGER J.M., RUN H.Y., CYR D.M., PATTERSON C., 2005, *Regulation of the cytoplasmic quality control protein degradation pathway by BAG2*, The Journal of Biological Chemistry, 280(4):38673-81.

DAY P.J., PINHEIRO T.J.T, ROBERTS L.M., LORD J.M., 2002, *Binding of Ricin A-Chain to Negatively Charged Phospholipid Vesicles Leads to Protein Structural Changes and Destabilizes the Lipid Bilayer*, Biochemistry, 41(8):2836-43.

DECAPRIO J.A., 1998, *The Role of the J-domain of SV40 Large T in Cellular Transformation*. Biologicals, 27(1):23-28.

DEEKS E.D., COOK J.P., DAY P.J., SMITH D.C., ROBERTS L.M., LORD J.M., 2002, *The low lysine content of ricin A chain reduces the risk of proteolytic degradation after translocation from the endoplasmic reticulum to the cytosol*, Biochemistry , 12;41(10):3405-13.

DE LOS RIOS P., BEN-ZVI A., SLUTSKY O., AZEM A., GOLOUBINOFF P., 2006, *Hsp70 chaperones accelerate protein translocation and the unfolding of stable protein aggregates by entropic pulling*, Proceedings of the National Academy of Science (USA), 103(16):6166-71.

DELABARRE B., CHRISTIANSON J.C., KOPITO R.R., BRUNGER A.T., 2006, *Central pore residues mediate the p97/VCP activity required for ERAD*, Molecular Cell, 22(4):451-462.

DEMAND J., LÜDERS J., HÖHFELD J., 1998, *The Carboxy-Terminal Domain of Hsc70 Provides Binding Sites for a Distinct Set of Chaperone Cofactors*, Molecular Cell Biology, 18(4):2023-2028.

DEMAND J., ALBERTI S.., PATTERSON C., HÖHFELD J., 2001, *Cooperation of a ubiquitin domain protein and an E3 ligase during chaperone/proteasome coupling*. Current Biology. 11(20):1569-77.

DI COLA A., FRIGERIO L., LORD J.M., CERIOTTI A., ROBERTS L.M., 2001, *Ricin A chain without its partner B chain is degraded after retrotranslocation from the endoplasmic reticulum to the cytosol in plant cells*. Proceedings of the National Academy of Science (USA), 98(25):14726-31.

DI COLA A., FRIGERIO L., LORD J.M., ROBERTS L.M., CERIOTTI A., 2005, *Endoplasmic reticulum-associated degradation of ricin A chain has unique and plant specific features.* Plant Physiology, 137(1):287-96.

DICKEY C.A., KAMAL A., LUNDGREN K., KLOSAK N., BAILEY R.M., DUNMORE J., ASH P., SHORAKA S., ZLATKOVIC J., ECKMAN C.B., PATTERSON C., DICKSON D.W., NAHMAN S. JR.,HUTTON M., BURROWS F., PETRUCELLI L., 2007, *The high-affinity HSP90-CHIP complex recognizes and selectively degrades phosphorylated tau client proteins*, Journal of Clinical Investigation, 117(3):648-658.

DOONG H., VRAILIS A., KOHN E.C., 2002, *What's in the 'BAG'? – a functional domain analysis of the BAG-family proteins.* Cancer Letters, 188(1-2):25-32.

DRIESSEN A.J. & NOUWEN N., 2008, *Protein translocation across the bacterial cytoplasmic membrane*, Annual Review of Biochemistry, 77:643-67.

DULBECCO R & FREEMAN G., 1959, *Plaque production by polyoma virus*, Virology, 8(3):396-7.

EHSES E., LEONHARDT R.M., HANSEN G., KNITTLER M.R., 2005, *Functional Role of C-Terminal Sequence Elements in the Transporter Associated with Antigen Processing.* The Journal of Immunology, 174:328-339.

ELETTO D., DERSH D., ARGON Y., 2010, *GRP94 in ER quality control and stress responses,* Seminars in Cell & Developmental Biology, doi:10.1016/j.semcdb.2010.03.004.

ELLGAARD L. & HELENIUS A., 2003, *Quality control in the Endoplasmic Reticulum,* Nature Reviews of Molecular Cell Biology, 4(3):181-191.

ELLIOTT E., TSVETKOV P., GINZBURG I., 2007, *BAG-1 Associates with Hsc70-Tau Complex and Regulates the Proteasomal Degradation of Tau Protein*. The Journal of Biological Chemistry. 282:37276-37284.

ELLIS R.J. & HARTL F.U., 1999, *Principles of protein folding in the cellular environment*, Current Opinion in Structural Biology, 9:102:110.

ENDO Y., MITSUI K., MOTIZUKI M., TSURUGI K., 1987, *The mechanism of action of ricin and related toxic lectins on eukaryotic ribosomes. The site and the characteristics of the modification in 28 S ribosomal RNA caused by the toxins.* Journal of Biological Chemistry. 262(12):5908-12.

ESSER C., ALBERTI S., HÖHFELD J., 2004, *Cooperation of molecular chaperones with the ubiquitin/proteasome system*, Biochimica et Biophysioca Acta, 1695:171-188.

FAGIOLI C., MEZGHRANI A., SITIA R., 2001, *Reduction of Interchain Disulfide Bonds Precedes the Dislocation of Ig-μ Chains from the Endoplasmic Reticulum to the Cytosol for Degradation*, Journal of Biological Chemistry, 276:40962-40967.

FELDMAN M. & VAN DER GOOT F.G., 2009, *Novel ubiquitin-dependent quality control in the endoplasmic reticulum*. Trends in Cell Biology, 19(8):357-63.

FELTS S.J. & TOFT D.O., 2003, *p23, a simple protein with complex activities.* Cell Stress Chaperones, 8(2):108-113.

FERMANI S., TOSI G., FARINI V., POLITO L., FALINI G., RIPAMONTI A., BARBIERI L., CHAMBERY A., BOLOGNESI A., 2009, *Structure/function studies on two type 1 ribosome inactivating proteins: Boughanin and lychnin.* The Journal of Structural Biology, 168(2):278-287.

FISCHER G., BANG H., MECH C., 1984, *Determination of enzymatic catalysis for the cis-trans-isomerization of peptide binding in proline-containing peptides*, Biomed Biochem Acta., 43(10):1101-11.

FISHER E.A., LAPIERRE L.R., JUNKINS R.D., MCLEOD R.S., *The AAA-ATPase p97 facilitates degradation of apolipoprotein B by the ubiquitin-proteasome pathway.* Journal of Lipid Research, 49(10):2149-60.

FLICK K., RAASI S., ZHANG H., YEN J.L., KAISER P., 2006, *A ubiquitin-interacting motif protects polyubiquitinated Met4 from degradation by the 26S proteasome*. Nature Cell Biology 8(5):509-15.

FLYNN G.C., POHL J., FLOCCO M.T., ROTHMAN J.E., 1991, *Peptide-binding specificity of the molecular chaperone BiP*. Nature, 353(6346):726-30.

FREEMAN B.C., TOFT D.O., MORIMOTO R.I., 1996, *Molecular chaperone machines: chaperone activities of the cyclophilin Cyp-40 and the steroid aporeceptor-associated protein p23*. Science, 274(5293):1718-20.

FRIGERIO L., VITALE A., LORD J.M., CERIOTTI J.M., ROBERTS L.M., 1998, *Free Ricin A Chain, Proricin, and Native Toxin Have Different Cellular Fates When Expressed in Tobacco Protoplasts,* The Journal of Biological Chemistry, 273:14194-14199.

FRIGERIO L., JOLLIFFE N.A., DI COLA A., FELIPE D.H., PARIS N., NEUHAUS J.M., LORD J.M., CERIOTTI A., ROBERTS L.M., 2001, *The internal propeptide of the ricin precursor carries a sequence-specific determinant for vacuolar sorting.* Plant Physiology, 126:167-175.

GARDNER R.G., SWARBRICK G.M., BAYS N.W., CRONIN S.R., WILHOVSKY S., SEELIG L., KIM C., HAMPTON R.Y., 2000, *Endoplasmic reticulum degradation requires lumen to cytosol signalling*, Journal of Cell Biology, 151(1):69-82.

GASPERI-CAMPANI A., BARBIERI L., LORENZINI E., MONTANARO L., SPERTI S., BONETTI E., STIRPE F., 1978, *Modeccin, the toxin of Adenia digitata*. *Purification, toxicity and inhibition of protein synthesis in vitro,* Biochemical Journal, 174:491-496.

GASTEIGER E., HOOGLAND C., GATTIKER A., DUVAUD S., WILKINS M.R., APPEL R.D., BAIROCH A., WALKER M.J., 2005, *The Proteomics Protocols Handbook*, Humana Press, pages 571-607.

GAUSS R., JAROSCH E., SOMMER T., HIRSCH C., 2006, *A complex of Yos9p and HRD ligase integrates endoplasmic reticulum quality control into the degradation machinery.* Nature Cell Biology, 8(8):849-54.

GENEVAUX P., LANG F., SCHWAGER F., VARTIKAR J.V., RUNDELL K., PIPAS J.M., GEORGOPOULOS C., KELLEY W.L., 2003, *Simian virus 40 T antigens and J domains: analysis of Hsp40 cochaperone functions in Escherichia coli.* Journal of Virology, 77(19):10706-13.

GILLECE P., PILON M., RÖMISCH K., 2000, *The protein translocation channel mediates glycopeptides export across the endoplasmic reticulum membrane.* Proceedings of the National Academy of Science (USA), 97(9):4609-14.

GIODINI A & CRESSWELL P., 2008, *Hsp90-mediated cytosolic refolding of exogenous proteins internalized by dendritic cells*. The EMBO Journal, 27:201-211.

GOLDFARB S.B., KASHLAN O.B., WATKINS J.N., SUAUD L., YAN W., KLEYMAN T.R., RUBENSTEIN R.C., 2006, *Differential effects of Hsc70 and Hsp70 on the intracellular trafficking and functional expression of epithelial sodium channels*. Proceedings of the National Academy of Sciences (USA), 103(15):5817-5822.

GOLDSTEIN R.F., NIRAJ A., SANDERSON T.P., WILSDON L.S., RAB A., KIM H., BEBOK Z., COLLAWN J.F., *VCP/p97AAA-ATPase does not interact with wild-type cystic fibrosis transmembrane conductance regulator*. American Journal of Respiratory Cell Molecular Biology, 36(6):706-14.

GÓMEZ-PUERTAS P., MARTIN-BENITO J., CARRASCOSA J.L., WILLINSON K.R., VALPUESTA J.M., 2004, *The substrate recognition mechanism in chaperonins*, Journal of Molecular Recognition, 17(2):85-94.

GNANN A., RIORDAN J.R., WOLF D.H., 2004, *Cystic fibrosis transmembrane conductance regulator degradation depends on the lectins Htm1p/EDEM and the Cdc48 protein complex in yeast*. Molecular Biology of the Cell, 15:4125-4135.

GRANNEMAN S., TOLLERVEY D., 2007, *Building Ribosomes: Even More Expensive Than Expected?* Current Biology, 17(11):415-416.

GROSS, M., AND HESSEFORT, S., 1996, *Purification and characterization of a 66-kDa protein from rabbit reticulocyte lysate which promotes the recycling of hsp 70* [*sic*]. Journal of Biological Chemisty, 271, 16833-16841.

GUERRA L., NEMEC K.N., MASSEY S., TATULIAN S.A., THELESTAM M., FRISAN T., TETER K., 2009, *A Novel Mode of Translocation for Cytolethal Distending Toxin*. Biochimica Biophysica Acta, 1793(3):489-495.

GUSAROVA V., CAPLAN A.J., BRODSKY J.L., FISHER E.A., 2001, *Apolipoprotein B Degradation is Promoted by the Molecular Chaperones hsp90 and hsp70* [*sic*], Journal of Biological Chemistry, 276:24891-900.

HALAWANI D. & LATTERICH M., 2006, *p97: The Cell's Molecular Purgatory*, Molecular Cell, 22:713-717.

HAMMAN B.D., CHEN J.C., JOHNSON E.E., JOHNSON A.E., 1997, *The aqueous pore through the translocon has a diameter of 40-60A during cotranslational protein translocation at the ER membrane*. Cell, 89(4):535-44.

HAMMOND C., HELENIUS A., 1994, *Folding of VSV G protein: sequential action of BiP and calnexin*, Science 266, 456-458.

HAMPTON R.Y., 2000, *ER stress response: Getting the UPR hand on misfolded proteins*, Current Biology, 10(14):518-521.

HASLBECK M., FRANZMANN T., WEINFURTNER D., BUCHNER J., 2005, *Some like it hot: the structure and function of small heat shock proteins*, Nature Structural & Molecular Biology, 12:842-846.

HATAKEYAMA S., YADA M., MATSUMOTO M., ISHIDA N., NAKAYAMI K.I., 2001, *U box proteins as a new family of ubiquitin-protein ligases.* Journal of Biological Chemistry, 276(35):33111-20.

HAUG G., AKTORIES K., BARTH H., 2004, *The Host Cell Chaperone Hsp90 Is Necessary for Cytotoxic Action of the Binary Iota-Like Toxins*, Infection and Immunity, 72(5):3066-3068.

HAZES B., & READ R.J., 1997, *Accumulating evidence suggests that several AB-toxins subvert the endoplasmic reticulum-associated degradation pathway to enter target cells*., Biochemistry, 36(37):11051-4.

HEBERT D.N., BERNASCONI R., MOLINARI M., 2010, *ERAD substrates: Which way out?* Seminars in Cell & Developmental Biology, 21(5):526-32.

HEGDE R., PODDER S.K., 2001, *Evolution of tetrameric lectin* Ricinus communis *agglutinin from two variant groups of ricin toxin dimers*. European Journal of Biochemistry, 254(3):596-601.

HERNÁNDEZ, M. P., SULLIVAN, W. P., AND TOFT, D. O., 2002, *The assembly and intermolecular properties of the hsp70-Hop-hsp90 molecular chaperone complex*. Journal of Biological Chemistry. 277, 38294-38304.

HERSHKO A. & ROSE I.A., 1987, *Ubiquitin-aldehyde: a general inhibitor of ubiquitin-recycling processes.* Proceedings of the National Academy of Sciences (USA), 84(7):1829-1833.

HESSLING M., RICHTER K., BUCHNER J., 2009, *Dissection of the ATP-induced conformational cycle of the molecular chaperone Hsp90*. Nature structural & molecular biology, 16(3):287-293.Or

HEUCK A.P., TWETEN R.K., JOHNSON A.E., 2003, *Assembly and Topography of the Prepore Complex in Cholesterol-dependent Cytolysines*. The Journal of Biological Chemistry, 278:31218-31225.

HIRSCH C., GAUSS R., HORN S.C., NEUBER O., SOMMER T., 2009, *The ubiquitylation machinery of the endoplasmic reticulum*. Nature, 458:453-460.

HOCHSTRASSER M., 2006, *Lingering mysteries of ubiquitin-chain assembly*, Cell, 124(1):27-34.

HÖHFELD J., CYR D.M., PATTERSON C., 2001, *From the cradle to the grave: molecular chaperones may choose between folding and degradation*. EMBO Reports, 2(10):885-890.

HÖHFELD J., HARTL F.U., 1994, *Post-translational protein import and folding.* Current Opinions in Cell Biology. 4:499-509.

HÖHFELD J. & JENTSCH S., 1997, *GrpE-like regulation of the Hsc70 chaperone by the anti-apoptotic protein BAG-1*. The EMBO Journal, 16(20:6209-6216.

HÖHFELD J., MINAMI Y., HARTL F.U., 1995, Hip, a novel cochaperone in the eukaryotic Hsc70/Hsp40 reaction cycle. Cell. 83(4):589-98.

HOSOMI A., TANABE K., HIRAYAMI H., KIM I., RAO H., SUZUKI T., 2010, *Identification of an Htm1 (EDEM)-dependent, Mns1-independent Endoplasmic Reticulum-associated Degradation (ERAD) Pathway in Saccharomyces cerevisiae APPLICATION OF A NOVEL ASSAY FOR GLYCOPROTEIN ERAD**, The Journal of Biological Chemistry, 285:24324-334.

HUDSON T.H., & NEVILLE D.J., 1987, *Temporal separation of Protein Toxin Translocation from Processing* Events, The Journal of Biological Chemistry, 262(34):16484-494.

HU C.Y., PETTITT B.M., ROESGEN J., 2009, *Osmolyte solutions and protein folding.* F1000 Biology Reports, 1:41 (doi: 10.3410/B1-41).

HUYER G., PILUEK W.F., FANSLER Z., KREFT S.G., HOCHSTRASSER M., BRODSKY J.L., MICHAELIS S., 2004, *Distinct machinery is required in Saccharomyces cerevisiae for the endoplasmic reticulum-associated degradation of a multispanning membrane protein and a soluble luminal protein*. Journal of Biological Chemistry, 279(37):38369-78.

HRIZO S.L., GUSAROVA V., HABIEL D.M., GOECKELER J.L., FISHER E.A., BRODSKY J.L., 2007, *The Hsp110 molecular chaperone stabilizes apolipoprotein B from endoplasmic reticulum associated degradation (ERAD)*, Journal of Biological Chemistry, 282(45):32665-75.

HRUSKA A.J., 1988, *Cyanogenic glucosides as defense compounds: a review of the evidence*, Journal of Chemical Ecology, 14(12):2213-2217.

IMAI J., MARUYA M., YASHIRODA H., YAHARA I., TANAKA K., 2003, *The molecular chaperone Hsp90 plays a role in the assembly and maintenance of the 26S proteasome*, EMBO Journal, 22(14):3557-67.

IMMORMINO R.M., DOLLINS E., SHAFFER P.L., SOLDANO K.L., WALKER M.A., GEWIRTH D.T., 2004, *Ligand-induced Conformational Shift in the N-terminal Domain of GRP94, an Hsp90 Chaperone*., Journal of Biological Chemistry, 279:46162-46171.

IRVIN J.D., 1975, *Purification and partial characterisation of the antiviral protein from* Phytolacca Americana *which inhibits eukaryotic protein synthesis.* Archives of Biochemistry and Biophysics. 169:522-528.

JACH G., GORNHARDT B., MUNDY J., LOGEMANN J., PINSDORF E., LEAH R., SCHELL J., MAAS C., 1995, *Enhanced quantitative resistance against fungal disease by combinatorial expression of different barley antifungal proteins in tobacco*. The Plant Journal, 8:97-109.

JANSE D.M., CROSAS B., FINLEY D., CHURCH G.M., 2004, *Localization to the Proteasome Is Sufficient for Degradation*. The Journal of Biological Chemistry, 279(2):21415-20.

JARIEL-ENCONTRE I., BOSSIS G., PIECHACZYK M., 2008, *Ubiquitin-independent degradation of proteins by the proteasome.* Biochimica et Biophysica Acta – Reviews on Cancer, 1786(2):153-177.

JENTSCH S., RUMPF S., 2006, *Cdc48 (p97): a 'molecular gearbox' in the ubiquitin pathway.* TRENDS in Biochemical Sciences, 32(1):6-11.

JEHNSEN R.E., & JOHNSON A.E., 1999, *Protein Translocation: Is Hsp70 pulling my chain?* Current Biology, 9(20):R779-782.

JIANG C., FANG S.L., XIAO Y.F., O'CONNOR S.P., NADLER S.G., LEE D.W., JEFFERSON D.M., KAPLAN J.M., SMITH A.E., CHENG S.H., 1998, *Partial restoration of cAMP-stimulated CFTR chloride channel activity in DeltaF508* [*sic*] *cells by deoxyspergualin.,* American Journal of Physiology, 275:171-8.

JIANG J., BALLINGER C.A., WU Y., DAI Q., CYR D.M., HÖHFELD J., PATTERSON C., 2001. *CHIP is a U-box-dependent E3 ubiquitin ligase: identification of Hsc70 as a target for ubiquitylation.* Journal of Biological Chemistry.

JOHNSON, B. D., SCHUMACHER, R. J., ROSS, E. D., AND TOFT, D. O., 1998, *Hop modulates hsp70/hsp90 interactions in protein folding*. Journal of Biological Chemistry, 273:3679-3686.

KABANI M. KELLEY S.S., MORROW M.W., MONTGOMERY D.L., SIVENDRAN R., ROSE M.D., GIERASCH L.M., BRODSKY J.L., 2003, *Dependence of endoplasmic reticulum-associated degradation on the peptide binding domain and concentration of BiP*, Molecular Biology of the Cell, 14(8):4347-48.

KABANI M., MCLELLAN C., RAYNES D.A., GUERRIERO V., BRODSKY J.L.., 2002, *HspBP1, a homologue of the yeast Fes1 and Sls1 proteins, is an Hsc70 nucleotide exchange factor*. FEBS Letters, 531(2):339-42

KAGANOVICH D., KOPITO R., FRYDMAN J., 2008, *Misfolded proteins partition between two distinct quality control compartments*. Nature, 454(28):1088-1096.

KALIA S.K., LEE S., SMITH P.D., LIU L., CROCKER S.J., THORARINSDOTTIR T.E., GLOVER J.R., FON E.A., PARK D.S., LOZANO D.S., 2004, *BAG5* [sic] *Inhibits Parkin and Enhances Dopaminergic Neuron Degradation*. Neuron. 44(6):931-45.

KAMPINGA H.H., KANON B., SALOMONS F.A., KABAKOV A.E., PATTERSON C., 2003, *Overexpression of the cochaperone CHIP enhances Hsp70-dependent folding activity in mammalian cells.* Molecular Cell Biology, 23(14):4948-58.

KAWAGUCHI, S. & D. T. W. NG, 2007, *SnapShot: ER-associated degradation pathways.* Cell. 129:1230.

KING F.W., WAWRZYNOW A., HÖHFELD J., ZYLICZ M., 2001, *Co-chaperones Bag-1, Hop and Hsp40 regulate Hsc70 and Hsp90 interactions with wild-type or mutant p53.* The EMBO Journal, 20(22):6297-305.

KIM H.T., KIM K.P., LLEDIAS F., KISSELEV A.F., SCAGLIONE K.M., SKOWYRA D., GYGI S.P., GOLDBERG A.L., 2007, *Certain pairs of ubiquitin-conjugating enzymes (E2s) and ubiquitin-protein ligases (E3s) synthesize nondegradable forked ubiquitin chains containing all possible isopeptide linkages.* Journal of Biological Chemistry. 282(24):17375-86.

KIM H.T., KIM K.P., UCHIKI T., GYGI S.P., GOLDBERG A.L., 2009, *S5a promotes protein degradation by blocking synthesis of nondegradable forked ubiquitin chains.* The EMBO Journal, 28:1867-1877.

KIM I., AHN J., LIU C., TANABE K., APODACA J., SUZUKI T., RAO H., 2006, *The Png1-Rad23 complex regulates glycoprotein turnover*, Journal of Cell Biology, 172(2):211-219.

KIM J.H., LUDGER J., GOUD B., ANTONY C., LINGWOOD C.A., DANEMAN R., GRINSTEIN S., 1998, *Noninvasive measurement of the pH of the endoplasmic reticulum at rest and during calcium release*. Proceedings of the National Academy of Science (USA), 95:2997-3002.

KIM T.S., JANG C.Y., KIM H.D., LEE J.Y., AHN B.Y., KIM J., 2006, *Interaction of Hsp90 with Ribosomal Proteins Protects from Ubiquitination and Proteasome-dependent Degradation*, Molecular Biology of the Cell, 17:824-833.

KINCAID M.M. & COOPER A.A., 2007, *ERADicate ER stress or die trying*. Antioxidant & Redox Signalling, 9(12):2373-87

KOBAYASHI T., MANNO A., KAKIZUKA A., 2007, *Involvement of valosin-containing protein (VCP)/p97 in the formation and clearance of abnormal protein aggregates*. Genes to Cells, 12:889-901.

KOONIN E.V., ARAVIND L., KONDRASHOV A.S., 2000, *The impact of comparative genomics on our understanding of evolution.* Cell, 101(6):573-6.

KOSMAOGLOU M., SCHWARZ N., BETT J.S., CHEETHAM M.E., 2008, *Molecular Chaperones and Photoreceptor Function*, Progress in Retinal and Eye Research, 27:434-449.

KOZLOWSKI L., 2008, *Calculation of protein isoelectric point*. Web-site: isoelectric.ovh.org

KUNDRAT L., & REGAN L., 2010, *Identification of Residues on Hsp70 and Hsp90 Ubiquitinated by the Cochaperone CHIP*, Journal of Molecular Biology, 395(3):587-594.

KREFT S.G., WANG L., HOCHSTRASSER M., 2006, *Membrane topology of the Yeast endoplasmic reticulum-localized ubiquitin ligase Doa10 and comparison with its human ortholog TEB4 (MARCH-VI),* The Journal of Biological Chemistry, 281:4646-4653.

LANDRY S.J., JORDAN R., MCMACKEN R., GIERASCH L.M., 1992, *Different conformations for the same polypeptide bound to chaperones DnaK and GroEL*. Nature, 355:455-457.

LAPPI D.A., ESCH F.S., BARBIERI L., STIRPE F., SORIA M., 1985, *Characterization of a Saporinaria officinalis seed ribosome-inactivating protein: immunoreactivity and sequence homologues.* Biochemical and biophysical research communications. 129(3):934-42.

LAUVRAK S.U., LLORENTE A., IVERSEN T., SANDVIG K., 2002, *Selective regulation of the Rab9-independent transport of ricin to the Golgi apparatus by calcium.* Journal of Cell Science, 115:3449-3456.

LEE P.J., BRAUWEILER A., RUDOLPH M., HOOPER J.E., DRABKIN H.A., GEMMILL R.M., 2010, *The TRC8 ubiquitin ligase is sterol regulated and interacts with lipid and protein biosynthetic pathways*. Molecular Cancer Research, 8(1):93-106.

LEE R.J., LIU C.W., HARTY C., MCCRACKEN A.A., LATTERICH M., RÖMISCH K., DEMARTINO G.N., THOMAS P.J., BRODSKY J.L., 2004, *Uncoupling retro-translocation and degradation in the ER-associated degradation of a soluble protein*. EMBO Journal, 23(11):2206-2215.

LENCER W.I., CONSTABLE C., MOE S., JOBLING M.G., WEBB H.M., RUSTON S., MADARA J.L., HIRST T.R., HOLMES R.K., 1995, *Targeting of cholera toxin and Escherichia coli heat labile toxin in polarized epithelia: role of COOH-terminal KDEL*. Journal of Cell Biology, 131(4):951-62.

LI S., SPOONER R.A., ALLEN S.C., GUISE C.P., LADDS G., SCHNOEDER T., SCHMITT M.J., LORD J.M., ROBERTS L.M., *2010, Folding-competent and folding-defective forms of Ricin A chain have different fates following retrotranslocation from the endoplasmic reticulum*. Molecular Biology of the Cell. [Epub ahead of print] PMID: 20519439.

LI W., & YE Y., 2008, *Polyubiquitin chains: functions, structures, and mechanisms.* Cell Molecular Life Sciences, 65(15):2397-406.

LI X.P., BARICEVIC M., SAIDASAN H., TUMER N.E., 2007, *Ribosome Depurination Is Not Sufficient for Ricin-Mediated Cell Death in Saccharomyces cerevisiae.* Infection and Immunity, 75(1):417-428.

LI Y.B., FRANKEL A.E., RAMAKRISHNAN S., 1992, *High-level expression and simplified purification of recombinant ricin A chain.* Protein Expression and Purification. 3(5):386-394.

LIPSON C., ALALOUF G., BAJOREK M., RABINOVICH E., ATIR-LANDE A., GLICKMAN M., BAR-NUN S., 2008, *A proteasomal ATPase contributes to dislocation of endoplasmic reticulum-associated degradation (ERAD) substrates.* Journal of Biological Chemistry, 283(11):7166-75.

LIU J., ZHANG J.P., QUINN T., BRADNER J., BEYER R., CHEN S., ZHANG J., 2009, *Rab11a and HSP90 Regulate Recycling of Extracellular α-Synuclein*, The Journal of Neuroscience, 29(5):1480-1485.

LIU Q., ZHAN J., CHEN X., ZHENG S., 2006, *Ricin A chain reaches the endoplasmic reticulum after endocytosis.* Biochemical and Biophysical Research Communications, 343(3):857-63.

LLOPIS J., MCCAFFREY J.M., MIYAWAKI A., FARQUHAR M.G., TSIEN R.Y., 1998, *Measurement of cytosolic, mitochondrial, and Golgi pH in single living cells with green fluorescent proteins.* Proceedings of the National Academy of Science (USA), 95(12):6803-8.

LLORENTE A., VAN DEURS B., GARRED Ø., EKER P., SANDVIG K., 2000, *Apical endocytosis of ricin in MDCK cells is regulated by the cyclooxygenase pathway*. Journal of Cell Science, 113:1213-1221.

LOO M.A., JENSEN T.J., CUI L., HOU Y., CHANG X., RIORDAN J.R., 1998, *Perturbation of Hsp90 interaction with the nascent CFTR prevents its maturation and accelerates its degradation by the proteasome.* The EMBO Journal, 17(23):6879-87.

LORD J.M., 1985, *Precursors of ricin and Ricinus communis agglutinin. Glycosyaltion during synthesis and intracellular transport.* European Journal of Biochemistry. 146(2):411-6.

LORD J.M., ROBERTS L.M., ROBERTUS J.D., 1994, *Ricin: structure, mode of action, and some current applications*. FASEB J., 8:201-208.

LORD, J.M. and ROBERTS, L.M.,1998, *Toxin Entry: Retrograde Transport through the Secretory Pathway*. The Journal of Cell Biology, 140(4):733-736.

LÜDERS J., DEMAND J., SCHÖNFELDER S., FRIEN M., ZIMMERMANN R., HÖHFELD J., 1998, *Cofactor modulation of the functional specificity of the molecular chaperone Hsc70.* Biological Chemistry, 379(10):1217-26.

LÜDERS J., DEMAND J., HÖHFELD J. 2000, *The ubiquitin-related BAG-1 provides a link between the molecular chaperones Hsc70/Hsp90 and the proteasome*. Journal of Biological Chemistry. 275(7):4613-7

MAJOUL I., SOHN K., WIELAND F.T., PEPPERKOK R., PIZZA M., HILLEMANN J., SÖLING H.D., *KDEL receptor (Erd2p)-mediated retrograde transport of the cholera toxin A subunit from the Golgi involves COPI, p23, and the COOH terminus of Erd2p.* Journal of Cell Biology, 143(3):601-12.

MÄÄTTÄNEN P., GEHRING K., BERGERON J.J.M., THOMAS D.Y., 2010, *Protein quality control in the ER: The recognition of misfolded proteins.* Seminars in Cell & Developmental Biology, 21:500-511.

MARKOSSIAN K.A. & KURGANOV B.I., 2004, *Protein Folding, Misfolding, and Aggregation. Formation of Inclusion Bodies and Aggresomes.* Biochemistry (Moscow), 69(9):971-98.

MARGUET D., SPILIOTIS E.T., PENTCHEVA T., LEBOWITZ M., SCHNECK J., EDIDIN M., 1999, *Lateral diffusion of GFP-tagged H2Ld molecules and of GFP-TAP1 reports on the assembly and retention of these molecules in the endoplasmic reticulum.* Immunity. 11:231-240.

MARSHALL R.S., JOLLIFFE N., CERIOTTI A., SNOWDEN C.J., LORD J.M., FRIGERIO L., ROBERTS L.M., 2008, *The Role of CDC48 in the Retro-translocation of Non-ubiquitinated Toxin Substrates in Plant Cells*. The Journal of Biological Chemistry. 283:15869-15877.

MARTOGLIO B. and DOBBERSTEIN B., 1998, *Signal Sequences: more than just greasy peptides.* Trends in Cell Biology, 8(10):410-415.

MAYERHOFER P.U., COOK J.P., WAHLMAN J., PINHEIRO T.T., MOORE K.A., LORD J.M., JOHNSON A.E., ROBERTS L.M., 2009, *Ricin A chain insertion into endoplasmic reticulum membranes is triggered by a temperature increase to 37°C*. The Journal of Biological Chemistry, 284(15):10232-42.

MCCRACKEN A.A., BRODSKY J.L., 2006, *Recognition and Delivery of ERAD Substrates to the Proteasome and Alternative Paths for Cell Survival*. Current Topics in Microbiology and Immunology, 300:17-40.

MCDONOUGH H., & PATTERSON C., 2003, *CHIP: a link between the chaperone and proteasome systems.* Cell Stress Chaperones. 8(4):303-308.

MCCLELLAN A.J., SCOTT M.D., FRYDMAN J., 2005, *Folding Quality Control of the VHL Tumor Suppressor through Distinct Chaperone Pathways*, Cell, 121(5):739-748.

MCCLELLAN A.J., TAM S., KAGANOVICH D., FRYDMAN J., 2005, *Protein quality control: chaperones culling corrupt conformations*. Nature Cell Biology, 7(8):736-740.

MCLELLAN C.A., RAYNES D.A., GUERRIERO V., 2003, *HspBP1, an Hsp70 cochaperone, has two structural domains and is capable of altering the conformation of the Hsp70 ATPase domain.* Journal of Biological Chemistry. 278(21):19017-22.

MEACHAM G.C., PATTERSON C., ZHANG W., YOUNGER J.M., CYR D.M., 2001, *The Hsc70 co-chaperone CHIP targets immature CFTR for proteasomal degradation*. Nature Cell Biology. 3(1):100-5.

MELDOLESI J., & POZZAN T., 1998, *The endoplasmic reticulum Ca^{2+} store: a view from the lumen*. TIBS 23:10-15.

METZGER M.B., MAURER M.J., DANCY B.M., MICHAELIS S., 2008, *Degradation of a cytosolic protein requires endoplasmic reticulum-associated degradation machinery,* Journal of Biological Chemistry, 283(47):32302-16.

MEUSSER B., HIRSCH C., JAROSCH E., SOMMER T., 2005, *ERAD: the long road to destruction*. Nature Cell Biology, 7(8):766-772.

MICKLER M., HESSLING M., RATZKE C., BUCHNER J., HUGEL T., 2009, *The large conformational changes of Hsp90 are only weakly coupled to ATP hydrolysis.* Nature Structural & Molecular Biology, 16(3):281-286.

MINAMI Y., HÖHFELD J., OHSTUKA K., HARTL F.U., 1996, *Regulation of the Heat-shock protein 70 Reaction Cycle by the Mammalian DnaJ homolog, Hsp40*., The Journal of Biological Chemistry, 271:19617-24.

MOISENOVICH M., TONEVITSKY A., MALJUCHENKO N., KOZLOVSKAYA N., AGAPOV I., VOLKNANDT W., BEREITER J., 2004, *Endosomal ricin transport: involvement of Rab4- and Rab5-positive compartments.* Histochemical Cell Biology, 121(6):429-439.

MOORE P., BERNARDI K.M., TSAI B., 2010, *The Ero1α-PDI Redox Cycle Regulates Retro-Translocation of Cholera Toxin*. Molecular Biology of the Cell, 21(7):1305-1313.

MORISHIMA Y., KANELAKIS K.C., MURPHY P.J.M., LOWE E.H., JENKINS G.J., OSAWA Y., SUNSHARA R.K., PRATT W.B., 2003, *The Hsp90 Cochaperone p23 Is the Limiting Component of the Multiprotein Hsp90/Hsp70-based Chaperone System in Vivo Where It Acts to Stabilize the Client Protein·Hsp90 Complex*. The Journal of Biological Chemistry, 278(49):48754-48763.

MORITO D., HIRAO K., ODA Y., HOSOKAWA N., TOKUNAGA F., CYR D.M., TANAKA K., IWAI K., NAGATA K., 2008, *Gp78 cooperates with RMA1 in endoplasmic reticulum-associate degradation of CFTRDeltaF508.* Molecular Biology of the Cell, 19(4):1328-36.

MORRE, D.J., MORRE, D.M., MOLLEHHAUER, H.H., REUTTER, W. (1987). Golgi apparatus cisternae of monensin-treated cells accumulate in the cytoplasm of liver slices. European Journal of Cell Biology 43(2):235-242.

MURATA S, MINAMI Y, MINAMI M, CHIBA T, TANAKA K. 2001, *CHIP is a chaperone-dependent E3 ligase that ubiquitylates unfolded protein.* EMBO Reports, 2(12):1133-8.

MURPHY P.J.M., MORISHIMA Y., CHEN H., GALIGNIANA M.D., MANSFIELD J.F., SIMONS S.S. Jr., Pratt W.B., 2003, *Visualization and Mechanism of Assembly of a Glucocorticoid Receptor·Hsp70 Complex That Is Primed for Subsequent Hsp90-dependent Opening of the Steroid Binding Cleft.* Journal of Biological Chemistry, 278:34764-773.

NADEAU K., NADLER S.G., SAULNIER M., TEPPER M.A., WALSH C.T., 1994, *Quantitation* [*sic*] *of the interaction of the immunosuppressant deoxyspergualin and analogs with Hsc70 and Hsp90.*, Biochemistry, 33(9):2561-7.

NADLER S.G., DISCHINO D.D., MALACKO A.R., CLEAVELAND J.S., FUJIHARA S.M., MARQUARDT H., 1998, *Identification of a binding site on Hsc70 for the immunosuppressant 15-deoxyspergualin.* Biochemical and Biophysical Research Communications, 253(1):176-180.

NAKATSUKASA K. & BRODSKY J.L., 2008, *The recognition and retrotranslocation of misfolded proteins from the endoplasmic reticulum*. Traffic, 9(6):861-870.

NG W., SERGEYENKO T., ZENG N., BROWN J.D., RÖMISCH K., 2007, *Characterization of the proteasome interaction with the Sec71 channel in the endoplasmic reticulum*. Journal of Cell Science, 120(4):682-91.

NOLLEN E.A., KABAKOV A.E., BRUNSTING J.F., KANON B., HÖHFELD J., KAMPINGA H.H., 2001. *Modulation of* in vivo *Hsp70 chaperone activity by Hip and Bag-1*. The Journal of Biological Chemistry. 276(7):4677-82.

ODUNUGA O.O., LONGSHAW V.M., BLATCH G.L., 2004, *HOP: more than an Hsp70/Hsp90 adaptor protein*, BioEssays, 26(10):1058-1068.

OH K.J., SENZEI L., COLLIER R.J., FINKELSTEIN A., 1999, *Translocation of the catalytic domain of diphtheria toxin across planar phospholipid bilayers by its own T domain.* Proceedings of the National Academy of Science (USA), 96(15):8467-70.

OLSNES S., PIHL A., 1982, *Ricin – a potent homicidal poison*. British Medical Journal, 278:350-351.

OLSNES S., PIHL A., 1973, *Different biological properties of the two constituent peptide chains of ricin, a toxic protein inhibiting protein synthesis*, Biochemistry, 12(16):3121-6.

OMURA T., KANEKO M., ONOGUCHI M., KOIZUMI S., ITAMI M., UEYAMA M., OKUMA Y., NOMURA Y., 2008, *Novel functions of ubiquitin ligase HRD1 with transmembrane and proline-rich domains*. Journal of Pharmacological Science, 106(3):512-9.

O'NEAL C.J., JOBLING M.J., HOLMES R.K., HOL W.G., *Structural basis for the activation of cholera toxin by human ARF6-GTP*. Science, 309(5737):1093-6.

ONO K., IKEMOTO M., KAWARABAYASHI T., IKEDA M., NISHINAKAGAWA T., HOSOKAWA M., SHOJI M., TAKAHASHI M., NAKASHIMA M., 2009, *A chemical chaperone, sodium 4-phenylbutyric acid, attenuates the pathogenic potency in human alpha-synuclein A30P + A53T transgenic mice*, Parkinsonism Related Disorders, 15(9):649-54.

OYADOMARI, S., YUN, C., FISHER, E.A., KREGLINGER, N., KREIBICH, G., OYADOMARI, M., HARDING, H.P., GOODMAN, A.G., HARANT, H., GARRISON, J.L., 2006, *Cotranslocational degradation protects the stressed endoplasmic reticulum from protein overload.* Cell, 126:727–739.

PANDE A.H., SCAGLIONE P., TAYLOR M., NEMEC K.N., TUTHILL S., MOE D., HOLMES R.K., TATULIAN S.A., TETER K., 2007, *Conformational instability of the Cholera Toxin A1 Polypeptide.* Journal of Molecular Biology, 375(4):1114-1128.

PANDE A.H., MOE D., JAMNADAS M., TATULIAN S.A., TETER K., 2008, *The Pertussis Toxin S1 Subunit is a Thermally Unstable Protein Susceptible to Degradation by the 20S Proteasome*. Biochemistry, 45(46):13734-13740.

PEEK L.J., BREY R.N., MIDDAUGH R., 2006, *A rapid, three-step process for the preformulation of a recombinant ricin toxin A-chain vaccine.* Journal of Pharmaceutical Sciences, 96(1):44-60.

PETRUCELLI L., DICKINSON D., KEHOE K., TAYLOR J., SNYDER H., GROVER A., DE LUCIA A., MCGOWAN E., LEWIS J., PRIHAR G., KIM J., DILLMANN W.H., BROWNE S.E., HALL A., VOELLMY R., TSUBOI Y., DAWSON T.M., WOLOZIN B., HARDY J., HUTTON M., 2004, *CHIP and Hsp70 regulate tau ubiquitination, degradation and aggregation*. Human Molecular Genetics, 13(7):703-714.

PILON M., SCHEKMAN R., RÖMISCH K., 1997, *Sec61p mediates export of a misfolded secretory protein from the endoplasmic reticulum to the cytosol for degradation*, EMBO Journal, 16(15):4540-4548.

PLATH K., RAPOPORT T.A., 2000, *Spontaneous release of cytosolic proteins from posttranslational substrates before their transport into the endoplasmic reticulum.* Journal of Cell Biology, 151(1):167-78.

PLOEGH H.L., 2007, *A lipid-based model for the creation of an escape hatch from the endoplasmic reticulum.* Nature, 448:435-8

POMORSKI T., MENON A.K., 2006, *Lipid flippases and their biological functions*, Cellular and Molecular Life Sciences, 63:2908-2921.

PRAPAPANICH V., CHEN S., SMITH D.F., 1998, *Mutation of Hip's Carboxy-Terminal Region Inhibits a Transitional Stage of Progesterone Receptor Assembly*. Molecular Cell Biology. 18(2): 944–952.

PRATT W.B., MORISHIMA Y., PENG H.M., OSAWA Y., 2010, *Proposal for a role of the Hsp90/Hsp70-based chaperone machinery in making triage decisions when proteins undergo oxidative and toxic damage*. Experimental Biology and Medicine, 235:278-289.

PRODROMOU C., & PEARL L., 2006, *Structure and Mechanism of the Hsp90 Molecular Chaperone Machinery*, Annual Review of Biochemistry, 75:271-294.

PYE V.E., DREVENY I., BRIGGS. L.C., SANDS C., BEURON F., ZHANG X., FREEMONT P.S., 2006, *Going through the motions: The ATPase cycle of p97.* Journal of Structural Biology, 156(1):12-28.

QIAN S.B., MCDONOUGH H., BOELLMANN F., CYR D.M., PATTERSON C., 2006, *CHIP-mediated stress recovery by sequential ubquitination of substrates and Hsp70*. Nature 440:551-555.

QUAN E.M., KAMIYA Y., KAMIYA D., DENIC V., WEIBEZAHN J., KATO K., WEISSMAN J.S., 2008, *Defining the glycan destruction signal for endoplasmic reticulum-associated degradation*. Molecular Cell, 32(6):870-877.

RAASI S. & WOLF D.H., 2007, *Ubiquitin receptors and ERAD: A network of pathways to the proteasome*. Seminars in Cell & Developmental Biology. 18:780-791.

RABINOVICH E., KEREM A., FRÖHLICH K.U., DIAMANT N., BAR-NUN S., 2002, *AAA-ATPase p97/Cdc48, a cytosolic chaperone required for endoplasmic reticulum-associated protein degradation*, Molecular Cell Biology, 22(2):626-34.

RABU S., WIPF P., BRODSKY J.L., HIGH S., 2008, *A precursor specific role for Hsp40/Hsc70 during tail-anchored protein integration at the endoplasmic reticulum*, The Journal of Biological Chemistry, 10(283):27504-13.

RAJAPANDI T., GREENE L.E., EISENBERG E., 2000, *The Molecular Chaperone Hsp90 and Hsc70 are Both Necessary and Sufficient to Activate Hormone Binding by Glucocorticoid Receptor.* 275(29):22597-22604.

RAO P.V. , JAYARAJ R., BHASKAR A.S., KUMAR O., BHATTACHARYA R., SAXENA P., DASH P.K., VIJAYARAGHAVAN R., 2005, *Mechanism of ricin-induced apoptosis in human cervical cancer cells.* Biochemical Pharmacology, 69(5):855-865.

RAPAK, A., FALNES, P.O., OLSNES, S., 1997, *Retrograde transport of mutant ricin to the endoplasmic reticulum with subsequent translocation to the cytosol.* Proceedings of the National Academy of Science U.S.A. 94(8):3783-3788.

RATTS R., ZENG H., BERG E.A., BLUE C., MCCOMB M.E., COSTELLO C.E., VANDERSPEK J.C., MURPHY J.R., *The cytosolic entry of diphtheria toxin catalytic domain requires a host cell cytosolic translocation factor complex*. Journal of Cell Biology, 160(7):1139-1150.

RAVID T., KREFT S.G., HOCHSTRASSER M., 2006, *Membrane and soluble substrates of the Doa10 ubiquitin ligase are degraded by distinct pathways.* EMBO Journal, 25(3):533-43.

REN J., SHARPE J.C., COLLIER R.J., LONDON E., 1999, *Membrane translocation of charged residues at the tips of hydrophobic helices in the T domain of diphtheria toxin*, Biochemistry, 38(3):976-984.

RETZLAFF M., STAHL M., EBERL H.C., LAGLEDER S., BECK J., KESSLER H., BUCHNER J., 2009, *Hsp90 is regulated by a switch point in the C-terminal domain.* EMBO Reports, 10(1):1147-1153.

RICHARDSON P.T., WESTBY M., ROBERTS L.M., GOULD J.H., COLMAN A., LORD J.M., 1989, *Recombinant proricin binds galactose but does not depurinate 28 S ribosomal RNA*. FEBS Letters, 255(1):15-20.

RICHTER K., REINSTEIN J., BUCHNER J., 2007, *A Grp on the Hsp90 Mechanism*, Molecular Cell 28:177-179.

ROBERTS L.M., & LORD J.M., 2004, *Ribosome-Inactivating Proteins: Entry into Mammalian Cells and Intracellular Routing*. Mini-Reviews in Medicinal Chemistry, 4(5):505-512.

RODNIN M.W., KYRYCHENKO A., KIENKER P., SHARMA O., POSOKHOV Y.O., COLLIER R.J., FINKELSTEIN A., LADOKHIN A.S., 2010, *Conformational Switching of the Diphtheria Toxin T Domain*. Journal of Molecular Biology, [Epub ahead of print].

ROE S.M., 1999, *Structural Basis for Inhibition of the Hsp90 Molecular Chaperone by the Antitumor Antibiotics Radicicol and Geldanamycin,* Journal of Medicinal Chemistry, 42:260-6.

RÖMISCH K., 2005, *Endoplasmic reticulum-associated degradation.* Annual Review of Cell & Developmental Biology. 21:435-456.

ROSSER M.F., & NICCHITTA C.V., 2000, *Ligand interactions in the adenosine nucleotide-binding domain of the Hsp90 chaperone, GRP94. I. Evidence for allosteric regulation of ligand binding.,* The Journal of Biological Chemistry, 275(30):22798-805.

RUBENSTEIN R.C., & LYONS B.M., 2001, *Sodium 4-phenylbutyrate downregulates HSC70 expression by facilitating mRNA degradation*. The American Journal of Physiology: Lung Cell Molecular Physiology, 281(1):39-42.

RUBENSTEIN R.C. & P.L., *Sodium 4-phenylbutyrate downregulates HSC70: implications for intracellular trafficking of DeltaF508-CFTR*, American Journal of Cell Physiology, 278(2):259-67.

RUTENBER E., ROBERTUS J.D., 1991, *The crystallographic refinement of ricin at 2.5Å resolution*. Proteins 10, 240-250.

SAHARA N., MURAYAMA M., MIZOROKI T., URUSHITANI M., IMAI Y., TAKAHASHI R., MURATA S., TANAKA K., TAKASHIMA A., 2005, *In vivo evidence of CHIP up-regulation attenuating tau aggregation*. Journal of Neurochemistry, 94(5):1254-63.

SANDVIG K., MADSHUS I.H., OLSNES S., 1984, *Dimethyl sulphide protects cells against polypeptide toxins and poliovirus.* Biochemical Journal, 219(3):935-40.

SANDVIG K., & PRYDZ K., HANSEN S.H., VAN DEURS B., 1991, *Ricin transport in brefeldin A-treated cells: correlation between Golgi structure and toxic effect*. Journal of Cell Biology, 115(4):971-81.

SANDVIG, K. & VAN DEURS, B., 2002, *Transport of protein toxins into cells: pathways used by ricin, cholera toxin and Shiga toxin.* FEBS Letters, 529(1):49-53.

SARKAR M., KURET J., LEE G., 2008, *Two Motifs Within the Tau Microtubule-binding Domain Mediate Its Association With the Hsc70 Molecular Chaperone.* Journal of Neuroscience Research, 86:2763-2773.

SASAKI T., KISHI M., SAITO M., TANAKA T., HIGUCHI N., KOMINAMI E, KATUNUMA N., MURACHI T., 1990, *Inhibitory effect of di- and tripeptidyl aldehydes on calpains and cathepsins*. Journal of Enzyme Inhibitors, 3(3):195-201.

SCHLOSSMAN D.M., SCHMID S.L., BRAELL W.A., ROTHMAN J.E., 1984, *An enzyme that removes clathrin coats: purification of an uncoating ATPase*. Journal of Cell Biology, 99(2):723-33.

SCHNEIDER C., SEPP-LORENZINO L., NIMMESGERN E., OUERFELLI O., DANISHEFSKY S., ROSEN N., HARTL F.U., 1996, *Pharmacologic shifting of a balance between protein refolding and degradation mediated by Hsp90.* Proceedings of the National Academy of Sciences (USA), 93(25): 14536–41.

SCHRÖDER M. & KAUFMAN R.J., 2004, *ER Stress and the unfolded protein response*, Mutation Research/Fundamental and Molecular Mechanisms of Mutagenesis, 569(1-2):29-63.

SCHUBERTH C. & BUCHBERGER A., *Membrane-bound Ubx2 recruits Cdc48 to ubiquitin ligases and their substrates to ensure efficient ER-associated protein degradation.* Nature Cell Biology, 7(10):999-1006.

SCHULTE T.W., AKINAGA S., SOGA S., SULLIVAN W., STENSGARD B., TOFT D., NECKERS L.M., 1998, *Antibiotic radicicol binds to the N-terminal domain of Hsp90 and shares impotant biologic* [*sic*] *activites with geldanamycin.*, Cell Stress Chaperones, 3(2):100-8.

SCHWIEGER I., LAUTZ K., KRAUSE E., ROSENTHAL W., WIESNER B., HERMOSILLA R., 2008, *Derlin-1 and p97/Valosin-Containing Protein Mediate the Endoplasmic Reticulum-Associated Degradation of Human V2 Vasopressin Receptors.* Molecular Pharmacology, 73:697-708.

SHA O., YEW D.T., NG T.B., YUAN L., KWONG W.H., 2010, *Different in vitro toxicities of structurally similar type I ribosome-inactivating proteins (RIPs)*, Toxicology in vitro, 24(4):1176-82.

SHARMA S.V., AGATSUMA T., NAKANO H., 1998, *Targeting of the protein chaperone, HSP90, by the transformation suppressing agent, radicicol.*, Oncogene, 16(20):2639-45.

SHANER L. & MORANO K.A., 2007, *All in the family: atypical Hsp70 chaperones are conserved modulators of Hsp70 activity*, Cell Stress & Chaperones, 12(1):1-8.

SHARP S.Y., BOXALL K., ROWLANDS M., PRODROMOU C., ROE S.M., MALONEY A., POWERS M., CLARKE P.A., BOX G.A., SANDERSON S., PATTERSON L., MATTHEWS T.P., CHEUNG K.J., BALL K., HAYES A., RAYNAUD F., MARAIS R., PEARL L., ECCLES S., AHERNE W., MCDONALD E. & WORKMAN P., 2007, In vitro *Biological Characterization of a Novel, Synthetic Diaryl Pyrazole Resorcinol Class of Heat Shock Protein 90 Inhibitors.*, Cancer Research, 67(5):2206-2216.

SHEN H.Y., HE J.C., WANG Y., HUANG Q.Y., CHEN J.F., 2005, *Geldanamycin induces heat shock protein 70 and protects against MPTP-induced dopaminergic neurotoxicity in mice*. Journal of Biological Chemistry, 280(48):39962-9.

SHEPHERD J., 1994, *Lipoprotein metabolism: an overview*, Drugs, 47(2):1-10.

SHIMURA H., SCHWARTZ D., GYGI S.P., KOSIK K.S., 2004, *CHIP-Hsc70 complex ubiquitinates phosphorylated tau and enhances cell survival.* Journal of Biological Chemistry, 279(6):4869-76.

SHU C.W., CHENG N.L., CHANG W.M., TSENG T.L., LAI Y.K., 2005, *Transactivation of hsp70-1/2 in geldanamycin-treated human non-small cell lung cancer H460 cells: involvement of intracellular calcium and protein kinase C.* Journal of Cell Biochemistry, 94(6):1199-209.

SILIGARDI G., PANARETOU B., MEYER P., SINGH S., WOOLFSON D.N., PIPER P.W., PEARL L.H., PRODROMOU C., 2002, *Regulation of Hsp90 ATPase Activity by the Co-chaperone Cdc37p/p50^{cdc37}*, The Journal of Biological Chemistry, 277(23):20151-20159.

SITTLER A., LURZ R., LUEDER G., PRILLER J., LEHRACH H., HAYER-HARTL M.K., HARTL F.U., WANKER E.E., 2001, *Geldanamycin activates a heat shock response and inhibits huntingtin aggregation in a cell culture model of Huntington's disease.* Human Molecular Genetics, 10(12):1307-15.

SLOMINSKA-WOJEWODZKA M., GREGERS T.F., WALCHLI S., SANDVIG K., 2006, *EDEM is involved in retrotranslocation of ricin from the endoplasmic reticulum to the cytosol*, Molecular Biology of the Cell, 17(4):1664-75.

SOLL J. & SCHLEIFF E., 2004, *Protein import into chloroplasts.* Nature Reviews Molecular Cell Biology, 5:198-208.

SONDERMANN H., SCHEUFLER C., SCHNEIDER C., HÖHFELD J., HARTL F.U., MOAREFI I., 2001, *Structure of a Bag/Hsc70Complex: Convergent Functional Evolution of Hsp70 Nucleotide Exchange Factors*, Science, 291:1553-1557.

SONG Y. & MASISON D.C., 2005, *Independent Regulation of Hsp70 and Hsp90 Chaperones by Hsp70/Hsp90-organizing Protein Sti1 (Hop1)*, The Journal of Biological Chemistry, 280(40):34178-85.

SIMPSON J.C., LORD J.M., ROBERTS L.M., 1995, *Point mutations in the hydrophobic C-terminal region of Ricin A chain indicate that Pro250 plays a key role in membrane translocation*. European Journal of Biochemistry. 232(2):458-63.

SIMPSON J.C., SMITH D.C., ROBERTS L.M., LORD J.M., 1998, *Expression of Mutant Dynamin Protects Cells against Diphtheria Toxin but Not against Ricin.* Experimental Cell Research, 239:293-300.

SONG B.L., SEVER N., DEBOSE-BOYD R.A., 2005, *Gp78, a Membrane-Anchored Ubiquitin Ligase, Associates with Insig-1 and Couples Sterol-Regulated Ubiquitination to Degradation of HMG CoA Reductase*. Molecular Cell, 19:829-840.

SPILSBERG B., HANADA K., SANDVIG K., 2005, *Diphtheria toxin translocation across cellular membranes is regulated by sphingolipids*, Biochemical and Biophysical Research Communications, 329(2):465-473.

SPOONER R.A., HART P.J., COOK J.P., PIETRONI P., ROGON C., HÖHFELD J., LORD J.M., 2008, *Cytosolic chaperones influence the fate of a toxin dislocated from the endoplasmic reticulum.*, Proceedings from the National Academy of Science (USA), 105(45):17408-13.

SPOONER R.A., WATSON P., SMITH D.C., BOAL F., AMESSOU M., LUDGER J., CLARKSON G.C., LORD J.M., STEPHENS D.J., ROBERTS L.M., 2008a, *The secretion inhibitor Exo2 perturbs trafficking of Shiga toxin between endosomes and the* trans*-Golgi network*, Biochemical Journal, 414(3):471-484.

SPOONER R.A., SMITH D.C., EASTON A.J., ROBERTS L.M., LORD J.M., 2006, *Retrograde transport pathways utilised by viruses and protein toxins.* Virology Journal, 3(26).

SPOONER R.A., WATSON P.D., MARSDEN C.J., SMITH D.C., MOORE K.A., COOK J.P., LORD J.M., ROBERTS L.M., 2004, *Protein disulfide-isomerase* [sic] *reduces ricin to its A and B chains in the endoplasmic reticulum.* Biochemical Journal, 383:285-293.

SPOONER R.A. & WATSON P., 2006, *Toxin entry and trafficking in mammalian cells*. Advanced Drug Delivery Reviews, 58(15):1581-96.

STEBBINS C.E., RUSSO A.A., SCHNEIDER C., ROSEN N., HARTL F.U., PAVLETICH N.P., 1997, *Crystal structure of an Hsp90-Geldanamycin Complex: Targeting of a protein Chaperone by an Antitumor Agent.*, Cell, 89(2):239-50.

STILLMARK H., 1888, *Über, ein giftiges Ferment aus den Samen von Ricinus comm. L. und einigen anderen Euphorbiaceen*, M.D. Dissertation, University of Dorpat, Dorpat.

STIRPE F. & BATTELLI M.G., 2006, *Ribosome-inactivating Proteins: Progresses and Problems*. Cellular and Molecular Life Sciences. 63:1850-1866.

STIRPE F., WILLIAMS D.G., ONYON L.J., LEGG R.F., STEVENS W.A., 1981, *Dianthins, ribosome-damaging proteins with anti-viral properties from Dianthus caryophyllus L. (carnation).* Biochemical Journal, 195:399-405.

STUBDAL H., ZALVIDE J., DECAPRIO J.A., 1996, *Simian Virus 40 Large T Antigen Alters the Phosphorylation State of the RB-Related Proteins p130 and p107*. Journal of Virology. 70(5):2781-88.

SUN L. & CHEN Z.J., 2004, *The novel functions of ubiquitination in signalling*, Current Opinions in Cell Biology, 16(2):119-126.

SWAMINATHAN R., HOANG C.P., VERKMAN A.S., 1997, *Photobleaching recovery and anisotropy decay of green fluorescent protein GFP-S65T in solution and cells: cytoplasmic viscosity probed by green fluorescent protein translational androtational diffusion*. Biophysics Journals 72:1900-1907.

SWANSON R., LOCHER M., HOCHSTRASSER M., 2001, *A conserved ubiquitin ligase of the nuclear envelope/endoplasmic reticulum that function in both ER-associated and Matalpha2 repressor degradation*. Genes & Development, 15(20):2660-74.

TAKAYAMA S. & REED J.C., 2001, *Molecular chaperone targeting and regulation by the BAG family proteins*. Nature Cell Biology, 3:E237-241.

TAKAYAMA S., BIMSTON D.N., MATSUZAWA S., FREEMAN B.C., AIME-SEMPE C., XIE Z., MORIMOTO R.I., REED J.C., 1997, *BAG-1 modulates the chaperone activity of Hsp70/Hsc70.* The EMBO Journal, 16:4887-4896.

TAYLOR M., NAVARRO-GARCIA F., HUERTA J., BURRESS H., MASEY S., IRETON K., TETER K., 2010, *Hsp90 is required for transfer of the cholera toxin A1 subunit from the endoplasmic reticulum to the cytosol*, Journal of Biological Chemistry, [Epub ahead of print].

TETER K., HOLMES R.K., 2002, *Inhibition of Endoplasmic Reticulum-Associated Degradation in CHO Cells Resistant to Cholera Toxin*, Pseudomonas aeruginosa *Exotoxin A, and Ricin.* Infection and Immunity, 70(11):6172-6179.

TETER K., JOBLING M.G., HOLMES R.K., 2003, *A Class of Mutant CHO Cells Resistant to Cholera Toxin Rapidly Degrades the Catalytic Polypeptide of Cholera Toxin and Exhibits Increased Endoplasmic Reticulum-Associated Degradation.* Traffic. 4(4):232-242.

THOMAS M., HARRELL J.M., MORISHIMA Y., PENG H.M., PRATT W.B., LIEBERMAN A.P., 2006, *Pharmacologic and genetic inhibition of hsp90-dependent trafficking reduces aggregation and promotes degradation of the expanded glutamine androgen receptor without stress protein induction.* Human Molecular Genetics, 15(11):1876-83.

THROWER J.S., HOFFMAN L., RECHSTEINER M., PICKART C.M., 2000, *Recognition of the polyubiquitin proteolyic signal*. EMBO Journal, 19(1):94-102.

TIAN P., ANDRICIOAEI I., 2006, *Size, motion, and function of the SecY translocon revealed by molecular dynamics simulations with virtual probes.* Biophysical Journal 90(8):2718-30.

TOMKIEWICZ D., NOUWEN N. & DRIESSEN A.J.M., 2007, *Pushing, pulling and trapping – Modes of motor protein supported translocation*. FEBS Letters, 581(15):2820-2828.

URUSHITANI M., KURISU J., TATENO M., HATAKEYAMA S., NAKAYAMA K., KATO S. & TAKAHASHI R., 2004, *CHIP promotes proteasomal degradation of familial ALS-linked mutant SOD1 by ubiquitinating Hsp/Hsc70*.Journal of Neurochemistry, 90(1):231-44.

UTSKARPEN A., SLAGSVOLD H.H., IVERSEN T.G., WÄLCHLI S., SANDVIG K., 2006, *Transport of ricin from endosomes to the Golgi apparatus is regulated by Rab6A and Rab6A'.*, Traffic 7(6):662-672.

VAGO R., MARSDEN C.J., LORD J.M., IPPOLITI R., FLAVELL D.J., FLAVELL S.U., CERIOTTI A., FABBRINI M.S., 2005, *Saporin and ricin A chain follow different intracellular routes to enter the cytosol of intoxicated cells.* FEBS Journal, 272:4983-4995.

VAN ANKEN E. & BRAAKMAN I., 2005, *Versatility of the Endoplasmic Reticulum Protein Folding Factory*. Critical Reviews in Biochemistry and Molecular Biology, 40:191-228.

VAN DEN BERG B., CLEMONS W.M. Jr., COLLINSON I., MODIS Y., HARTMANN E.,HARRISON S.C., RAPOPORT T.A., 2004, *X-ray structure of a protein-conducting channel.* Nature, 427:36-44.

VAN DEN BERG B., ELLIS R.J., DOBSON C.M., 1999, *Effects of macromolecular crowding on protein folding and aggregation*. The EMBO Journal, 18:6927-33.

VAN DEURS, B., SANDVIG, K., PETERSEN, O.W., OLSNES, S., SIMONS, K., GRIFFITHS, G.,1988, *Estimation of the Amount of Internalised Ricin That reaches the trans-Golgi Network.* The Journal or Cell Biology, 106:253-267.

VAN DEURS, B., TONNESSEN T.I., PETERSEN O.W., SANDVIG K., OLSNES S., 1986, *Routing of internalized ricin and ricin conjugates to the Golgi complex.* Journal of Cell Biology, 102(1):37-47.

VAN NOCKER S., DEVERAUX Q., RECHSTEINER M., VIERSTRA R.D., 1996, *Arabidopsis MBP1 gene encodes a conserved ubiquitin recognition component of the 26S proteasome*, Proceedings of the National Academy of Science (USA), 93(2):856-60.

VANHOVE M., USHERWOOD Y.K., HENDERSHOT L.M., 2001, *Unassembled Ig heavy chains do not cycle from BiP in vivo but require light chains to trigger their release.* Immunity, 15(1):105-14.

VAUGHAN C.K., PIPER P.W., PEARL L.H., PRODROMOU C., 2008, *A common conformationally coupled ATPase mechanism for yeast and human cytoplasmic HSP90s.* The FEBS Journal, 276(1):199-209.

VENDEVILLE A., RAYNE F., BONHOURE A., BETTACHE N., MONTCOURRIER P., BEAUMELLE B., 2004, *HIV-1 Tat Enters T Cells Using Coated Pits before Translocating from Acidified Endosomes and Eliciting Biological Responses*, Molecular Biology of the Cell, 15:2347-2360.

WALES, R., ROBERTS, L.M., LORD, J.M. (1993). Addition of an Endoplasmic Reticulum Retrieval Sequence to Ricin A Chain Significantly Increases Its Cytotoxicity to Mammalian Cells. *The Journal of Biological Chemistry* 268(32):23986-23990.

WALSH P., BURSAC D., LAW Y.C., CYR D., LITHGOW T., 2004, *The J-protein family: modulating protein assembly, disassembly and translocation*. EMBO reports, 5(6):567-571.

WANG C.T., MENG M., ZHANG J.C., JIN C.J., JIANG J.J., REN H.S., JIANG J.M., QIN C.Y., YU D.Q., Chinese Medical Journal 121(17):1707-11.

WANG S. & NG D.T.W., 2008, *Lectins sweet-talk proteins into ERAD.* Nature Cell Biology, 10:251-253.

WANG Q., SONG C., LI C.C.H., 2004, *Molecular perspectives on p97-VCP: progress in understanding its structure and diverse biological functions.* Journal of Structural Biology, 146:1-2:44-57.

WANG X., HERR R.A., RABELINK M., HOEBEN R.C., WIERTZ E.J., & HANSEN T.H., 2009, *Ube2j2 ubiquitinates hydroxylated amino acids on ER-associated degradation substrates.* Journal of Cell Biology, 187(5):655-68.

WEDIN G.P.., NEAL J.S., EVERSON G.W., KRENZELOK E.P., 1986, *Castor Bean Poisoning*, The American Journal of Emergency Medicine, 4(3):259-261.

WEI C.H. & EINSTEIN J.R., 1974, *Preliminary crystallographic datafor a new crystalline form of abrin.* Journal of Biological Chemistry, 249, 2985-2986.

WERNER E.D., BRODSKY J.L., MCCRACKEN A.A., 1996, *Proteasome-dependent endoplasmic reticulum-associated protein degradation: an unconventional route to a familiar fate*. Proceedings of the National Academy of Science (USA), 93(24):13797-801.

WESCHE J., MAŁECKI J., WIĘDŁOCHA A., SKJERPEN C.A. CLAUS P., 2006, *FGF-1 and FGF-2 Require the Cytosolic Chaperone Hsp90 for Translocation into the Cytosol and the Cell Nucleus.* Journal of Biological Chemistry, 281(16):11405-12.

WESCHE, J., RAPAK, A., OLSNES, S., 1999, *Dependence of Ricin Toxicity on the Translocation of the Toxin A-chain from the Endoplasmic Reticulum to the Cytosol.* The Journal of Biological Chemistry 274(48):34443-34449.

WESTHOFF B., CHAPPLE P., VAN DER SPUY J., HÖHFELD J., CHEETHAM M.E., 2005, *HSJ1 Is a Neuronal Shuttling Factor for the Sorting of Chaperone Clients to the Proteasome*, Current Biology, 15:1058-64.

WHITESELL L. & COOK P., 1996, *Stable and specific binding of heat shock protein 90 by geldanamycin disrupts glucocorticoid receptor function in intact cells.* Molecular Endocrinology, 10(6):705-12.

WHITESELL L. & LINDQUIST S.L., 2005, *Hsp90 and the chaperoning of cancer*, Nature Reviews Cancer 5:761-72.

WHITESELL L., MIMNAUGH E.G., DE COSTA B., MYERS C.E., NECKERS L.M., 1994, *Inhibition of heat shock protein HSP90-pp60v-src heteroprotein complex formation by benzoquinone ansamycins: essential role for stress proteins in oncogenic transformation.* Proceedings of the National Academy of Science (USA), 91(18):8324-8.

WIEDEMANN N., FRAZIER A.E., PFANNER N., 2004, *The protein import machinery of mitochondria.* The Journal of Biological Chemistry, 279:14473-6.

WIEDERKEHR T., BUKAU B., BUCHBERGER A., 2002, *Protein Turnover: a CHIP Programmed for Proteolysis.* Current Biology, 12(1):R26-R28.

WILLER M., FORTE G.M.A., STIRLING C.J., 2008, *Sec61p Is Required for ERAD-L: GENETIC DISSECTION OF THE TRANSLOCATION AND ERAD-L FUNCTION OF SEC61P USING NOVEL DERIVATIVES OF CPY**. The Journal of Biological Chemistry, 283:33883-8.

YAN Q. PRESTWICH D.G., LENNARZ W.J., 1999, *The Ost1p subunit of yeast oligosaccharyl transferase recognizes the peptide glycosylation site –Asn-X-Ser/Thr-*, Journal of Biological Chemistry, 274(8):5021-5.

YE Y., SHIBATA Y., YUN C., RON D., RAPOPORT T.A., 2004, *A membrane protein complex mediates retro-translocation from the ER lumen into the cytosol*. Nature, 429:841-847.

YE Y. MEYER H.H., RAPOPORT T.A., 2003, *Function of the p97-Ufd1-Npl4 complex in retrotranslocation from the ER to the cytosol: dual recognition of nonubiquitinated polypeptide segments and polyubiquitin chains*. Journal of Cell Biology, 162(1):71-84.

YOUNG J.C., AGASHE V.R., SIEGERS K., HARTL F.U., 2004, *Pathways of chaperone-mediated protein folding in the cytosol*. Nature Reviews in Molecular Cell Biology, 5:781-791.

YOUNG J.C., BARRAL J.M. & HARTL F.U., 2003, *More than folding: localized functions of cytosolic chaperones*. Trends in Biochemical Sciences, 28(10):541-547.

YOUNG J.C., MOAREFI I., HARTL F.U., 2001, *Hsp90 a specialized but essential protein-folding tool*. Journal of Cell Biology, 154(2):267-274.

YOSHIDA Y., CHIBA T., TOKUNAGA F., KAWASAKI H., IWAI K., SUZUKI T., ITO Y., MATSUOKA K., YOSHIDA M., TANAKA K., TAI T., 2002, *E3 ubiquitin ligase that recognizes sugar chains.* Nature, 418(6896):438-42.

YOSHINARI T., CHEN C., ZHANG M., WU H.C., 1991, *Disruption of the Golgi apparatus by brefeldin A inhibits the toxicity of ricin, modeccin and* Pseudomonas *toxin*. Experimental Cellular Research, 192:389-395.

ZACHOWSKI A., 1993, *Phospholipids in animal eukaryotic membranes: transverse asymmetry and movement*. Biochem. Journal, 294:1-14.

ZARA V., FERRAMOSCA A., ROBITAILLE-FOUCHER P., PALMIERI F., YOUNG J.C., 2009, *Mitochondrial carrier protein biogenesis: role of the chaperones Hsc70 and Hsp90.* Biochemical Journal, 419:369-375.

ZHAN, J., STAYTON, P., PRESS, O.W., 1998, *Modification of ricin A chain, by addition of endoplasmic reticulum (KDEL) or Golgi (YQRL) retention sequences, enhances its cytotoxicity and translocation.* Cancer Immunology and Immunotherapy, 46(1):55-60.

ZHANG M., BOTËR M., LI K., KADOTA Y., PANARETOU B., PRODROMOU C., SHIRASU K., PEARL L.H., 2008, Structural and functional coupling of Hsp90- and Sgt1-centred multi-protein complexes, *The EMBO Journal*, 27:2789-2798.

ZHANG J., BAKER M.L., SCHRÖDER G.F., DOUGLAS N.R., REISSMANN S., JAKANA J., DOUGHERTY M., FU C.J., LEVITT M., LUDTKE S.J., FRYDMAN J., CHIU W., 2010, *Mechanism of folding chamber closure in a group II chaperonin.* Nature Letters, 463:379-384.

Software

Chimera

Molecular graphics images were produced using the UCSF Chimera package from the Resource for Biocomputing, Visualization, and Informatics at the University of California, San Francisco (supported by NIH P41 RR-01081).

ISISDraw

Figures showing the chemical structures of small molecule inhibitors were produced using ISISDraw V2.5.4 (MDL Information Systems).

Microsoft Excel

Microsoft's Excel was used for linear regression of datasets, Student's T-tests (paired and unpaired), where stated.

PaintShopPro Photo X2

Graphics depicting model pathways were produced using PaintShopPro Photo X2 (CorelDraw).

TotalLab Quant

All electrophoretic gels and blots derived from them were quantified using TotalLab Quant, 2003 (GE Healthcare).

CHAPTER 8:

Appendix

8.1 The activity of deoxyspergualin degrades on prolonged storage

As referred to in text in section 5.11.3, the activity of deoxyspergualin degrades after opening and protracted storage dissolved in water. Figure 8.1 compares the effect of an old stock of DSG to a freshly dissolved batch.

8.2 The turbidity of RTA can be measured during a heat treatment

As referred to in section 4.3, dilute RTA was incubated in a MOPS/KCl buffer (in 10 mM MOPS / 50 mM KCl, pH7.2) and the absorbance at 320nm was recorded over time. Two methods were used. An "aliquot method", where the absorbance of a 20μL sample from an larger incubation (of 700μL) was taken and its absorbance measured. This method used a water bath to heat the sample. A second approach used a spectrophotometer with a heated chamber to measure the absorbance of a "whole sample" in a cuvette, without the need for aliquots.

The whole sample method produces much more reliable results, but the capacity of the heated spectrophotometer's chamber was limited. Moreover, the temperature control was unreliable over time and varied across the chamber. The aliquot method, on the other hand, would have allowed parallel samples to be taken, but the results it generated seemed too unreliable to waste precious purified proteins upon.

Figure 8.1 – The activity of deoxyspergualin degrades on prolonged storage

a) & b) Show exemplar dose-response curves from sets of three independent assays. 100 µg.mL^{-1} lactose (○); 100 µg.mL^{-1} lactose and 50 µg.mL^{-1} DSG (●). In a) a stock of DSG which had been frozen at 20°C in water for 6 months. In b) a freshly dissolved batch was used. c) Shows the calculated protective effect in each instance (from an average of the three assays (error bars show standard deviation). d) Shows the effect of DSG itself upon protein synthesis relative to lactose treatment.

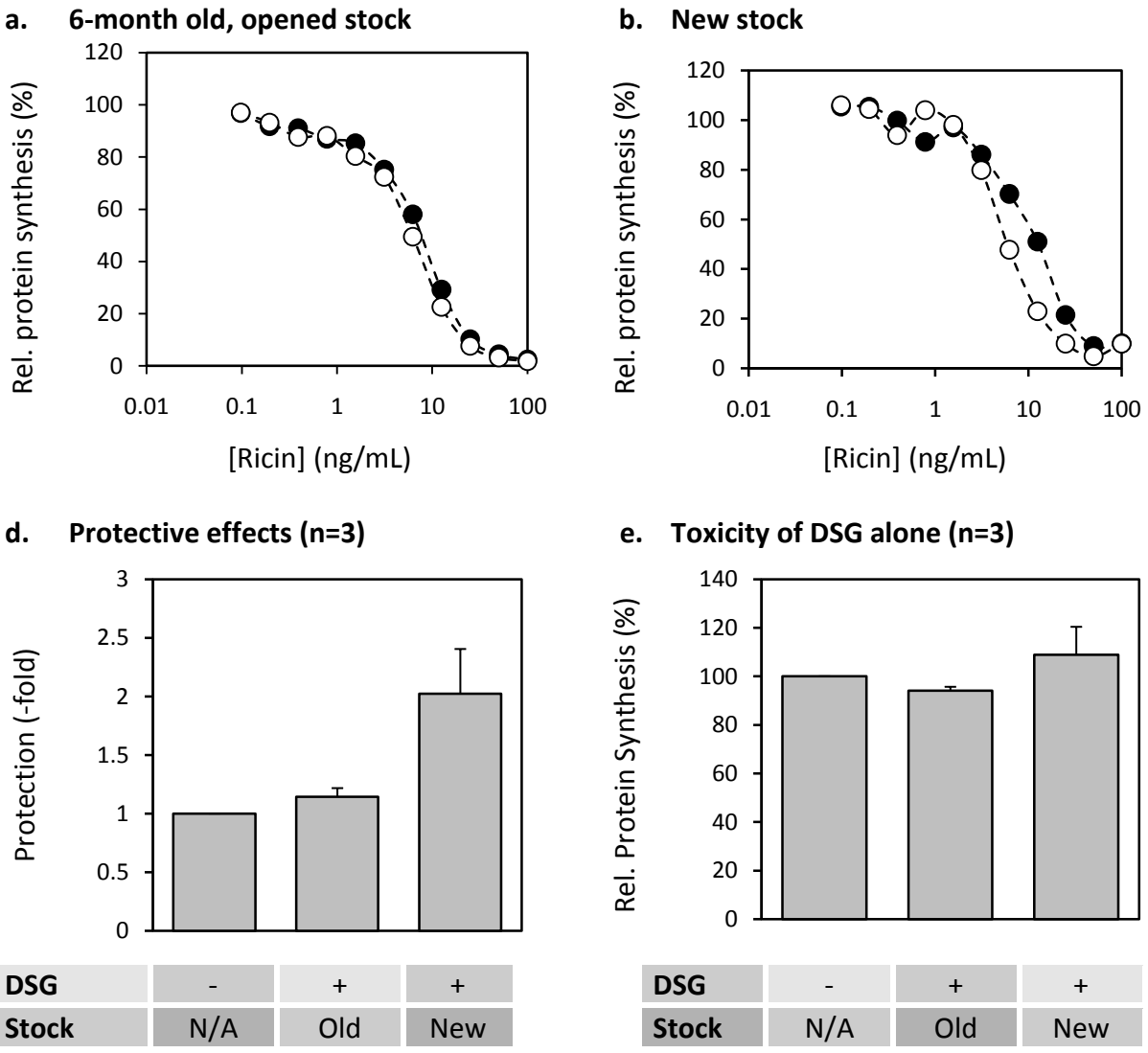

Figure 8.2 – The increasing turbidity of an RTA solution during a heat treatment

The absorbance of RTA (in 10 mM MOPS / 50 mM KCl, pH7.2) at 320 nm was measured over time. Two techniques were attempted: using a waterbath to heat the sample, from which aliquots were taken and analysed in a spectrophotometer separately (the "aliquot method"). Alternatively, a spectrophotometer with temperature control was used, so the absorbance of the whole sample rather than an aliquot was taken at each timepoint (the "whole sample method"). Experiments were conducted with 1.38 µM RTA, with 0.46 µM RTA, or no RTA. Two temperatures were used: 21°C or 45°C.

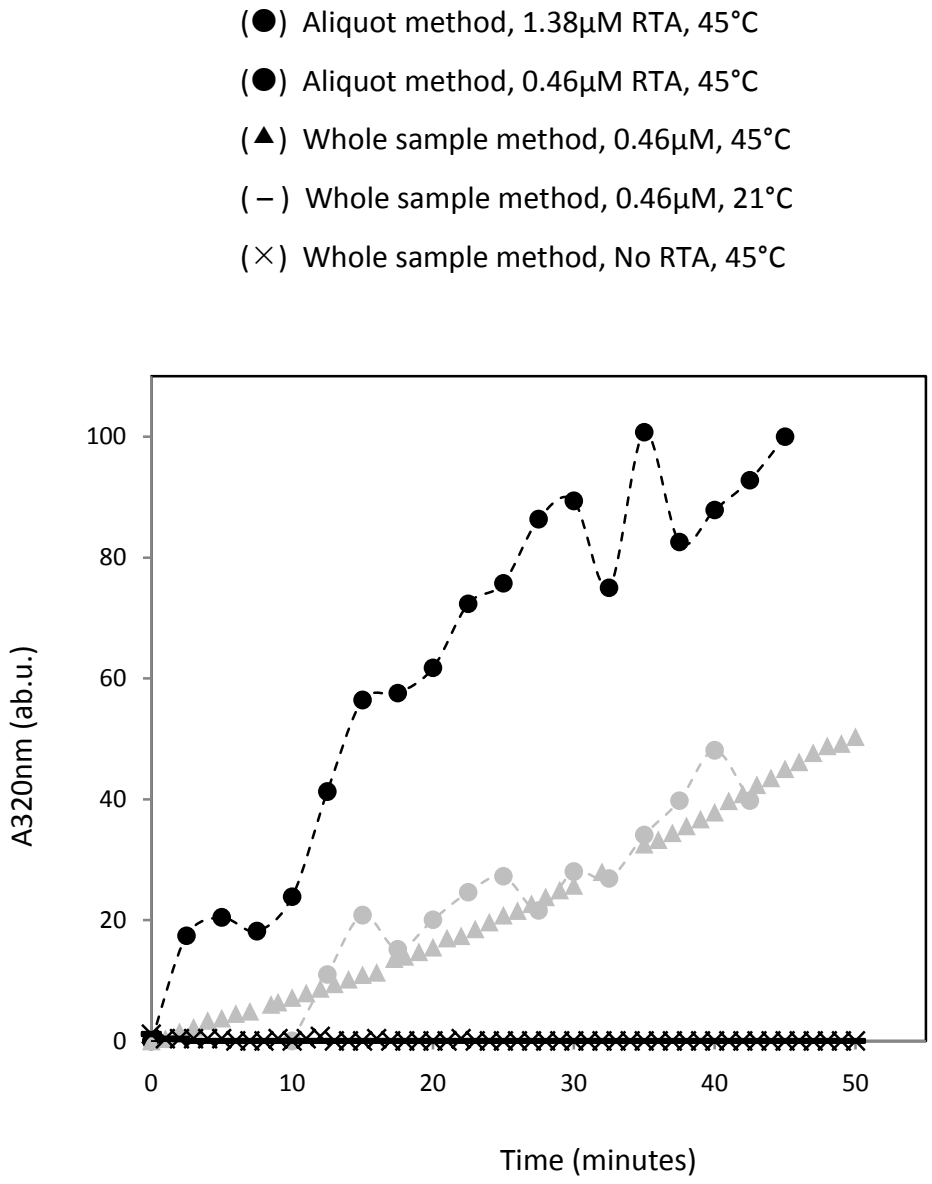

Cytosolic chaperones influence the fate of a toxin dislocated from the endoplasmic reticulum

Robert A. Spooner[a,1], Philip J. Hart[a], Jonathan P. Cook[a], Paola Pietroni[a], Christian Rogon[b], Jörg Höhfeld[b], Lynne M. Roberts[a], and J. Michael Lord[a]

[a]Department of Biological Sciences, University of Warwick, Coventry CV4 7AL, United Kingdom; and [b]Institut für Zellbiologie, Rheinische Friedrich Wilhelms-Universität Bonn, Ulrich-Haberland-Strasse 61a, 53121 Bonn, Germany

Communicated by Ellen S. Vitetta, University of Texas Southwestern Medical Center, Dallas, TX, September 24, 2008 (received for review January 30, 2008)

The plant cytotoxin ricin enters target mammalian cells by receptor-mediated endocytosis and undergoes retrograde transport to the endoplasmic reticulum (ER). Here, its catalytic A chain (RTA) is reductively separated from the cell-binding B chain, and free RTA enters the cytosol where it inactivates ribosomes. Cytosolic entry requires unfolding of RTA and dislocation across the ER membrane such that it arrives in the cytosol in a vulnerable, nonnative conformation. Clearly, for such a dislocated toxin to become active, it must avoid degradation and fold to a catalytic conformation. Here, we show that, *in vitro*, Hsc70 prevents aggregation of heat-treated RTA, and that RTA catalytic activity is recovered after chaperone treatment. A combination of pharmacological inhibition and cochaperone expression reveals that, *in vivo*, cytosolic RTA is scrutinized sequentially by the Hsc70 and Hsp90 cytosolic chaperone machineries, and that its eventual fate is determined by the balance of activities of cochaperones that regulate Hsc70 and Hsp90 functions. Cytotoxic activity follows Hsc70-mediated escape of RTA from an otherwise destructive pathway facilitated by Hsp90. We demonstrate a role for cytosolic chaperones, proteins typically associated with folding nascent proteins, assembling multimolecular protein complexes and degrading cytosolic and stalled, cotranslocational clients, in a toxin triage, in which both toxin folding and degradation are initiated from chaperone-bound states.

Hsc70 | Hsp90 | ricin

Endoplasmic-reticulum (ER) associated protein degradation (ERAD) comprises coordinated disposal systems that recognize and remove misfolded and unassembled proteins in the ER, dislocating them across the ER membrane to the cytosol for proteasomal destruction. Degradation is normally facilitated by polyubiquitylation, usually on internal lysyl residues of the target protein. Both membrane-bound and soluble ER proteins can be disposed of by ERAD (1, 2).

The plant cytotoxin ricin traffics to the ER lumen of mammalian cells where it is reduced to its RTA and RTB subunits before RTA dislocation (3). RTA does not penetrate the ER membrane directly; instead it exploits pre-existing protein-conducting channels as a nonnative species, mimicking ER proteins dispatched via ERAD (4, 5). Thus, it enters the cytosol in a form susceptible to proteolysis or aggregation. A proportion must evade these fates to gain a catalytic conformation that depurinates target ribosomes, stopping protein synthesis. The paucity of lysine residues in RTA may facilitate uncoupling from ERAD by reducing the potential for polyubiquitylation, thereby hampering proteasomal degradation (6). This, in turn, may provide opportunities for spontaneous or chaperone-assisted folding not normally sanctioned for ERAD substrates.

We show an interaction of RTA with the cytosolic heat shock (cognate) protein Hsc70. From the chaperone-bound state, nonnative cytosolic RTA can achieve a catalytic conformation or can be inactivated. Its ultimate fate depends on the activities of cochaperones that regulate Hsc70.

Results

Inhibition of Hsc70 Protects HeLa Cells from Ricin. Ricin binds exposed galactosyl residues, opportunistically exploiting a huge number of surface glycoproteins (3). Consequently, trafficking pathways are diverse with <5% of the cell-surface bound toxin reaching the TGN (7). Of this, only a tiny proportion reaches the ER (8) and subsequently the cytosol. RTA is not modified in transit, so the toxic cytosolic fraction cannot be distinguished from the overwhelming noncytotoxic majority at the cell surface and in the endomembrane system by immunoblotting, cellular fractionation, indirect immunofluorescence, or coimmunoprecipitation approaches. However, ricin cytotoxicity correlates strongly with ribosome depurination, so it can be used as a measure of the relative amount of native RTA in the cytosol (9).

Deoxyspergualin (DSG) alters the ATPase activity of the cytosolic heat-shock (cognate) protein Hsc70 *in vitro*, and *in vivo* permits expression of functional cystic fibrosis transmembrane conductance regulator (CFTR) in cells expressing mutant ΔF508CFTR, presumably by inhibiting interactions with Hsc70 chaperone complexes that target it to proteasomes (10, 11). When DSG was added with ricin to HeLa cells, the cells became ~3-fold more resistant to toxin (Fig. 1 *A* and *B*), suggesting that an increased proportion of toxin remained inactive. DSG alone had no effect on protein synthesis (Fig. 1*C*). The ER Hsp70 counterpart BiP is not affected by DSG (12), suggesting that protection occurred in the cytosol. After ricin challenge, a distinct lag before the onset of cytotoxicity that represents trafficking time from cell surface to the first destruction of ribosomes (13) is unchanged by DSG treatment (Table 1), confirming that the effect of DSG occurs in the cytosol, and not by interfering with toxin delivery. Because unfolding is necessary to render RTA competent for dislocation (5), then folding must be required for catalytic activity in the cytosol, and this appears to involve Hsc70. In contrast, DSG had no effect on the potency of diphtheria toxin (DTx, Fig. 1 *A* and *B*), which enters the cytosol from acidified endosomes, refolding spontaneously in the cytosol (14).

Inhibition of Hsp90 Sensitizes Cells to Ricin. DSG also interacts with the cytosolic chaperone Hsp90 (10). To clarify its most upstream target, we used geldanamycin (GA) and radicicol (RA), competitive inhibitors of the Hsp90 ATP-binding site (15). Treatment with 1 μM GA or RA resulted in a ~1.5- to 2-fold sensitization of cells to ricin (Fig. 2 *A* and *B*), without altering toxin trafficking times (Table 1). Treatments with GA or RA alone have little, if any, effect on protein synthesis (Fig. 2*C*).

Author contributions: R.A.S., J.H., L.M.R., and J.M.L. designed research; R.A.S., P.J.H., J.P.C., and P.P. performed research; C.R. contributed new reagents/analytic tools; R.A.S., J.H., L.M.R., and J.M.L. analyzed data; and R.A.S., J.H., L.M.R., and J.M.L. wrote the paper.

The authors declare no conflict of interest.

Freely available online through the PNAS open access option.

[1]To whom correspondence should be addressed. E-mail: r.a.spooner@warwick.ac.uk.

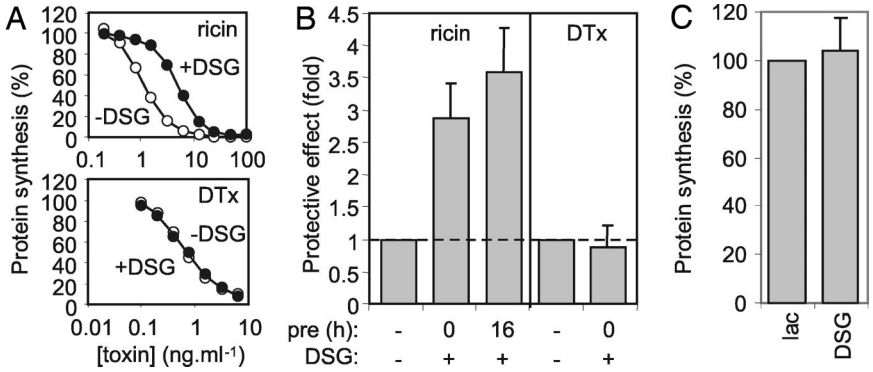

Fig. 1. Deoxyspergualin (DSG) protects HeLa cells from ricin intoxication. (*A*) Cells were treated for 4 h with graded doses of ricin or diphtheria toxin (DTx) in growth medium containing 50 μg ml^{-1} DSG/100 μg ml^{-1} lactose (filled circles) or 100 μg ml^{-1} lactose carrier only (open circles), and their subsequent ability to synthesize proteins was determined by measuring incorporation of [^{35}S]-Met into acid-precipitable material. Typical single assays are shown. (*B*) Control cells and cells pretreated (pre) with DSG/lactose were treated as in *A*, sensitivities to toxin (IC_{50}, toxin concentration required to reduce protein synthesis to 50% that of nontoxin treated controls) were determined, and fold protection (IC_{50} DSG-treated cells: IC_{50} control cells) is displayed. Means of three (DTx, ricin 16-h DSG pretreatment) or six (ricin, no DSG pretreatment) independent experiments are displayed. (Bars, $\pm$1 S.D.; broken line, no protective effect over that of treatment with lactose carrier only). (*C*) Cells were treated with lactose (lac) or lactose/DSG only as appropriate for 4 h, and remaining protein synthesis ability was determined. (n = 3; bars, $\pm$1 S.D.).

Prolonged inhibition of Hsp90 by GA up-regulates Hsp72 (16). We saw the same, confirming activity of GA and RA under our conditions (Fig. 2*D*). Our sensitizing effects were obtained by using acute drug treatments, before up-regulation of Hsp72, but even with a 4-h drug pretreatment, cells were still sensitized to ricin (data not shown). Thus, the effects of GA and RA do not arise through augmented levels of Hsp72. GA and RA also interact with GRP94, the ER counterpart of Hsp90. NECA (N-ethylcarboxamidoadenosine), a GRP94 inhibitor that does not affect Hsp90 (17) protected cells slightly from ricin (1.48 $\pm$ 0.34 -fold, n = 5), confirming that the sensitizing effects of GA and RA arose from inhibition of cytosolic Hsp90 and not GRP94 (Fig. 2*B*). It also suggests a role for GRP94 in preparing RTA for dislocation, consistent with its ability to direct the null Hong Kong variant of α1-antitrypsin to ERAD (18).

These data suggest that the fate of RTA is determined by cytosolic triage, with an activation arm (toxin-sensitizing) inhibited by DSG and an inactivation arm (protective) inhibited by GA and RA. Combined treatment with DSG and RA gave a net protective effect against ricin (Fig. 2*B*), demonstrating a sequential process with the step promoted by Hsc70 lying upstream of the step mediated by Hsp90.

Hsc70 Interacts with RTA *in Vitro*. Because the minuscule amounts of cytosolic RTA preclude detection except by monitoring the consequences of its catalytic action, interactions with Hsp70 and its cochaperone Hsp40 were examined *in vitro*. Brief heating to 45°C destabilizes RTA structure (19). RTA became insoluble (P, pellet) after such treatment (15 min), with ~10% remaining soluble (S) after centrifugation (Fig. 3*A*, upper panel, upper graph). Incremental increases in recovery of soluble material were obtained by adding Hsp40, Hsp70, or both before heating. Maximal chaperone-mediated solubility required ATP. These data suggest that a potential role for these chaperones *in vivo* could be to prevent vulnerable dislocated RTA from aggregating. Hsp40 was insoluble after heat treatment, alleviated by addition of Hsc70. Repeating these assays in the absence of RTA showed that this is its normal behavior (Fig. 3*A*, middle panel).

Table 1. Ricin cell-surface to cytosol trafficking times

Treatment	T, min
100 μg ml^{-1} lactose carrier	62.4 $\pm$ 1.2
50 μg ml^{-1} DSG/ lactose	64.7 $\pm$ 1.8
0.001% DMSO vehicle	68.0 $\pm$ 6.3
1 μM geldanamycin/DMSO	63.4 $\pm$ 9.8
1 μM radicicol/DMSO	65.2 $\pm$ 8.3

T, n = 3–6, $\pm$ 1 SD.

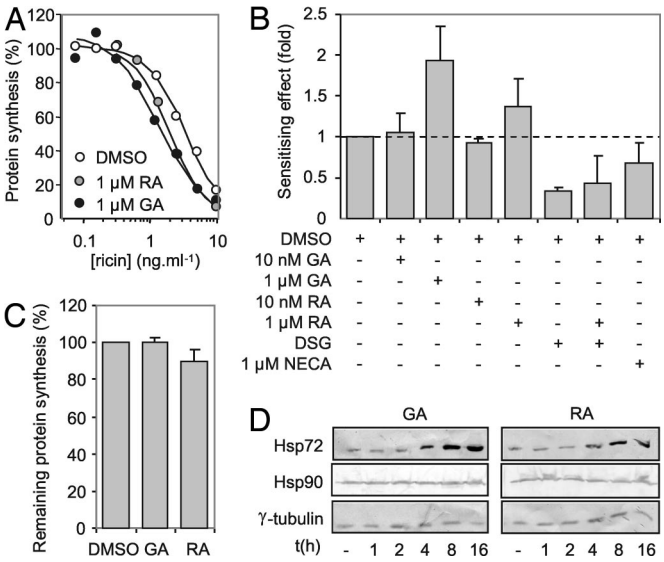

Fig. 2. Geldanamycin (GA) and radicicol (RA) sensitize HeLa cells to ricin challenge. (*A*) Cells were treated (4 h) with increasing doses of ricin in medium containing GA/DMSO (black circles), RA/DMSO (gray circles), or DMSO vehicle only (white circles), and their subsequent ability to synthesize proteins was determined as in Fig. 1*A*. Typical single assays are shown. (*B*) Cells were challenged as in (*A*), IC_{50} values were determined as in Fig. 1*B*, and the effects of GA and RA are displayed as fold sensitizations (IC_{50} GA- or RA-treated cells: IC_{50} control DMSO-treated cells). Also shown are the effects of treatment with NECA, and combined treatments with RA, DSG, and DMSO. Means of three independent experiments are displayed, except for NECA treatment, where n = 5. (Bars, $\pm$1 S.D.; broken line, no effect over that of treatment with DMSO vehicle only) (*C*) Cells were treated with vehicle DMSO, DMSO/GA, or DMSO/RA as appropriate for 4 h, and remaining protein synthesis ability was determined. (n = 3; bars, $\pm$1 S.D.) (*D*) Immunoblots of detergent soluble cell extracts (25 μg protein per lane) from cells incubated for various lengths of time (t) in growth medium containing 1 μM GA or 1 μM RA were probed for Hsp72 (upper strip), Hsp90 (middle strip), or γ-tubulin (lower strip).

CELL BIOLOGY

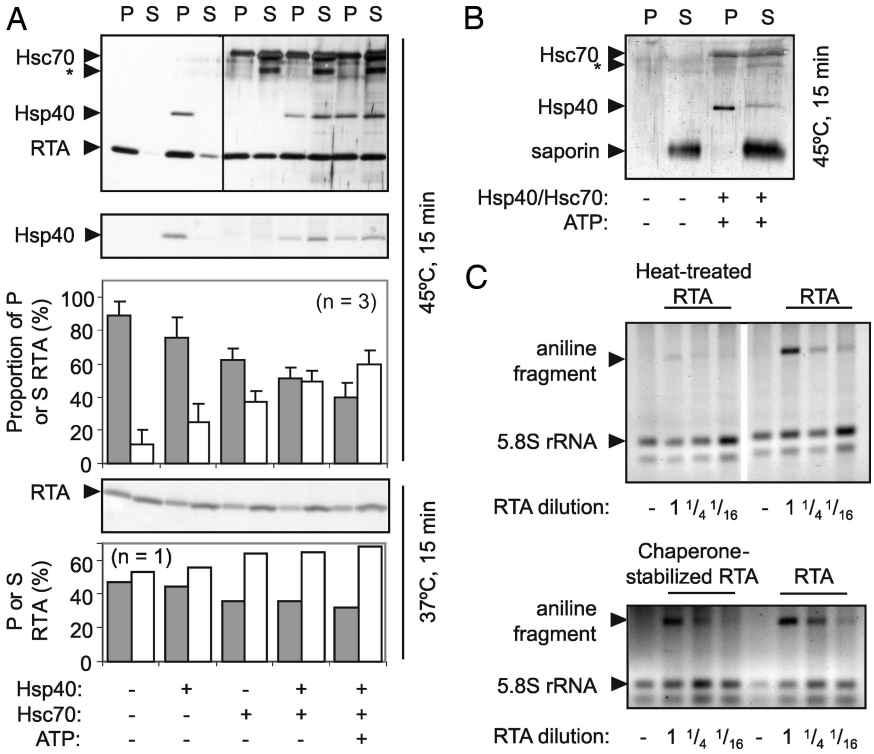

Fig. 3. *In vitro* interactions of RTA and Hsp40 and Hsc70 chaperones. (*A*) RTA (500 ng) was incubated at the indicated temperatures for 15 min in 20 μl of 20 mM Mops pH 7.2, 100 mM KCl, in the presence or absence of Hsp40, Hsc70, or ATP (shown below the panels). Aggregated (P) and soluble (S) fractions were separated by centrifugation, heated in reducing SDS sample buffer, and analyzed by SDS/PAGE and subsequent silver staining. *, proteolytic fragment of Hsc70 lacking the C-terminal regulatory domain. Proportions (%) of aggregated (gray) and soluble (white) RTA are shown. (Bars, $\pm$1 S.D.) (*B*) Reaction mixtures where RTA was replaced by saporin were treated as in (*A*). (*C*) Dilutions of the soluble fractions from 375 ng of heat-treated RTA (upper panel), 375 ng of chaperone-stabilized RTA (lower panel), and 375 ng of native RTA were added to yeast ribosomes for 2 h at 30°C. After cleavage of any depurinated 28S rRNA with acetic-aniline, rRNAs were extracted, electrophoresed in denaturing conditions (1.2% agarose, 50% formamide), and gels were stained with ethidium bromide before quantifying (22).

When RTA was heated for 15 min with or without chaperones at 37°C, the chaperones had a similar although less pronounced effect (Fig. 3*A*, lower panel, lower graph). Saporin has a largely indistinguishable tertiary structure relative to RTA with identical, superimposable active site residues and has identical activity against ribosomes (20), but it lacks the C-terminal hydrophobic stretch that in RTA has been implicated in membrane interactions preceding dislocation (21). Saporin showed no thermal instability (Fig. 3*B*) after heating at 45°C. This result contrasts with the instability of RTA and its recognition by Hsp40/Hsc70 even at 37°C, and suggests that interactions with Hsc70 might be a normal feature of folded RTA in the cytosol.

To investigate whether chaperone-treated RTA had catalytic activity, dilutions of the soluble fractions from heat-treated RTA and chaperone-stabilized RTA were added to yeast ribosomes, which were subsequently treated with acidified aniline. Correctly folded RTA specifically depurinates yeast 26S rRNA, and aniline treatment cleaves the phosphodiester bond at the depurination site, releasing a small diagnostic fragment of RNA (22). As expected, a small amount of RTA activity remained after heat-treatment, but almost full activity was recovered from chaperone-stabilized RTA (Fig. 3*C*). We conclude that the major proportion of denatured RTA with chaperone-mediated solubility is, or can become, competent to gain catalytic activity.

Hsc70 Cochaperone Activity Determines the Fate of Dislocated RTA *in Vivo*. Having established that RTA interacts with Hsc70 *in vitro* and that catalytic activity can be recovered from the chaperone-bound state, we examined the effects of modulating Hsc70 cochaperone activities *in vivo*.

The dual cochaperone Hsc70-Hsp90 organizing protein (Hop) recruits Hsp90 to pre-existing Hsc70-client complexes, transferring client proteins from Hsc70 to Hsp90 (23). Transient overexpression of Hop protected cells from ricin challenge (Fig. 4 *A* and *C*), suggesting that increased links between Hsc70 and Hsp90 lead to increased toxin turnover, consistent with the sensitizing effects of GA/RA that block entry into the Hsp90 cycle. Thus, sequential interaction with Hsc70 and Hsp90 directs cytosolic RTA toward net inactivation.

BCL2-associated athanogene protein (BAG-1) isoforms are nucleotide exchange factors that stimulate release of Hsc70-bound clients and bear a ubiquitin-like (ubl) motif that interacts with the proteasome (24). Transient overexpression of BAG-1 protected cells against ricin (Fig. 4 *B* and *D*). Thus, BAG-1 may stimulate release of Hsc70-bound RTA on a path toward inactivation, consistent with the increased sensitivity of cells to ricin reported after inhibition of proteasome activity (25).

Both Hsc70- and Hsp90- complexes can become sorting machines that promote client destruction. C terminus of Hsp70-interacting protein (CHIP) is an E3 ubiquitin ligase that interacts with Hsc70 and Hsp90, and with its partner ubiquitin-conjugating enzymes initiates proteasomal sorting by ubiquitylating chaperone-bound substrates. Transient over-expression of CHIP resulted in enhanced inactivation of RTA, seen as increased resistance of cells to ricin (Fig. 4 *B* and *E*).

To investigate whether Hsc70 can also promote toxin activity *in vivo*, we overexpressed Hsp70-interacting protein (Hip), a Hsc70 cochaperone, which stabilizes ADP-bound Hsc70, in-

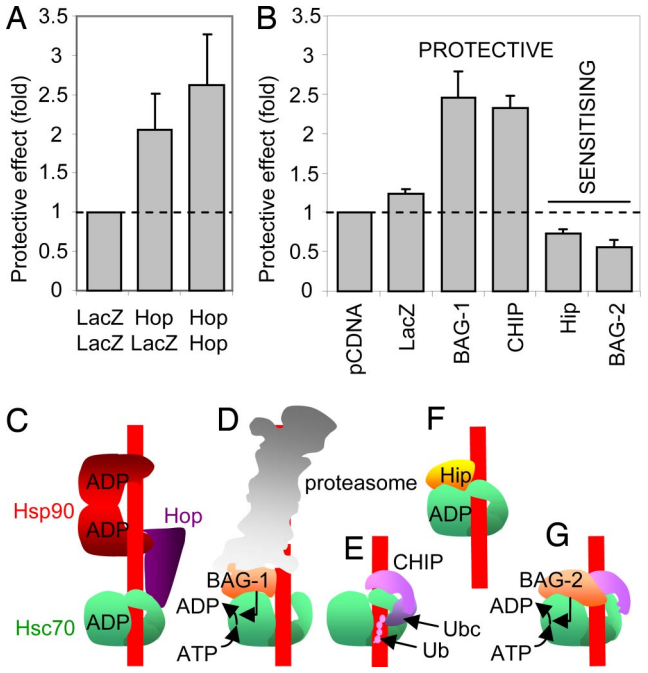

Fig. 4. Hsc70 cochaperone activity determines the fate of dislocated RTA *in vivo*. (*A*) Cells transiently transfected with an expression plasmid expressing Hop (Hop/Hop), with an equimolar mixture of plasmids expressing LacZ and Hop (Hop/LacZ), or with a plasmid expressing LacZ (LacZ/LacZ) were assayed for ricin sensitivity. Values were corrected for transfection efficiency, determined as 35% by epifluorescent examination of cells transiently transfected with a plasmid expressing GFP. Dotted line, no effect over that of LacZ transfection. (*B*) Cells were transfected, as in (*A*), with expression plasmids expressing LacZ, BAG-1S [the small (S) isomer of BAG-1], CHIP, Hip, or BAG-2 and were assayed for ricin sensitivity compared with cells transfected coevally with vector alone. Dotted line, no protective effect over vector transfection. (*C–G*) Interactions of cochaperones with Hsc70 and client protein (red line).

creasing client residence and presumably permitting greater opportunity for productive folding (26). Over-expression of Hip-sensitized cells to ricin challenge (Fig. 4 *B* and *F*); thus, Hip controls an activation arm of RTA triage.

The BAG-2 nucleotide exchange factor lacks the ubl domain of BAG-1 and thus, cannot link a client:chaperone complex directly to the proteasome. It also inhibits CHIP activity (27). These properties allow it to facilitate maturation of newly synthesized CFTR, diverting the receptor from the proteasome pathway (28). Consistent with this, BAG-2 overexpression increased the sensitivity of cells to ricin (Fig. 4 *B* and *G*), demonstrating diversion of RTA from a destructive fate. We conclude that the ultimate fate of cytosolic RTA is determined by the relative expression levels of Hsc70 cochaperones.

RTA Can Be a Substrate for CHIP. Our inhibitor and expression data demonstrate that activation and inactivation arms for RTA proceed from Hsc70, and suggest that inactivation may require a ubiquitin signal, either indirectly [via the interlaced ubl domain of BAG-1 or perhaps in a piggy-back mechanism through Hsc70 ubiquitylation (29)], or directly (as CHIP-mediated RTA ubiquitylation). To examine the latter, purified RTA was added to reaction mixtures in which CHIP activity can be recapitulated *in vitro* (30), which were then incubated for 2 h at 30°C. In complete reaction mixtures and also when E1 (ubiquitin activating enzyme), E2 (ubiquitin conjugating enzyme), CHIP, or Hsp40/Hsc70 were individually absent from the reconstitutions, no ubiquitylation of RTA was seen (data not shown). However, after mild thermal denaturation (45°C, 10 min) followed by incubation at 30°C in complete reaction mixture not only was Hsc70 ubiquitylated (Fig. 5*A*, Ub-Hsc70, upper panel) but so was a small proportion of RTA (Fig. 5*A*, Ub-RTA, lower panel). An even smaller proportion of RTA was a substrate for isolated CHIP.

The scrutiny of native RTA at 37°C by Hsc70 complexes that was noted previously (Fig. 3*A*) was also seen with Hsc70/CHIP complexes. After incubation at 37°C for 2 h in the absence of E1, there was no ubiquitylation of Hsc70, CHIP, or RTA (Fig. 5*B*). Upon addition of E1, both Hsc70 and CHIP became ubiquitylated, events that occur *in vivo* that reflect regulation of Hsc70 by CHIP (28). Not all proteins are ubiquitylated in these conditions, for example, BAG-2 inhibits CHIP activity without becoming ubiquitylated (28). A recombinant version of RTA containing four extra lysyl residues (RTA 6K) was more heavily ubiquitylated under these conditions, consistent with its enhanced propensity for proteasomal degradation (25). A small proportion of native wild-type RTA (2K) was also a substrate for the Hsc70/CHIP cochaperone machinery (Fig. 5*B*).

Hsp90 also prevented aggregation of heat-treated RTA *in vitro*, but in an ATP-independent manner (Fig. 5*C*, upper panel and graph), but, unlike Hsc70, had no effect at 37°C (Fig. 5*C*, lower panel and graph). Furthermore, in *in vitro* CHIP-mediated ubiquitylation assays at 37°C, Hsp90 alone could not direct CHIP efficiently toward RTA, but in the presence of Hsc70 and HOP, Hsp90 promoted RTA ubiquitylation, thus providing a rationale for the net protective effect of Hsp90 *in vivo* (Fig. 5*D*). We conclude that both nonnative and native RTA at the physiological temperature for ricin intoxication can be substrates for Hsc70- and Hsp90-CHIP complexes, and that sequential Hsc70-Hsp90 interactions lead to net RTA inactivation.

Discussion

Molecular chaperones are widely regarded as cellular protein folding factors governing folding of nascent and damaged protein clients, and as protein assembly factors. During ER translocation, yeast cytosolic chaperones target ER import-incompetent proteins to the proteasome (31). In mammalian cells, roles for Hsc70 have been demonstrated in CFTR triage (32) and in cotranslocational destruction of apoB that has stalled in the import translocon (33). Here, we demonstrate that a luminal protein that exploits the ERAD pathway for dislocation is also scrutinized by the same machineries. Prevailing concentrations of Hsc70 cochaperones determine the proportion of toxin that can recover catalytic activity and the proportion that is destroyed. The simplest model to account for our findings is shown in Fig. 5*E*, illustrating chaperone-mediated triage of cytosolic RTA. After dislocation, RTA is recognized by the Hsc70 chaperone machinery. Cochaperones BAG-2 and Hip promote RTA activity *in vivo*, resulting in increased sensitivity of cells to ricin. Inactivation arms also proceed from Hsc70, controlled by BAG-1 and CHIP, protecting the cell from ricin toxicity. In addition, the dual cochaperone Hop coordinates a sequential Hsc70-Hsp90 triage whose net effect is to render dislocated RTA inactive. Inactivation may be mediated by ubiquitylation machineries. Both gain of catalytic conformation and degradation of RTA proceed from chaperone-bound states. This is highly reminiscent of the Hsc70-Hsp90 mediated regulation of signaling proteins (34), but may be unprecedented for a soluble protein that is dislocated from the ER lumen, because soluble ERAD substrates typically interact with other membrane-associated chaperone machineries (35), whereas cytosolic domains of misfolded membrane proteins typically interact with Hsc70 complexes (36). Our findings emphasize the central role of Hsc70-Hsp90 chaperone machineries in cytosolic protein triage. A minimal role for Hsc70 appears to be to prevent aggregation of dislocated RTA in the cytosol, but the possibility

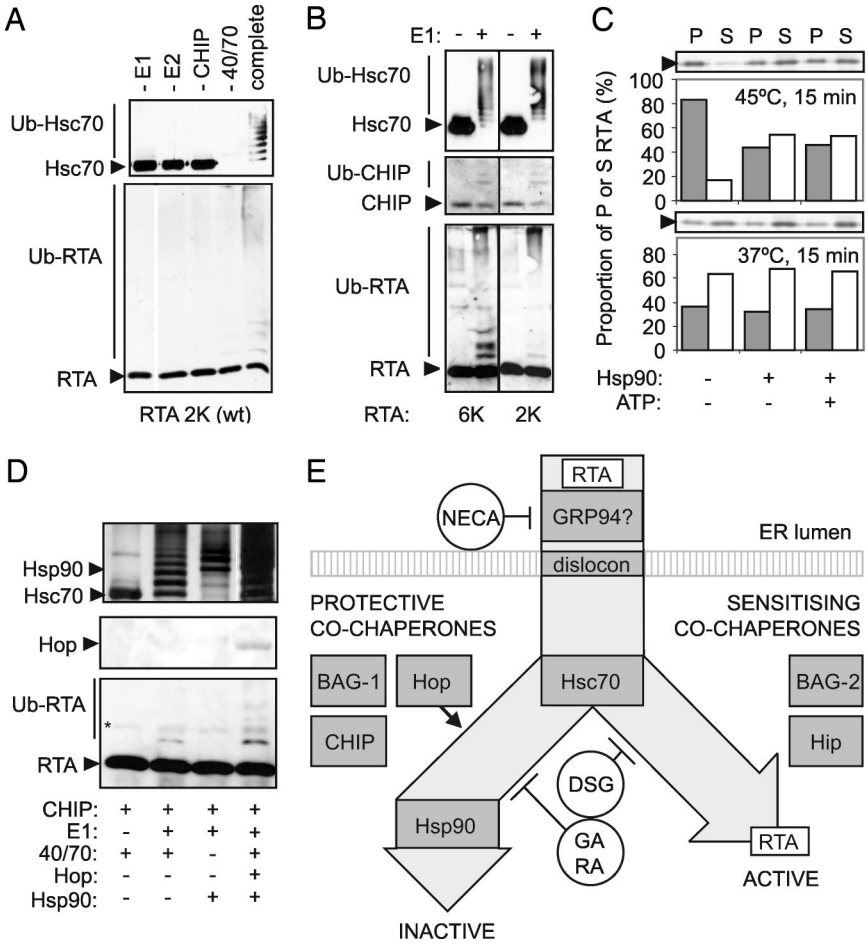

Fig. 5. RTA is a substrate for CHIP. (*A*) RTA was added to a reaction mixture (complete), which can recapitulate CHIP activity (28), and to mixtures lacking E1 ubiquitin activating enzyme, E2 (UbcH5 ubiquitin conjugating enzyme), CHIP, or Hsp40/Hsc70 (40/70) as indicated. After heating (45°C, 10 min), reactions were activated by addition of 5 mM $MgCl_2$, 10 mM DTT, and 5 mM ATP, incubated (2h, 30°C), and products were identified by reducing SDS/PAGE and immunoblotting for Hsc70 and RTA. (*B*) Addition of E1 to a reaction mixture containing RTA, Hsp40, Hsc70, E2, CHIP, and ubiquitin as in *A*, and incubation at 37°C for 2 h results in CHIP-mediated ubiquitylation of Hsc70 (upper panel, Ub-Hsc70), CHIP (middle panel, Ub-CHIP), and both RTA 6K and RTA (lower panel, Ub-RTA) as revealed by immunoblots. (*C*) RTA (500 ng) was incubated (45°C or 37°C, 15 min) in the presence or absence of Hsp90 or ATP (shown below the panels). Aggregated (P) and soluble (S) fractions were separated by centrifugation, heated in reducing SDS sample buffer, and analyzed by SDS/PAGE and subsequent silver staining. Proportions (%) of aggregated (gray) and soluble (white) RTA are shown. (*D*) RTA was added to CHIP recapitulation mixtures as in *A*, but containing Hsp40 and Hsp70 (40/70), HOP, and Hsp90 as indicated below the panels, incubated (2 h, 37°C), and products were identified by reducing SDS/PAGE and immunoblotting for HOP and RTA, and by silver staining for Hsc70 and Hsp90. *, cross-reacting contaminant. (*E*) Proposed cytosolic triage of dislocated RTA.

of Hsc70 supporting the folding of RTA directly cannot yet be discounted.

Folding of heat-denatured RTA *in vitro* is favored in the presence of ribosomes, implicating the toxin's substrate in its own activation (19). It remains to be seen whether human homologues of ribosome-tethered chaperones that assist folding of nascent proteins (37, 38) also contribute to posttranslational folding of cytosolic RTA and how significant a role they have relative to the soluble chaperone complexes.

Materials and Methods

Cytotoxicity Measurements. HeLa cell responses to 4-h challenges with graded doses of ricin or diphtheria toxin (DTx) were measured as previously described (3). For pharmacological studies, cells were treated coevally with graded doses of toxin in medium containing carrier or solvent vehicle (control) and with toxin dilutions in medium containing both carrier/vehicle and pharmacological agent. Each cytotoxicity curve was normalized to controls not treated with toxin, but containing agent or vehicle as appropriate, so any effects of agent alone on protein synthesis were accounted for. Toxin trafficking times from cell surface to first destruction of ribosomes were measured as previously described (13). DSG was supplied by Worldwide Clinical Development, Nippon Kayaku Co., Ltd., 31–12, Shimo 3-chome, Kita-ku, Tokyo 115-0042, Japan.

Overexpression Studies. HeLa cells were transfected with vectors expressing cochaperones, using previously published conditions (3). Two days posttransfection, cells were seeded into 96-well plates and grown overnight for cytotoxicity studies. Overexpression of cochaperones was confirmed by using FLAG-tagged versions of these proteins, and immunoblotting using an anti-FLAG antibody (data not shown).

***In Vitro* Ubiquitylation, Aggregation, and RTA Activity Studies.** Recombinant RTA was added to reaction mixtures containing 0.1 μM E1 ubiquitin activating enzyme, 0.3 μM Hsp40, 3 μM Hsc70, 3 μM HOP, 3 μM Hsp90, 4 μM UbcH5 (E2 conjugating enzyme), 3 μM CHIP, and 2 $mg.ml^{-1}$ ubiquitin in 20 mM Mops, pH 7.2, 100 mM KCl, 5 mM $MgCl_2$, 5 mM ATP, 10 mM DTT buffer as previously described (28) and to reaction mixtures lacking components as appropriate. After incubation (2 h) at 30°C or 37°C as appropriate, products were identified by reducing SDS/PAGE and immunoblot. When required, reaction mixes lacking ATP and $MgCl_2$ were heated to 45°C for 10 min followed by cooling to the required reaction temperature and activation of the reaction by addition of ATP and $MgCl_2$. For aggregation studies, reaction mixtures lacking E1, E2, CHIP, and Ub were used, and RTA was heated to 37°C or 45°C in the presence or absence of Hsp40, Hsc70, Hsp90, and ATP. Aggregated and soluble fractions were separated by centrifugation (16,000 $\times$ *g*, 10 min), solubilized in reducing SDS sample buffer, and analyzed by SDS/PAGE and silver staining. Catalytic activity of RTA from soluble fractions was assayed by quantifiying the RNA

fragment released from yeast 26S rRNA after RTA-mediated depurination of intact ribosomes and cleavage with acetic-aniline. rRNA species were resolved by denaturing gel electrophoresis, and fragments quantified in relation to the amount of 5.8S rRNA (22). Bands on silver-stained and ethidium bromide stained gels were quantified by using TotalLab software.

ACKNOWLEDGMENTS. We thank Prof. John R. Ellis for critical readings and encouragement. This work was supported by National Institutes of Health Grant 5U01AI65869-02, Wellcome Trust Programme Grant 080566Z/06/Z, Biotechnology and Biological Sciences Research Council, U.K., and the Deutsche Forschungsgemeinschaft SFB635.

1. Brodsky JL (2007) The protective and destructive roles played by molecular chaperones during ERAD (endoplasmic-reticulum-associated degradation). *Biochem J* 404:353–363.
2. Meusser B, Hirsch C, Jarosch E, Sommer T (2005) ERAD: The long road to destruction. *Nat Cell Biol* 7:766–772.
3. Spooner RA, *et al.* (2004) Protein disulphide-isomerase reduces ricin to its A and B chains in the endoplasmic reticulum. *Biochem J* 383:285–293.
4. Wesche J, Rapak A, Olsnes S (1999) Dependence of ricin toxicity on translocation of the toxin A-chain from the endoplasmic reticulum to the cytosol. *J Biol Chem* 274:34443–34449.
5. Argent RH, *et al.* (1994) Introduction of a disulfide bond into ricin A chain decreases the cytotoxicity of the ricin holotoxin. *J Biol Chem* 269:26705–26710.
6. Hazes B, Read RJ (1997) Accumulating evidence suggests that several AB-toxins subvert the endoplasmic reticulum-associated protein degradation pathway to enter target cells. *Biochemistry* 36:11051–11054.
7. van Deurs B, *et al.* (1988) Estimation of the amount of internalized ricin that reaches the trans-Golgi network. *J Cell Biol* 106:253–267.
8. Rapak A, Falnes PO, Olsnes S (1997) Retrograde transport of mutant ricin to the endoplasmic reticulum with subsequent translocation to cytosol. *Proc Natl Acad Sci USA* 94:3783–3788.
9. Wales R, Roberts LM, Lord JM (1993) Addition of an endoplasmic reticulum retrieval sequence to ricin A chain significantly increases its cytotoxicity to mammalian cells. *J Biol Chem* 268:23986–23990.
10. Nadeau K, *et al.* (1994) Quantitation of the interaction of the immunosuppressant deoxyspergualin and analogs with Hsc70 and Hsp90. *Biochemistry* 33:2561–2567.
11. Meacham GC, *et al.* (2001) The Hsc70 co-chaperone CHIP targets immature CFTR for proteasomal degradation. *Nat Cell Biol* 3:100–105.
12. Brodsky JL (1999) Selectivity of the molecular chaperone-specific immunosuppressive agent 15-deoxyspergualin: Modulation of Hsc70 ATPase activity without compromising DnaJ chaperone interactions. *Biochem Pharmacol* 57:877–880.
13. Hudson TH, Neville DM, Jr (1987) Temporal separation of protein toxin translocation from processing events. *J Biol Chem* 262:16484–16494.
14. Ramsay G, Montgomery D, Berger D, Freire E (1989) Energetics of diphtheria toxin membrane insertion and translocation: Calorimetric characterization of the acid pH induced transition. *Biochemistry* 28:529–533.
15. Roe SM, *et al.* (1999) Structural basis for inhibition of the Hsp90 molecular chaperone by the antitumor antibiotics radicicol and geldanamycin. *J Med Chem* 42:260–266.
16. Lawson B, Brewer JW, Hendershot LM (1998) Geldanamycin, an hsp90/GRP94-binding drug, induces increased transcription of endoplasmic reticulum (ER) chaperones via the ER stress pathway. *J Cell Physiol* 174:170–178.
17. Rosser MF, Nicchitta CV (2000) Ligand interactions in the adenosine nucleotide-binding domain of the Hsp90 chaperone, GRP94 I: Evidence for allosteric regulation of ligand binding. J Biol Chem 275:22798–22805.
18. Christianson JC, Shaler TA, Tyler RE, Kopito RR (2008) OS-9 and GRP94 deliver mutant alpha1-antitrypsin to the Hrd1-SEL1L ubiquitin ligase complex for ERAD. *Nat Cell Biol* 10:272–282.
19. Argent R H, *et al.* (2000) Ribosome-mediated folding of partially unfolded ricin A-chain. *J Biol Chem* 275:9263–9269.
20. Savino C, *et al.* (2000) The crystal structure of saporin SO6 from Saponaria officinalis and its interaction with the ribosome. *FEBS Lett* 470:239–243.
21. Day PJ, Pinheiro TJ, Roberts LM, Lord JM (2002) Binding of ricin A-chain to negatively charged phospholipid vesicles leads to protein structural changes and destabilizes the lipid bilayer. *Biochemistry* 41:2836–2843.
22. Chaddock JA, Roberts LM (1993) Mutagenesis and kinetic analysis of the active site Glu177 of ricin A-chain. *Protein Eng* 6:425–431.
23. Chen S, Smith DF (1998) Hop as an adaptor in the heat shock protein 70 (Hsp70) and hsp90 chaperone machinery. *J Biol Chem* 273:35194–35200.
24. Luders J, Demand J, Hohfeld J (2000) The ubiquitin-related BAG-1 provides a link between the molecular chaperones Hsc70/Hsp70 and the proteasome. *J Biol Chem* 275:4613–4617.
25. Deeks ED, *et al.* (2002) The low lysine content of ricin A chain reduces the risk of proteolytic degradation after translocation from the endoplasmic reticulum to the cytosol. *Biochemistry* 41:3405–3413.
26. Hohfeld J, Minami Y, Hartl FU (1995) Hip, a novel cochaperone involved in the eukaryotic Hsc70/Hsp40 reaction cycle. *Cell* 83:589–598.
27. Dai Q, *et al.* (2005) Regulation of the cytoplasmic quality control protein degradation pathway by BAG2. *J Biol Chem* 280:38673–38681.
28. Arndt V, *et al.* (2005) BAG-2 acts as an inhibitor of the chaperone-associated ubiquitin ligase CHIP. *Mol Biol Cell* 16:5891–5900.
29. Urushitani M, *et al.* (2004) CHIP promotes proteasomal degradation of familial ALS-linked mutant SOD1 by ubiquitinating Hsp/Hsc70. *J Neurochem* 90:231–244.
30. Jiang J, *et al.* (2001) CHIP is a U-box-dependent E3 ubiquitin ligase: Identification of Hsc70 as a target for ubiquitylation. *J Biol Chem* 276:42938–42944.
31. Park SH, *et al.* (2007) The cytoplasmic Hsp70 chaperone machinery subjects misfolded and endoplasmic reticulum import-incompetent proteins to degradation via the ubiquitin-proteasome system. *Mol Biol Cell* 18:153–165.
32. Younger JM, *et al.* (2006) Sequential quality-control checkpoints triage misfolded cystic fibrosis transmembrane conductance regulator. *Cell* 126:571–582.
33. Gusarova V, Caplan AJ, Brodsky JL, Fisher EA (2001) Apoprotein B degradation is promoted by the molecular chaperones hsp90 and hsp70. *J Biol Chem* 276:24891–24900.
34. Arndt V, Rogon C, Hohfeld J (2007) To be, or not to be–molecular chaperones in protein degradation. *Cell Mol Life Sci* 64:2525–2541.
35. Nakatsukasa K, Brodsky JL (2008) The recognition and retrotranslocation of misfolded proteins from the endoplasmic reticulum. *Traffic* 9:861–870.
36. Nakatsukasa K, Huyer G, Michaelis S, Brodsky JL (2008) Dissecting the ER-associated degradation of a misfolded polytopic membrane protein. *Cell* 132:101–112.
37. Otto H, *et al.* (2005) The chaperones MPP11 and Hsp70L1 form the mammalian ribosome-associated complex. *Proc Natl Acad Sci USA* 102:10064–10069.
38. Hundley H, *et al.* (2002) The *in vivo* function of the ribosome-associated Hsp70, Ssz1, does not require its putative peptide-binding domain. *Proc Natl Acad Sci USA* 99:4203–4208.